Caractérisation et étude des vibrations dans la pratique sportive

Robin Trama

N°d'ordre NNT : 2021LYSE1128

THESE de DOCTORAT DE L'UNIVERSITE DE LYON
opérée au sein de
l'Université Claude Bernard Lyon 1

Ecole Doctorale N° 205
Ecole Doctorale Interdisciplinaire Sciences-Santé (EDISS)

Spécialité de doctorat :
Sciences et Techniques des Activités Physiques et Sportives (STAPS)

Soutenue publiquement le 09/07/2021, par :
Robin Trama

Caractérisation et étude des vibrations dans la pratique sportive

---

Devant le jury composé de :

Chèze Laurence (PU)	Université Claude Bernard Lyon 1	Présidente
Colson Serge (PU)	Université Côte d'Azur	Rapporteur
Nordez Antoine (PU)	Université de Nantes	Rapporteur
Bertucci William (PU)	Université de Reims Champagne-Ardenne	Examinateur
Hintzy Frédérique (MCU-HDR)	Université Savoie Mont Blanc	Examinatrice
Hautier Christophe (MCU-HDR)	Université Claude Bernard Lyon 1	Directeur de thèse
Blache Yoann (MCU)	Université Claude Bernard Lyon 1	Co-directeur de thèse
Colson, Serge (PU)	Université Côte d'Azur	Invité

TABLE DES MATIERES

TABLE DES ILLUSTRATIONS

RESUMES

Résumé

La course à pied et les différentes pratiques sportives induisent des chocs et des vibrations transitoires au niveau des tissus mous à chaque impact. Ces impacts et vibrations peuvent générer un stress mécanique important, qui accroit le risque de fatigue et de blessure de sur-sollicitation. Le premier objectif de la thèse était consacré au développement de méthodes de traitement du signal d'accélération et d'analyse statistique afin de mieux caractériser les impacts et vibrations subies par le sportif. Le second objectif était de définir les facteurs externes, tels que le type de mouvement, le matériel sportif, ou la fatigue neuromusculaire, qui faisaient varier le comportement vibratoire en pratique écologique. Avec le développement de méthodes de traitement du signal (transformée en ondelettes continue) et statistiques (Statistical nonParametric Mapping), nous avons montré que la vibration des tissus mous était différente de la vibration musculaire. Ainsi, les accéléromètres ne permettaient de caractériser que partiellement la vibration du muscle par rapport à une échographe ultra rapide. De plus, l'augmentation de la vitesse de course et les mouvements effectués lors de la pratique de sports collectifs génèrent des impacts à plus grande amplitude et à plus haute fréquence, ainsi que des vibrations des tissus mous plus amples que la course en ligne droite. Parmi le matériel sportif évalué, seul un revêtement sportif coulissant a permis de réduire l'amplitude de l'impact au sol. Une identification du type de mouvement a été rendu possible grâce à la mesure des impacts et l'usage d'un réseau de neurones convolutifs, permettant de franchir une première étape dans l'évaluation de la dose vibratoire subie par un sportif lors de sa pratique. Enfin, une étude réalisée lors des courses de l'UTMB a permis d'observer une stratégie de protection de l'organisme après des efforts de type trail en diminuant l'amplitude et la fréquence des vibrations des muscles les plus sollicités. Il reste nécessaire d'améliorer la caractérisation de la vibration musculaire avec des accéléromètres fixés sur la peau et de déterminer l'effet de l'exposition répétée à des vibrations transitoires sur le système neuromusculaire et musculo-squelettique.

Abstract

Running and various team sports generate transient vibrations in the soft tissues of the lower limb at each impact between the foot and the ground. These impacts and vibrations can generate significant mechanical stress, which increases the risk of overuse injury when not properly managed. The first objective of the thesis was devoted to the development of signal processing and statistical analysis methods to better characterize the impacts and vibrations encountered by athletes. The second objective was to define the external factors, such as practices, sports equipment, or neuromuscular fatigue, that modify the vibratory behavior in ecological practice. With the development of signal processing methods (continuous wavelet transform) and statistical methods (Statistical nonParametric Mapping), we highlighted that soft tissue vibration was different from muscle vibration. Thus, accelerometers allow only a salient characterization of the muscle vibration compared to an ultrafast ultrasound. Besides, increasing running speed and sport specific tasks generated higher impact amplitude and frequency, as well as greater soft tissue vibration compared to in-line running. Among the sports equipment evaluated, only a sliding sports surface reduced the amplitude of the impact on the ground. An identification of the type of movement was made possible thanks to the measurement of the impacts and a convolutional neural network, allowing to cross the first step in the evaluation of the vibratory dose undergone by an athlete. Finally, a study carried out during the UTMB races put forward a strategy of protection of the neuromuscular system after trail-type efforts by decreasing the amplitude and the frequency of the vibrations of the most solicited muscles. It is now necessary to improve the characterization of muscle vibration with accelerometers fixed to the skin and to determine the effect of repetitive exposure to transient vibrations on the neuromuscular and musculoskeletal system.

REMERCIEMENTS

C'était une longue aventure… cinq ans déjà.

Merci à Christophe et Yoann, mes deux directeurs de thèse, qui m'ont tout d'abord fait confiance pour mener à terme ce projet et qui m'ont formé sur tous les aspects de la recherche et de l'enseignement. Merci à Christophe qui a su me faire me poser les bonnes questions pour orienter mes différentes approches : « L'important c'est la question, pas la réponse ». Merci à Yoann de m'avoir encouragé à travailler dès le début avec ce qui est devenu mon meilleur pote, Matlab : « Si tu ne trouves pas, cherche, et si dans une semaine tu n'as pas trouvé, tu viendras me voir ». Le fait de m'avoir motivé à me mettre tôt à la programmation m'a permis d'être rapidement indépendant et m'a permis de réfléchir autrement sur beaucoup de sujets, même autres que scientifiques. Evidemment il n'y a pas eu que du travail et j'ai énormément apprécié les moments de détente : « C'est pas moi, j'étais au bar ! ». Un grand merci à vous deux !

Merci aux collègues avec qui j'ai partagé plusieurs de ces années riches en sorties grimpes, courses et apéros. La vie de labo n'aurait pas été la même sans vous.

C'était une longue aventure… quinze ans déjà.

Merci à mes amis d'enfance, même si vous me m'avez pas soutenu à proprement parlé durant ce travail, vous m'avez supporté, et ça, c'est déjà pas mal. Ces années auraient été différentes si je ne vous avais pas vu régulièrement les weekends.

C'était une longue aventure… vingt-sept ans déjà.

Merci Papa et Maman pour votre soutien inconditionnel. Désolé, je sais que vous vouliez que je rentre après mes études mais cela a pris plus de temps qu'initialement imaginé… et qui sait ce que nous réserve l'avenir ? Mais je sais que même au bout du monde vous serez là pour moi.

Merci à mon frangin Max et à Vérane qui ont toujours été là pour moi, surtout dans les moments difficiles.

Merci à toute ma famille, qui est la meilleure du monde, évidemment.

PUBLICATIONS

Sont soulignés les articles et résumés repris dans la thèse.

Articles dans des revues internationales à comité de lecture

Acceptés

R. Trama, C. Hautier, Y. Blache (2021). fctSnPM: Factorial ANOVA and post-hoc tests for Statistical nonParametric Mapping in MATLAB. Journal of Open Source Software, 6(63), 3159, https://doi.org/10.21105/joss.03159

R. Trama, C. Hautier, R. Souron, T. Lapole, A. Fouré, Y. Blache (2021). Is accelerometry an effective method to assess muscle vibrations in comparison to ultrafast ultrasonography? IEEE Transactions on Biomedical Engineering, Vol 68, No. 4, pp. 1409-1416. 10.1109/TBME.2020.3035838

Q. Zhang, B. Morel, **R. Trama**, C. Hautier (2021). Influence of Fatigue on the Rapid Hamstring/Quadriceps Force Capacity in Soccer Players. Frontiers in Physiology, Vol 12, pp. 35. 10.3389/fphys.2021.627674

R. Trama, C. Hautier, Y. Blache (2020). Input and Soft-Tissue Vibration Characteristics during Sport-Specific Tasks. Medicine & Science in Sports & Exercise, Vol. 52, No. 1, pp. 112–119. 10.1249/MSS.0000000000002106

Q. Zhang, F. Pommerell, A. Owen, **R. Trama**, C. Martin, C. Hautier (2020). Running patterns and force-velocity sprinting profiles in elite training young soccer players: A Cross-Sectional Study. European Journal of Sport Science, pp. 1-25. 10.1080/17461391.2020.1866078

Q. Zhang, **R. Trama**, A. Fouré, C. Hautier (2020). The Immediate Effects of Self-Myofacial Release on Flexibility, Jump Performance and Dynamic Balance Ability. Journal of Human Kinetics, Vol. 75, No. 1, pp. 139–148. 10.2478/hukin-2020-0043

R. Trama, Y. Blache, C. Hautier (2019). Effect of rocker shoes and running speed on lower limb mechanics and soft tissue vibrations. Journal of Biomechanics, Vol. 82, pp. 171–177. 10.1016/j.jbiomech.2018.10.023

P. Balducci, Saboul. D, **R. Trama** (2019). Monitoring heart rates to evaluate pacing on a 75-km MUM. The Journal of Sports Medicine and Physical Fitness, Vol. 59, No. 7. 10.23736/S0022-4707.18.08861-8

P. Balducci, M. Clémençon, **R. Trama**, C. Hautier (2017). The Calculation of the Uphill Energy Cost of Running from the Level Energy Cost of Running in a Heterogeneous Group of Mountain Ultra Endurance Runners. Asian Journal of Sports Medicine, Vol. 8, No. 1. 10.5812/asjsm.42091.

P. Balducci, M. Clémençon, R. Trama, Y. Blache, C. Hautier (2017). Performance Factors in a Mountain Ultramarathon. International Journal of Sports Medicine, Vol. 38, No. 11, pp. 819-826. 10.1055/s-0043-112342.

Soumis

R. Trama, Y. Blache, F. Hintzy, J. Rossi, G. Y Millet, C. Hautier. Does neuromuscular fatigue generated by mountain ultra-marathon modify foot impact and soft-tissue vibrations during running? Medicine & Science in Sports & Exercise. MSSE-D-20-01167

R. Trama, M-C Play*, G. Y Millet, C. Hautier, M. Giandolini, J. Rossi. Soft Tissue Vibrations in Running: A Narrative Review. Journal of Biomechanics. BM-D-20-01498

Résumés de congrès

Accepté

R. Trama, C. Hautier, Y. Blache. (2019). Sport-related impact classification through a convolutional neural network. Computer Methods in Biomechanics and Biomedical Engineering, Vol. 22, No. sup1, pp. 267–269. 10.1080/10255842.2020.1714908

R. Trama, T. Le Solliec, Y. Blache, C. Hautier. Heel Impact, Tibial Shock and Soft Tissue Vibrations in young basketball players: influence of movements and court construction. Congrès de la Société de Biomécanique 2021. Computer Methods in Biomechanics and Biomedical Engineering (Accepté).

Communications orales

R. Trama, T. Le Solliec, Y. Blache & C. Hautier. (2021). Impact au sol et vibrations des tissus mous des membres inférieurs en tennis : comparaison avec des mouvements standardisés. 2eme colloque international: Le tennis dans la société de demain, Dijon, France (en visioconférence).

R. Trama, Y. Blache, C. Hautier. (2017). Muscle Tuning Paradigm. Effet de la vitesse de course. Association des Chercheurs en Activités Physiques et Sportives (ACAPS), Dijon, France.

R. Trama, A. Fouré, Y. Blache, C. Hautier. (2019). Does accelerometer measure muscle vibrations? European Congress of Sport Science (ECSS), Prague, Tchéquie.

R. Trama, C. Hautier, Y. Blache. (2019). Sport-related impact classification through a convolutional neural network. Société de Biomécanique (SB), Poitiers, France.

Articles de vulgarisation

R. Trama, Y. Blache, C. Hautier. (2020). Comparaison de moyennes en une et deux dimensions : la cartographie statistique paramétrique (SPM) pour tous. Blog de la Société de Biomécanique : https://www.biomecanique.org/index.php/fr/blog/179-outils-comparaison-de-courbes-et-de-cartes-la-cartographie-statistique-parametrique-spm-pour-tous et Blog de l'Association des Chercheur en Activité Physique et Sportive (ACAPS) : https://www.acaps.asso.fr/comparaison-de-moyennes-en-une-et-deux-dimensions-la-cartographie-statistique-parametrique-spm-pour-tous/

1 INTRODUCTION GENERALE

Selon le rapport de 2020 de l'Institut National de la Jeunesse et de l'Education Populaire, 66% de la population française de plus de 15 ans avait pratiqué au moins une activité sportive au cours de l'année. De plus, avec plus d'un demi-milliard de pratiquants à travers le monde (Hulteen et al., 2017), la course à pied est l'un des sports les plus pratiqués. Malgré les nombreux effets positifs de la course à pied sur la santé, tels qu'une meilleure santé cardiovasculaire et cardiorespiratoire rallongeant l'espérance de vie (Lee et al., 2017), une amélioration de la résistance du système ostéo-articulaire (Chen et al., 2016) et un sentiment d'accomplissement et d'intégration sociale (Major, 2001), une gestion inappropriée de la charge d'entraînement peut causer un risque accru de blessure (Hreljac, 2004; Kiernan et al., 2018).

Une des causes d'occurrence des blessures en course à pied est un excès de stress mécanique, qui endommage les différents tissus comme les muscles, les cartilages et les os (Zadpoor & Nikooyan, 2011). Le stress mécanique se caractérise par une succession de contractions musculaires, d'impacts entre le pied et le sol, et de vibrations provoquées par cet impact (Zadpoor & Nikooyan, 2011). Alors que les adaptations chroniques à l'exposition aux vibrations sont bénéfiques pour améliorer la force musculaire grâce à des adaptations nerveuses (Souron et al., 2017b) et structurelles (Necking et al., 1996b) les vibrations aiguës peuvent être néfastes pour le système neuromusculaire à court terme (Necking et al., 2002; Souron et al., 2017a). En effet, il a été montré que des vibrations continues à 40 Hz provoquent des lésions musculaires (Necking et al., 1996a, 1992) tandis que des vibrations entre 80 et 120 Hz peuvent causer une fatigue neuromusculaire (Souron et al., 2017b, 2017a). Les vibrations provoquées par les impacts entre le pied et le sol, avec des fréquences allant de 10 à 130 Hz (Enders et al., 2012) sont, quant à elles, l'un des facteurs pouvant être à l'origine de la fatigue neuromusculaire et des lésions musculaires, augmentant à terme le risque de blessure chronique (Mair et al., 1996).

Bien que plusieurs études aient porté sur la caractérisation de la vibration des tissus mous (i.e., le complexe peau, graisse et muscle) grâce à des accéléromètres (Wakeling & Nigg, 2001a), une certaine incertitude demeure quant à la capacité de ces capteurs à caractériser la vibration musculaire (Lai & Hodson-Tole, 2020; Yamada et al., 2018). De plus, de nombreuses études se sont intéressées à la course

à pied (Boyer & Nigg, 2004) et aux réceptions de sauts (Fu et al., 2015), cependant, les vibrations induites par des mouvements spécifiques à diverses pratiques sportives n'ont pas été étudiées. Enfin, même si des liens ont été établis entre les caractéristiques de la vibration et la génération de fatigue ou de dommages musculaires (Necking et al., 1992; Souron et al., 2017a), il est à noter que la vibration induite était continue et générée de manière artificielle (i.e., induite par un excitateur extérieur) et non générée par un impact entre le pied et le sol.

Par conséquent, l'étude des vibrations musculaires dans diverses pratiques et de leurs effets sur le système neuromusculaire permettra d'apporter de nouvelles informations pour compléter l'analyse multifactoriel de la fatigue, de la performance et de la blessure. Pour mieux comprendre ces vibrations musculaires, un premier axe de la thèse portera sur l'identification et le développement de méthodes de mesures et d'analyse de la vibration, tandis qu'un second axe sera orienté sur la quantification des vibrations dans diverses conditions de pratiques.

2 REVUE DE LITTERATURE

2.1 LA VIBRATION CHEZ L'ETRE HUMAIN

2.1.1 Définition

Une vibration est un phénomène mécanique qui correspond aux variations de vitesse d'un corps physique (i.e., son accélération), oscillant autour de sa position de repos (Piéron, 1935). La vibration est une perturbation qui se propage dans un milieu matériel, avec transport d'énergie mais sans transport de matière ; c'est donc une onde mécanique. La vibration est principalement quantifiée grâce à des accéléromètres (Coza et al., 2010; Wakeling & Nigg, 2001a) et est caractérisée par son amplitude et sa fréquence. L'amplitude de la vibration diminuant au cours du temps par un phénomène d'amortissement dans l'organisme humain, son coefficient d'amortissement est aussi caractérisé (Khassetarash et al., 2015a). La vibration dans le corps humain peut donc être modélisée comme une force s'appliquant sur un système masse-ressort-amortisseur (Figure 1).

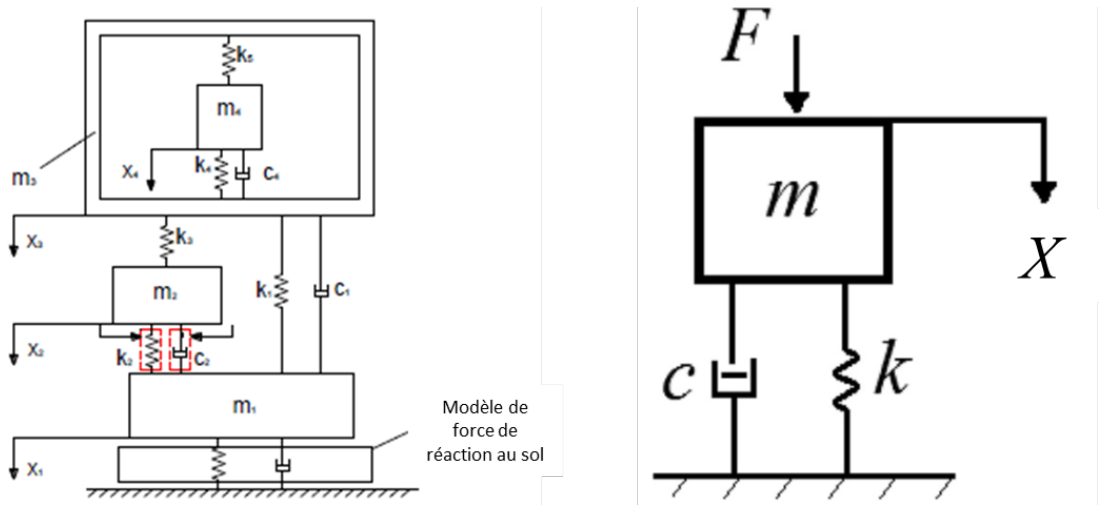

Figure 1 : Modèle masses-ressorts-amortisseurs (gauche) adapté de Nikooyan et Zadpoor (2012) et modèle masse-ressort-amortisseur simplifié (droite) adapté de Khassetarash et al. (2015b). m représente la masse du système, k sa raideur et c son coefficient d'amortissement. X est le déplacement de la masse engendré par la force de réaction au sol (modèle de gauche) ou par la force appliquée sur la masse (modèle de droite).

2.1.2 La vibration des tissus mous

Les tissus mous sont composés du complexe muscle-tendon et des tissus superficiels l'entourant tels que la graisse sous-cutanée et la peau (Figure 2). La vibration du muscle devrait être au centre des recherches car c'est lui qui est effecteur du mouvement et qui peut être fatigué ou lésé. Or, la localisation profonde du muscle rend la caractérisation de sa vibration difficile et ne permet pas de la dissocier de la vibration de l'ensemble des tissus mous (Smeathers, 1989). Ainsi, la plupart des études utilisent le terme de « vibration des tissus mous » et non de « vibration musculaire ».

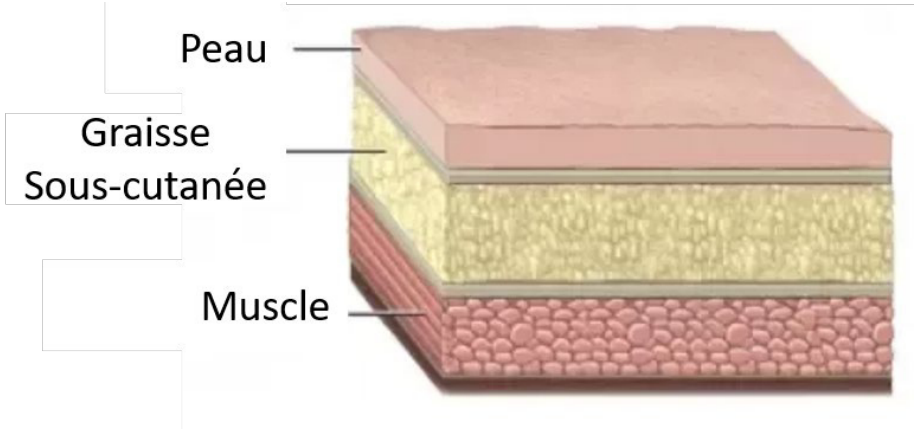

Figure 2 : Organisation des différentes couches de tissus mous. Le muscle, tissu profond, se retrouve sous la graisse sous-cutanée (quelques millimètres à plusieurs centimètres d'épaisseur) et la peau (moins de 1 millimètre d'épaisseur).

2.1.3 Cadre juridique sur l'exposition aux vibrations

Dans le cadre du travail, plusieurs décrets et directives viennent réguler l'exposition aux vibrations. Notamment les articles r4442, r4443, r4444 et r4445 du code du travail, le décret n° 2005-746 du 4 juillet 2005 et la directive 2002/44/ce du parlement européen et du conseil du 25 juin 2002. Ces textes sont relatifs aux prescriptions de sécurité et de santé applicables en cas d'exposition des travailleurs aux risques dus aux vibrations mécaniques et modifiant le code du travail. Ils obligent les employeurs à 1) organiser l'espace de travail pour limiter les travailleurs à l'exposition de vibrations ; 2) évaluer cette exposition, la mesurer et la comparer à la valeur seuil établie par le décret 2005-746 du 4 juillet 2005, dépendant de l'amplitude et de la durée de la vibration ; 3) engager diverses actions pour réduire l'exposition aux vibrations et informer les employés des bons comportements à adopter afin de protéger le travailleur. Cependant, le parallèle dans le cadre sportif ne peut pas être fait, car aucun règlement ne vient contrôler l'exposition aux vibrations des sportifs durant leur pratique.

2.2 LA VIBRATION DANS LA PRATIQUE SPORTIVE

2.2.1 Caractéristiques de la vibration

Bien que plusieurs paramètres soient présentés dans la littérature pour décrire la vibration dans la pratique sportive, ces paramètres se réfèrent toujours à l'une des trois composantes suivantes : l'amplitude, la fréquence, et l'amortissement.

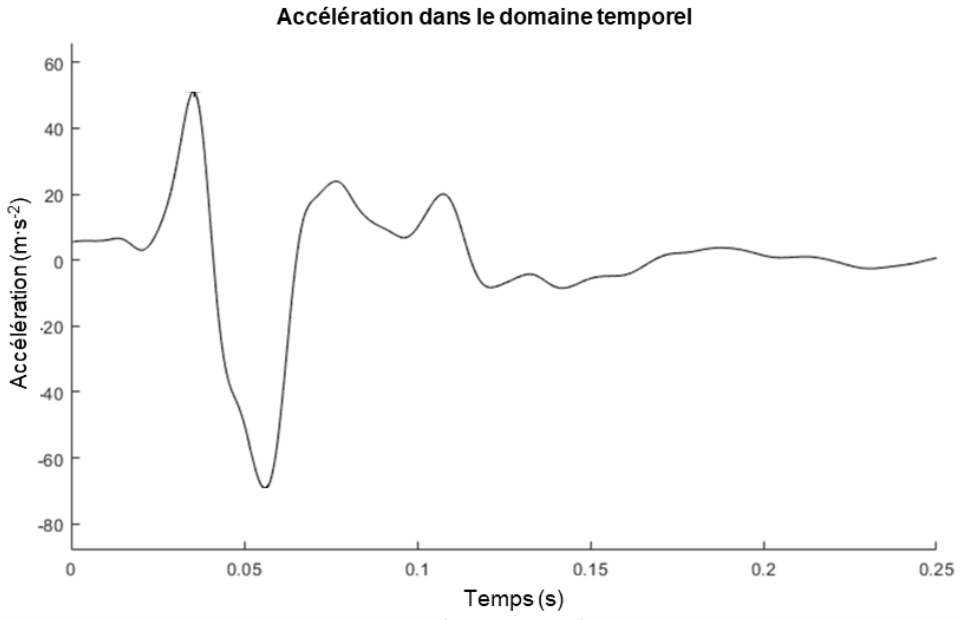

Figure 3: Signal d'accélération verticale type recueilli au niveau du gastrocnemius medialis après un impact entre le pied et le sol en course à pied

2.2.1.1 Amplitude

L'amplitude ou encore l'intensité de la vibration est caractérisée par sa valeur ou son amplitude maximale (i.e., au sens mathématique, c'est-à-dire la différence entre son maximum et son minimum). Plus l'amplitude est grande, plus la vibration entrainera un déplacement important pour une fréquence donnée. L'amplitude correspond donc à l'intensité de la force (N ou $m \cdot s^{-2} \cdot kg$) normalisée par la masse (kg) du système (Équation 1). Elle est donc exprimée en $m \cdot s^{-2}$ ou en g (1 g = 9.81 $m \cdot s^{-2}$)(Figure 3).

$$\alpha = F/m, \qquad \textit{Équation 1}$$

avec α l'amplitude de la vibration, F la force externe au système et m la masse du système.

2.2.1.2 Fréquence

La fréquence de vibration est définie par le nombre d'oscillations par seconde du signal vibratoire et est exprimée en Hz (s^{-1}). La fréquence propre d'une structure (ω_0), peut être définie de deux manières. Premièrement, elle correspond à la fréquence à laquelle va naturellement osciller une structure après avoir été déplacée de sa position de repos. Secondement, la fréquence propre est aussi appelée fréquence de résonnance, et correspond à la fréquence à laquelle l'amplitude de la vibration est maximale lorsque la structure est soumise à des vibrations extérieures (Wakeling et al., 2002; Wang et al., 2007). Quelle que soit la définition utilisée, la fréquence propre ou de résonnance est corrélée à la raideur de la structure (i.e., sa résistance à la déformation en N/m ou s^{-2}·kg), et inversement corrélée à sa masse (Équation 2).

$$\omega_0 = \sqrt{k/m}, \qquad \textit{Équation 2}$$

avec k la raideur et m la masse du système.

2.2.1.2.1 Fréquence propre et transfert d'énergie

Pour déterminer la fréquence de propre des tissus mous, des vibrations continues sont générées via un excitateur externe, comme une plateforme vibrante (Wakeling et al., 2002) ou un vibrateur (Wang et al., 2007). Les tissus mous vibreront à la fréquence induite par la source de la vibration, c'est-à-dire dans ce cas-ci à la fréquence de l'excitateur externe, avec une amplitude plus ou moins importante en fonction de l'amplitude de la vibration de l'excitateur et au regard de la proximité entre la fréquence de l'excitateur et la fréquence propre des tissus mous. La fréquence à laquelle l'amplitude de vibration de la structure est maximale détermine la fréquence de résonnance de la structure, alors que des fréquences plus ou moins élevées par rapport à cette fréquence entraineront une vibration de plus faible amplitude (Wakeling et al., 2002; Wang et al., 2007). Le transfert d'énergie en fonction de la fréquence (*T(f),* Équation 3) peut être calculé pour déterminer la quantité d'énergie transmise de la source jusqu'aux tissus mous. La totalité de l'énergie de la source est transférée sous forme de vibration lorsque *T(f)* = 0%, une amplification d'énergie à lieu lorsque *T(f)* > 0%, et une atténuation lorsque *T(f)* < 0% (Figure 4).

$$\mathrm{T(f)} = 100 \cdot \left(\frac{E_s(f)}{E_{tm}(f)} - 1\right) \qquad \textit{Équation 3}$$

avec T(f) le pourcentage d'énergie à chaque fréquence transféré de la source $E_s(f)$ vers les tissus mous $E_{tm}(f)$.

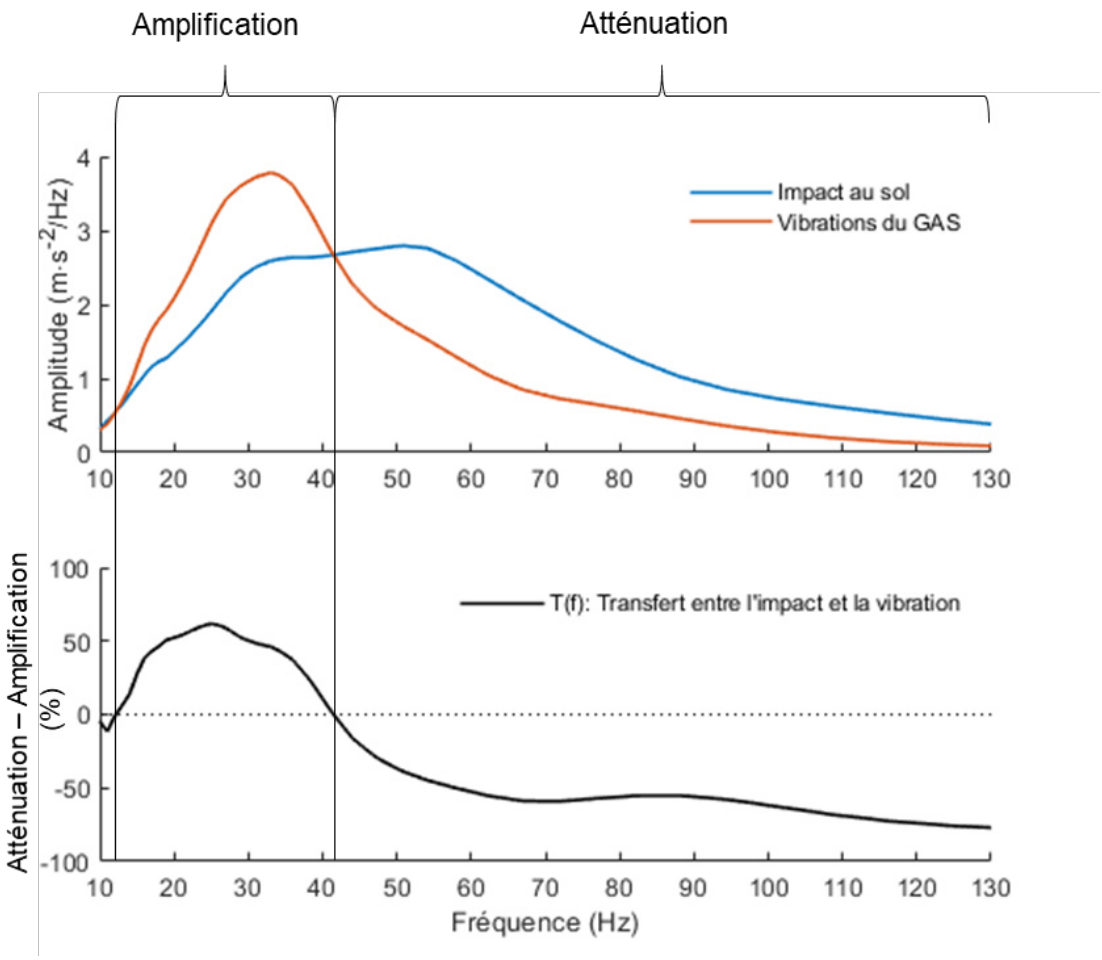

Figure 4 : Exemple de spectre fréquentiel d'un impact (bleu) et de la vibration du gastrocnemius medialis en résultant (rouge). Une amplification de l'impact a lieu entre 12 et 42 Hz, alors qu'une atténuation se produit au-delà de 42 Hz.

2.2.1.3 Amortissement

L'amortissement d'une vibration peut être caractérisé par plusieurs variables différentes représentant la grandeur de décroissance de l'amplitude de la vibration au cours du temps. Concernant les tissus mous, l'amortissement est pseudo-périodique, c'est-à-dire que son taux d'amortissement (ζ) est compris entre 0 et 1. Le taux d'amortissement correspond au ratio entre le coefficient amortissement mesuré (en s^{-1}) et l'amortissement critique de la structure (Équation 4). Pour une même structure, plus le coefficient d'amortissement est important, plus le taux d'amortissement sera important (Figure 5).

$$\zeta = c \,/\, 2\sqrt{km}, \qquad \textit{Équation 4}$$

avec ζ le taux d'amortissement, c le coefficient d'amortissement, k la raideur et m la masse du système.

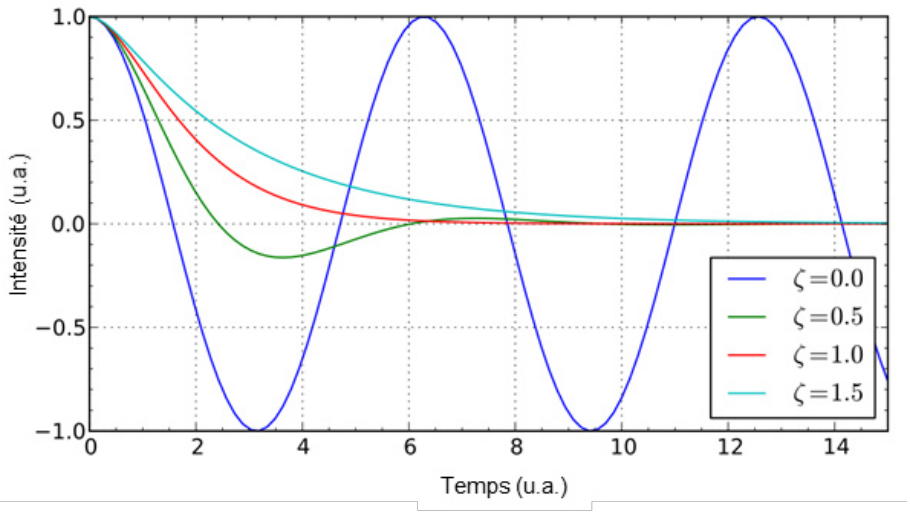

Figure 5 : Evolution de l'amplitude de la vibration au cours du temps en fonction du taux d'amortissement.

En connaissant la fréquence propre et le coefficient d'amortissement de la structure, le taux d'amortissement peut être calculé (Équation 5), notamment lorsque la vibration est modélisée (Wakeling & Nigg, 2001b).

$$\zeta = \frac{c}{\omega_0 \sqrt{4\pi^2 + \frac{c^2}{\omega_0^2}}},$$

Équation 5

avec ζ le taux d'amortissement, c le coefficient d'amortissement, et ω_0 la fréquence propre du système.

2.2.2 La vibration continue

La vibration continue, aussi appelée vibration contrainte ou entretenue, est caractérisée par sa fréquence et son amplitude. Son caractère continu est dû à une source ou excitateur externe, comme une plateforme vibrante (Wakeling et al., 2002) ou un vibrateur local (Wang et al., 2007), qui maintient la vibration à une amplitude constante. L'arrêt de l'activité de la source laisse donc le temps au muscle d'amortir la vibration, qui revient à une amplitude nulle au bout de quelques oscillations.

L'exposition aiguë aux vibrations continues peut créer de la fatigue neuromusculaire et des dommages structurels en fonction de la fréquence (Necking et al., 1996a, 1992; Souron et al., 2017a). En effet, des vibrations continues à 40 Hz provoquent des lésions musculaires (Necking et al., 1996a, 1992) alors que la fatigue neuromusculaire peut être générée par des vibrations entre 80 et 120 Hz (Souron et al., 2017b, 2017a). Ces phénomènes s'expliquent par le fait que les basses fréquences de vibrations ont un potentiel

plus important pour créer du déplacement et léser les fibres musculaires (de Hoyo et al., 2013; Necking et al., 1996a), tandis que les vibrations à hautes fréquences peuvent activer des afférences nerveuses provoquant de la fatigue neuromusculaire (Rittweger et al., 2003; Souron et al., 2017a, 2017b). De plus, des études ont montré une augmentation inefficace de l'activité musculaire lorsque le sportif est soumis à des vibrations continues (Hintzy et al., 2019; Munera et al., 2017), avec pour conséquence une augmentation de la consommation d'oxygène (Rittweger et al., 2002).

Bien que les vibrations continues soient utilisées lors de protocoles d'entrainement spécifiques comme de la réathlétisation (Rittweger, 2010; Souron et al., 2017a), les résultats obtenus dans ces études permettent d'extrapoler leurs effets à ceux des vibrations transitoires rencontrées lors de la pratique sportive.

2.2.3 La vibration transitoire

La vibration induite par la pratique sportive est qualifiée de transitoire car une fois initiée, celle-ci est amortie (Khassetarash et al., 2015a). D'une manière générale, la vibration est provoquée lorsque deux structures rentrent en collision l'une avec l'autre. En course à pied, la vibration des tissus mous des membres inférieurs est initiée lors d'un freinage brusque du corps qui a lieu à chaque impact entre le pied et le sol. Dans le cas du tennis, un impact entre la balle et le tamis de la raquette provoque la vibration de la raquette, transmise au squelette et aux tissus mous du membre supérieur. Cet impact, représentant la source de la vibration, initie une onde de choc qui remonte le long des structures musculo-tendineuses et se propage aux tissus mous. La fréquence de l'impact étant proche de la fréquence propre des tissus mous, un phénomène de résonnance à lieu (Wakeling et al., 2003, 2002; Wang et al., 2007) et la vibration se retrouve amplifiée (Équation 3, Figure 4 et Figure 6). Cependant, l'organisme est capable de s'adapter grâce à des ajustements du système nerveux central qui peut modifier les activations musculaires afin d'améliorer l'amortissement de la vibration et de limiter son transfert (Jalali et al., 2019; Wakeling et al., 2003, 2002). Ce phénomène porte le nom de « muscle tuning » (Nigg & Wakeling, 2001) et permet de limiter l'amplitude de vibration et les potentiels effets néfastes associés.

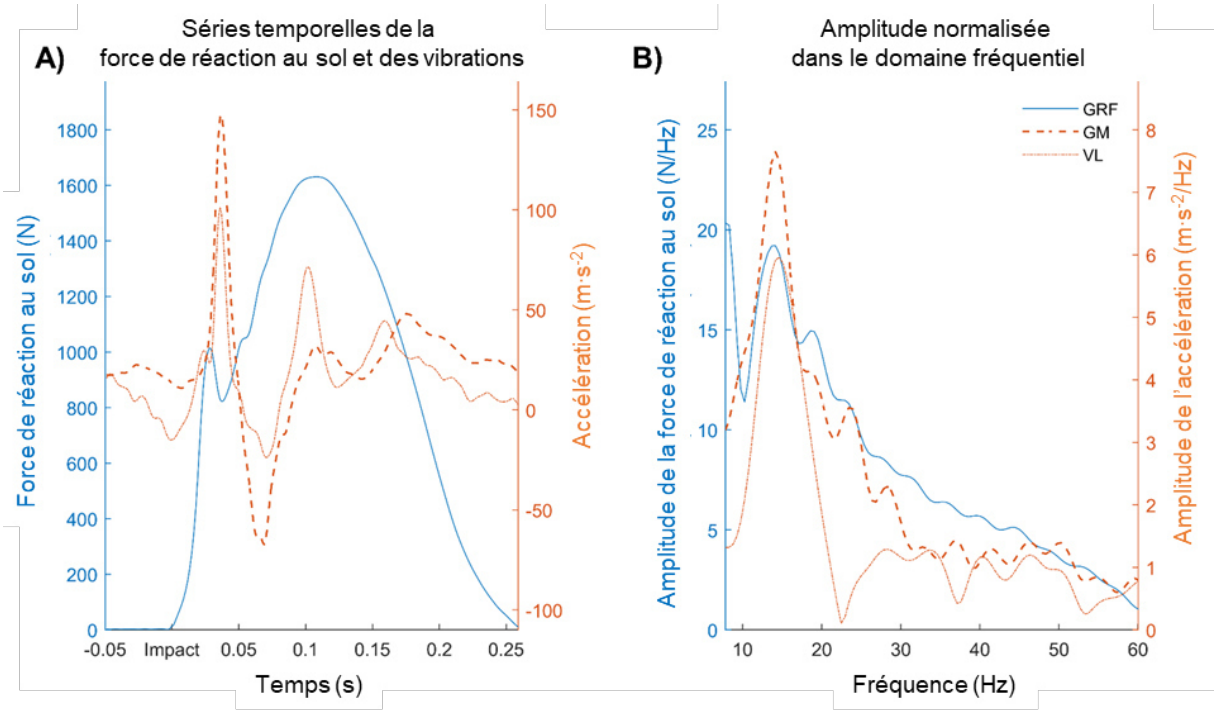

Figure 6 : A) Force de réaction au sol (GRF, bleu) et vibrations des tissus mous (orange) du gastrocnemius medialis (GM) et vastus lateralis (VL) dans le domaine temporel. Représentation des mêmes signaux dans le domaine fréquentiel. La synchronisation des pics montre le phénomène de résonance. Adapté de Trama, Play et al. (soumis).

2.2.3.1 Le « muscle tuning paradigm »

Un paradigme appelé "muscle tuning" a été proposé par Nigg et Wakeling afin de comprendre comment le système musculo-squelettique s'adaptait aux différents impacts entre le pied et le sol (Nigg, 2001, 1997; Nigg et al., 1987; Nigg & Liu, 1999; Wakeling & Nigg, 2001b). Ce paradigme suggère que les coureurs ajustent leurs activations musculaires avant le contact entre le pied et le sol, modifiant les angles et raideurs articulaires afin de minimiser l'amplitude des vibrations (Boyer, 2006; Boyer & Nigg, 2004). En effet, une augmentation de l'activation musculaire avant le contact pied-sol a été observée lors de conditions où la fréquence de l'impact était proche de la fréquence de résonnance des tissus mous (Boyer & Nigg, 2004; Wakeling et al., 2002). Cette pré-activation musculaire conduit à une amélioration de l'amortissement des vibrations et à une légère augmentation de la fréquence (Wakeling et al., 2002), cependant pas assez importante pour s'éloigner de la fréquence de l'impact (Figure 7). En d'autres termes, la stratégie employée par le système neuromusculaire pour réduire l'amplitude des vibrations est d'améliorer le coefficient d'amortissement, et non pas d'éloigner la fréquence de résonnance des tissus mous de celle de l'impact. Un mauvais ajustement des activations musculaires par le système

nerveux central (Jalali et al., 2019) entraine donc une augmentation de l'amplitude des vibrations (Boyer, 2006).

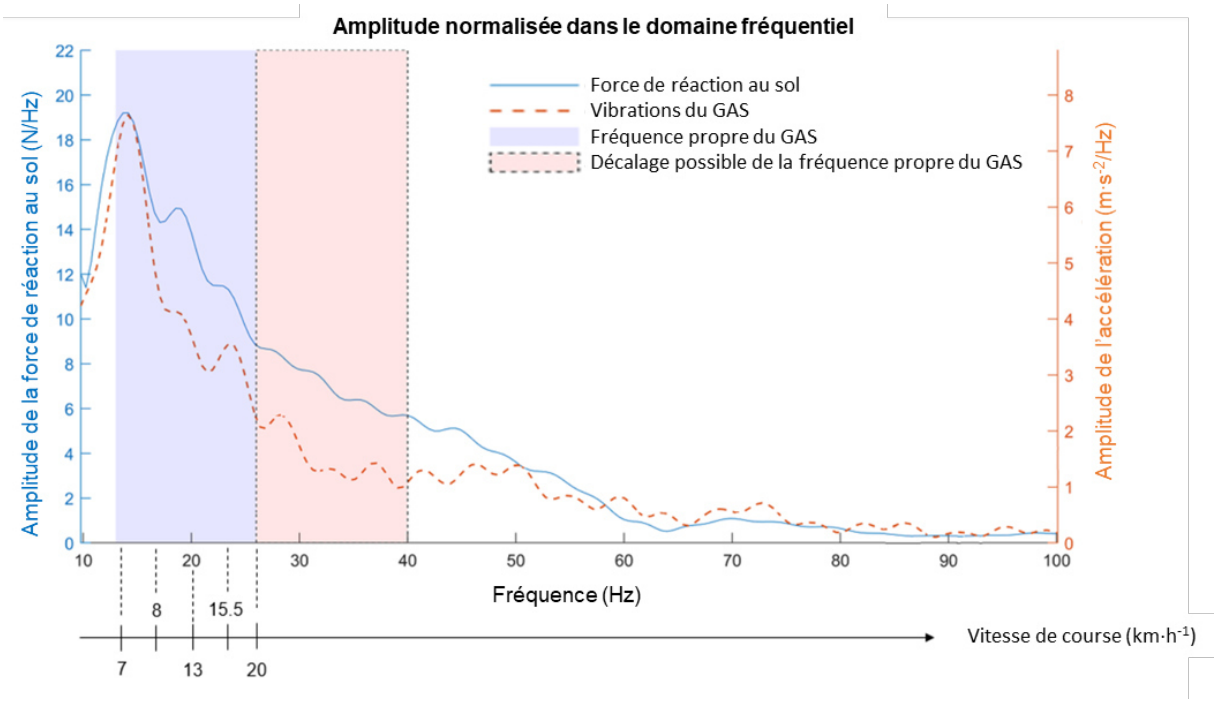

Figure 7 : Force de réaction au sol (bleu) et vibrations des tissus mous du gastrocnemius medialis (orange-GAS) dans le domaine fréquentiel. La zone bleu correspond à la fréquence propre du muscle (Martínez et al., 2019; Wakeling & Nigg, 2001b), ce qui coïncide avec les différentes fréquences d'impacts mesurées lors de la course à pied à différentes vitesses (Boyer & Nigg 2004; Trama et al. 2019). Le décalage de la fréquence propre du muscle n'est pas suffisante et coïncide toujours avec la fréquence de l'impact (Wakeling et al., 2002). Adapté de Trama, Play et al. (soumis).

2.2.3.2 Caractéristiques musculaires faisant varier les vibrations

2.2.3.2.1 Masses musculaires

Pour un impact donné, l'amplitude et la fréquence de la vibration sont inversement liées à la masse du système sur lequel la vibration est mesurée (Équation 1 et Équation 2, respectivement). Plus la masse est importante, moins l'amplitude et la fréquence sont élevées. Bien que ce postulat soit vrai pour une structure mécanique passive, celui-ci n'a pas été vérifié en course à pied puisqu'aucune étude expérimentale n'a fait le lien entre la masse du muscle, son amplitude de vibration et sa fréquence. Néanmoins, des amplitudes de vibrations plus importantes pour le *quadriceps* en comparaison au *triceps surae*, et des fréquences de vibration très proches entre le *quadriceps* et le *tibialis anterior* (Boyer & Nigg, 2004) ont été observées en course à pied. Bien que ces muscles soient de masses différentes, d'autres facteurs comme la proximité avec l'impact, les activations musculaires et les propriétés

mécaniques du muscle peuvent moduler ces caractéristiques vibratoires. Enfin, la masse locale, celle de l'accéléromètre et des tissus mous vibrant avec lui, pourrait être à considérer à la place de la masse du muscle et des tissus mous (Smeathers, 1989).

2.2.3.2.2 Raideur musculaire

La fréquence de vibration est proportionnelle à la raideur du système étudié (Équation 2). Sur un muscle, la fréquence est proportionnelle à la raideur de l'ensemble des tissus mous. Une étude récente a montré que des haltérophiles avaient une fréquence de vibration propre plus grande que des coureurs (Chen et al., 2020). Bien que d'autres facteurs puissent être avancés pour expliquer cette différence (e.g., moins de tissus adipeux, plus de pourcentage de fibres rapides), l'hypothèse la plus probable est celle d'une raideur musculaire accrue chez les haltérophiles.

2.2.3.2.3 Contraction musculaire

Sur un impact isolé, il a été montré que la contraction musculaire a pour effet d'augmenter la raideur des tissus mous par l'augmentation de la raideur musculaire, et par conséquent, d'augmenter la fréquence de la vibration (Équation 2), l'amortissement critique (Équation 4) et le coefficient d'amortissement (Wakeling & Nigg, 2001b). En course à pied, l'amplitude et la fréquence de l'impact étant modulées par les activations musculaires (Boyer, 2006; Boyer & Nigg, 2004), le lien entre la contraction musculaire et les caractéristiques de la vibration ne sont pas aussi évident.

2.2.3.3 Facteurs externes faisant varier les vibrations

2.2.3.3.1 Matériel sportif

2.2.3.3.1.1 Chaussures

Le marché de la chaussure de course est en évolution constante, avec des modes qui ne cessent de varier. Certaines marques mettent l'accent sur des chaussures avec des semelles très épaisses, dites maximalistes, tandis que d'autres prônent le retour au naturel avec des chaussures avec très peu d'amorti, dites minimalistes (Gellaerts et al., 2017). Ces deux extrêmes sont minoritaires tant la plupart des marques se situent entre les deux. Au-delà de faire varier l'épaisseur de la semelle, les marques proposent des matériaux viscoélastiques différents, ayant pour but d'amortir l'impact en augmentant la

viscosité (Éthylène-acétate de vinyle (EVA) ou autres technologies déposées) ou renvoyer de l'énergie en augmentant l'élasticité (polyuréthanes thermoplastiques (TPU) ou autres technologies déposées) (Giandolini et al., 2020). Faire varier les propriétés mécaniques de la semelle permet aussi de modifier la dureté (indice Asker C) de la chaussure (Boyer & Nigg, 2004; Nigg et al., 1987). Enfin, d'autres fabricants font varier la forme de la semelle, en proposant des semelles incurvées appelées « rocker » (Sobhani et al., 2016).

L'effet de ces différentes modifications est encore difficile à percevoir au niveau de la vibration des tissus mous bien que quelques tendances ont été mises en évidence. Une semelle plus épaisse ou plus visqueuse tend à réduire l'amplitude des vibrations mesurées pendant la course (Gellaerts et al., 2017; Giandolini et al., 2020), tandis que la modification de la dureté ne modifierait pas le comportement vibratoire (Boyer & Nigg, 2004).

Comme des modifications d'impacts et de vibrations variées ont été observées après la même modification de chaussure (c'est-à-dire des résultats spécifiques au sujet), le concept de groupes fonctionnels a été proposé. En effet, tous les individus ne présentent pas les même caractéristiques anthropométriques et musculaires. Certains individus entrainés en force peuvent présenter une raideur musculaire plus importante et avoir ainsi une fréquence propre de vibration plus importante (Chen et al., 2020), tandis qu'il existe des personnes capables d'amortir plus efficacement les vibrations que d'autres (Martínez et al., 2019). Un groupe fonctionnel est donc défini comme un groupe de sportifs réagissant de manière similaire à une intervention spécifique sur la chaussure (Hoerzer et al., 2015). Dans ce sens, le ressenti du coureur est essentiel. En effet, une chaussure diminuant l'amplitude de l'impact et de la vibration chez ce coureur aura tendance à être ressentie comme amortissante (coefficient de corrélation r<0.3) (Horvais et al., 2019).

2.2.3.3.1.2 Cuissard de compression

Les vêtements compressifs font maintenant partie intégrante de l'équipement du coureur, qu'il soit traileur ou coureur sur route. Ce type d'équipement a d'abord été développé pour être porté au niveau de la jambe pour faciliter le retour veineux à l'effort comme au repos. Le développement de cuissards ou de manchons adaptés à la cuisse est plus récent et leur adoption est encore faible, comme le montre

les chiffres sur une cohorte de 52 participants à l'UTMB 2019. En effet seulement 8% des coureurs en portaient alors que 25% avaient une compression au niveau des jambes (données non publiées).

L'effet des cuissards compressifs est très efficace (taille d'effet >0.8) pour diminuer l'amplitude de la vibration (Borràs et al., 2011; Broatch et al., 2019; Coza & Nigg, 2008; Ehrström et al., 2018; Fu et al., 2015; Gellaerts et al., 2017; Hintzy et al., 2019; Lussiana et al., 2015; Valle et al., 2013). Cet effet est expliqué par un maintien mécanique au niveau musculaire, permettant aussi d'accroitre l'amortissement de la vibration (Coza & Nigg, 2008; Fu et al., 2015).

D'autres effets protecteurs sont aussi à mettre en avant, comme la diminution des douleurs et des dommages musculaires (Borràs et al., 2011; Valle et al., 2013) ou la réduction des activations musculaires (Hintzy et al., 2019). Cependant, aucune donnée n'existe quant au lien entre l'altération de la fonction neuromusculaire et la diminution de l'amplitude de vibration.

2.2.3.3.1.3 Revêtement du sol

Il existe assez peu d'informations quant à l'effet du sol sur les vibrations des tissus mous. Une étude a montré qu'un sol plus dur entrainait une amplitude de vibration plus importante, résultat étant dû à un pic passif plus important (Boyer, 2006). Une autre étude se concentrant sur la force de réaction au sol sur l'axe antéro-postérieur a montré qu'un sol moins raide et « coulissant » permettait de réduire la vitesse de montée en force et la fréquence de l'impact (Chen et al., 2019). Cependant le lien entre la force de réaction au sol et la raideur du sol fait l'objet de controverses car certaines études ne reportent pas de changement du pic passif (Kerdok et al., 2002). Bien que la raideur du sol soit modifiée, la raideur effective du coureur reste inchangée, cela étant dû à une adaptation de la raideur de la jambe qui vient se compresser de manière plus importante (diminution de raideur) lorsque le sol est très raide (Kerdok et al., 2002). En conséquence, le sol sportif a un potentiel pour modifier la raideur de la jambe, et donc, les caractéristiques des vibrations des tissus mous (Boyer, 2006).

2.2.3.3.2 Fatigue neuromusculaire

Dans ce paragraphe, la fatigue est définie comme une incapacité temporaire d'un muscle à produire de la puissance (Bigland-Ritchie et al., 1978; Gandevia, 2001). Cette fatigue étant réversible avec le temps (récupération) et non chronique, ce facteur a été considéré comme externe au pratiquant.

Il a été démontré que les ajustements d'activités musculaires décrites par le muscle tuning se produisaient au niveau des muscles non fatigués (Wakeling et al., 2003; Wakeling & Nigg, 2001b). Différentes études ont montré que la fatigue entrainait une augmentation de l'amplitude de la vibration de 10 à 30% (Ehrström et al., 2018; Friesenbichler et al., 2011; Khassetarash et al., 2019, 2015a; Nikooyan & Zadpoor, 2012). Pour l'amortissement, deux études menées par Khassetarash et al. (2015a et 2019) ont montré un résultat inverse par rapport aux résultats d'un modèle informatique de Nikooyan et Zadpoor (2012), puisqu'une augmentation de 15 à 20% de l'amortissement a été constatée. Bien qu'il n'y ait pas d'explication claire à cette augmentation puisque l'activité musculaire n'a pas été modifiée, les auteurs ont spéculé que l'augmentation de l'amortissement pourrait être due à des changements dans les propriétés des composants passifs (c'est-à-dire non contractiles) de l'ensemble des tissus mous. Cependant, il convient de mentionner que les protocoles utilisés n'ont peut-être pas été assez longs pour induire une fatigue neuromusculaire importante et pour diminuer la capacité d'amortissement des muscles. Enfin, une seule étude a évalué l'effet de la fatigue sur la fréquence de vibrations, sans altération de celle-ci avec la fatigue (Friesenbichler et al., 2011).

2.3 MESURE DES VIBRATIONS

Une vibration est un phénomène mécanique qui correspond aux variations de vitesse d'un corps physique (i.e., son accélération), oscillant autour de sa position de repos (Piéron, 1935). La vibration est principalement quantifiée grâce à des accéléromètres (Wakeling & Nigg, 2001a), mais peut aussi être mesurée grâce des marqueurs réfléchissants et des caméras haute fréquence (Coza et al., 2010), ou de l'échographie ultra-rapide (Yamada et al., 2018).

2.3.1 Mesure par accéléromètre

Les accéléromètres sont des capteurs permettant de quantifier l'accélération linéaire d'un corps. Bien que l'unité du système international soit le $m \cdot s^{-2}$, la plupart des capteurs mesurent le signal en g, correspondant à l'accélération causée par l'attraction terrestre environ égale à 9.81 $m \cdot s^{-2}$. Lorsque ces capteurs sont utilisés, il faut donc prendre en considération l'accélération de la pesanteur. La pesanteur étant une force constante, il est nécessaire d'utiliser un filtre passe-haut pour enlever les basses fréquences du signal ou des capteurs prenant en considération l'effet de la force de gravité.

La position de l'accéléromètre a elle aussi une importance car l'amplitude de la vibration est réduite au fur et à mesure que l'on s'éloigne de son site d'initiation, c'est-à-dire en remontant vers la partie proximale du segment lorsque l'impact est initié au niveau du pied (Boyer & Nigg, 2006; Lucas-Cuevas et al., 2017). Cependant, il n'existe pas de consigne fixe pour positionner de manière reproductible les accéléromètres. Nous retrouvons donc des placements légèrement différents entre les études, bien que la partie proéminente du chef musculaire étudié, proche des électrodes d'électromyographie si utilisées conjointement, soit souvent préconisée comme site de fixation (Boyer & Nigg, 2007a). Il est donc essentiel de marquer la localisation du capteur si des mesures répétées sont effectuées. De plus, les accéléromètres peuvent être utilisés pour quantifier l'impact au sol (Boyer & Nigg, 2007b). Pour cela, le capteur est placé au niveau du talon, sur la peau ou sur la tige postérieure de la chaussure.

Pour fixer le capteur sur la peau, de la colle médicale ou du scotch double face peuvent être utilisés. Cependant, la fixation des accéléromètres est souvent renforcée grâce à des bandes collantes de type straps ou autres tissus venant envelopper le membre sur lequel l'accéléromètre est fixé. Cette procédure

a pour effet de venir comprimer la jambe et peut avoir un effet sur le signal vibratoire (Lussiana et al., 2015). Il est donc conseillé d'appliquer la même pression lors que la mesure est répétée, et si possible de la vérifier à l'aide de capteurs de pression. Pour fixer le capteur au niveau du talon la même méthodologie peut être employée, ou des systèmes de fixations supplémentaires où l'accéléromètre est encastré peuvent aussi être utilisés pour assurer un meilleur maintien (Giandolini et al., 2015).

Les accéléromètres permettent un échantillonnage des données à de hautes fréquences, généralement supérieures à 1000 Hz. La vibration des tissus mous étant majoritairement composée de fréquences inférieures à 130 Hz (Khassetarash et al., 2015a), cette fréquence d'échantillonnage est suffisante. Cependant, certains capteurs, notamment lorsque intégrés à des électrodes d'électromyographie, peuvent avoir des fréquences de l'ordre de 150 Hz (Gellaerts et al., 2017). Bien que cette fréquence d'échantillonnage permette d'analyser des signaux oscillant à une fréquence allant jusqu'à 75 Hz selon le théorème de Nyquist-Shannon, et d'avoir une estimation correcte de la fréquence principale de la vibration (Wakeling et al., 2002), une fréquence d'au moins 500 Hz semble nécessaire pour pouvoir analyser de plus hautes fréquences (Enders et al., 2012).

Il existe parmi ces capteurs des modèles uni-axiaux ou tri-axiaux. Le premier type de capteur peut être par exemple employé pour de la détection d'évènements, comme un impact au sol (Khassetarash et al., 2019), tandis que les seconds seront préférés pour la caractérisation de la vibration. Cependant, même avec des capteurs tri-axiaux, certains auteurs se sont focalisés sur l'analyse de l'accélération sur l'axe colinéaire à l'axe longitudinal de la structure étudiée (Wakeling & Nigg 2001a; Boyer & Nigg 2004; Enders et al. 2012; Khassetarash, Hassannejad, Enders, et al. 2015; Trama et al. 2019; Giandolini et al. 2020). Lorsque plusieurs axes sont analysés, une analyse indépendante (Giandolini et al., 2019) ou de la norme des axes, aussi appelée accélération résultante (Ehrström et al., 2018), peut être effectuée. Lors de l'analyse d'un ou plusieurs axes de manière indépendante, un alignement sur les segments corporels est nécessaire, tandis que l'analyse de la norme du signal peut se faire sans alignement particulier car elle considère les trois axes simultanément.

La masse de l'accéléromètre peut, elle aussi, avoir un effet sur le signal vibratoire. En effet, si la masse de l'accéléromètre est trop importante par rapport à la masse du muscle étudié, le capteur peut avoir une

incidence forte sur le signal recueilli (Smeathers, 1989). Les avancées technologiques permettent l'utilisation d'accéléromètres pesant moins de 5 grammes limitant ainsi fortement les effets néfastes de la masse de l'accéléromètre sur le signal vibratoire (Figure 8).

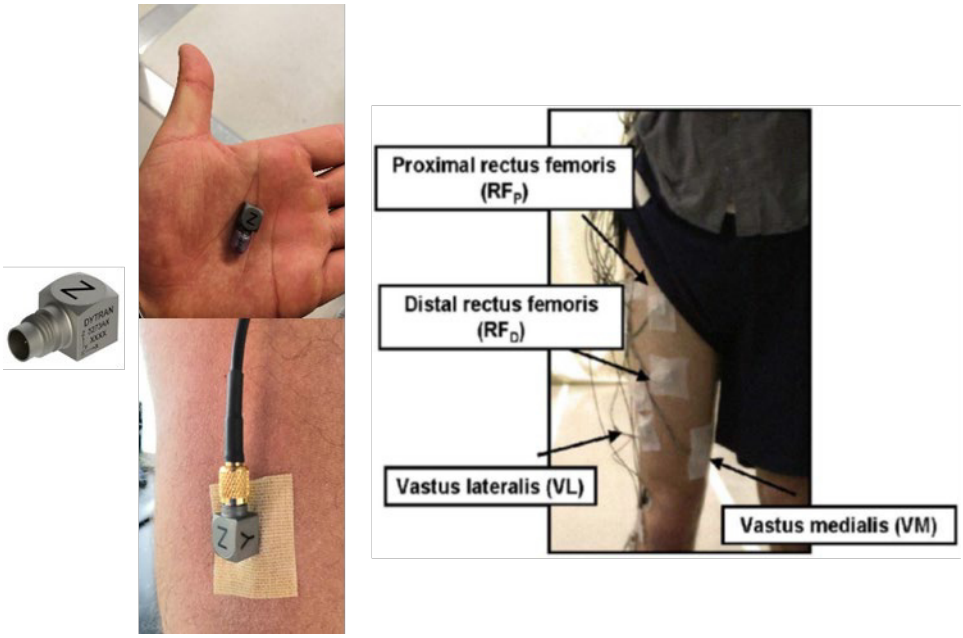

Figure 8 : Exemple d'un accéléromètre tri-axial léger (≈2.7 grammes) et compact (≈1.08 cm^3) à gauche et positionnement de différents accéléromètres sur la cuisse (à droite). Tiré de Boyer and Nigg (2006).

2.3.2 Mesure par caméra haute fréquence

La mesure par caméra haute fréquence se fait en suivant la position d'un marqueur sphérique (Borràs et al., 2011; Broatch et al., 2019) ou d'un marqueur en forme de « L » fixé sur la peau (Coza et al., 2010) (Figure 9) grâce à plusieurs caméras optoélectroniques. Le suivi de la trajectoire de ces marqueurs se fait avec une erreur résiduelle inférieure à quelques millimètres (Borràs et al., 2011). La fréquence d'acquisition est limitée à quelques centaines de Hertz, limitant les chercheurs utilisant cette technologie à des fréquences d'acquisition allant de 200 à 500 Hz (Borràs et al., 2011; Broatch et al., 2019; Coza et al., 2010). Une limite majeure de cette méthode réside dans son caractère non ambulatoire. Bien que son utilisation soit possible lors de course à pied sur tapis avec une zone de mesure restreinte, l'étude de mouvements nécessitant un déplacement important ou une mesure écologique sont impossibles (Giandolini et al., 2015). Cette méthode est limitée en termes de fréquence d'acquisition et de déplacement, et reste donc marginalement utilisée.

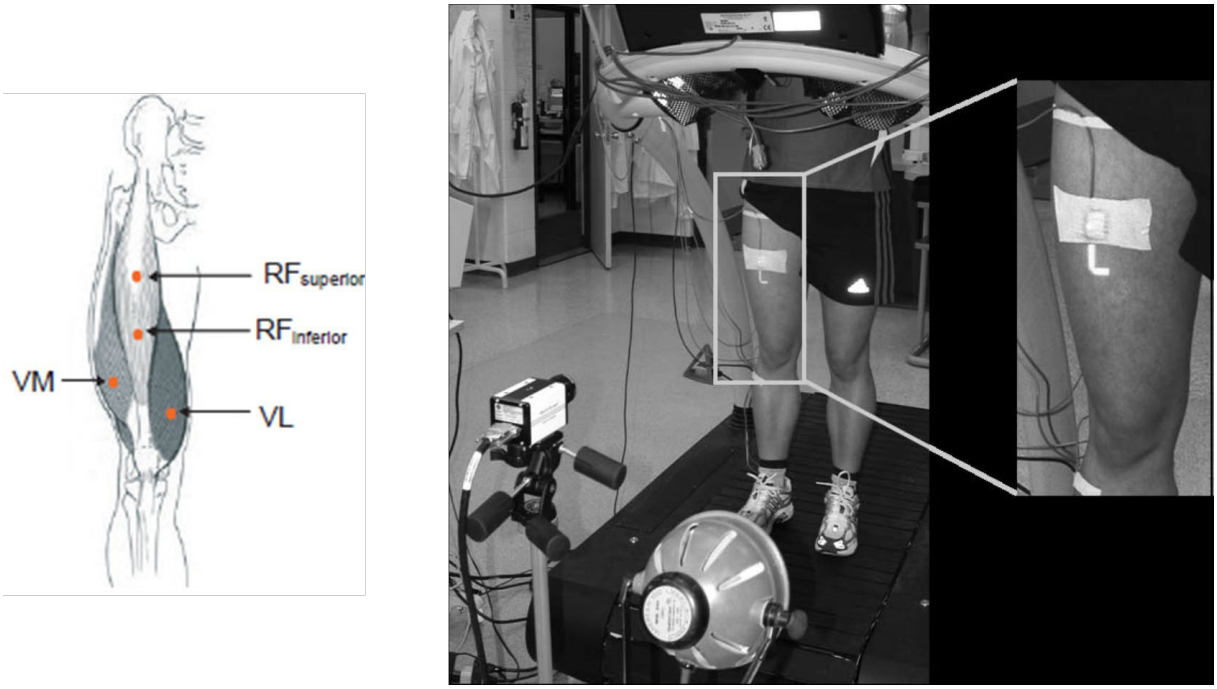

Figure 9 : Matériel utilisé pour mesurer conjointement la vibration à l'aide d'un accéléromètre et de vidéo à haute fréquence. Gauche : Position des marqueurs sphériques utilisés par Borràs et al. (2011) et droite : Marqueur en forme de « L » utilisé par Coza et al. (2010).

2.3.3 Mesure par échographe ultra-rapide

Un échographe est une machine envoyant et réceptionnant des ultrasons à travers une sonde, et permet d'étudier directement le tissu musculaire profond. Le mode B des échographes permet d'obtenir des images et des vidéos du muscle, cependant, les fréquences d'acquisitions maximales de 100 Hz ne suffisent pas pour caractériser correctement le déplacement rapide du muscle lorsqu'il est soumis à un choc. Bien qu'une étude ait utilisé une fréquence de 80 Hz pour caractériser la vibration musculaire (Lai & Hodson-Tole, 2020), certains échographes disposent depuis 2009 d'un mode ultra-rapide permettant d'obtenir des vidéos avec une fréquence d'échantillonnage allant jusqu'à 20 000 Hz (Bercoff, 2011). D'un point de vue technique, l'échographe ultra-rapide est capable d'utiliser simultanément tous les émetteurs et récepteurs d'ultrasons de la sonde, alors qu'une acquisition en mode B utilise ces capteurs en série. Les désavantages de cette technique sont que la durée d'une vidéo est de quelques secondes au maximum, demandant parfois plusieurs essais pour acquérir la vibration dans son intégralité. Ce désavantage est accentué par le fait que l'image ne soit pas visualisable en temps réel, requérant un traitement ultérieur. De plus, la qualité de la vidéo est légèrement dégradée par rapport à une vidéo obtenue en mode B, et la distance entre deux pixels est d'un à deux millimètres (256 x 180 pixels pour

un champ de vue de 5 x 2.5 cm). Néanmoins, les vidéos ultra-rapides couplées avec un algorithme de suivi de points permettent de retrouver le déplacement des structures musculaires soumises à une vibration (Figure 10) (Lai & Hodson-Tole, 2020; Yamada et al., 2018). Cette méthode permettant d'analyser la vibration du muscle uniquement, et non de tous les tissus mous comme pour les accéléromètres et les caméras, est prometteuse. Cependant, certaines limites comme sa mobilité (bien que des échographes portables existent, la technologie ultra-rapide n'est pas disponible sur ceux-ci), la complexité du suivi d'image ou la prise en compte du mouvement relatif de la sonde en font une méthode en développement mais encore peu utilisée dans l'étude des vibrations.

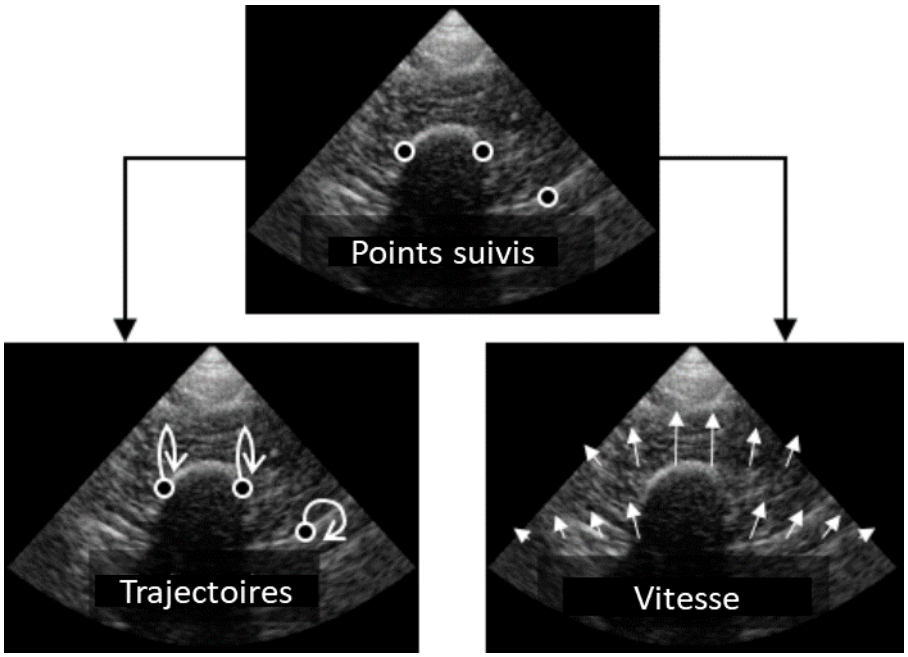

Figure 10 : Suivi de la trajectoire de différents points d'intérêts au niveau musculaire grâce à de l'échographie ultra-rapide. Adapté de Yamada et al. (2018).

2.4 TRAITEMENT DU SIGNAL VIBRATOIRE

2.4.1 Filtrage du signal

Lors de mouvements humains, les accéléromètres enregistrent aussi bien la vibration que le mouvement du squelette. Le mouvement étant à des fréquences inférieures à 10 Hz, un filtre passe haut est généralement appliqué pour s'affranchir de ce bruit nuisible à la caractérisation de la vibration. De plus, un bruit dû à certains systèmes de fixations à base de bois ont conduit les chercheurs à filtrer le signal avec un filtre passe bas à 50 ou 60 Hz (Shorten & Winslow, 1992). Lors d'une analyse fréquentielle ou temps-fréquence, ces filtres ont moins d'importance car l'analyse du signal permet de dissocier le mouvement et le bruit à haute fréquence de la vibration en elle-même. Par exemple, il est possible de calculer uniquement l'énergie de la vibration en prenant l'énergie se trouvant entre 10 et 50 Hz (Giandolini et al., 2020). Cependant, lors d'une analyse temporelle ou d'une modélisation de la vibration, ces filtres sont essentiels pour ne pas biaiser l'analyse.

2.4.2 Analyse temporelle

L'analyse temporelle se base uniquement sur la représentation temporelle du signal brut ou filtré de la vibration recueillie (Figure 11). Les différents paramètres d'amplitudes correspondent à l'accélération pic ou à l'amplitude pic à pic (Boyer & Nigg, 2004; Nikooyan & Zadpoor, 2012), à la déviation standard du signal (Gellaerts et al., 2017) ou à la valeur moyenne quadratique (root mean square, rms) du signal (Ehrström et al., 2018). La fréquence dominante de la vibration est calculée comme la valeur inverse du double de la période entre deux pics successifs (Boyer & Nigg, 2004) . Ce type d'analyse peut permettre d'estimer le coefficient d'amortissement grâce à l'enveloppe du signal, mais n'a été utilisé que sur des modes spécifiques de vibrations (Khassetarash et al., 2015a).

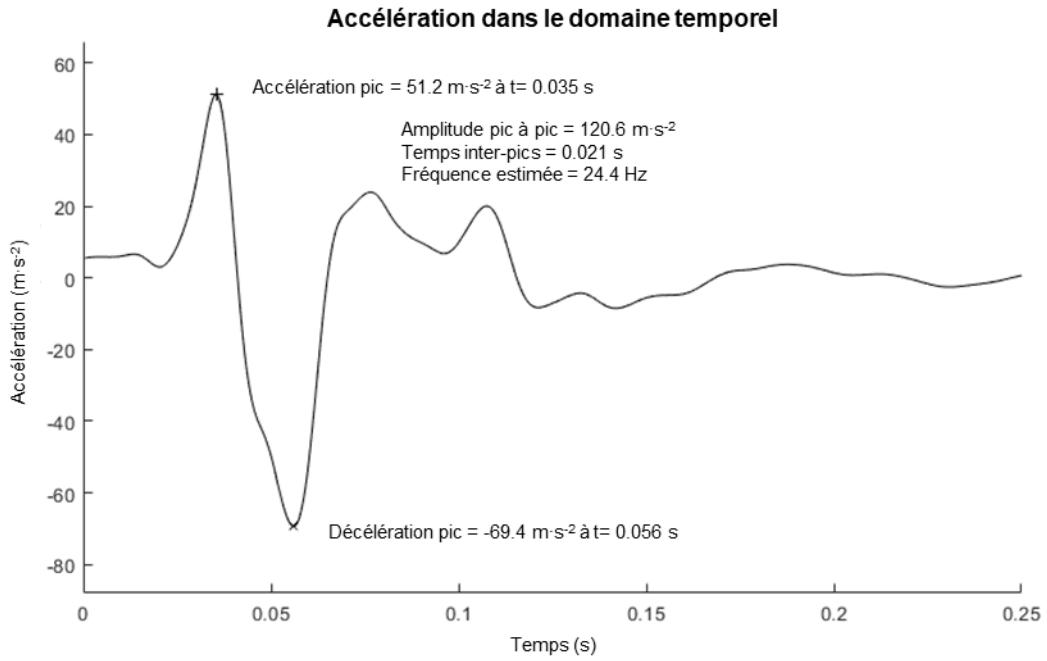

Figure 11 : Analyse temporelle d'un signal de vibration.

2.4.3 Analyse fréquentielle par transformée de Fourier rapide

La transformée de Fourier rapide (Équation 6), transforme le signal en somme de fonctions sinus d'amplitudes données (Figure 12). Cet algorithme permet de calculer le spectre fréquentiel (transformé de Fourier discrète), et d'en extraire des informations comme la fréquence principale (fréquence avec le plus d'amplitude), médiane et moyenne (Figure 13). Certains paramètres d'amplitude comme l'amplitude pic ou l'air sous la courbe peuvent aussi être calculés. Cette analyse permet donc de comparer le contenu fréquentiel de différents signaux, cependant, la notion de temporalité est perdue.

$$S(k) = \sum_{n=0}^{N-1} s(n) e^{-2i\pi k \frac{n}{N}}, \text{pour } 0 \leq k < N$$

Équation 6

avec S(k) la transformée de Fourier discrète obtenue avec une transformée de Fourier rapide d'un signal s de N d'échantillons.

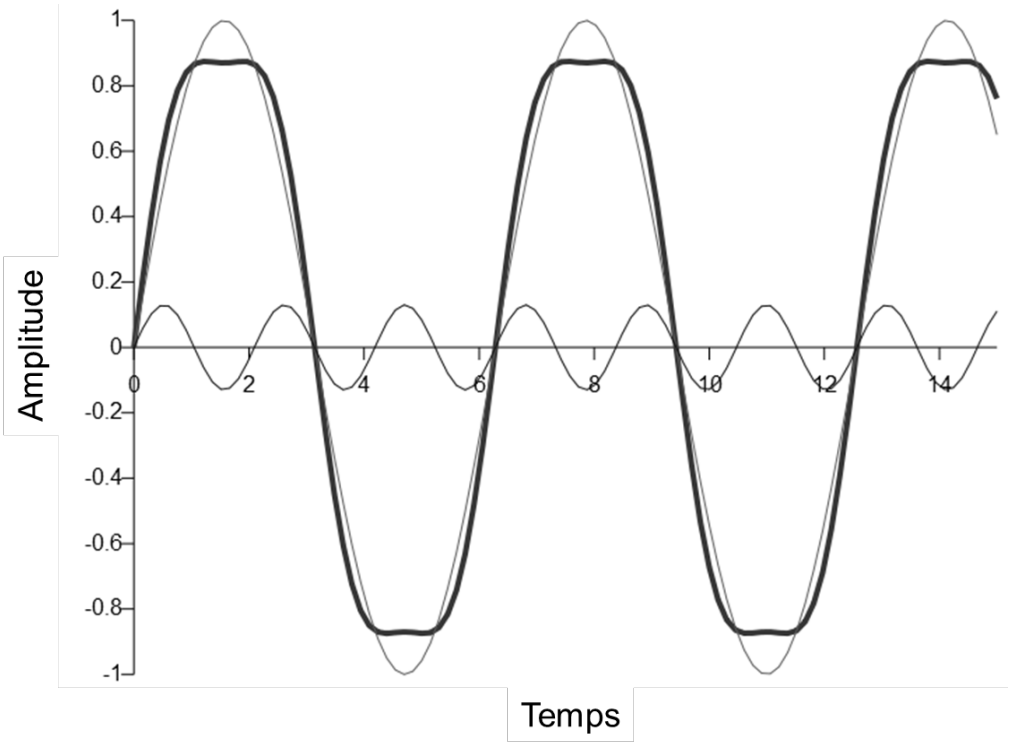

Figure 12 : Illustration de la transformée de Fourier rapide. Le signal en tracé épais est décomposé en deux sinus de fréquences différentes (tracés fins).

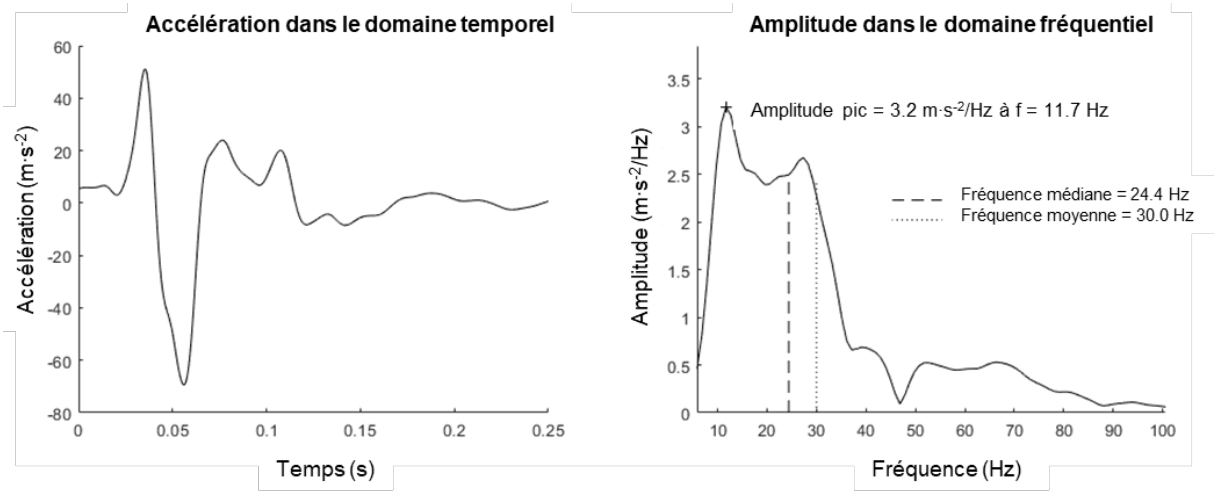

Figure 13 : Signal dans le domaine temporel et son spectre fréquentiel obtenu après une transformée de Fourier rapide.

2.4.4 Modélisation

Un signal vibratoire composé d'une seule fréquence amortie peut être modélisé suivant l'Équation 7 (Fu et al., 2015; Wakeling & Nigg, 2001b). Cette modélisation est effectuée en optimisant les paramètres d'amplitude, fréquence et amortissement pour que le signal modélisé soit le plus proche du signal mesuré.

$$s(t) = \alpha e^{-ct} \sin(2\pi f t + \rho), \qquad \text{Équation 7}$$

avec s(t) le signal en fonction du temps, α l'amplitude maximale du signal, c le coefficient d'amortissement, f la fréquence du signal et ρ le coefficient de phase temporelle.

Bien que cette modélisation permette d'obtenir tous les paramètres de la vibration, elle requiert un second découpage du signal au niveau du premier pic (Figure 14) ou en prenant la vibration « libre » après 50 millisecondes (Wakeling & Nigg, 2001b). De plus, cette méthode est limitée à une seule fréquence, ce qui n'est pas le cas de la vibration dans le corps humain où la vibration est composée de plusieurs fréquences distinctes.

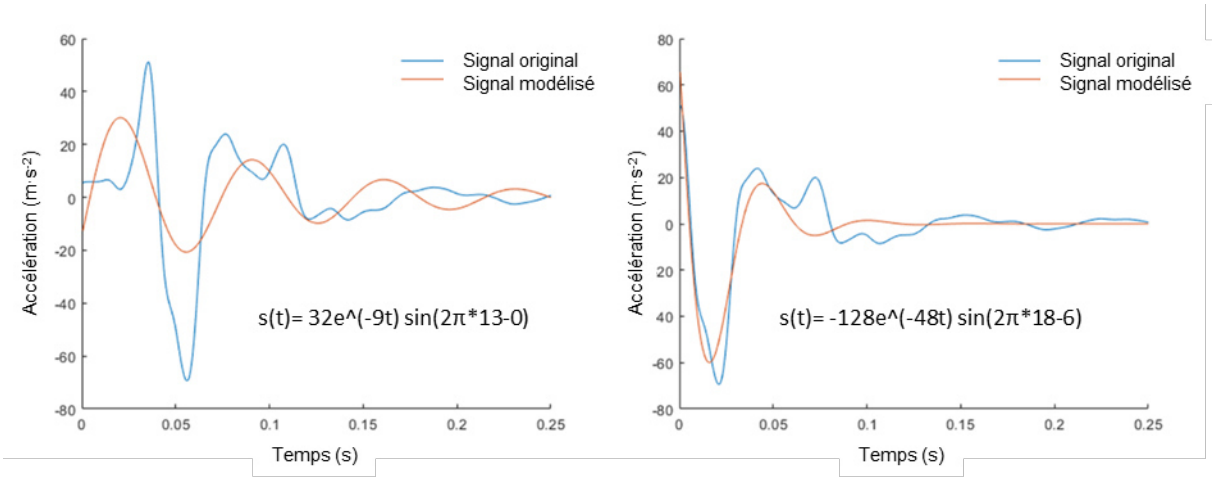

Figure 14 : Modélisation du signal temporel sous forme d'un sinus amorti en découpant le signal au niveau de l'impact au sol (gauche) ou au niveau du premier pic (droite). Dans le second cas, le signal à une amplitude de -128 m·s^{-2}, une fréquence de 18 Hz, et un coefficient d'amortissement de -48 s^{-1}.

2.4.5 Analyse temps-fréquence

Chacune des méthodes présentées ci-dessus présentent des faiblesses évidentes dues aux caractères multimodal (i.e., le signal est composé de différentes fréquences) et non stationnaire (i.e., le signal ne se répète pas dans le temps de manière identique, il est amorti) du signal vibratoire. En conséquence, la méthode temporelle estime uniquement la fréquence au moment des pics et ne permet pas le calcul de l'amortissement, la modélisation est limitée à un signal unimodale, tandis que l'analyse fréquentielle par transformé de Fourier enlève toutes les données temporelles tout en étant peu adapté à un signal non stationnaire.

C’est pour cela que les chercheurs se sont tournés vers des méthodes d’analyse temps-fréquence permettant de répondre aux caractéristiques multimodale et non stationnaire du signal vibratoire (Enders et al., 2012; Khassetarash et al., 2015a).

2.4.5.1 Transformée en ondelettes continue

2.4.5.1.1 Principes généraux

La transformée en ondelettes continue est un type d’analyse temps-fréquence consistant en une convolution (i.e., multiplication point par point) du signal avec une ondelette fille à chaque échantillon de temps du signal d’origine (Équation 8). Le produit de convolution, aussi appelé coefficient d’ondelettes, représente l’adéquation entre le signal et l’ondelette à chaque échantillon du signal grâce au paramètre β. Si ce coefficient est important la vibration est, à ce moment donné, à la fréquence de l’ondelette utilisée. A l’inverse, si le coefficient est faible, la vibration n’est pas à cette fréquence à ce moment donné (Figure 15).

$$Wf(\alpha,\beta) = \int_{-\infty}^{+\infty} f(x) * \psi_{\alpha,\beta}\,, \text{pour } \alpha > 0 \text{ et } \beta \in \mathbb{R} \qquad \textit{Équation 8}$$

*avec $Wf(\alpha,\beta)$ le coefficient d’ondelettes pour le facteur de dilatation α et de translation β, f(x) le signal mesuré, * le symbole de convolution, $\psi_{\alpha,\beta}$ l’ondelette fille.*

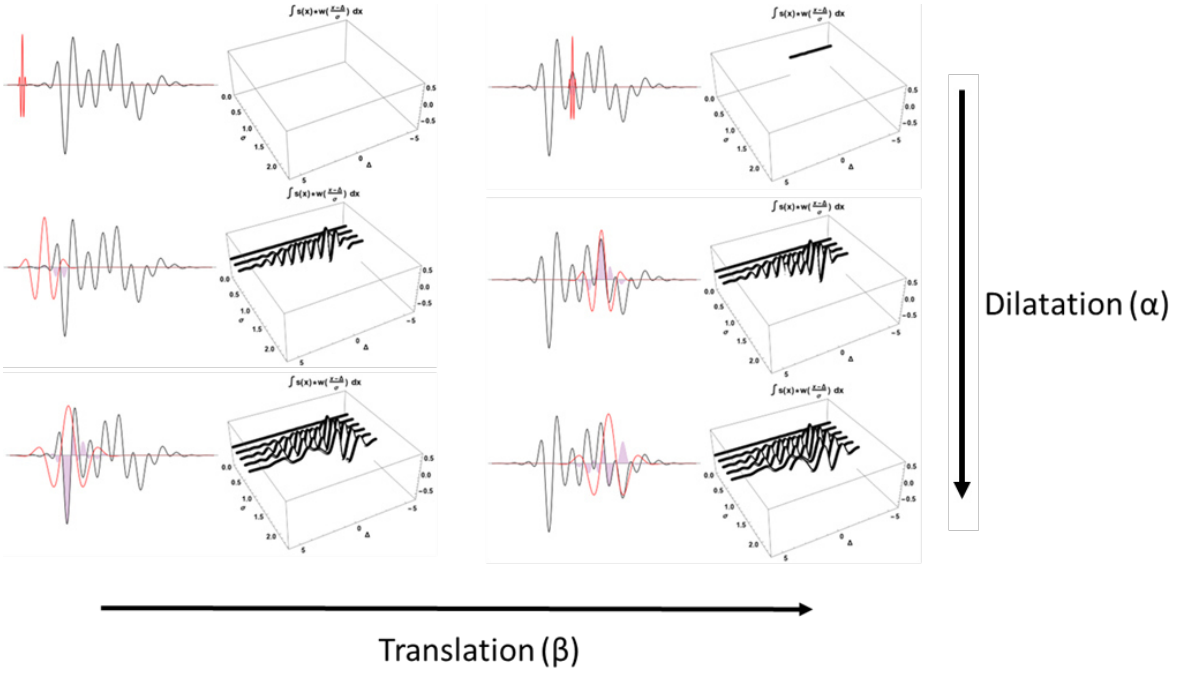

Figure 15 : Exemple de translation et dilatation lors d'une transformée en ondelettes continue. L'intégrale de la zone grise, correspondant à la convolution de l'ondelette fille (rouge) et du signal (noir), est reportée sur la carte de droite, à la fréquence donnée par α et au temps donnée par β.

Chaque ondelette est dérivée d'une ondelette mère en la compressant (augmentant sa fréquence) ou la dilatant (diminuant sa fréquence) grâce au paramètre de dilatation α. Chaque ondelette est donc définie dans le temps et possède donc une résolution temporelle et fréquentielle dépendantes de α. Plus l'ondelette sera dilatée, plus elle permettra de repérer des basses fréquences, plus sa résolution fréquentielle sera élevée, et moins sa résolution temporelle le sera. A l'inverse, plus l'ondelette sera compressée, plus elle permettra de repérer des hautes fréquences, plus sa résolution temporelle sera élevée, et moins sa résolution fréquentielle le sera. Donc plus la résolution fréquentielle est importante, moins la résolution temporelle l'est, c'est le compromis temps-fréquence (Figure 16).

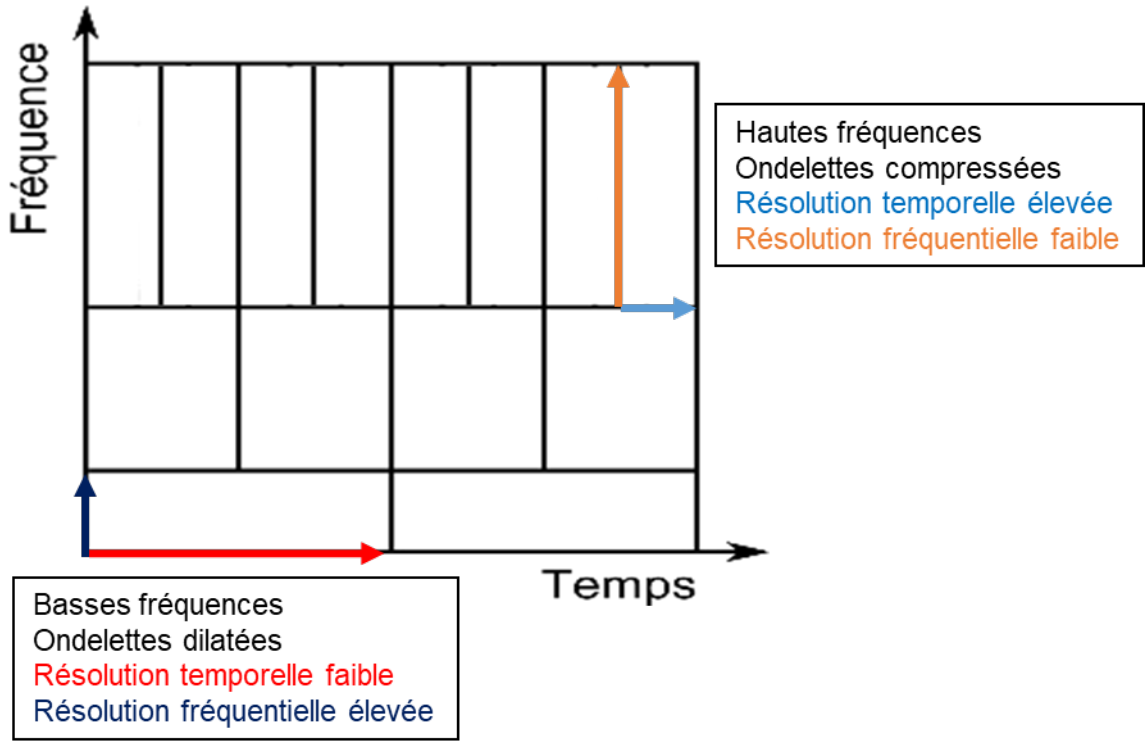

Figure 16 : Pavage temps-fréquence de l'analyse en ondelette. Les basses fréquences sont bien définies dans le domaine fréquentiel et moins bien dans le domaine temporel alors que l'inverse est rencontré pour les hautes fréquences.

En appliquant cette méthode sur le signal d'accélération, il est donc possible d'obtenir une carte temps-fréquence des coefficients d'ondelettes (Figure 17). Nous voyons sur cette figure que l'amplitude du signal est importante jusqu'à 0.25 secondes après l'impact à une fréquence de 11 Hz, durant 0,12 secondes à des fréquences comprises entre 25 et 30 Hz, et entre 0,03 et 0,06 secondes entre 60 et 80 Hz. Cette analyse permet donc de prendre en considération à la fois la temporalité et la fréquence de la vibration.

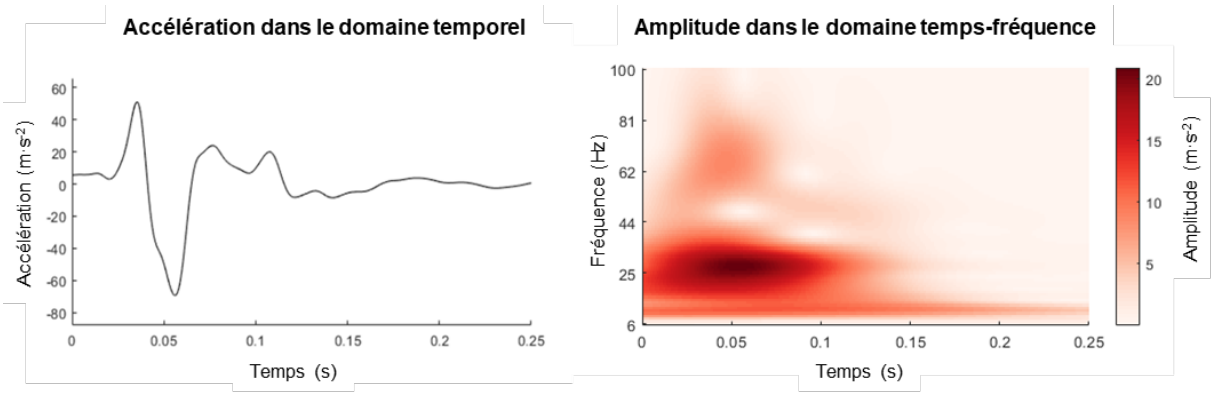

Figure 17 : Exemple d'une transformée en ondelettes continue sur un signal d'accélération. La carte à droite représente les coefficients d'ondelettes.

Il est ensuite possible de revenir à une représentation temporelle (Équation 9) pour calculer l'amortissement (Figure 18) ou fréquentielle (Équation 10) pour calculer les indicateurs de fréquence (Figure 18).

$$P(t) = \int_{f_{min}}^{f_{max}} p(t,f)df, \qquad \text{Équation 9}$$

avec P(t) l'énergie en fonction du temps t, p(t,f) le coefficient d'ondelettes au temps t et à la fréquence f, f allant de f_{min} à f_{max}.

$$P(f) = \int_{t_0}^{t_{max}} p(t,f)dt, \qquad \text{Équation 10}$$

avec P(f) l'énergie en fonction de la fréquence f, p(t,f) le coefficient d'ondelettes à la fréquence f et au temps t, t_{max} étant la durée du signal.

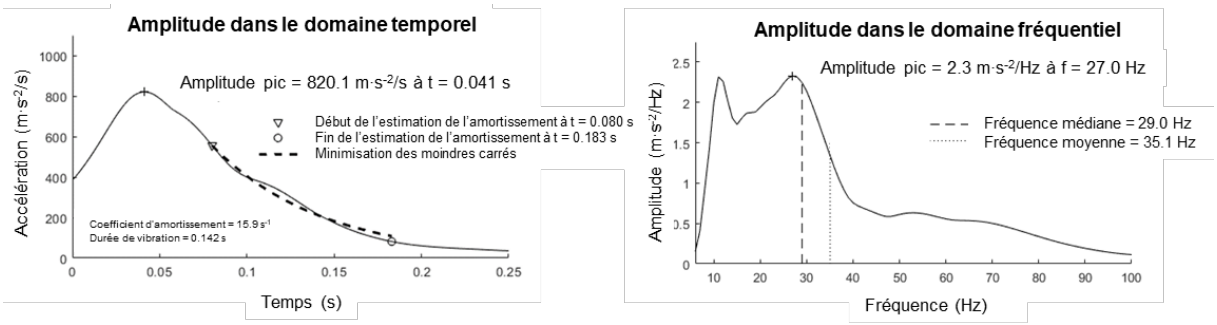

Figure 18 : Amplitude totale du signal dans le domaine temporel avec calcul de l'amortissement (gauche), et spectre fréquentiel avec calcul des fréquences d'intérêt (droite).

Ici, l'amortissement est calculé avec une optimisation du coefficient d'amortissement (c) afin que l'erreur entre la décroissance du signal et une décroissance exponentielle soit minimale (Équation 11).

$$min\left(\sum_{t=T1}^{T2}(P_{T1}\cdot e^{-c\cdot t} - P(t))^2\right), \qquad \text{Équation 11}$$

avec T1 l'instant auquel la décroissance est maximale, P_{T1} la puissance à t=T1, T2 l'instant où la puissance atteint 10% de P_{T1}, $P(t)$ le signal mesuré et $P_{T1}\cdot e^{-c\cdot t}$ la décroissance théorique du signal.

2.4.5.1.2 Choix de l'ondelette mère

Comme décrit ci-dessus, les ondelettes sont toutes dérivées d'une ondelette mère ayant des caractéristiques bien précises. Il existe plusieurs dizaines de familles d'ondelettes mères, avec plusieurs

dizaines d'ondelettes dérivées faisant partie de la même famille, qui peuvent être réelles ou aussi comporter une partie imaginaire. Une méthode a été développée pour choisir la meilleure ondelette mère afin de d'enlever le bruit d'un signal (Phinyomark et al., 2009), cependant, son application à l'analyse du signal en tant que telle n'est pas nécessairement obligatoire.

Une « super famille » d'ondelettes analytiques, lui permettant d'obtenir des valeurs d'amplitude nulles dans les fréquences négatives, se nommant Morse a été développée (Lilly & Olhede, 2012, 2009). La caractéristique analytique de cette famille est intéressante car elle permet de retranscrire à l'identique l'amplitude du signal. Dans ce sens, si une oscillation à une amplitude de de 1 $m \cdot s^{-2}$, le coefficient d'ondelettes sera lui aussi de 1 $m \cdot s^{-2}$. De plus, deux caractéristiques permettent de moduler soit son type (pour passer d'une ondelette Morse à Cauchy par exemple), soit le rapport de la résolution temps-fréquence (Figure 19). Ces différents choix ont un impact direct sur l'estimation des fréquences, mais aussi et surtout de l'amortissement du signal vibratoire.

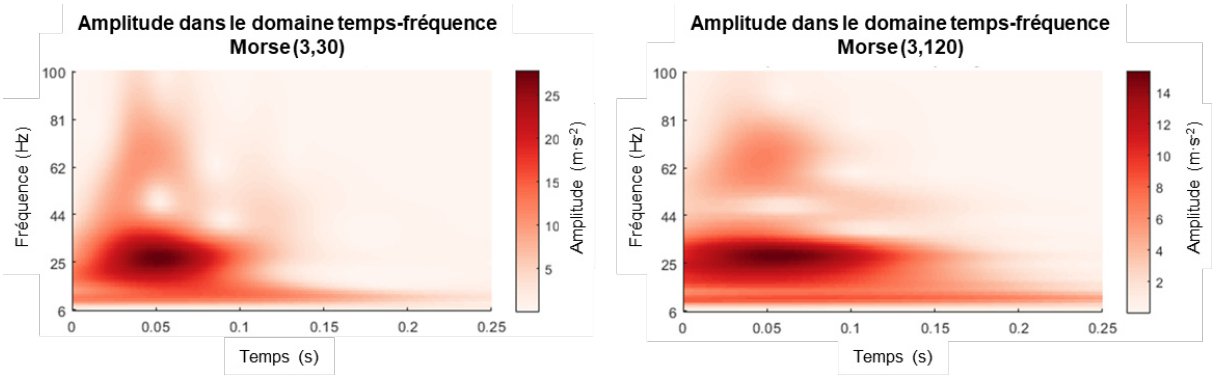

Figure 19 : Transformée en ondelettes continue du même signal avec la même famille d'ondelette (Morse), avec une meilleure localisation temporelle (gauche) ou fréquentielle (droite).

2.4.5.2 Décomposition en modes intrinsèques

La décomposition en modes intrinsèques est une méthode d'analyse temps-fréquence qui s'affranchit du choix de l'ondelette mère (Khassetarash et al., 2015a). En effet, cette méthode utilise la forme du signal comme base de décomposition, ce qui a pour effet d'avoir une forme adaptée à chaque signal analysé (Figure 20). Cependant, le nombre et la fréquence des modes varient d'un signal à l'autre, ce qui demande d'interpréter les résultats modes par modes et non pas par fréquences (Khassetarash et al., 2015a). De plus, une analyse supplémentaire est nécessaire pour obtenir l'amortissement ou la fréquence

de chaque mode. Une transformée de Fourier rapide est généralement réalisée pour obtenir la fréquence principale de chaque mode alors qu'une analyse temporelle permet d'estimer l'amortissement de chaque mode. Ainsi, la fréquence et l'amortissement total du signal sont estimés par ces deux mêmes méthodes sur le signal complet.

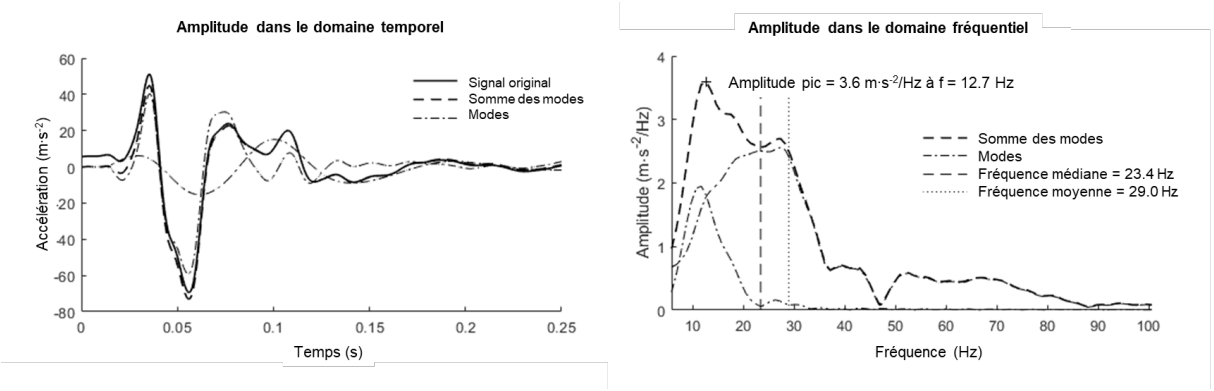

Figure 20 : Décomposition en modes intrinsèques (gauche) et transformée de Fourier rapide des différents modes (droite). Ici, le signal est composé de deux modes distincts.

3 OBJECTIFS DE LA THESE

La littérature sur l'étude des vibrations dans la pratique sportive est vaste, multidisciplinaire et hétérogène. En effet, celle-ci elle concerne aussi bien l'influence de différents matériels (Blache et al., 2017; Boyer & Nigg, 2004; Chadefaux et al., 2016; Ehrström et al., 2018; Giandolini et al., 2020; Manin et al., 2012), que l'effet de la fatigue (Ehrström et al., 2018; Friesenbichler et al., 2011; Khassetarash et al., 2019, 2015a; Nikooyan & Zadpoor, 2012) ou encore des interactions avec l'activité musculaire (Wakeling et al., 2003; Wakeling & Nigg, 2001b). Les différents paramètres décrits pour caractériser les vibrations manquent d'uniformisation car les approches pour traiter le signal et l'analyser ont été multiples. La principale explication serait que l'étude des vibrations n'est pas exclusif au domaine sportif, et les études venant de champs disciplinaires comme les sciences de l'ingénieur et des matériaux apportent leur propres moyens d'analyse (Manin et al., 2012). De plus, les différentes avancées dans le traitement du signal (Enders et al., 2012) et des statistiques (Pataky, 2010) appliquées au domaine sportif ont encore multiplié le nombre d'approches. En parallèle, les évolutions dans le domaine de l'imagerie médicale, notamment les échographes ultra-rapides, ont permis de visualiser des variations de mouvement brèves directement au niveau musculaire (Lai & Hodson-Tole, 2020; Yamada et al., 2018). Combiner ces différentes avancées pourrait donc permettre de caractériser plus précisément l'exposition du système musculaire, et non de l'ensemble des tissus mous, aux vibrations.

Au-delà des différentes méthodes existantes pour mesurer et caractériser les vibrations, certains facteurs externes modifient le comportement vibratoire. Premièrement, le paradigme du « muscle tuning » défini dans le début des années 2000 suggère que l'impact, sa transmission, et les vibrations des tissus mous sont modulés par l'activité musculaire afin de limiter l'exposition du système neuromusculaire aux vibrations (Nigg, 2001; Nigg & Wakeling, 2001). Ce paradigme, considéré comme un mécanisme de protection, a été défini sur des activités de marche (Wakeling et al., 2003), de course à pied (Boyer, 2006; Boyer & Nigg, 2007a, 2004), ou lors de vibrations induites (Wakeling et al., 2002). Cependant, et à l'exception de réceptions de saut (Fu et al., 2017, 2015), il n'existe aucune information sur les caractéristiques de l'impact et la vibrations des tissus mous lors de différentes pratiques sportives. En

considérant que la vibration peut avoir un effet délétère sur l'individu en augmentant la fatigue et en créant des dommages musculaires (Ehrström et al., 2018; de Hoyo et al., 2013; Rittweger et al., 2003), caractériser ces vibrations durant la pratique de sports collectifs permettrait de mettre en évidence les contraintes de ces pratiques par rapport à la course, et ainsi d'obtenir une meilleure appréhension de l'exposition aux vibrations de ces pratiquants.

En complément du muscle tuning, d'autres méthodes comme le matériel sportif ont été utilisées pour réduire l'exposition aux vibrations.. L'objectif principal était d'amortir l'impact et de limiter la propagation des vibrations, afin d'assister le muscle dans son travail d'amortissement et retarder l'apparition de fatigue (Ehrström et al., 2018). Les travaux sur la chaussure de sport ont permis d'évaluer l'influence de l'épaisseur (Gellaerts et al., 2017), du matériau (Giandolini et al., 2020) ou de la dureté de la semelle (Boyer & Nigg, 2004), mais aucune étude ne s'est intéressée à la forme de la semelle. En effet, de plus en plus de chaussures à forme arrondies dites « rocker » sont commercialisées. Bien que ces chaussures puissent modifier la cinématique et la cinétique de course, leurs effets sur la force de réaction au sol sont encore débattus (Boyer & Andriacchi, 2009; Lin et al., 2017; Sobhani et al., 2016), alors que leurs effets sur les vibrations des tissus mous restent inconnu. De plus, l'influence du revêtement du sol sportif a reçu peu d'intérêt dans l'étude des vibrations des tissus mous où une seule étude a montré qu'une augmentation de la raideur verticale du sol entrainait une amplitude de vibrations plus importante (Boyer, 2006). Parallèlement, une diminution de la raideur dans l'axe horizontal permettraient une réduction de l'amplitude et de la fréquence d'impact sur l'axe antéro-postérieur (Chen et al., 2019).

Enfin, le mécanisme de protection du muscle tuning étant lié à l'‘activité musculaire, l'influence de la fatigue musculaire a fait l'objet de plusieurs études (Ehrström et al., 2018; Friesenbichler et al., 2011; Khassetarash et al., 2019, 2015a; Nikooyan & Zadpoor, 2012), néanmoins cette fatigue n'était souvent pas caractérisée et était induite par des protocoles de course de courte durée (<10 km). Les résultats de ces études n'étant que partiellement en adéquation avec la fatigue modélisée par un modèle informatique (Nikooyan & Zadpoor, 2012), il semble qu'une fatigue plus extrême permettrait de mieux comprendre

les perturbations et les mécanismes de protection mis en place pour gérer les contraintes vibratoires après fatigue (Wakeling et al., 2002).

Cette thèse s'articule donc autour de deux objectifs :

1) Développer des méthodes innovantes en termes de mesure, traitement du signal et d'analyse statistique afin de mieux caractériser la vibration musculaire.
2) Définir les facteurs externes (pratiques, matériels et fatigue) faisant varier le comportement vibratoire des tissus mous en pratique écologique.

4 ETUDES EXPERIMENTALES

4.1 DEVELOPPEMENT DE METHODES DE MESURE, DE TRAITEMENT DU SIGNAL ET D'ANALYSE STATISTIQUE POUR CARACTERISER LA VIBRATION MUSCULAIRE

R. Trama, M-C Play*, G. Y Millet, C. Hautier, M. Giandolini, J. Rossi. Soft Tissue Vibrations in Running: A Narrative Review. Journal of Biomechanics. (Soumis)

R. Trama, C. Hautier, Y. Blache. fctSnPM: Factorial ANOVA and post-hoc tests for Statistical nonParametric Mapping in MATLAB. Journal of Open Source Software, 6(63), 3159, https://doi.org/10.21105/joss.03159

R. Trama, C. Hautier, R. Souron, T. Lapole, A. Fouré, Y. Blache (2021). Is accelerometry an effective method to assess muscle vibrations in comparison to ultrafast ultrasonography? IEEE Transactions on Biomedical Engineering. Vol. 68, No. 4, pp. 1409–1416. 10.1109/TBME.2020.3035838

Développement méthodologique

L'ensemble des traitements référencés dans la partie 2.4 sont disponibles en téléchargement à l'adresse suivante : https://github.com/tramarobin/vibAnalyzer

4.1.1 Traitement du signal vibratoire et analyse statistique des nouveaux indicateurs

Il existe de nombreuses différences entre les études en ce qui concerne la mesure des vibrations et son traitement. Ces différences sont dues à un manque de lignes directrices sur le sujet alors que de telles directives existent pour l'électromyographie de surface (Stegeman & Hermens, 2007) ou la cinématique en trois dimensions (Wu et al., 2005, 2002) par exemple. Cependant, bien que diverses méthodes existent pour caractériser la vibration, trois indicateurs sont majoritairement rapportés dans la littérature : l'amplitude, la fréquence et l'amortissement. Pour une vibration transitoire, ces trois caractéristiques ne sont pas stables dans le temps. La vibration étant amortie, le signal vibratoire mesuré est non stationnaire et son amplitude décroit en fonction du temps. De plus, le signal est multimodal car son spectre fréquentiel comporte plusieurs fréquences distinctes. Ces fréquences sont amorties de manière différenciée et causent une variation du contenu fréquentiel au cours du temps. Ainsi, les méthodes d'analyse temps-fréquence développées permettent d'observer ces changements temporels et fréquentiels au cours du temps (Enders et al., 2012; Khassetarash et al., 2015a).

Notre revue de littérature (Trama, Play et al., soumis) a mis en avant que la tendance actuelle soit d'effectuer un traitement temps-fréquence sur le signal afin d'analyser l'évolution de l'amplitude dans ces deux domaines. Ces deux domaines sont cependant encore analysés de manière majoritairement indépendante, en regroupant l'énergie par bande de fréquences (Giandolini et al., 2020; Khassetarash et al., 2015a) ou en faisant la somme des ondelettes ou des modes pour représenter l'énergie dans le domaine temporel (Enders et al., 2012; Khassetarash et al., 2015a). Les indicateurs qui sont extraits lors de cette analyse restent donc scalaires, ils contiennent une seule information et omettent deux dimensions parmi le temps, la fréquence et/ou l'amplitude. Ces indicateurs comportent donc une indication unique sur l'amplitude, la fréquence ou l'amortissement, et sont donc plus pauvres en information que les indicateurs temporels (e.g., évolution de l'amplitude au cours du temps) et/ou fréquentiels (e.g., évolution de l'amplitude en fonction de la fréquence). La faible proportion de tels indicateurs dans la littérature en faveur d'indicateurs scalaires est due au manque d'outils statistiques permettant d'analyser des courbes ou des cartes.

Pour analyser statistiquement les spectres de fréquences ou l'évolution de l'amplitude au cours du temps, une méthode nommée cartographie statistique paramétrique (Statistical Parametric Mapping, SPM, https://spm1d.org) a été adaptée du domaine de la neuro-imagerie (Pataky, 2010). Cette méthode permet de comparer plusieurs évolutions distinctes d'un paramètre donné, les variables sont de dimensions 1D-1D (ou simplement appelé 1D), a l'inverse des indicateurs scalaires qui sont eux de dimensions 1D-0D (ou 0D). Pour répondre à notre problématique qui est d'analyser l'évolution de l'amplitude en fonction du temps et de la fréquence, une adaptation de cette méthode pour l'analyse de cartes de coefficient d'ondelettes, de dimension 1D-2D (ou 2D), a été développée (https://github.com/tramarobin/fctSnPM, Trama et al. (2021)). Pour effectuer les inférences statistiques sur les différences d'amplitude (i.e., les coefficients d'ondelettes) à chaque temps et fréquence, cette méthode se base sur une approche non paramétrique (Statistical nonParametric Mapping, SnPM) consistant en des tests de permutations de labels (Nichols & Holmes, 2002). Les tests de permutations de labels consistent a effectué le test statistique (ANOVA ou test-t) sur différentes organisations de données. En se basant sur le résultat du test statistique et de différentes permutations de labels (« mon résultat est-il plus significatif si ces deux personnes inversent leurs groupes ? »), il est possible de calculer la distribution des données de manière empirique. Prenons l'exemple mis en avant par Nichols & Holmes (2002), avec une série de 6 mesures étant organisées sous les labels ABABAB. En testant toutes les permutations possibles de ces labels, 20 possibilités sont obtenues (Figure 21).

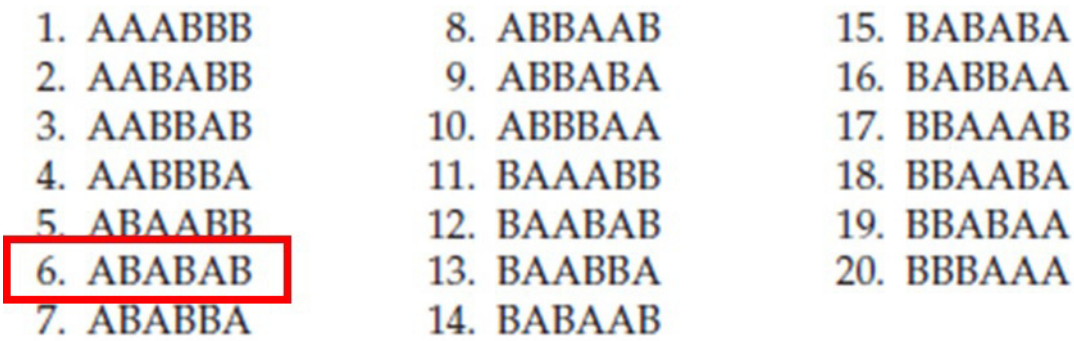

Figure 21 : Liste des 20 labélisations possible pour une série de 6 mesures avec des labels originaux de ABABAB.

A chacun de ces 20 tests correspond la valeur du test réalisé, ici un test t entre le groupe A et le groupe B (Figure 22). Si le résultat était dû à la chance, la labélisation avec le plus haut (ou bas) score statistique

aurait pu être n'importe laquelle des 20 labellisations. Cependant, le résultat avec le plus haut score est bien la labellisation d'origine, montrant qu'il y avait 1/20 chance que cela se produise. Ce résultat est donc significatif à 1/20, soit 5%. A noter que la situation 15, obtenant le score le plus bas, est simplement une inversion des labels A et B.

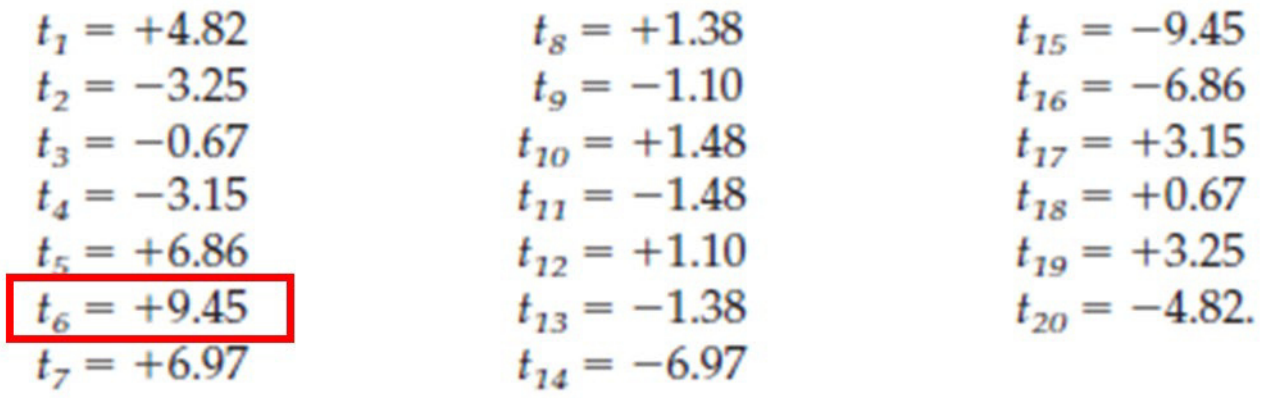

Figure 22 : Liste des 20 valeurs du test t entre les groupes A et B, pour chaque labellisation possible.

Cette méthodologie est ensuite appliquée à chaque point (aussi appelé nœud) de la courbe ou de la carte. Le nœud ayant la labellisation avec la plus grande valeur statistique définie la distribution statistique maximale, qui sera utilisée comme référence par la suite. Cette distribution est alors ordonnée de la plus grande à la plus petite valeur. Si 100 labellisations sont réalisées pour un risque de 5%, la 5ème valeur la plus grande représente le seuil des 5%. Pour avoir un risque inférieur à 5% le seuil statistique est défini avec la valeur inférieure à ce risque, soit la 4ème valeur. Par la suite, les valeurs (t ou F) de chaque nœud étant supérieures à ce seuil sont considérées comme significatives. Pour chacun des tests effectués avec des données différentes, un nouveau seuil et une nouvelle distribution sont calculés. C'est-à-dire que les différents effets d'une ANOVA, ou les différents test t composant le post-hoc n'auront pas le même seuil. Le seuil étant défini par un seul nœud, il est important que les nœuds soient liées et appartiennent à un même continuum de données, c'est-à-dire qu'ils appartiennent au même mouvement, voire phase d'un mouvement. De plus, il est important d'avoir suffisamment de participants pour obtenir un nombre suffisant de permutations afin d'atteindre la précision statistique requise. En effet, l'algorithme mathématique utilise des permutations aléatoires et deux tests peuvent donner des résultats légèrement différents. La précision et la répétabilité de ce test est grandement dépendant du nombre de permutations

effectué, et plus ce nombre sera grand, plus deux tests seront similaires et répétables. L'objectif de cet algorithme est de simplifier l'analyse des cartes (2D) et de courbes (1D) avec la méthode SnPM afin qu'un plus grand nombre de chercheurs puissent extraire des informations multidimensionnelles de leurs signaux vibratoires. Cette fonction est en accès libre (https://github.com/tramarobin/fctSnPM) et est décrite dans un article (Trama et al., 2021), et a fait l'objet d'une communication vulgarisée publié dans le blog de l'ACAPS (https://www.acaps.asso.fr/comparaison-de-moyennes-en-une-et-deux-dimensions-la-cartographie-statistique-parametrique-spm-pour-tous/) et dans le blog de la société de Biomécanique (https://www.biomecanique.org/index.php/fr/blog/179-outils-comparaison-de-courbes-et-de-cartes-la-cartographie-statistique-parametrique-spm-pour-tous).

4.1.2 Caractérisation de la vibration musculaire

La mesure de la vibration par accéléromètre est la plus adaptée en condition écologique, mais ces capteurs mesurent la vibration de l'ensemble des tissus mous et non uniquement du muscle. En considérant que le muscle et les tissus superficiels ne partagent pas la même raideur (Smeathers, 1989), il est possible que ces tissus superficiels modifient les caractéristiques de la vibration mesurée à la surface. Deux études ont montré qu'il était possible de quantifier le déplacement musculaire, et a postériori son accélération, grâce à de l'échographie (Lai & Hodson-Tole, 2020; Yamada et al., 2018). Cependant, aucune comparaison n'a été faite entre la mesure de la vibration par échographe et par accéléromètre.

L'objectif de cette étude était ainsi d'évaluer le biais de mesure du signal vibratoire par accélérométrie en comparaison à une évaluation par échographie ultra-rapide.

Un choc a été induit sur la partie latérale de la cuisse, sur un muscle relâché ou contracté à 40% de son activation maximale, et la vibration des tissus mous a été mesurée par accélérométrie tandis que celle du muscle par échographie ultra-rapide. Pour quantifier le déplacement, et a postériori l'accélération au niveau musculaire, un suivi de point a été effectué sur les vidéos issues de l'échographe (https://www.youtube.com/watch?v=Q5IvmxSmHSQ). Une transformée en ondelettes continue a été effectuée sur les signaux vibratoires. Les cartes de coefficients d'ondelettes ont été comparées grâce à

la méthode SnPM, tandis que les indicateurs d'amplitude, fréquence, et amortissement ont été statistiquement analysés avec des modèles linéaires mixtes. Des corrélations entre les différences relatives des différents paramètres lorsque mesurés avec les deux moyens de mesures et l'épaisseur du plis sous-cutanés ont aussi été réalisées.

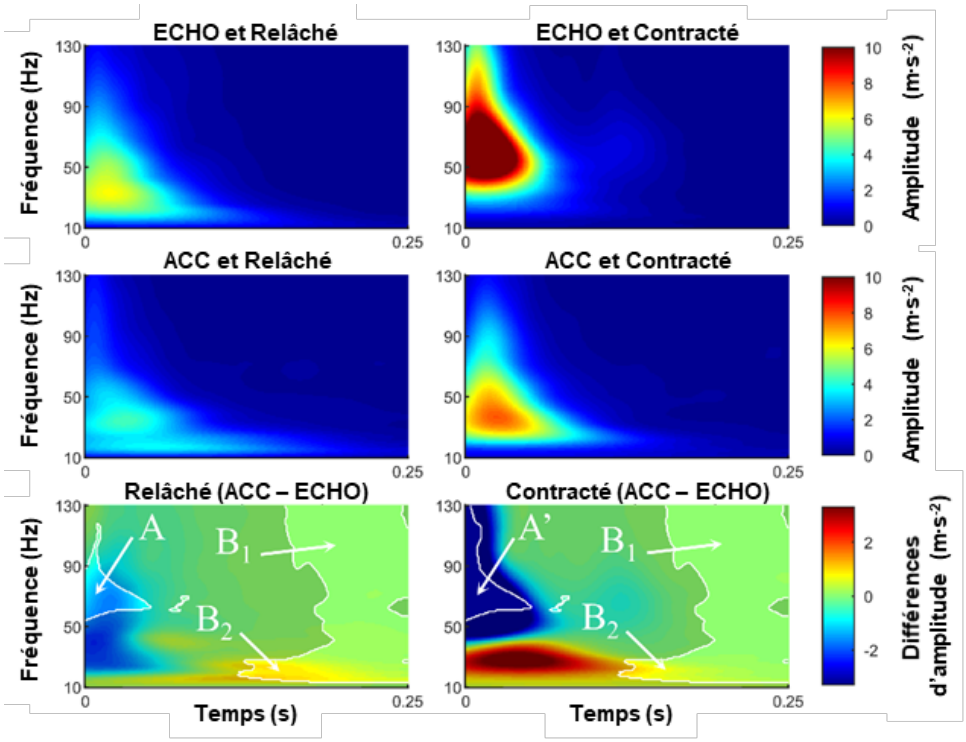

Figure 23 : Comparaison des cartes de coefficients d'ondelettes entre la mesure par accéléromètres (ACC) et échographie (ECHO). Les clusters clairs (A, B1 et B2) représentent les différences significatives entre les deux moyens de mesures obtenus avec une analyse SnPM.

Les résultats ont montré que l'accéléromètre permettait de quantifier les principales caractéristiques de la vibration musculaire et qu'il était sensible aux modifications induites par la contraction musculaire. Cependant, l'accéléromètre sous estimait l'amplitude de la vibration musculaire à des fréquences supérieures à 50 Hz juste après l'impact, et surestimait l'amplitude de vibration à des fréquences inférieures à 20 Hz à partir de 0.1 secondes après l'impact (Figure 23). De plus, l'accéléromètre sous-estimait la fréquence (18.5 ± 4.6 Hz contre 28.3 ± 8.1 Hz) et l'amortissement (14.9 ± 3.4 s^{-1} contre 25.7 ± 7.5 s^{-1}) de la vibration comparé à l'échographie, avec des différences plus marquées lorsque le muscle était contracté (27.7 ± 7.0 Hz contre 54.6 ± 6.8 Hz pour la fréquence et 26.7 ± 4.8 s^{-1} contre 40.7 ± 5.8 s^{-1} pour l'amortissement) (Figure 23). Aussi, une augmentation de l'épaisseur du pli sous-cutané entrainait une augmentation de la différence de mesure entre les deux méthodes (Figure 24).

Les tissus superficiels, avec une raideur plus faible comparée à celle du muscle (Smeathers, 1989), agissaient comme un filtre passe-bas atténuant les hautes fréquences de vibrations (>50 Hz). De plus, ces tissus étant passifs et non contractiles, l'amortissement de la vibration était réduit, notamment pour les basses fréquences (<20 Hz), entrainant une augmentation de l'énergie totale sur ces fréquences. Suite à ces résultats, nous avons conseillé de filtrer les fréquences inférieures à 20 Hz, notamment sur un muscle contracté où la fréquence de vibration du muscle est bien supérieure à celle des tissus superficiels, et de sélectionner des participants avec un faible pourcentage de masse grasse.

Cette procédure expérimentale possède certaines limitations quant à son application plus globale à la course à pied et sur différents muscles. Les vibrations induites par le pendule, bien que d'amplitude et fréquence similaire aux vibrations générées en course à pied, ont été mesurées dans deux axes du *vastus lateralis* uniquement. Il est possible que l'architecture musculaire, les muscles environnants ou encore la composition des graisses l'entourant puisse engendrer des résultats différents sur d'autres muscles. Des mesures complémentaires sur des conditions de courses à pied seront nécessaires pour développer des algorithmes de correction du signal afin de mieux caractériser la vibration musculaire par accélérométrie.

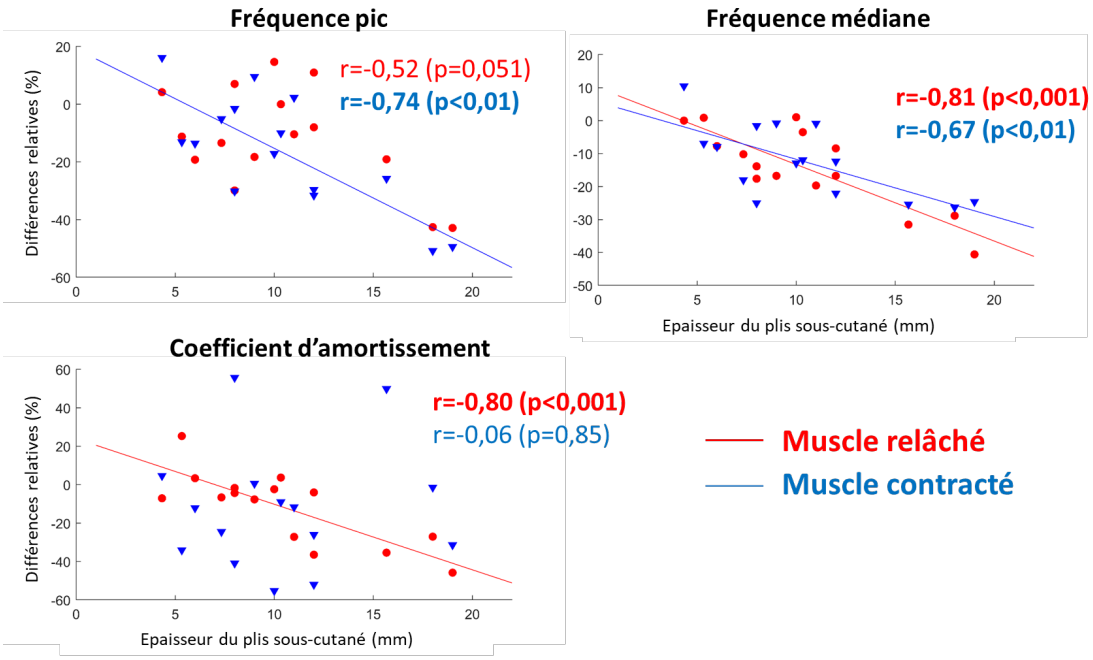

Figure 24 : Corrélations entre les différences relatives du paramètre mesuré avec échographie ou accélérométrie et l'épaisseur du plis sous-cutané localisé sous le moyen de mesure. Adapté de Trama et al.(2021).

1 **Soft Tissue Vibrations in Running: A Narrative Review**

2

3 Marie-Caroline Play (ORCID 0000-0002-9790-3286)[1*], Robin Trama (ORCID 0000-0001-
4 6807-0505)[2*], Guillaume Y Millet (ORCID 0000-0002-6395-0762)[1,3], Christophe Hautier
5 (ORCID 0000-0002-9845-2456)[2], Marlène Giandolini (ORCID 0000-0003-1507-8356)[4],
6 Jérémy Rossi (ORCID 0000-0002-0559-208X)[1]

7 1. Univ Lyon, UJM-Saint-Etienne, Inter-university Laboratory of Human Movement Biology,
8 EA 7424, F-42023, Saint-Etienne, France

9 2. Univ Lyon, University Claude Bernard Lyon I, Inter-university Laboratory of Human
10 Movement Biology, EA 7424, F-69622 Lyon, France

11 3. Institut Universitaire de France (IUF)

12 4. Amer Sports Footwear Innovation and Sport Sciences Lab, Salomon SAS, Annecy, France

13 * Both authors contributed equally to this manuscript

14 **Corresponding author:**

15 Dr. Jérémy ROSSI

16 LIBM, Campus Santé Innovations, 10 chemin de la Marandière, 42270 Saint-Priest-en-Jarez,
17 France

18 Tel: +334 77 42 18 75 – Email: jeremy.rossi@univ-st-etienne.fr

19

20

21 **Abstract**

22 During running, the human body is subjected to successive impacts generating vibrations in
23 soft tissue packages (i.e. soft tissue vibrations - STV). Repetitive vibrations may affect comfort
24 and performance, explaining why STV has recently attracted substantial research attention. The
25 objectives of this narrative review are to: (i) provide a comprehensive overview of the literature
26 on STV during running, especially why and how STV occurs; (ii) provide an overview of the
27 various approaches and output parameters used for quantifying STV with their strengths and
28 limitations; (iii) summarise the factors that affect STV. A wide set of parameters are employed
29 to characterise STV and there is a need to understand which ones should be used. This review
30 suggests that amplitude of STV quantifies the mechanical stress undergone by the soft-tissue
31 packages and should be completed by time-frequency approaches to better characterize
32 neuromuscular adaptations. Regarding sports gear, the present literature review shows that
33 compression apparels seem to be effective in reducing STV. In contrast, the effects of footwear
34 are heterogeneous and responses to footwear interventions are highly individual. The creation
35 of functional groups has recently been suggested as a promising way to better adapt the
36 characteristics of the shoes to the runners 'anthropometrics. Finally, fatigue was found to
37 increase vibration amplitude during short and intense running bouts but should be investigated
38 for prolonged running exercises and include an evaluation of neuromuscular fatigue. This
39 review permits to make recommendations about STV measurements which must be considered
40 for future studies and running footwear development.

41

42 **Keywords:** *Accelerometer, Compression, Fatigue, Footwear, Soft Tissue Vibrations,*

43

1 INTRODUCTION

The principal aim of Research & Development departments in sport companies are to guarantee comfort, limit the rate of injury and improve performance through the development of innovative products for active population as well as athletes. Accordingly, impact-related stress applied to the musculoskeletal system has received considerable attention as the human body experiences repetitive shocks each time the foot hits the ground during running. These inputs generate vibrations to the musculoskeletal system. Although local or whole-body vibration is used as a training intervention as it may improve strength through neural adaptations [1], vibrations may have detrimental effects on the musculoskeletal structures [2,3], and can also affect comfort [4] and performance [5]. Consequently, runners tend to minimise STV through biomechanical and neuromuscular adaptations, or by wearing adequate equipment such as compressive apparel and footwear. Furthermore, STV may also be affected by fatigue. Despite that reducing STV dose is of interest from a performance and injury prevention perspective, no literature review has addressed STV during running yet. Thus, the aims of this narrative review are to (i) provide a comprehensive overview of the literature on STV during running; (ii) present several output parameters and explain the various approaches with their strengths and limitations for quantifying STV; (iii) summarise the factors that may minimize STV.

Twenty-five articles were obtained by searching the electronic bases of PubMed-NCBI, ScienceDirect, Web of Science and Google Scholar, using the following keywords in title/abstract linked with the following Boolean operators: Soft Tissue Vibrations AND Running AND (Fatigue OR Shoe OR Footwear OR Compression OR Muscle Tuning). Electronic database searching was supplemented by examining the references of 34 relevant articles. A total of 59 articles have been integrated for the present narrative review.

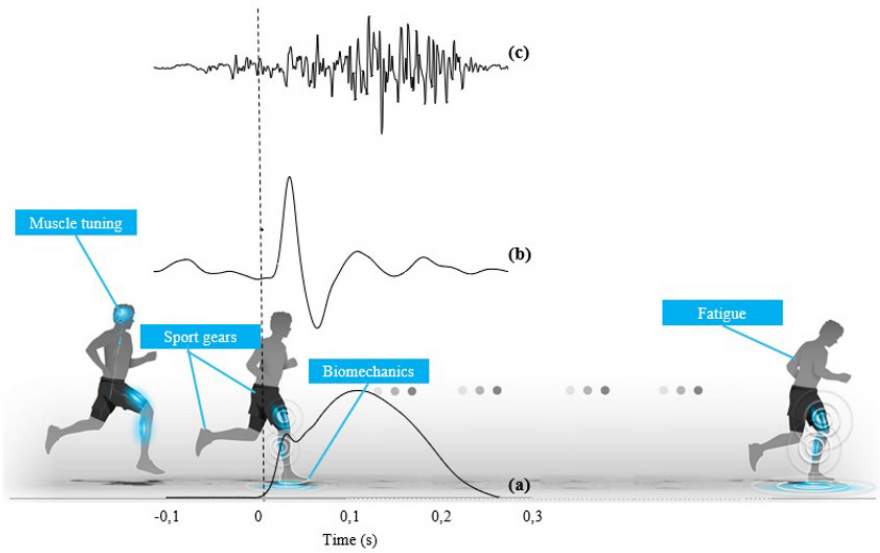

Figure 1. Overview of factors affecting soft tissue vibrations: muscle tuning, foot strike pattern, sport gears (compressive garments and footwear), and fatigue. Typical signals of vertical ground reaction force (a), *gastrocnemius medialis* acceleration (b) and electromyographic activity (c) are also represented.

2 SOFT-TISSUE VIBRATIONS IN RUNNING

2.1 Background

During running, each contact between the foot and the ground causes an impact (e.g. an average impact peak of 2.15 body weight at 4 m/s, [6]), considered as an input into the musculoskeletal system (Fig. 1a). This involves a sudden deceleration of certain parts of the body, such as the lower limb's skeleton and soft tissue packages (including muscles, tendons, adipose tissue, ligaments, skin), reaching 10 g.= 100 $m \cdot s^{-2}$ [7]. Because of the shock wave generated beneath the foot which travels up the body to the head, soft-tissue packages oscillate in all directions. As soft tissue packages are considered as oscillating masses, these displacements are characterised by their frequency, amplitude and damping. The number of oscillations performed by soft tissue packages in one second corresponds to its frequency (expressed in Hz, where 1 Hz = 1 oscillation per second) and gives information on the soft-

84 tissue package properties. Indeed, each soft-tissue package tends to vibrate at a specific
85 frequency, called natural (or free) vibration frequency. The natural frequency of bones is
86 significantly higher (200-900 Hz, [8]) than those of soft-tissue packages, that oscillate at about
87 10 Hz when relaxed and increases up to 60 Hz when muscles are fully contracted [9]. The
88 frequency of impact forces during running are close to the natural frequency of soft-tissue
89 packages [6], as the peak impact force at heel strike is reached within 30 ms and so has an
90 excitation frequency in the range of 10-30 Hz [10]. Thus, STV may occur because of a resonance
91 phenomenon in soft tissue packages.

92 2.2 Measurement of Soft Tissue Vibrations

93 The current literature suggests different ways to quantify STV, either with skin-mounted
94 accelerometers or passive filmed markers, the first method being the most widely used. As
95 accelerometers and motion capture will quantify different aspect of the soft tissue motion, we
96 suggest a close attention to indicate whether magnitude refers to displacement or acceleration.

97 The accelerometer placement is important as magnitude of STV differs within one soft
98 tissue compartment [11]. However, no standardised guidelines have been published yet. In
99 running, STV occurs in three dimensions: vertical – also called longitudinal, axial or proximo-
100 distal; antero-posterior – also called transverse; and medio-lateral. Some authors have analysed
101 only the longitudinal axis [12,13], which requires a careful alignment of the accelerometer along
102 the longitudinal axis of the segment. Other studies highlighted the importance of transversal
103 components of the acceleration signal because vibration magnitude can be equally, if not more,
104 important along the transverse axis compared to the longitudinal axis [7,14,15]. To the best of our
105 knowledge, only few authors have quantified the resultant acceleration [16,17]. It is worth
106 mentioning that changes along one axis could be compensated by changes along other axes.
107 For tibial vibrations measurement, it has been noticed that considering all axes, either

individually or using the resultant (i.e. square root of the three axes) improves the repeatability and the reliability of the measurements [14].

Video tracking with passive markers has also been used to quantify STV [16,18]. However, only vibration amplitude can be assessed with this method because of the low frequency resolution. Indeed, while most researchers have used a sampling rate over 1000 Hz with tri-axial accelerometers, sampling frequency as low as 150 Hz has been widely used both with video tracking [18,19] and accelerometers [16]. Even though the Nyquist's theorem is respected, the accuracy of these video tracking measurements remains questionable.

Table 1 : Variables and type of analysis used in the literature to assess soft-tissue vibrations

Type of analysis	Variable (unit)	Description / Computation	References
AMPLITUDE			
Temporal	Peak acceleration ($m \cdot s^{-2}$)	Maximum of the absolute value of the acceleration signal	Trama et al. (2019) Boyer & Nigg (2004, 2006, 2007) Nikooyan & Zadpoor (2012) Giandolini et al. (2020)
	Root mean square acceleration ($m \cdot s^{-2}$)	Average root mean square of the signal with a 0.01s window	Ehrström et al. (2018)
	Standard deviation of accelerations ($m \cdot s^{-2}$)	Standard deviation of the acceleration signal	Gellearts et al. (2017)
	Maximal displacement (m)	Difference between the maximum and minimum position of the soft-tissue markers relative to the segment of interest	Borràs et al. (2011) Broatch et al. (2019, 2020)
Fast Fourier Transform	Normalised Fourier Transform ($m \cdot s^{-2}/Hz$)	Fourier Transform normalised by the frequency resolution Represent the amplitude at each frequency	Boyer & Nigg (2006, 2007) Enders et al. (2012) Khassetarash (2015b)
	Power Spectral Density ($m^2 \cdot s^{-4}/Hz$)	Square of the Fourier Transform normalised by the inverse of the product of the signal length by the sample frequency Represent the power at each frequency	Giandolini et al. (2020) Friesenbichler et al. (2011)
Continuous Wavelet Transform	Time integral of wavelet coefficients for different frequency bands ($m \cdot s^{-2}/Hz$)	Equivalent to the Normalised Fourier Transform	Trama et al. (2019, 2020)
	Sum of wavelets power	Non-indicated (normalised)	Khassetarash et al. (2019)
FREQUENCY			
Temporal	Peak frequency estimate	Inverse of the duration between the two first peaks after heel strike	Boyer & Nigg (2004)
Fast Fourier Transform	Peak frequency (Hz)	Frequency with the most amplitude	Enders et al. (2014) Giandolini et al. (2020)
	Mean frequency (Hz)	Weighted average product of the amplitude of the frequency by the frequency	Friesenbichler et al. (2011) Enders et al. (2014)

	Median frequency (Hz)	Frequency that split the amplitude or power spectrum in half	Enders et al. (2014)
Continuous Wavelet Transform	Peak frequency (Hz)	See above	Trama et al. (2019, 2020)
DAMPING			
Continuous Wavelet Transform	Damping coefficient (s^{-1})	Decrement of logarithm power or logarithm decrement of power (estimation via least-square minimisation)	Enders et al. (2012, 2014) Khassetarash et al. (2015b, 2019) Trama et al. (2019, 2020)
	Settling time (s)	Time between maximum amplitude and 10% amplitude	Khassetarash et al. (2019)
	Energy dissipation ($J \cdot kg^{-1}$)	Product of the time integral of the square vibration speed by the double of damping coefficient	
Partly Ensemble Empirical Mode Decomposition	Damping coefficient (s^{-1})	See above	Khassetarash et al. (2015a)
	Damping ratio (ø)	Damping coefficient relative to the critical damping of the frequency dampened	
	Energy dissipation ($J \cdot kg^{-1}$)	See above	

2.3 Outcome variables

The amplitude, frequency, and damping of STV are reported in numerous studies since each of these three parameters brings different information.

1) The amplitude of the vibration provides information on the magnitude of stress undergone by the musculoskeletal system as:

$$a = \frac{F}{m} \qquad \text{(Eq. 1)}$$

with a the acceleration in $m \cdot s^{-2}$, F the force in $kg \cdot m \cdot s^{-2}$, and m the mass in kg.

2) The frequency corresponds to the number of oscillations undergone by soft-tissue packages during one second (expressed in Hz), and as depicted by Eq. 2, gives information on the natural frequency of the soft-tissue packages [20]:

$$f = \sqrt{\frac{k}{m}} \qquad \text{(Eq. 2)}$$

with f the frequency in Hz, k the stiffness in $N \cdot m^{-1}$.

3) The damping coefficient is an indicator of how the muscle damps the vibration. A greater damping means that the vibration decay is quicker. It is expressed in "per second". The notation s^{-1} is preferred to Hz.

As the vibratory signal of soft-tissues during running is multi-modal (i.e., the signal is composed of several frequencies) and non-stationary (i.e., the characteristics of the signal change over time), several methods have been developed to assess the three parameters above. Each of them can be described by different variables and obtained from different types of analysis (Table 1 and Fig. 2).

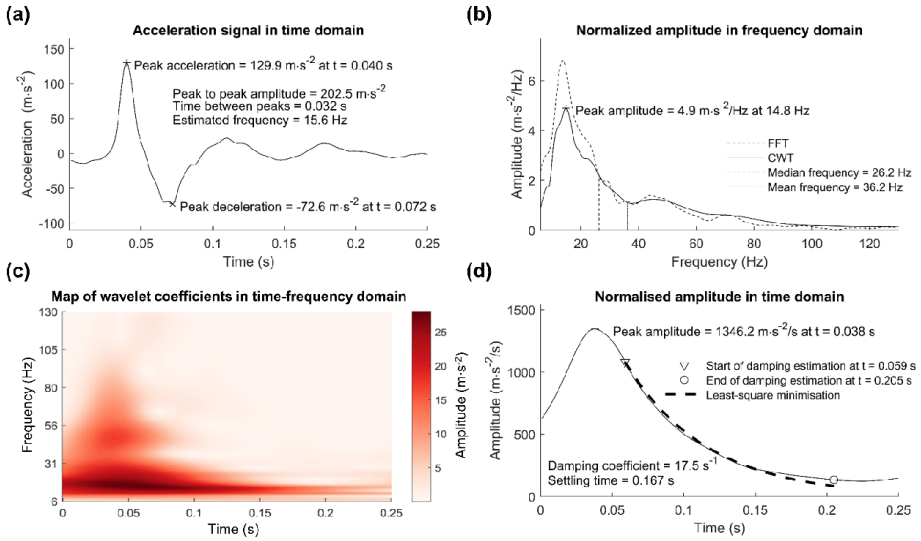

Figure 2. Authors' data during running for the *gastrocnemius medialis* (GM): (a) amplitude variables obtained with time analysis; (b) frequency variables obtained by frequency analysis; (c) map resulting from time-frequency analysis; (d) damping variables in time domain resulting from time-frequency analysis.

2.3.1 Time analysis

Time analysis (Fig. 2a) is the simplest method to analyse vibratory signals. From the time representation of the acceleration signal (Fig. 1b), one can compute the peak acceleration [13,21–23], the mean standard deviation [16], or the root mean square acceleration [17]. A temporal analysis

146 of passive marker displacement allows the calculation of the maximum displacement of the
147 soft-tissue [18,19]. With these amplitude characteristics, the intensity of the mechanical stress
148 undergone by the soft-tissue package can be quantified. The total vibration exposure was
149 defined as the product between the vibration amplitude, duration, and stride frequency [24] In
150 addition, it is possible to estimate the frequency of the vibration, which corresponds to the
151 inverse of the time period between two consecutive peaks [21]. Although this method is the
152 simplest to implement, it is very sensitive to the filters applied on the raw signals. In running,
153 one study has applied a low-pass filter at 50 Hz on the signal [25] while the others did not filter
154 the signal. It is possible to compute damping from a temporal analysis (e.g., model or logarithm
155 decrement between peaks) [26]. However, due to the multi-modal and non-stationary
156 characteristics of the vibratory signal in running, damping is commonly computed with other
157 methods.

158 *2.3.2 Frequency Analysis*

159 The multi-modal characteristics of the vibratory signal have incited researchers to use other
160 approaches lying in the frequency domain analysis. The most common algorithm employed is
161 the Fast Fourier Transforms (FFT). FFT allows the calculation of the Fourier Transform (FT),
162 which is often normalised (nFT) by the frequency bin width (i.e., FFT resolution) to ease the
163 comparison between studies and methods (Fig. 2b). By squaring the FT and dividing by the
164 frequency resolution, it is possible to calculate the power spectral density of the signal (PSD).
165 NFT represents the amplitude of the signal in function of the frequency, in our case expressed
166 in $m \cdot s^{-2}/Hz$, while PSD represent the power in function of the frequency, in $m^2 \cdot s^{-4}/Hz$ [27].
167 These spectrums allow the calculation of the peak frequency (i.e. the frequency with the highest
168 amplitude) associated with the peak amplitude or peak power [12,25,28,29]. It is also possible to
169 compute the median [30] or the mean [29,30] frequency, which allows to characterize how the energy
170 is distributed over the frequency continuum. If the peak, mean, and median frequencies are

close to each other, the energy is localized near the peak frequency. However, if these metrics are far apart, the acceleration signal may be composed of several distinct frequencies. Knowing that muscle activity modulates STV frequency[26], it is of great interest to have a detailed description of the frequency characteristics of STV in order to presuppose the effect of a given condition (e.g. gears, footwear, fatigue) on muscle activation [21]. Subsequently, frequency analysis allows to calculate the total amplitude or power within a given frequency range by integrating the nFT or PSD curve, respectively [13,31] . These parameters are related to the vibration amplitude and duration. Consequently, they could be more suitable to characterise the total vibration exposure compared to time analysis.

2.3.3 Time-frequency Analysis

The non-stationary characteristic of the signal has led authors to employ time-frequency analyses, such as continuous wavelet transforms (CWT)[28,29,32,33] or empirical mode decomposition based method (EMD) [32]. The difference between these two methods is that CWT works on all the frequency range, while EMD extracts intrinsic mode functions. The major limit of the CWT is the choice of the mother wavelet which can differ between studies. The limit of EMD is that mode functions are specific to the signal, meaning that their numbers and frequency are not identical for all signals. These limits complicate the comparisons between studies and/or individuals. Time-frequency analyses permit the quantification of the vibration amplitude evolution as function of time and frequency (Fig. 2c). By choosing the wavelets or mode functions analysed, mainly between 6 and 130 Hz (the frequencies below and above corresponding to movement and noise, respectively), it is possible to calculate different indicators for different time and frequency ranges. To illustrate the major advantage of time-frequency analysis over the frequency analysis, one can consider a signal with a first frequency with high power during a short time period, and a second frequency with low power for a long time. The frequency analysis will depict a spectrum with two frequency peaks of

196 similar energy, without the possibility to identify if the power of these frequencies were
197 different. Concurrently, the time-frequency analysis will display a map of wavelet coefficients
198 on which differences in power over frequency and time could be clearly identified. This
199 information, though it is not yet widespread in literature, allows a better description of the
200 vibration amplitude throughout the stance phase (i.e., braking, mid-stance, propulsion), and
201 permits a better understanding of the effect of vibrations on the musculoskeletal and
202 neuromuscular systems.

203 No study has used the map of wavelet coefficients (Fig 2c) as a descriptive variable
204 during running. Instead, maps are used to extract variables[29,32,33] . First, by integrating the map
205 in function of time, one can compute an equivalent of the nFT and obtain the same information
206 as those obtained with FFT analysis. Although the frequency domain is well estimated by CWT
207 (Fig. 2b), these methods are a compromise between the time and frequency resolution, and
208 thus, are often used in parallel of frequency analysis. Second, by integrating the map in function
209 of the frequency[33] or by summing the wavelets power [12,24,28,30], one can compute the overall
210 amplitude of the vibration in the time domain. The result of this computation depends on the
211 frequency range analysed, and/or of the wavelets summed. As the theoretical overall power
212 decay is known and linked to the damping properties of the soft tissues, it allows to estimate
213 damping (Eq. 3). In addition, the same decay can be obtained from the envelope of the intrinsic
214 mode functions computed with EMD [32].

215 $$p(t) = P_0 e^{-dt} \qquad \text{(Eq.3)}$$
216
217 where P_0 is the power of the sum of the wavelets, d the damping coefficient, and t the time.

218 As the power decay is exponential, the logarithm of the decay is linear. The damping
219 can be estimated with least-square minimization, the damping coefficient being the slope of

220 the regression line [12,28,30,32]. Another method is to use an optimization function[33] to minimised
221 the error between the measured decay and the modelled decay (Eq.3 and Fig. 2d).

222 Other methods have been proposed to assess the damping of the vibration. For instance,
223 one can calculate the settling time of the vibration, that corresponds to the duration between
224 the time at maximal power, and the time when the power is dampened at 90% [24]. The greater
225 the damping, the shorter the settling time. The dissipation of energy, depending on the damping
226 and speed, can be computed [12,24,32]. Several studies depicted that the higher frequencies of
227 vibrations were more dampened[32,33] but dissipated less energy [32]. Knowing that damping can
228 be altered by foot strike pattern [30] or fatigue [12,24], this indicator can inform on the neuromuscular
229 adaptions and strategies to limit the vibration exposure.

230 In addition, the transfer of amplitude between the input (i.e. impact quantified with
231 ground reaction force or heel/tibial accelerometer) and the STV[33,34] , or between two locations
232 on the same muscle [11] can be quantified. The transfer corresponds to the ratio between the two
233 locations for one amplitude parameter, such as peak amplitude, PSD, or entire power spectrum.
234 Transfer can be expressed as a percentage of variation [33] or as a transmissibility function
235 expressed in dB[35]. Consequently, the transfer gives information about the relative movement
236 of the soft tissues compared to the bones. Changes in transfer function, instead of changes in
237 vibration amplitude, can better inform on the presence of neuromuscular adaptions induced by
238 the muscle tuning [34,35]. Indeed, muscle tuning adaptations can lead to a decrease in the transfer
239 of the vibration from the bones to soft tissue packages (i.e., the bones and soft tissues are more
240 united), by different strategies explained in another section of this review (see 3.2).

241 3 PARAMETERS INFLUENCING SOFT TISSUE VIBRATIONS

242 Both intrinsic (biomechanical and muscle pattern) and extrinsic (sports gears) parameters of
243 the runner have an effect on STV (Fig. 1). Creation of functional groups will allow researchers

244 to group individuals who react in a similar way to a specific sportwear intervention and see
245 whether these runners have the same morphological and functional characteristics.

246 3.1 Biomechanics

247 Each runner automatically and naturally adopts a specific biomechanical pattern, which has
248 been termed 'preferred movement path' [36]. One macroscopic feature describing part of one's
249 preferred movement path is his/her foot strike pattern [37]. In level running, it is well known that
250 runners strike the ground either with their heel (rearfoot strikers) or with their midfoot/forefoot.
251 Foot strike patterns are characterised by differences in muscle activation, kinetics and
252 kinematics [38–40]. Rearfoot strikers usually demonstrate a more extended knee and dorsiflexed
253 ankle at foot strike. Conversely, greater knee flexors and plantar flexors activities, more flexed
254 knee and more plantarflexed ankle at foot strike have been observed in midfoot/forefoot strikers
255 [41]. Based on these considerations, all of these biomechanical differences could affect the shock
256 wave propagation through the lower limb and the damping of STV. Indeed, it has been
257 observed that natural frequencies and damping of STV were affected by the knee flexion angle
258 during isometric contractions [9]. In line with the preferred movement path paradigm, it is worth
259 mentioning that STV damping on medial gastrocnemius muscle was impaired when heel
260 strikers were asked to run with a forefoot strike pattern and vice-versa [30]. It is suggested that
261 runners demonstrate the best damping of STV with their preferred foot strike pattern.

262

263 3.2 Implications of muscle tuning

264 A paradigm called "muscle tuning" was proposed to understand how the body reacts to
265 repetitive impact forces [42]. Muscles are suggested to be vibration modulators that induce
266 damping or natural frequency shifts to minimize vibration It suggests that runners tune muscle
267 activation before foot strike in order to minimise STV. Indeed, in response to an input signal
268 (i.e. ground reaction forces) with a frequency close to the soft tissue natural frequency, an

increase in muscular activation before foot-ground contact has been noticed [21,43]. In running, earlier studies have suggested that muscles are vibration modulators, inducing two different mechanisms used to minimize vibrations. Increase in the damping coefficient[9,29] has been vastly more reported than shifts in the natural frequency [9], not substantial enough to move away from those due to the impact forces (Fig.3). These neuromuscular adjustments seem to be subject-specific. Based on equation 2, we can assume that vibration frequency is negatively associated with mass. In particular, larger muscles may use natural frequency shifts as a preferred adaptation mechanism to minimize vibrations [44]. An earlier study focusing on compositions of muscle fibre types showed that power-trained athletes exhibited higher soft tissue compartment vibration frequencies during running, indicating that fast-twitch fibres might have been activated to accommodate the demands of locomotion and muscle tuning. [45].

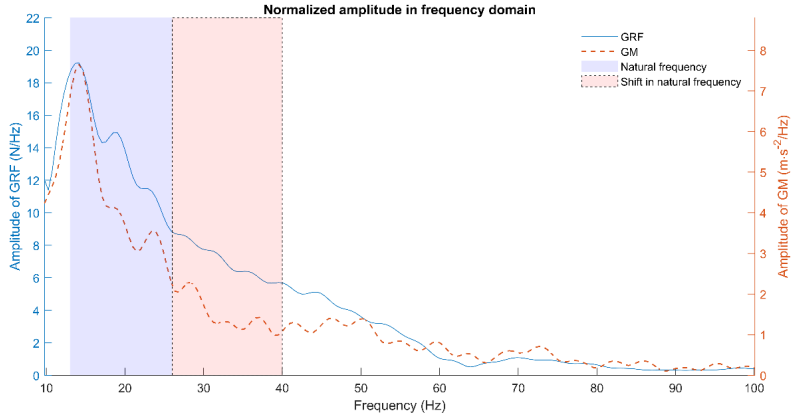

Figure 3. Representation of the frequency signals of the ground reaction force (full line) and gastrocnemius acceleration (dotted line) during running. The blue area is equivalent to the natural muscle frequencies (Wakeling et al. (2001)), which coincide with impact frequencies during different running velocities (from Trama et al. (2019) and Boyer et al. (2004)). Shifts in natural frequency are not enough important and still match with GRF frequency content.

Finally, if muscles are not tuned properly by central nervous system [46] in response to input changes, STV amplitude increase [35]. Soft-tissue packages may then oscillate

288 substantially because of the resonance phenomena. In this case, the muscle-tendon units may
289 be exposed to high forces, which increases the risk of injuries.

290

291 ## 3.3 Sportgears

292 ### *3.3.1 Compressive garments*

293 An effective method to attenuate STV during dynamic activities is the use of sports
294 compressive garments. To the best of our knowledge, five studies investigated the effects of
295 compressive garments on STV during downhill [17,19] or flat running [16,18,47]. The main findings
296 are summarised in Table 2. In the literature, two types of garments have been used when
297 studying STV: tights compressing both calves and thighs, and shorts compressing thighs only.
298 Vibrations have been measured with tri-axial accelerometers or 3D motion capture where the
299 sensors (accelerometers or markers, respectively) were put either under [17] or on top of the
300 garments [16,18,19,47]. One could suggest that setting the device under the garments may affect the
301 compressive pressure and/or applied an extra pressure on the device which could underestimate
302 the benefit and/or distort the accelerations signals.

303 All studies, both during flat and downhill running, noticed up to a 20% decrease in STV
304 when the pressure exerted by the garments increased. The observed differences in STV
305 between garments seem to be independent of the degree of compression applied [18]. For
306 instance, the coefficient of determination for the relationship between the degree of pressure
307 and the reduction of oscillation at 10 km/h for the vastii muscles was estimated to be 0.4 [16,18].
308 As pressure was measured at rest and not during running, it could be suggested that this
309 coefficient remains relatively low and there is a state of uncertainty on the garment's capacity
310 to maintain pressure during running [18]. The authors suggested that further research should
311 investigate the degree of pressure applied by garments during running.

312 Compressive garments have been shown to be more effective in reducing oscillations
313 on vastii muscles than gastrocnemii muscles [18]. Soft-tissue masses are greater for thighs than
314 for calves. Given the elastic nature of muscle and surrounding soft tissues, the capacity for soft-
315 tissue displacement following foot strike is likely greater for bigger soft-tissue masses.
316 Therefore, compression is likely to have a greater damping effect on vastii muscles.
317 It has been shown that compressive garments also minimise the harmful effects of
318 impact forces during running by decreasing muscle activation [18]. In other words, as wearing
319 compression garment decreases STV amplitude, the requirement for 'muscle tuning' is lower
320 which may reduce neuromuscular fatigue. Indeed, for a given downhill running bout (slope: –
321 8.5°, 40-min at a velocity associated with 55% of VO_{2max} [17]), perceived muscle soreness
322 measured one day after the running test was found to be significantly lower for the quadriceps.
323 Additionally, for a similar downhill running protocol (slope: -10°, 40-min at a velocity
324 associated with 85% of VO_{2max} [19]), muscular biopsies performed 48 h after running test
325 highlighted higher inflammation and sarcomere injuries without compression. Moreover, the
326 decrease in STV also induced a faster recovery of peripheral and central neuromuscular
327 function and a lower impairment in running economy [17]. Overall, compression apparels seem
328 to minimise STV and muscle activity in running leading to a reduction in soft-tissue damages
329 and fatigue.
330
331 *3.3.2 Footwear*
332 Footwear characteristics have the potential to influence impact and STV. Five studies have
333 assessed the effects of changing a) midsole materials (viscoelasticity and/or hardness) and b)
334 midsole geometry (thickness and/or curvature) on STV during running (Table 2).
335 *Midsole materials*

Viscoelasticity: A viscous midsole has been found to reduce initial vibratory input of STV for calf and thigh muscles [22,48]. In the viscous condition, the vertical amplitude decreased by 8 to 12% for the *vastus medialis* (VM) and *gastrocnemius medialis* (GM), equivalent to an about 1-g decrease in the acceleration peaks [22]. In addition, the vertical PSD was reduced by ~20-27% for GM, VM and the *tibialis anterior*. Concerning viscoelasticity effect on the damping mechanism, there was a better damping for the viscous midsole condition for VM. However, it seems that changing midsole viscoelasticity has no significant effect on vibration frequency. It is worth mentioning that changes in leg STV amplitude and damping were associated with a decrease of EMG activity. Indeed, EMG activity before foot strike was lower for the viscous condition which might explain the better damping and the reduction in the amplitude of STV. [22].

Hardness: It has been shown that changing midsoles hardness from Asker 40C (soft) to 70C (hard) did not change STV [21]. Even if harder shoes elicit higher impact peak force and loading rate [21], no significant effects of hardness were found on peak acceleration and peak frequency. These results agree with a model studying the effects of footwear on impact forces and vibration during running. It has been proposed that the central nervous system guarantees an acceptable vibration threshold above which central functions (e.g. vision, vestibular function) may be impaired through muscle tuning [49–51]. It is however worth mentioning that neither PSD nor damping have been calculated yet in previous studies assessing the effects midsole hardness on STV. This is an important consideration given that a previous model suggested that soft shoes showed a 2 to 3 times greater damping coefficient than hard shoes [46].

Midsole geometry

No significant effect of midsole curvature (rocker) were found on STV, ground reaction forces or EMG activity [13]. When comparing minimalist to maximalist footwear, the latter being

360 characterised by a thick and curved midsole, muscular oscillations were about 19% lower with
361 maximalist shoes compared to minimalist ones [16]. Thus, large changes in midsole geometry
362 affect STV. However, in this study, both midsole thickness and curvature were different so that
363 no definitive conclusion can be made on the independent effect of midsole curvature and
364 thickness on STV. Moreover, differences in data analysis should be mentioned: [16] considered
365 the three axes while [13] only focused on the longitudinal axis.

366 To sum up, footwear effect on vibratory responses is more complicated that for the
367 garments and needs to assume both the STV and EMG outcomes for the effect of footwear to
368 be interpreted.

369 *Functional groups*

370 As the same shoe modification produces different reactions among runners (i.e. subject specific
371 results), the concept of functional groups has been proposed. In footwear science, a functional
372 group is defined as a group of subjects who respond similarly to a specific shoe intervention
373 [52]. A recent study recorded STV of the *gastrocnemius* during 5-min treadmill run [53]. When
374 running with the same shoe condition, the 42 participants demonstrated very different degrees
375 of damping. As this study noticed no changes in muscle activation, input or natural frequency
376 between the groups, we suggest that anthropometric differences and muscle tuning strategies
377 enounced previously could participate in determining the neuromuscular response to footwear
378 changes. For instance, not all individuals have the same anthropometrics and muscle
379 characteristics. Chen et al. (2021) showed that powerlifters had a higher STV frequency than
380 runners, which was explained by a greater muscle stiffness or less fat thickness [54]. Besides,
381 population has been split between dampeners or frequency shifters [44] so that it is likely that the
382 neuromuscular response to sports gears differ between these two populations. When testing
383 sports gears, we suggest to define functional groups based on both anthropometric

384 measurements and STV characteristics measured in a controlled condition. Functional groups
385 can be determined by using methods such as principal component analysis [52] or vector
386 representation, as there are powerful and promising tools to identify clusters of subjects with
387 similar characteristics [55].

388 **Table 2** : Effect of equipment on soft tissue vibrations

Reference		Participants details (Level | Gender | Age | Weight | Height)	COMP / TEST details (Type | Pressure (mm Hg)) / Shoe characteristics)	Running protocol	Device measuring STV | Locations | Frequency	Effects of COMP / TEST
APPAREL						
FLAT RUNNING	Coza et al. (2008)	Young and active subjects M = 2 | F = 2 | n.i.	n. i.	Treadmill 5 speeds × 3 shoes per COMP	Tri-axial accelerometers VM, GL, BF 2400 Hz	Damping ↗ (+8 %)
	Gellaerts et al. (2017)	Healthy men | M = 11 | 25.1 ± 2.7 yrs | 67.5 ± 1.3 kg | 175.5 ± 1.8 cm	Shorts| COMP1 (Thigh): 20.4 ± 1.7 COMP2 (Thigh): 14.5 ± 1.3 COMP3 (Thigh): 9.6 ± 0.8	Treadmill 10 km/h 1 minute per COMP	Tri-axial accelerometers on textile VM and RF 150 Hz	SD Ar ↘ (from -5.15 to -16.2 %) for all muscles and garments
	Broatch et aL (2019)	Recreational athletes | M = 13 | 22 ± 3 yrs | 84.1 ± 9.4 kg | 185.5 ± 5.5 cm	Tight | COMP (Thigh) 12.1 ± 2.3 (Calf) 17.2 ± 6.2	Two 4 min treadmill running 12 and 15 km/h with 30 min rest	3D motion capture Markers on textile VAS and GAS 250 Hz	v. MD ↘ (-3 %) for VAS at 12 km/h m. l. MD ↘ (-13 %) for GAS at 12 km/h a. p. MD ↘ (-20 %) for GAS at all speed RMS Ar ↘ for VAS at 12 km/h
	Broatch et al. (2020)	Recreational athletes| M = 14 | 27 ± 5 yrs | 77.8 ± 8.4 kg | 180.9 ± 7.3 cm	Tight | COMP1 (Thigh) 12.1 ± 2.3 (Calf) 17.2 ± 6.2 COMP2 (Thigh) 12.9 ± 2.7 (Calf) 14.6 ± 4.9 COMP3 (Thigh) 13.2 ± 3.1 (Calf) 11.4 ± 4.7	4 × 9 min continuous treadmill 3 min at 8 / 10 / 12 km/h) with 30 min rest	3D motion capture, Markers on textile VAS and GAS 250 Hz	v. MD ↘ (-10 %) for VAS for all garments m. l. MD ↘ (-20 %) for VAS for all garments v. MD ↘ (-4 %) for GAS for COMP1 (m. l. MD ↘ (-11 %) for GAS for COMP1
DOWNHILL RUNNING	Ehrstrom et al. (2018)	Well-trained runners M = 13 | 38.6 ± 5.7 yrs | 72.1 ± 4.7kg | 175.8 ± 5.1 cm	Tight | COMP (Thigh) 16-18 (Calf) 20-25	Outside 40 min DHR -8.5 % slope 55 % VO2max	Tri-axial accelerometers under textile VL and GM 1000 Hz	RMS Ar ↘ (-5 %) only for VAS
	Borras et al. (2011)	Moderately train soccer player M = 9 | 27.7 ± 10.9 yrs | 76.1 ± 6.1 kg | 176.8 ± 3.6 cm	Shorts| n. i.	Treadmill 40 min DHR -10 % slope 85 % VO2max	3D motion capture Markers on textile RF and VAS 200 Hz	MD ↘ (-7.8 %)
FOOTWEAR						
MIDSOLE COMPOSITION	Giandolini et al. (2020)	Recreational and competitive runners | M = 12 | 42 ± 10 yrs | 75.2 ± 8.4 kg | 178 ± 4 cm	COND: Elastic (full EVA 55C-Asker) TEST: Viscous (bi-material 42 and 52C-Asker)	20-m indoor track | 3.33 m/s | 5 trials per shoe.	Tri-axial accelerometers on VM and GM 2000 Hz	For GM: v. a_{peak} ↘ (-8.2 ± 3.5 %) v. PSD ↘ (-17.5 ± 6.2 %) v. f_{peak} ↔ v. Damping ↔ For VM: v. a_{peak} ↘ (-12 ± 3.7 %)

						v. PSD ↘ (-19.7 ± 6.2 %) v. f_{peak} ↔ v. Damping ↘ (-19.3 ± 17.1 %)
	Giandolini et al. (2017)	n. i. | M = 8 | n. i. | n. i. | n. i.	COND: EVA, 60C-Asker (hard) TEST: eTPU 40C-Asker (elastic and soft)	treadmill | 3.33 m/s | 2 trials per shoe. during 5min.	Tri-axial accelerometers TA, GL, RF and BF 2560 Hz	For TA: v. PSD ↗ (+26.7 ± 20%) For RF: a.p. PSD ↗ (+42.6 ± 35.5 %) For GL and BF: PSD ↔
	Boyer et al. (2004)	Regularly runners | M = 10 | 25 ± 4.2 yrs	COND: Elastic (52C-Asker) TEST1: Viscous (50C-Asker) TEST2: Visco-elastic (40C-Asker) TEST3: Visco-elastic (55C-Asker) TEST4: Visco-elastic (70C-Asker)	16-m indoor track| 2, 3, 4 and 5.5 m/s| 3 trials per shoe and surface	Tri-axial accelerometers TA, GM, VL and BF 2400 Hz	For all muscles: v. a_{peak} ↔ v. f_{peak} ↔
MIDSOLE SHAPE	Trama et al. (2019)	Recreational runners | M = 20 | 23.9 ± 2.1 yrs | 73.6 ± 7.4 kg | 177 ± 5 cm	COND: Flat (h_{toe}=40 mm, h_{heel}=55 mm, Δh=15 mm) TEST: Rocker (h_{toe}=41 mm, h_{heel}=58 mm, Δh=17 mm)	Indoor track| 8, 10.5, 13 and 15.5 km/h | 5 trials per shoe and running speed	Tri-axial accelerometers GM and VL 1000 Hz	For VL and GM: v. a_{peak} ↔ v. f_{peak} ↔ Damping ↔
	Gellaerts et al. (2017)	Healthy men | M=11 | 25.1 ± 2.7 yrs | 67.5 ± 1.3 kg | 175.5 ± 1.8 cm	COND: minimalist (h_{toe}=4 mm, h_{heel}=4 mm, Δh=0 mm) TEST: maximalist (h_{toe}=29 mm, h_{heel}=33 mm, Δh=4 mm)	Treadmill| 10 km/h| 1 minute per shoe	Tri-axial accelerometers RF and VM 150 Hz	For RF: MD ↘ (-20.6 ± 6.6 %) For VM: MD ↘ (-18.8 ± 2.5 %)

M: Male, F: Female, n. i.: non-indicated, COMP: Compression Tested, COND: Condition, TEST: Shoe Tested, h_{toe}: Height under the toe, h_{heel}: Height under the heel, Δh: Height difference between heel and toe, DHR: Downhill running, VM: Vastus Medialis, VL: Vastus Lateralis, GM: Gastrocnemius Medialis, GL: Gastrocnemius Lateralis, BF: Biceps Femoris, RF: Rectus Femoris, VAS: Vastii, GAS: gastrocnemii, TA: Tibialis Anterior, SD Ar: Standard Deviation of Acceleration resultant, RMS Ar: Rot Mean Square of Acceleration resultant, MD: Muscle Displacement, a_{peak}: peak acceleration, f_{peak}: peak frequency, PSD: Power Spectral Density, v.: vertical, a. p.: anterior-posterior, m. l.: medio-lateral, ↘: significant decrease, ↔: no significant change, ↗ significant increase.

4 EFFECTS OF FATIGUE ON SOFT TISSUE VIBRATIONS

Muscle tuning has been shown to occur in non-fatigued muscle. However, muscle tuning requires an increase in muscle activity that could be impaired by fatigue. Whether or not this protective mechanism is affected by neuromuscular fatigue is a relevant question. Five studies published between 2011 and 2019 focused on the effects of fatigue on STV [12,17,24,29,56] (Table 3). The protocols employed to induce fatigue can be classified in three categories:

1) a computer model with implemented fatigue [56],

2) level running until exhaustion [12,24,29],

3) downhill running [17].

406 The predictions of the computer model confirmed the hypothesis that the protective mechanism
407 of muscle tuning is altered with fatigue. This predicted that fatigue will induce an increase in
408 vibration amplitude and a decrease in damping, but no change in peak impact. It has been
409 proposed that neuromuscular fatigue induced by short and intense running, impacting more
410 specifically the fatigable type II fibres, can decrease muscle function and its damping capacity.
411 Yet the results obtained in two studies conducted by Khassetarash [12,24] found the opposite
412 result, as a 15% to 20% increase in damping was noted. While there are no clear explanations
413 for this increase since the muscular activity was not changed, the authors speculated that it may
414 be due to changes in the properties of the passive (i.e. non contractile) components of the soft-
415 tissue package. However, it is worth mentioning that the protocols used by Khassetarash et al.
416 may not have been long enough to induce a substantial neuromuscular fatigue and to diminish
417 the damping capacity of the muscles.

418 The amplitude of vibrations, which is the only parameter that was systematically studied
419 across the five studies, increased by 10 to 30% [12,17,24,29], as expected by the model [56]. The only
420 exception was for the GM after downhill protocol where amplitude was not modified [17]. To
421 explain this latter results, it was suggested that downhill running was more strenuous for knee
422 extensor muscles as a consequence of greater braking forces, and therefore, altered more the
423 *vastus lateralis* than the GM, which may not be the case in level running. The causes of the
424 increase in vibrations amplitude are not yet fully understood. Unlike is the model prediction [56],
425 concomitant increase in the passive peak of ground reaction force and vibration amplitude have
426 been reported [24]. Moreover, if the increase in vibrations amplitude was solely due to change in
427 impact forces, all muscles should behave similarly, which was not the case in the study of [17].
428 After efforts inducing neuromuscular fatigue similar to the one observed by Ehrstöm et al.
429 (2018), impact intensity was not modified, either when quantified with force plates [57,58] or tibial
430 accelerations [59]. Since a greater vibration amplitude was denoted without kinematics alterations

431 after short and intense exercises, these results confirmed that the protective mechanism of
432 muscle tuning is altered by fatigue.

433 Among the four experimental studies on fatigue and STV, only [17] quantified the
434 peripheral and central origins of neuromuscular fatigue. In the other experiments on short and
435 intense running exercise [12,24,29], neuromuscular fatigue was not assessed and runners were
436 considered exhausted when unable to maintain the pace. One experimental study quantified
437 changes in vibration frequency after fatigue and found no changes in the vibration peak
438 frequency [29]. As the vibration frequency is related to the mass and stiffness of the muscle (Eq.2)
439 [20], the stability of vibration frequency after exhaustion may reflect that the soft tissue stiffness
440 and mass were not altered in fatigued state. However, no definitive conclusion can be made as
441 only one study investigated this parameter, and more studies are needed to confirm this finding.

442

443 **Table 3.** Effect of fatigue on soft tissue vibrations

Reference	Participants details (Level | Gender | Age | Weight | Height)	Running protocol (Surface | Intensity | Duration | End of protocol)	Device measuring STV| Locations | Frequency | Time measurement	Effects of Fatigue
DOWNHILL				
Ehrström et al. (2018)	Well trained male runners | M = 13 | 38.6 ± 5.7 yrs | 72.1 ± 4.7 kg | 175.8 ± 5.1 cm	Treadmill with -8.5° slope | 55% $VO2_{max}$= 4.2 ± 0.3 m/s| 40 min | 40 min	Tri-axial accelerometers VL and GM 1000 Hz Non-FAT: 4-5 min and 9-10 min FAT: 34-35 min and 39-40 min	For VL: RMS Ar ↗ (11.6 ± 5.9 %) For GM: RMS Ar ↔
FLAT EXHAUSTION				
Friesenbichler et al. (2011)	Recreational runners | M = 3 | 26.7 ± 2.3 yrs | 65.3 ± 3.3 kg | 173.8. ± 3.8 cm F = 7 | 31.7 ± 7.3 yrs | 60.1 ± 6.4 kg | 165.5 ± 4.3 cm	230-m outdoor track|F : 3.1 ± 0.2 m/s, M : 3.8 ± 0.3 m/s | 10.4 ± 2.4 km | No longer able to maintain the required speed for 3 consecutive laps (690 m)	Tri-axial accelerometer TS 2400 Hz Non-FAT : 50 steps during the first 5 laps FAT : 50 steps during the last 5 laps	For TS: v. PSD ↗ (n.i) v. f_{mean} ↔ Time to peak ↗ (n.i.)
Khassetarash et al. (2015b)	Professionnal male runners | M = 8 | 26 ± 3.6 yrs | 65 ± 12kg | 175 ± 6 cm	Treadmill | 4 m/s | 9.6 ± 1.2 km | No longer able to run at the given speed or running distance more than 10 km	Tri-axial accelerometer GM 2000 Hz Non-FAT: first minute FAT: last minute	For GM: v. $f_{amplitude}$ ↗ (between 20 and 300 %) Damping ↗ (20.3 ± 2.3 %)
Khassetarash et al. (2019)	Semi-professional middle- and long-distance male runners | M = 11 | 32.7 ± 9.94 yrs | 65.9 ± 9.86 kg | 174.3 ± 4.63 cm	Treadmill | 4.3 ± 0.3 m/s | 15 ± 1.75 km| No longer able to maintain their preferred high level of effort speed.	Tri-axial accelerometer GL 2000 Hz Non-FAT and FAT: 5 strides average within 10 equal intervals (88 ± 26 sec)	For GL v. a_{peak} ↗ (29.8 ± 3.44 %) Damping ↗ (15.5 ± 0.65 %) Energy dissipation ↗ (70.6 ± 0.49 %) Settling time ↔

444 *M: Male, F: Female, n. i.: non-indicated, VL: Vastus Lateralis, GM: Gastrocnemius Medialis, GL: Gastrocnemius*
445 *Lateralis, TS: Triceps Surae, Non-FAT: non-fatigued state, FAT: fatigued state, RMS Ar: Root Mean Square*
446 *Acceleration resultant, PSD: Power Spectral Density,* f_{mean}*: Mean frequency,* $f_{amplitude}$*: Amplitude frequency,*
447 a_{peak}*: Peak acceleration, v.: vertical, ↘: significant decrease, ↔: no significant change, ↗ significant increase.*

448 ## 5 FINAL COMMENTS AND RECOMMENDATIONS

449 From a methodological point of view, STV should be quantified with skin-mounted
450 accelerometers at a sampling frequency equal or greater than 1000 Hz. In addition, all
451 acceleration axis, and/or the resultant acceleration, should be analysed. For data processing,
452 time-frequency approaches such as CWT or EMD should be employed as they are the most
453 adapted in extracting the relevant STV parameters for non-stationary signals. Vibration should
454 be described with at least one parameter for the amplitude, frequency and damping.

455 Quantification of input signals (i.e. ground reaction forces, acceleration at the tibia or the
456 heel), lower limb muscle activity and identification of the foot strike pattern seem necessary to

assess whether neuromuscular adaptations occur. Thus, investigating the effect of footwear or fatigue on STV requires a complete biomechanical assessment (i.e. electromyography, kinetics, kinematics, accelerometry).

A number of future research directions regarding STV are worth considering. Specifically, the relationship between running kinematics and STV should be assessed to better understand how motor organisation may affect STV properties. In addition, research on sport shoes should focus on identifying functional groups in order to better adapt the characteristics of the shoes to the subjects' ones. The differences between female, male, young and old runners STV should be explored in the future. Finally, the effects of fatigue on STV should be investigated for prolonged running exercises, and include an evaluation of the neuromuscular fatigue such as the loss of force, and if possible, more specific information on central and peripheral fatigue.

Acknowledgments: This study was partly funded by Amer Sports Footwear. The authors would like to thank Dr Callum Brownstein for the English editing of the manuscript.

Author's contribution:

M.C.P. and R.T. selected references, summarise them, and wrote the initial draft. These authors have contributed equally to this work.

M.G., C.H., J.R. and G.Y.M conceived the presented idea and did specifically critical review, commentary and revision.

Conflicts of interest: none declared

479

480

25

481 6 REFERENCES

482 1. Souron R, Besson T, Millet GY, Lapole T. Acute and chronic neuromuscular adaptations
483 to local vibration training. *European Journal of Applied Physiology.*
484 2017;117(10):1939-1964. doi:10.1007/s00421-017-3688-8

485 2. Lafortune MA, Lake MJ. D O M I N a N T Role of Interface Over Knee Angle for
486 Cushioning Impact Loading a N D Regulating Initial. *Journal of biomechanics.*
487 1996;29(12):1523-1529.

488 3. Milner CE, Ferber R, Pollard CD, Hamill J, Davis IS. Biomechanical factors associated
489 with tibial stress fracture in female runners. *Medicine and Science in Sports and*
490 *Exercise.* 2006;38(2):323-328. doi:10.1249/01.mss.0000183477.75808.92

491 4. Du BB, Bigelow PL, Wells RP, Davies HW, Hall P, Johnson PW. The impact of
492 different seats and whole-body vibration exposures on truck driver vigilance and
493 discomfort. *Ergonomics.* 2018;61(4):528-537. doi:10.1080/00140139.2017.1372638

494 5. Chadefaux D, Rao G, Androuet P, Berton E, Vigouroux L. Active tuning of stroke-
495 induced vibrations by tennis players. *Journal of Sports Sciences.* 2017;35(16):1643-
496 1651. doi:10.1080/02640414.2016.1227868

497 6. Shorten M, Mientjes MIV. The "heel impact" force peak during running is neither "heel"
498 nor "impact" and does not quantify shoe cushioning effects. *Footwear Science.*
499 2011;3(1):41-58. doi:10.1080/19424280.2010.542186

500 7. Chadefaux D, Gueguen N, Thouze A, Rao G. 3D propagation of the shock-induced
501 vibrations through the whole lower-limb during running. *Journal of Biomechanics.*
502 2019;96(xxxx):109343. doi:10.1016/j.jbiomech.2019.109343

503 8. Nassar AA, Almudhaffar MA. Vibration of bones: A case study on human femur.

504 *Journal of Engineering Sciences*. 2014;14(2):229-239. doi:10.17605/OSF.IO/E546S

505 9. Wakeling JM, Nigg BM. Modification of soft tissue vibrations in the leg by muscular
506 activity. *Journal of Applied Physiology*. 2001;90(2):412-420.
507 doi:10.1152/jappl.2001.90.2.412

508 10. Cavanagh and Lafortune MA. GRF in distance running. *Journal of Biomechanics*.
509 1980;13.

510 11. Boyer KA, Nigg BM. Soft tissue vibrations within one soft tissue compartment.
511 2006;39:645-651. doi:10.1016/j.jbiomech.2005.01.027

512 12. Khassetarash A, Hassannejad R, Ettefagh MM, Sari-Sarraf V. Fatigue and soft tissue
513 vibration during prolonged running. *Human Movement Science*. 2015;44:157-167.
514 doi:10.1016/j.humov.2015.08.024

515 13. Trama R, Blache Y, Hautier C. Effect of rocker shoes and running speed on lower limb
516 mechanics and soft tissue vibrations. *Journal of Biomechanics*. 2019;82:171-177.
517 doi:10.1016/j.jbiomech.2018.10.023

518 14. Sheerin KR, Reid D, Besier TF. The measurement of tibial acceleration in runners—A
519 review of the factors that can affect tibial acceleration during running and evidence-
520 based guidelines for its use. *Gait and Posture*. 2019;67:12-24.
521 doi:10.1016/j.gaitpost.2018.09.017

522 15. Lafortune MA. Three-dimensional acceleration of the tibia during walking and running.
523 *Journal of Biomechanics*. 1991;24(10). doi:10.1016/0021-9290(91)90166-K

524 16. Gellaerts J, Pirard M, Muzic J, Peseux M, Ménétrier A. Maximalist vs. minimalist shoes:
525 Dose-effect response of elastic compression on muscular oscillations. *Journal of Sports*
526 *Medicine and Physical Fitness*. 2017;57(10):1290-1298. doi:10.23736/S0022-

4707.16.06721-9

17. Ehrström S, Gruet M, Giandolini M, Chapuis S, Morin J-B, Vercruyssen F. Acute and Delayed Neuromuscular Alterations Induced by Downhill Running in Trained Trail Runners: Beneficial Effects of High-Pressure Compression Garments. *Frontiers in Physiology*. 2018;9(November). doi:10.3389/fphys.2018.01627

18. Broatch JR, Brophy-Williams NED, Phillips EJ, et al. Compression Garments Reduce Muscle Movement and Activation during Submaximal Running. *Medicine and Science in Sports and Exercise*. 2020;52(3):685-695. doi:10.1249/MSS.0000000000002182

19. Borràs X, Balius X, Drobnic F, Til L, Turmo A, Valle J. Effects of lower body compression garment in muscle oscillation and tissular injury during intense exercise. *Portuguese Journal of Sport Sciences*. 2011;11(2):685-688.

20. Smeathers JE. Transient Vibrations Caused by Heel Strike. *Proceedings of the Institution of Mechanical Engineers, Part H: Journal of Engineering in Medicine*. 1990;204(2):135-137. doi:10.1243/PIME_PROC_1990_204_244_02

21. Boyer KA, Nigg BM. Muscle activity in the leg is tuned in response to impact force characteristics. *Journal of Biomechanics*. 2004;37(10):1583-1588. doi:10.1016/j.jbiomech.2004.01.002

22. Giandolini M, Romain J-P, Horvais N, Nigg BM. Midsole Properties Affect the Amplitude of Soft-Tissue Vibrations in Heel–Toe Runners. *Medicine & Science in Sports & Exercise*. 2019;(October):1. doi:10.1249/mss.0000000000002194

23. Nikooyan AA, Zadpoor AA. Mass-spring-damper modelling of the human body to study running and hopping-an overview. *Proceedings of the Institution of Mechanical Engineers, Part H: Journal of Engineering in Medicine*. 2011;225(12):1121-1135.

550 doi:10.1177/0954411911424210

551 24. Khassetarash A, Hassannejad R, Ettefagh MM, Oskouei AE. Vibration settling time of
552 the gastrocnemius remains constant during an exhaustive run in rear foot strike runners.
553 *Journal of Biomechanics*. 2019;93(July):140-146. doi:10.1016/j.jbiomech.2019.06.026

554 25. Boyer KA, Nigg BM. Quantification of the input signal for soft tissue vibration during
555 running. *Journal of Biomechanics*. 2007;40(8):1877-1880.
556 doi:10.1016/j.jbiomech.2006.08.008

557 26. Nigg BM, Wakeling JM. Impact forces and muscle tuning: A new paradigm. *Exercise*
558 *and Sport Sciences Reviews*. 2001;29(1):37-41. doi:10.1097/00003677-200101000-
559 00008

560 27. Martyn R. S, Darcy S. W. Spectral Analysis of impact Shock During Running.
561 *International Journal of sport biomechanics*. 1992:288-304.

562 28. Enders H, von Tscharner V, Nigg BM. Analysis of damped tissue vibrations in time-
563 frequency space: A wavelet-based approach. *Journal of Biomechanics*.
564 2012;45(16):2855-2859. doi:10.1016/j.jbiomech.2012.08.027

565 29. Friesenbichler B, Stirling LM, Federolf P, Nigg BM. Tissue vibration in prolonged
566 running. *Journal of Biomechanics*. 2011;44(1):116-120.
567 doi:10.1016/j.jbiomech.2010.08.034

568 30. Enders H, von Tscharner V, Nigg BM. The effects of preferred and non-preferred
569 running strike patterns on tissue vibration properties. *Journal of Science and Medicine*
570 *in Sport*. 2014;17(2):218-222. doi:10.1016/j.jsams.2013.03.015

571 31. Giandolini M, Bartold S, Horvais N. Interaction between body composition and impact-
572 related parameters in male and female heel-toe runners. *Gait and Posture*.

2019;70(March):355-360. doi:10.1016/j.gaitpost.2019.03.026

32. Khassetarash A, Hassannejad R, Enders H, Ettefagh MM. Damping and energy dissipation in soft tissue vibrations during running. *Journal of Biomechanics*. 2015;48(2):204-209. doi:10.1016/j.jbiomech.2014.11.051

33. Trama R, Hautier C, Blache Y. Input and Soft-Tissue Vibration Characteristics during Sport-Specific Tasks. *Medicine & Science in Sports & Exercise*. 2019;(20):1. doi:10.1249/mss.0000000000002106

34. Boyer KA, Nigg BM. Changes in muscle activity in response to different impact forces affect soft tissue compartment mechanical properties. *Journal of Biomechanical Engineering*. 2007;129(4):594-602. doi:10.1115/1.2746384

35. Boyer KA, Nigg BM. Muscle Tuning During Running : Implications of an Un-tuned Landing. 2016;128(December 2006). doi:10.1115/1.2354202

36. Nigg BM, Baltich J, Hoerzer S, Enders H. Running shoes and running injuries: Mythbusting and a proposal for two new paradigms: "Preferred movement path" and "comfort filter." *British Journal of Sports Medicine*. 2015;49(20):1290-1294. doi:10.1136/bjsports-2015-095054

37. Giandolini M, Poupard T, Gimenez P, et al. A simple field method to identify foot strike pattern during running. *Journal of Biomechanics*. 2014;47(7):1588-1593. doi:10.1016/j.jbiomech.2014.03.002

38. Ahn AN, Brayton C, Bhatia T, Martin P. Muscle activity and kinematics of forefoot and rearfoot strike runners. *Journal of Sport and Health Science*. 2014;3(2):102-112. doi:10.1016/j.jshs.2014.03.007

39. Hamill J, Gruber AH, Derrick TR. Lower extremity joint stiffness characteristics during

596 running with different footfall patterns. *European Journal of Sport Science.*
597 2014;14(2):130-136. doi:10.1080/17461391.2012.728249

598 40. Kulmala JP, Avela J, Pasanen K, Parkkari J. Forefoot strikers exhibit lower running-
599 induced knee loading than rearfoot strikers. *Medicine and Science in Sports and*
600 *Exercise.* 2013;45(12):2306-2313. doi:10.1249/MSS.0b013e31829efcf7

601 41. Almeida MO, Davis IS, Lopes AD. BIOMECHANICAL DIFFERENCES OF FOOT
602 STRIKE PATTERNS DURING RUNNING : A SYSTEMATIC REVIEW WITH
603 META-ANALYSIS Masters and Doctoral Program in Physiotherapy , Universidade
604 Cidade de São Paulo (UNICID), SP , Brasil Department of Physical Medicine and
605 Rehabili. *Journal of Orthopaedic & Sports Physical Therapy.* 2015;45(10):738-755.
606 https://pubmed.ncbi.nlm.nih.gov/26304644/.

607 42. Nigg BM, Wakeling JM. Impact forces and muscle tuning: A new paradigm. *Exercise*
608 *and Sport Sciences Reviews.* 2001;29(1):37-41. doi:10.1097/00003677-200101000-
609 00008

610 43. Wakeling JM, Nigg BM, Rozitis AI. Muscle activity damps the soft tissue resonance
611 that occurs in response to pulsed and continuous vibrations. *Journal of Applied*
612 *Physiology.* 2002;93(3):1093-1103. doi:10.1152/japplphysiol.00142.2002

613 44. Martínez A, Lam CKY, von Tscharner V, Nigg BM. Soft tissue vibration dynamics after
614 an unexpected impact. *Physiological Reports.* 2019;7(2):1-11.
615 doi:10.14814/phy2.13990

616 45. Chen CH, Yang WW, Chen YP, Chen VCF, Liu C, Shiang TY. High vibration frequency
617 of soft tissue occurs during gait in power-trained athletes. *Journal of Sports Sciences.*
618 2021;39(4):439-445. doi:10.1080/02640414.2020.1824366

619 46. Jalali P, Noorani MRS, Hassannejad R, Ettefagh MM. Modeling the central nervous
620 system functionality in controlling the calf muscle activity during running with sport
621 shoes. *Proceedings of the Institution of Mechanical Engineers, Part H: Journal of*
622 *Engineering in Medicine*. 2019;233(2):254-266. doi:10.1177/0954411918821390

623 47. Coza A. Compression apparel effects on soft tissue vibrations. 2008.
624 doi:10.16258/j.cnki.1674-5906.2006.01.022

625 48. Giandolini M, Munera M, Chiementin X, Bartold S, Horvais N. Footwear influences
626 soft-tissue vibrations in rearfoot strike runners. *Footwear Science*. 2017;9(May):S25-
627 S27. doi:10.1080/19424280.2017.1313902

628 49. Gruber AH, Boyer KA, Derrick TR, Hamill J. Impact shock frequency components and
629 attenuation in rearfoot and forefoot running. *Journal of Sport and Health Science*.
630 2014;3(2):113-121. doi:10.1016/j.jshs.2014.03.004

631 50. Edwards WB, Derrick TR, Hamill J. Musculoskeletal attenuation of impact shock in
632 response to knee angle manipulation. *Journal of Applied Biomechanics*.
633 2012;28(5):502-510. doi:10.1123/jab.28.5.502

634 51. Zadpoor AA, Nikooyan AA. Modeling muscle activity to study the effects of footwear
635 on the impact forces and vibrations of the human body during running. *Journal of*
636 *Biomechanics*. 2010;43(2):186-193. doi:10.1016/j.jbiomech.2009.09.028

637 52. Hoerzer S, Tscharner V Von, Nigg BM. Defining functional Groups based on running
638 kinematics using self-Organizing Maps and support vector Machines. *Journal of*
639 *Biomechanics*. 2015. doi:10.1016/j.jbiomech.2015.03.017

640 53. Behling AV, Tscharner V von, Giandolini M, Nigg B. Strategies to reduce soft-tissue
641 vibrations in running. *Footwear Science*. 2019;11(sup1):S210-S211.

642 doi:10.1080/19424280.2019.1606338

643 54. Trama R, Hautier CA, Souron R, Lapole T, Fouré A. Is accelerometry an effective
644 method to assess muscle vibrations in comparison to ultrafast ultrasonography ?
645 2020;(june 2019). doi:10.1109/TBME.2020.3035838

646 55. Hoerzer S, Trudeau MB, Edwards WB, Nigg BM. Intra-rater reliability of footwear-
647 related comfort assessments. *Footwear Science*. 2016;8(3):155-163.
648 doi:10.1080/19424280.2016.1195451

649 56. Zadpoor AA, Nikooyan AA. The effects of lower-extremity muscle fatigue on the
650 vertical ground reaction force: A meta-analysis. *Proceedings of the Institution of*
651 *Mechanical Engineers, Part H: Journal of Engineering in Medicine*. 2012;226(8):579-
652 588. doi:10.1177/0954411912447021

653 57. Vernillo G, Aguiar M, Savoldelli A, et al. Regular changes in foot strike pattern during
654 prolonged downhill running do not influence neuromuscular, energetics, or
655 biomechanical parameters. *European Journal of Sport Science*. 2020;20(4):495-504.
656 doi:10.1080/17461391.2019.1645212

657 58. Degache F, Guex K, Fourchet F, et al. Changes in running mechanics and spring-mass
658 behaviour induced by a 5-hour hilly running bout. *Journal of Sports Sciences*.
659 2013;31(3):299-304. doi:10.1080/02640414.2012.729136

660 59. Giandolini M, Gimenez P, Temesi J, et al. Effect of the fatigue induced by a 110-km
661 ultramarathon on tibial impact acceleration and lower leg kinematics. *PLoS ONE*.
662 2016;11(3). doi:10.1371/journal.pone.0151687

The Journal of Open Source Software

fctSnPM: Factorial ANOVA and post-hoc tests for Statistical nonParametric Mapping in MATLAB

Robin Trama[1], **Christophe A Hautier**[1], **and Yoann Blache**[1]

1 Univ. Lyon, UCBL-Lyon 1, Laboratoire Interuniversitaire de Biologie de la Motricité, EA 7424, F 69622, Villeurbanne, France

DOI: 10.21105/joss.03159

Software

- Review
- Repository
- Archive

Editor: Christopher R. Madan

Reviewers:

- @0todd0000
- @nicholst

Submitted: 12 November 2020
Published: 14 July 2021

Summary

Statistical Parametric Mapping (SPM) is a statistical method originally used in neuroimaging developed in the early 90's in biomedical imaging, allowing to determine which brain zones were solicited during a functional MRI (Friston et al., 1995). Originally developed for a three dimensional analysis, the application of this method to the analysis of vectors or matrices was made possible thanks to Pataky (2010) whom allows to perform statistical inference on curves (vectors - 1D) or maps (matrices - 2D).

As in "classical" statistics on scalar values (0D), there is a parametric and a non-parametric approach to the SPM method. While the parametric method is based on random gaussian fields, the non-parametric method is based on label permutation tests (Nichols & Holmes, 2002), and thus, on re-sampling and randomness to make statistical inference. The main advantage of the non-parametric approach is that a gaussian distribution of the data is not required, making possible it to work with both curves and maps.

Statement of need

Most of physiological data measured during human movement are continuous and expressed in function of time. However, researchers predominantly analyze extracted scalar values from the continuous measurement, as the mean, the maximum, the amplitude, or the integrated value over the time. Analyzing continuous values (i.e., time series) can provide more information than extracted indicators, as the later discards one dimension of the data among the magnitude and localization in time. In addition, oscillatory signals such as muscle vibrations and electromyograms contain information in the temporal and frequency domains. However, scalar analysis reduces the information at only one dimension by discarding two dimensions among the magnitude and the localization in the time and/or frequency domain.

To analyze all the dimensions of a signal without losing information, the analysis of curves or maps was proposed, coded, and put online by Pataky. However, the use of the proposed functions does not allow the analysis of 2D data automatically. Moreover, a rather frequent error is to consider only the significance of the last statistical test performed and not the intersection between the post-hoc tests and the ANOVA. Indeed, a difference between two samples can be significant if, and only if the ANOVA is significant in the same areas. The spm1d package, redistributed with fctSnPM at `./fctSnPM/src/spm1d_Pataky` is published elsewhere, and thus is not part of this JOSS review.

The Journal of Open Source Software

fctSnPM

The function we propose meets two objectives. 1/ to allow statistical inferences on curves and maps with a standardized format and 2/ to simplify analyses by comparing means while considering intersections with tests performed upstream (ANOVA and post-hoc of main effects).

The statistical tests are performed taking into account the independent and repeated measure effects provided in the obligatory function inputs. ANOVA, up to three-way ANOVA with three repeated measures, is performed if required, and followed by post-hoc tests as paired or independent Student t-tests. By default, the ANOVA is performed with an alpha risk of 5%, while post-hoc tests alpha risk is adjusted with Bonferronni correction. A number of 10/alpha permutations (200 for a 5% risk) is defined for each test. Statistical parameters are customizable via optional inputs, like `multiPerm` which can be used to increase the number of permutations and achieve numerical stability and reliable analysis (Nichols & Holmes, 2002). A Matlab (.mat) file containing the number of permutations, the significant clusters, the statistical thresholds, and the raw data used in the analysis is also generated for each test family.

To interpret the results, figures directly usable for presentations and/or articles are available. In one dimension, the main figure contains the mean and standard deviations for each group of the analyzed condition, and the results of the post-hoc tests corrected with the result of the ANOVA. In two dimensions, the mean maps and the standard deviations are on two separate figures, and the result of the statistical analysis is displayed on the map of differences between two modalities. Therewith, other figures that display absolute and relative differences, effect sizes, and the raw value of the statistical test and its threshold are available.

To personalize the figures, Matlab (.fig) files are implemented to perform a posteriori modifications, and optional inputs are available to a priori customize the figures. These parameters are gathered in three categories: 1/ general plot parameters working identically for one and two dimensions, acting on axis labels and limits, image resolution and size 2/ one dimension parameters that act on the characteristics of the curves like color and transparency, or the position of the statistical analysis relatively to curves 3/ two dimensions parameters acting on the colormap and its limits, as well as the color of the statistical test displayed on map of differences.

This function was already used in Trama et al. (2021) to compare soft-tissue and muscle vibrations of the *vastus lateralis*. It is currently used to assess modifications of soft-tissue vibrations caused by mountain ultra-marathons, the effect of the pedaling phase on *quadriceps* soft-tissue vibrations, and differences in isokinetic torque after ACL operation and rehabilitation.

References

Friston, KJ., Holmes, AP., Worsley, KJ., Poline, JB., Frith, CD., & Frackowiak, RSJ. (1995). Statistical parametric maps in functional imaging: a general linear approach. *Human Brain Mapping*, *2*, 189–210. https://doi.org/10.1002/hbm.460020402

Nichols, TE., & Holmes, AP. (2002). Nonparametric permutation tests for functional neuroimaging: a primer with examples. *Human Brain Mapping*, *15*, 1–25. https://doi.org/10.1002/hbm.1058

Pataky, TC. (2010). Generalized n-dimensional biomechanical field analysis using statistical parametric mapping. *Journal of Biomechanics*, *43*, 1976–1982. https://doi.org/10.1016/j.jbiomech.2010.03.008

Trama, R., Hautier, C., Souron, R., Lapole, T., Fouré, A., & Blache, Y. (2021). Is accelerometry an effective method to assess muscle vibrations in comparison to ultrafast

ultrasonography. *IEEE Transactions on Biomedical Engineering*, *68*, 1409–1416. https://doi.org/10.1109/TBME.2020.3035838

Author's unedited version
IEEE article at : https://ieeexplore.ieee.org/document/9248640?denied=
Accepted 04 Nov. 2020 : 10.1109/TBME.2020.3035838

Is accelerometry an effective method to assess muscle vibrations in comparison to ultrafast ultrasonography?

Robin Trama, Christophe A. Hautier, Robin Souron, Thomas Lapole, Alexandre Fouré, and Yoann Blache

***Abstract*— *Objective:* The purpose of this study was to assess whether accelerometry effectively reflects muscle vibrations measured with ultrafast ultrasonography. *Methods:* Vibration characteristics initiated on the *vastus lateralis* muscle by an impactor were compared when assessed with accelerometry and ultrasonography. Continuous wavelet transforms and statistical parametric mapping (SPM) were performed to identify discrepancies in vibration power over time and frequency between the two devices. *Results:* The SPM analysis revealed that the accelerometer underestimated the muscle vibration power above 50 Hz during the first 0.06 seconds post impact. Furthermore, the accelerometer overestimated the muscle vibration power under 20 Hz, from 0.1 seconds after the impact. Linear regression revealed that the thicker the subcutaneous fat localized under the accelerometer, the more the muscle vibration frequency and damping were underestimated by the accelerometer. *Conclusion:* The skin and the fat tissues acted like a low-pass filter above 50 Hz and oscillated in a less damped manner than the muscle tissue under 20 Hz. *Significance:* To eliminate some artifacts caused by the superficial tissues and assess the muscle vibration characteristics with accelerometry, it is suggested to 1) high-pass filter the acceleration signal at a frequency of 20 Hz, under certain conditions, and 2) include participants with less fat thickness. Therefore, the subcutaneous thickness must be systematically quantified under each accelerometer location to clarify the differences between subjects and muscles.**

***Index Terms*—Acceleration, Continuous wavelet transforms, Damping, Statistical parametric mapping**

I. Introduction

SOFT tissue vibrations have been widely studied for various purposes over the past three decades. The first objective of these studies was to assess the vibration characteristics, such as amplitude, main and median frequencies, and damping properties [1]–[6]. Thereafter, studies aimed to better understand muscular activity tuning in response to impact and its effect on vibration (i.e., the muscle tuning paradigm) [7]–[12]. Then, some researchers demonstrated that muscular fatigue generated an increase in the vibration amplitude [13]–[15]. Currently, there is growing interest in assessing the influence of sports equipment on the decrease of soft tissue vibrations [15]–[21]. Notably, in all the aforementioned studies, soft tissue vibrations were quantified with accelerometers attached to the skin. Although accelerometry is the most applicable method for assessing soft tissue vibrations, this approach involves the recording of the accelerations of all the soft tissue packages, namely, the skin, the subcutaneous fat, and the muscle. Considering that muscle injuries [22], [23] and fatigue [24] can be caused by vibrations, the characterization of muscle vibrations, rather than the vibrations of the overall soft tissue package, is of greater interest. A previous study reported that muscle and other soft tissues do not share the same mechanical properties [25]; therefore, soft tissue vibrations measured by accelerometry might not accurately reflect muscle vibrations.

Recently, ultrafast ultrasound devices have been used to quantify continuous vibrations of a spinal bone [26] and the quadriceps muscles vibrating at frequencies below 10 Hz [27]. Analysis of such vibrations was performed using high-frequency image recording combined with image tracking algorithms. Although the vibrations were of a lower frequency and amplitude than those usually observed during sports activities, ultrasonography is a promising tool to assess impact-induced muscle vibrations without influence from the vibrations of the other soft tissues (i.e., the skin or subcutaneous fat). To the best of our knowledge, no study has assessed whether significant differences between accelerometry and ultrasonography may be observed when estimating muscle vibrations. Nevertheless, identifying such potential discrepancies could contribute to a better characterization of muscle vibrations assessed in realistic conditions with accelerometry.

Consequently, the purpose of this study was to determine whether a skin-mounted accelerometer reflects muscle vibrations assessed with ultrafast ultrasonography in a relaxed or contracted muscle. Based on a previous study [25], we hypothesized that soft tissue vibrations assessed with an accelerometer would be of greater amplitude, of lower frequency, and with reduced damping properties than muscle vibrations assessed with ultrasonography.

R. Trama, C. A. Hautier, A. Fouré, and Y. Blache are with the Univ. Lyon, UCBL-Lyon 1, Laboratoire Interuniversitaire de Biologie de la Motricité, EA 7424, F-69622, Villeurbanne, France (e-mail: robin.trama@univ-lyon1.fr).

R. Souron, and T. Lapole are with Univ. Lyon, UJM-Saint-Etienne, Laboratoire Interuniversitaire de Biologie de la Motricité, EA 7424, F-42023, Saint-Etienne, France.

IEEE article at : https://ieeexplore.ieee.org/document/9248640?denied=
Accepted 04 Nov. 2020 : 10.1109/TBME.2020.3035838

II. Material and Methods

A. Participants

A group of 15 participants composed of 12 men and 3 women (25.1 ± 4.4 years, 176 ± 6 cm, 70.7 ± 9.8 kg) volunteered to participate in this study. All the participants were healthy and free from lower-limb injury. The study was approved by the local university ethics committee, according to the statement of ethical principles of the Declaration of Helsinki, and the participants signed an informed consent document.

B. Instrumentation

An electromyogram (EMG) of the *vastus lateralis* of the right leg was recorded at 1000 Hz with pairs of surface electrodes (Delsys, Natick, Massachusetts, USA). An Aixplorer ultrasound device was used with an SL15-4 probe (Supersonic Imagine, Aix-en-Provence, France) to obtain video of the *vastus lateralis* vibrations (1000 Hz). The soft tissue acceleration of the thigh as well as the probe acceleration (± 50 g, 1000 Hz) were recorded with two biaxial accelerometers (Mega Electronics, Kuopio, Finland).

C. Procedure and data collection

Participants were seated on a custom-built isometric knee-extensor ergometer, with the hip and knee angles set at 90° and the chest secured with a safety belt. After having shaved and cleaned the skin with alcohol, surface electromyographic electrodes were placed on the *vastus lateralis* belly, according to SENIAM recommendations [28]. Before the experiment, participants performed a standardized warm-up consisting of ten incremental isometric knee extensions of 5 seconds. After a 3-minute rest period, participants performed two maximum voluntary isometric contractions to determine the maximal EMG signal and normalize the *vastus lateralis* activation level (see Data treatment section below).

Testing consisted of an assessment of *vastus lateralis* accelerations induced by an external shock, using a pendulum impactor (i.e., a reflex hammer was dropped from an angle of 45° with respect to the vertical). The position of the impactor was adjusted so that the impact was administered 6 cm distally from the location of the muscle-vibration measurement device. Shocks were administered under a relaxed condition (4 shocks) and a contracted condition (4 shocks at 40% of the maximal activation). Visual feedback of the 0.05-second normalized root-mean-square EMG of the *vastus lateralis* was displayed on a computer screen to help the participant achieve the 40% ± 10% target activation level. The impact was administered when the activation level was reached.

For each condition, two-dimensional *vastus lateralis* vibrations were measured with both an ultrasound device and an accelerometer. The ultrasound probe was positioned perpendicularly to the longitudinal axis of the thigh and proximally to the EMG electrodes. The position of the probe, ensuring two-dimensional analysis of the muscle vibrations along the mediolateral and anteroposterior axes of the thigh (Fig. 1), was marked on the skin, and the probe was clamped with a mechanical arm. A water-based gel was applied between the skin and the probe to avoid probe-skin contact. The position of the probe was adjusted between the relaxed and contracted conditions to keep the probe out of contact with the skin when the muscle expanded and, therefore, avoid any pressure from the probe on the skin. Once all the shocks were administered, the probe was replaced by the accelerometer, which was placed at the same location and oriented in the same direction as the probe. Thereafter, the same procedure was performed. Finally, the subcutaneous thigh fat thickness was measured with a skin caliper (the average of three measurements) at the location of the ultrasound probe and the accelerometer.

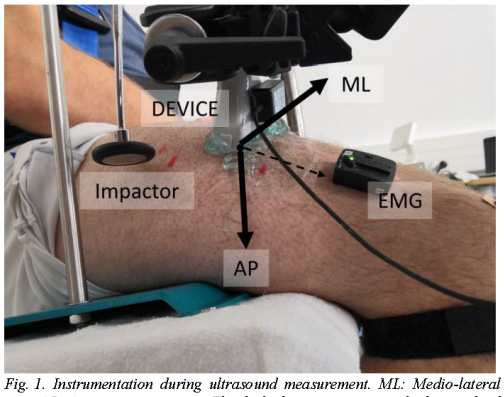

Fig. 1. Instrumentation during ultrasound measurement. ML: Medio-lateral axis; AP: Antero-posterior axis. The dashed arrow represents the longitudinal axis, orthogonal to the two others, but was not quantified in this study. DEVICE: Accelerometer or Ultrasonography.

D. Data treatment

The entire data treatment process was computed with MATLAB R2018b (MathWorks, Natick, Massachusetts, USA). Raw EMG signals of the *vastus lateralis* were run through a Butterworth bandpass filter between 10 Hz and 499 Hz. Thereafter, the root-mean-square envelope of the signal was calculated with a window length of 0.05 seconds. The signals were normalized for each participant with the mean values of the greatest 0.5-second plateau obtained during the two maximal contractions. The mean EMG was calculated from 0.5 seconds to the 0.05 seconds before the impact to avoid the noise caused by the shock [29].

Vastus lateralis accelerations were firstly computed from ultrasonographic images (bandwidth = 7.5 MHz, acquisition frequency = 1000 Hz, resolution = 256 pixels [width] x 180 pixels [height], field of view = 5 cm [width] x 2.5 cm [height]). When the *vastus lateralis* was located at the center of the image while relaxed or contracted, the upper zone of the muscles just below the subcutaneous fat was manually selected. Then, the binary robust invariant scalable keypoints (BRISK) algorithm [30], [31] was used to detect a maximum of 300 points within the selected zone. The point trajectories over time were then tracked to obtain the mediolateral and anteroposterior displacements of each point (videos are presented in supplementary files). A Butterworth bandpass filter between 10 Hz and 130 Hz was applied to the displacement of the points, and then the displacement signal was derived twice to obtain

IEEE article at : https://ieeexplore.ieee.org/document/9248640?denied=
Accepted 04 Nov. 2020 : 10.1109/TBME.2020.3035838

the point acceleration in the two directions. Points with a maximum acceleration above 5 m·s^{-2} were included, and the mean acceleration of these points was analyzed. Acceleration signals from the accelerometers (i.e., the skin and probe) were filtered with a Butterworth bandpass filter between 10 Hz and 130 Hz.

Acceleration signals of the tissues assessed with ultrasonography and accelerometry in the two-dimensional axis were investigated in the time-frequency domain with a continuous wavelet transform, using a filter bank with a Morse mother wavelet with $\gamma = 3$ and $P^2 = 60$ [32]. The modulus of the coefficients produced by the wavelet transform was computed and expressed as power as a function of time and frequency, $p(t, f)$. The mean maps of the four trials for each condition and each participant were considered for analysis. Only the signal powers ranging from 10 Hz to 130 Hz during the 0.25 seconds after the impact were analyzed [6], [33]. Consequently, the power maps were composed of 30250 nodes (250 nodes [time] x 121 nodes [frequency])

Additionally, three variables (main frequency, median frequency, and damping properties) were extracted from the power maps. The energy spectrum, *E(f)*, representing the energy at each frequency, was computed by integrating the signal power of each frequency over the time interval (1):

$$E(f) = \int_{t=0}^{0.25} p(t,f)\, dt. \quad (1)$$

The main and median frequencies were computed from the energy spectrum. The main frequency corresponded to the frequency with the most energy and the median frequency to the frequency that split the spectrum into two equal parts.

The overall measured power as a function of time, *P(t)*, was computed by integrating the power with respect to the frequency (2):

$$P(t) = \int_{f=10}^{130} p(t,f)\, \mathrm{d}f. \quad (2)$$

The damping properties (*D*) were computed from the overall signal power with an optimization algorithm, which minimized the sum of the squared difference between the measured and the theoretical power decay of the vibration [12], [33]. The algorithm optimized the *D* between the instants when the power decay was maximal (T1) and when the power was equal to 10% of the power at T1 (T2) (3):

$$\min_{D} \mathrm{J} = \sum_{t=T1}^{T2} (P_{T1} \cdot e^{-D \cdot t} - P(t))^2, \quad (3)$$

where P_{T1} is the measured power at T1, and $P_{T1} \cdot e^{-D \cdot t}$ is the theoretical power decay.

Finally, trials for which the peak acceleration of the probe of the ultrasound device was above 5 m·s^{-2} for at least one axis were excluded from the data analysis.

E. Statistics

Using the spm1d package for MATLAB [34], statistical parametric mapping (SPM) analysis was conducted in two dimensions on the power maps obtained from the wavelet transform. The SPM analysis requires a 1D-1D continuum, while power maps corresponded to a 2D-1D continuum (i.e., the power [1D] is represented as a function of time and frequency [2D]). In line with a previous study using 2D-1D SPM analysis [35], the maps were flattened into a 1D-1D continuum to allow for comparisons between the conditions and then reshaped to their original dimensions for interpretation of the results. Power maps were analyzed with a two-way analysis of variance (ANOVA) on repeated measures (i.e., *device*: accelerometer vs. ultrasound; *muscle activation level*: relaxed vs. contracted). Considering the independent analysis of the mediolateral and anteroposterior axes, the level of significance was set at 2.5% (α = 0.05/2). Then, post hoc tests with the Bonferroni correction were performed when appropriate. To find the *F*- or *t*-value corresponding to the level of significance mentioned above, a permutation test was used. The latter is a non-parametric statistical approach consisting of permutations of the labels between the different conditions, which allows the derivation of the appropriate statistical distribution directly from the data [36]. To achieve numerical stability, the number of permutations was set at 100/α (e.g., 4000 permutations for each ANOVA).

Using R software (v3.5.0, R Core Team, Vienna, Austria), linear mixed models [37] were used to investigate the effect of the device (fixed effect) and muscular activation level (fixed effect) on the *vastus lateralis* mean EMG, main and median frequencies, and damping properties. All the trials were included in the models, and the fixed effects were set as random intercepts and slopes to adapt the model to each participant's performance. The χ^2 and p-values were obtained from likelihood ratio tests, which were conducted by testing the full model against the model without the effect tested. The alpha error (5%) was corrected with the Holm-Bonferroni method. When an interaction was observed, the two fixed effects were tested independently in each category of the other effect. Then, Tukey HSD post hoc comparisons were performed. The normality, homoscedasticity, and linearity of the linear mixed model residuals were graphically controlled.

Therewith, effect sizes (ESs) were calculated with Hedges' *g* for each node of the power maps and each variable. Furthermore, the ESs for the power maps were corrected for a non-normal data distribution [38].

The mean relative differences between the values obtained with accelerometry and ultrasonography were calculated for the main and median frequencies and damping properties. Linear regressions were performed between these mean relative differences and the subcutaneous fat thickness for each axis and level of activation. A total of 12 regressions were performed, and the alpha risk (5%) was corrected with the Holm-Bonferroni method. When statistically significant, correlations were classified as *strong* if Pearson's $|r|$ range was between 0.6 and 0.79 and *very strong* if greater than or equal to 0.8.

IEEE article at : https://ieeexplore.ieee.org/document/9248640?denied=
Accepted 04 Nov. 2020 : 10.1109/TBME.2020.3035838

III. Results

The thigh fat thickness assessed with the skin caliper ranged from 4 mm to 18 mm (mean ± *SD*: 9.7 ± 4.1 mm). The mean peak accelerations of the probe in the mediolateral and anteroposterior directions were 2.1 ± 0.5 $m \cdot s^{-2}$ and 2.2 ± 0.6 $m \cdot s^{-2}$, respectively. These accelerations were, respectively, 20.3 ± 8.2 and 16.1 ± 7.0 times lower than the peak acceleration of the muscle assessed with ultrasonography. Concerning the muscular activation, linear mixed models depicted no interaction (p = 0.71, χ^2 = 0.1) or device effect (p = 0.98, χ^2 = 0.0), whereas the contracted condition led to a significantly greater mean EMG compared to the relaxed condition (p < 0.001, ES = 8.1; Fig. 2).

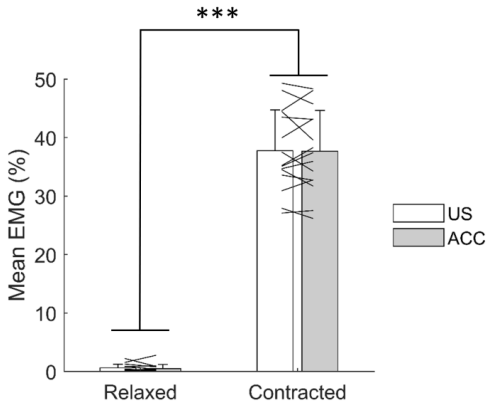

Fig. 2. Vastus lateralis *activation (mean ± SD) for the two conditions and the two devices. Black lines represent subject specific changes. US: Ultrasonography, ACC: Accelerometry. ***: p<0.001.*

A. Power map analysis

1) Mediolateral axis

The SPM ANOVA of the power maps (Fig. 3) revealed an interaction between the activation level and the device (clusters A' and C'), as well as the main effects of the device (clusters A, B_1, and B_2) and activation level (clusters C and D).

The effect of the device was observed in three clusters. Firstly, signal power between 50 Hz and 90 Hz during the first 0.06 seconds (cluster A) was 30% to 50% lower (-3 au on average) measured with accelerometry compared to ultrasonography (ES: 0.9 to 1.3). Due to an interaction effect, cluster A' was larger (up to 130 Hz) when the muscle was contracted. Secondly, cluster B may be divided into two sub-clusters. The signal power between 20 Hz and 130 Hz from 0.15 seconds (B_1) measured 150% to 250% greater (0.2 au on average) with accelerometry than with ultrasonography (ES: 2.0 to 3.0). By contrast, under 20 Hz (B_2), the signal power was 300% to 600% greater (1 au on average) when measured with accelerometry (ES: 1.4 to 1.8).

Furthermore, the effect of the activation level was represented by two distinct clusters. The first cluster (C), located between 45 Hz and 130 Hz during the first 0.1 seconds, depicted an increased power of 100% to 400% (4 au on average) for the contracted condition (ES: 1 to 1.5). Due to an interaction effect, this cluster was larger for ultrasonography (C'). The second cluster (D) was located between 10 Hz and 20 Hz during the first 0.2 seconds and exhibited a lower power of 30% to 60% (2.5 au on average) for the contracted condition (ES: 1.2 to 2).

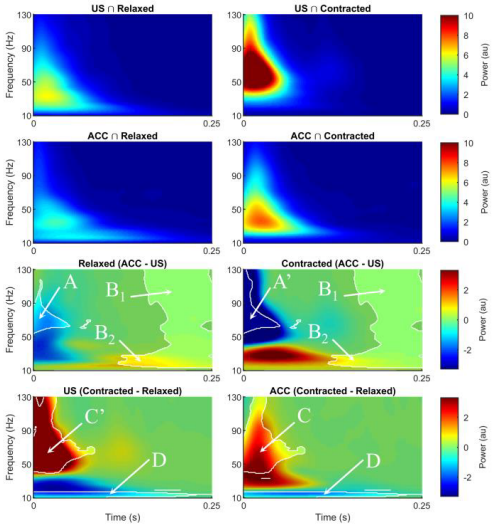

Fig. 3. From top to bottom; rows 1 and 2: mean power map for each condition of the medio-lateral axis; row 3: differences between devices for each activation condition, row 4: differences between activation conditions for each device. The enlighten clusters (A, B_1, B_2, C, and D) correspond to significant differences between two conditions. Clusters with an apostrophe (C') depicted an interaction effect within the cluster. US: Ultrasonography, ACC: Accelerometry.

2) Anteroposterior axis

The SPM ANOVA of the power maps (Fig. 4) revealed an interaction effect between the activation level and the device (clusters E', F', and G'), as well as the main effects of the device (clusters E, F, G, and H) and the activation level (clusters I and J).

The effect of the device was represented by four clusters. Firstly, from 0.05 to 0.12 seconds and between 70 Hz and 130 Hz (clusters E and E'), signal power was 40% to 60% (1 au on average) and 150% to 200% (3 au on average) greater when measured with accelerometry (ESs: 0.5 to 1.2 and 1 to 1.8) for a relaxed and contracted muscle, respectively. Secondly, power between 20 Hz and 50 Hz during the first 0.12 seconds (cluster F) was 200% to 500% (6 au on average) greater when measured with accelerometry (ES: 1.9 to 2.3). The third cluster (G) was located under 15 Hz and depicted 250% to 350% (1 au average) more power when measured with accelerometry (ES: 0.5 to 0.8). Due to an interaction effect, clusters F' and G' were larger and interrelated when the muscle was relaxed. The power between 20 Hz and 130 Hz from 0.15 seconds (cluster H) was

IEEE article at : https://ieeexplore.ieee.org/document/9248640?denied=
Accepted 04 Nov. 2020 : 10.1109/TBME.2020.3035838

300% to 600% (0.2 au on average) greater when measured with accelerometry (ES: 2.0 to 4.0).

Furthermore, the effect of the activation level on the power maps was observed in two distinct clusters. The first cluster (I), between 50 Hz and 120 Hz during the first 0.12 seconds, depicted 100% to 500% (6 au) more power when the muscle was contracted (ES: 1.2 to 2.2). The second cluster (J) was located between 15 Hz and 20 Hz during the first 0.2 seconds and exhibited 30% to 60% (3 au average) less power for the contracted condition (ES: 0.8 to 1.4).

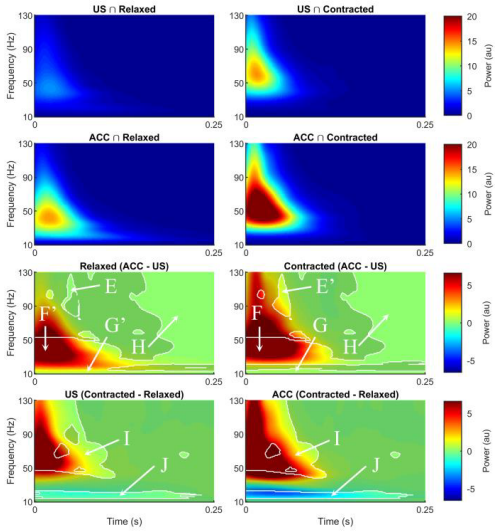

Fig. 4. From top to bottom; rows 1 and 2, mean power map for each condition of the antero-posterior axis; row 3: differences between devices for each activation condition, row 4: differences between activation conditions for each device. The enlighten clusters (E, F, G, H, I, and J) correspond to significant differences between two conditions. Clusters with an apostrophe (E', F', and G') depicted an interaction effect within the cluster. US: Ultrasonography, ACC: Accelerometry.

B. *Extracted variables*

Firstly, interaction effects on the main frequency were revealed for both axes ($p < 0.001$, $\chi^2 = 80.2$ and $p < 0.01$, $\chi^2 = 10.0$ for the mediolateral and anteroposterior axes, respectively; Table 1). Lower main frequencies were computed with accelerometry compared to ultrasonography, more significantly for a contracted muscle than for a relaxed one (-49%, $p < 0.001$, ES = 3.9 compared to -35%, $p < 0.001$, ES = 1.5 and -18%, $p < 0.01$, ES = 1.2 compared to -13%, $p < 0.01$, ES = 0.6 for the mediolateral and anteroposterior axes, respectively). Moreover, higher main frequencies were observed when the muscle was contracted than relaxed, though less significantly when quantified with accelerometry rather than ultrasonography (+50%, $p < 0.001$, ES = 1.6 compared to +93%, $p < 0.001$, ES = 3.5 and +46%, $p < 0.001$, ES = 1.6 compared to +53%, $p < 0.001$, ES = 2.5 for the mediolateral and anteroposterior axes, respectively).

Secondly, interaction effects were revealed for the mediolateral axis on the median frequency ($p < 0.001$, $\chi^2 = 102.6$; Table 1). Lower median frequencies were observed when quantified with accelerometry than with ultrasonography, more significantly for a contracted muscle than for a relaxed one (-38%, $p < 0.001$, ES = 4.1 compared to -20%, $p < 0.001$, ES = 1.2). Higher frequencies were observed for a contracted muscle than for a relaxed one, less significantly when quantified with accelerometry compared to ultrasonography (+25%, $p < 0.001$, ES = 2.2 compared to +44%, $p < 0.001$, ES = 3.3). Additionally, for the anteroposterior axis, only the main effects of the activation level and device were found (Table 1). Lower median frequencies were quantified with accelerometry compared to ultrasonography (-14%, $p < 0.001$, ES = 0.9), and higher frequencies were observed when the muscle was contracted rather than relaxed (+29%, $p < 0.001$, ES = 2.1).

Finally, the main effects of the activation level and device on the damping properties were calculated (Table 1). Reduced damping properties were found when quantified with accelerometry compared to ultrasonography (-37%, $p < 0.001$, ES = 1.4 and -15%, $p < 0.01$, ES = 0.7 for the mediolateral and anteroposterior axes, respectively). Greater damping properties were observed for a contracted muscle compared to a relaxed one (+66%, $p < 0.001$, ES = 1.6 and +14%, $p < 0.01$, ES = 0.6 for the mediolateral and anteroposterior axes, respectively).

TABLE I
VIBRATIONS CHARACTERISTICS

Variables	Axes	US ∩ Relaxed	ACC ∩ Relaxed	US ∩ Contracted	ACC ∩ Contracted
Main Frequency (Hz)	ML	28.3 ± 8.1 *	18.5 ± 4.6	54.6 ± 6.8 #$	27.7 ± 7.0 *
	AP	35.4 ± 7.9 *	30.7 ± 8.4	54.2 ± 7.0 #$	44.7 ± 8.6 *
Median Frequency (Hz)	ML	42.5 ± 6.5 *	35.6 ± 4.4	61.2 ± 4.5 #$	44.4 ± 3.7 *
	AP	49.6 ± 4.8 *	42.2 ± 5.5	63.5 ± 5.2 #$	55.4 ± 5.4 *
Damping (/s)	ML	25.7 ± 7.5 *	14.9 ± 3.4	40.7 ± 5.8 #$	26.7 ± 4.8 *
	AP	34.5 ± 4.0 *	30.3 ± 6.5	40.4 ± 9.9 #$	33.5 ± 7.6 *

Mean ± SD of the main, median frequencies and damping. US: Ultrasonography; ACC: Accelerometry. ML: medio-lateral axis; AP: antero-posterior axis. * means different of ACC ∩ Relaxed; # for different of US ∩ Relaxed; $ when different of ACC ∩ Contracted.

C. *Correlation with thigh fat thickness*

Significant correlations were found for the anteroposterior axis (Fig.5). For an increase of 1 mm of subcutaneous fat, the relative difference of the main frequency between ultrasonography and accelerometry increased on average by 3.4% for a contracted muscle (*strong*). The relative differences for the median frequency between the two devices also increased on average by 2.4% and 1.7% per 1 mm of fat thickness for a relaxed (*very strong*) and contracted (*strong*) muscle, respectively. The relative differences in damping

properties increased on average by 3.4% per 1 mm of fat for a relaxed muscle (*very strong*).

IV. Discussion

The purpose of this study was to determine whether a skin-mounted accelerometer reflects muscle vibrations assessed with ultrafast ultrasonography in a relaxed and contracted muscle. Compared to the ultrasound, the accelerometer overestimated the muscle vibration power under 20 Hz at the end of the vibration and underestimated the muscle vibration power above 50 Hz during the first 0.06 seconds after an impact for both the relaxed and contracted conditions. These discrepancies made the accelerometer underestimate the main and median frequencies, as well as the damping properties of the muscle. Furthermore, the differences observed between the two devices were greater when thigh fat thickness increased.

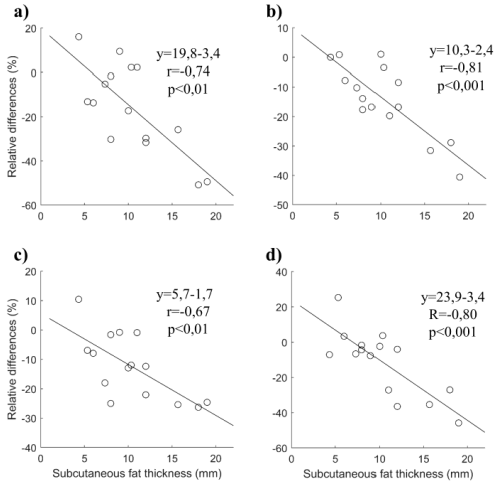

Fig. 5. Linear correlations between the subcutaneous fat thickness and the mean relative differences among accelerometry and ultrasonography on the antero-posterior axis for a) the main frequency on a contracted muscle, b) the median frequency for a relaxed and c) for a contracted muscle, d) the damping properties on a relaxed muscle.

A. Methodological considerations

To better characterize muscle behavior after an external impact, some methodological choices were made. Considering that a muscle tends to damp the vibrations as soon as an impact is initiated [3], the location of the probe and accelerometer with respect to the muscle belly had to be the same when comparing the measurement methods. Consequently, the recordings could not be performed simultaneously with the two devices. Therefore, precautions were taken to ensure that the two measurements were performed on the same location under uniform conditions. To that end, the mean muscular activation had to be similar when vibrations were recorded with either accelerometry or ultrasonography. We also ensured that vibrations generated by the impactor were minimally transmitted to the ultrasound probe during ultrasonographic measurement.

Different factors were considered in analyzing the ultrasound imaging videos. Our tracking method differed from previous studies aimed at tracking vibrations with ultrasound videos [26], [27]. As the muscle does not behave like a rigid body, a sliding window was not suitable for our purpose. Likewise, previous analysis of the data indicated that corner detection methods such as the Kanade-Lucas-Tomasi algorithm were not optimal, as the points tracked often disappeared during maximal amplitude acceleration. Thus, the BRISK algorithm [30] for detecting features (i.e., corners and the zones around them) appeared to be more appropriate. Furthermore, as the shockwave did not travel through all the points tracked, some points remained motionless over time. Therefore, a minimum limit of 5 $m \cdot s^{-2}$ was set to ensure that only the points undergoing vibration were included in the computation of average acceleration.

Consequently, the acceleration signals obtained from the ultrasound videos were considered to reflect the vibrations of the muscle only and not those of the other soft tissues.

B. Bias induced by superficial tissues

The extracted variables quantified with accelerometry aligned with a previous study reporting that the soft tissue vibrations of the *vastus lateralis* induced by an impactor have a main frequency ranging from 10 Hz to 40 Hz and damping properties from 10 s^{-1} to 60 s^{-1} for a relaxed and fully activated muscle, respectively [1]. However, these values were lower than those obtained from the muscle with ultrasonographic measurement. The power map analysis revealed that superficial tissues biased the vibration signal of the muscle by amplifying the power under 20 Hz and attenuating it above 50 Hz when estimated with accelerometry. The additional power observed with the accelerometer under 20 Hz at the end of the vibration may be explained by the lower stiffness and damping properties of the superficial tissues [25]. On the contrary, the lower power observed with the accelerometer above 50 Hz just after the impact may be the consequence of the superficial tissues acting like a low-pass filter [25]. Furthermore, we observed that an increase in the fat thickness intensifies the underestimation of the frequency content and damping properties of the muscle vibrations. This outcome aligns with the map analyses; on one hand, a lower power above 50 Hz causes a lower median frequency, and on the other hand, a greater power under 20 Hz at the end of the vibration involves decreased damping properties and a lower main frequency. Other differences in power at the end of the vibration and above 20 Hz were observed. These differences were small (0.2 au) relative to the total vibration power and may correspond to signal noise.

Similarly to a previous study [1], increasing muscular activation led to increased damping properties and higher main and median frequencies. More specifically, the increase in the frequency content from the relaxed to contracted muscle was greater when observed with ultrasonography compared to accelerometry. As discussed above, these discrepancies may be explained by the superficial tissues amplifying energy under 20 Hz and attenuating energy above 50 Hz. Thus, the

superficial tissues decrease the sensitivity of the accelerometer to capture changes in vibration characteristics between a relaxed and contracted muscle, especially when the subcutaneous fat is thicker

Accurate characterization of muscle vibrations could engender a better understanding of the muscle tuning paradigm [7], help in assessing muscle properties [1], and clarify the effects of fatigue or sports equipment on soft tissue vibration characteristics [15]. For instance, previous studies indicated that little or none of the energy of the input localized above 50 Hz was transmitted to the soft tissues [2], [39]. This result might be due to the underestimation of the vibration power above this limit by the accelerometer. Thus, muscles might vibrate at frequencies above 50 Hz during activities like running. Moreover, some authors have defined damping properties as the work performed by the muscle to damp vibration [5], [7]. Hence, the underestimation of damping when measured with an accelerometer may lead to an underestimation of the work performed by the muscle.

C. *Practical applications*

The use of accelerometry during sports activities is the most applicable method for soft tissue vibration assessment outside a laboratory. Despite some under- and over-estimations, accelerometry can reflect the effects of muscular activation and can be used to detect differences in frequency content or damping during sports activities. However, our results indicate that accelerometers should be used with caution, and some suggestions are proposed for using the full potential of accelerometry. Firstly, a muscle contracted at 40% vibrates at a higher frequency than the superficial tissues. In this case, a 20-Hz high-pass filtering of the signal can remove some artifacts caused by the superficial tissues vibrating at a frequency below 20 Hz. However, as a relaxed muscle vibrates at a frequency around 20 Hz, this filter may also remove some muscle vibrations and, therefore, should not be used. Secondly, the inclusion of subjects with thinner subcutaneous fat tissue can limit the under- and over-estimation of the power induced by the accelerometry method at some frequencies. Quantification of the subcutaneous fat thickness under the location of each accelerometer is recommended, especially when comparisons between individuals are performed (e.g., men vs. women). Since our experimental protocol was not designed to develop correction algorithms for the accelerometry signal, further studies are needed to address this issue.

D. *Limitations*

The results in the present study were obtained after an administered shock to the lateral part of the *vastus lateralis* muscle, which may differ from values recorded during sports activities, as the amplitude of the vibrations was smaller than in running or landing [39]. Furthermore, only the upper zone of the *vastus lateralis* muscle was studied, and our outcomes may not be inferred to other muscles. Moreover, as the muscle damps the vibrations along its fibers, further explorations are needed to determine the effect of the spatial location of the measuring device on the findings of the present study.

All measurements were firstly performed with ultrasonography and then with accelerometry. No randomization between the conditions could have been made, as the ultrasonography measurement had to be completed before the accelerometry measurement to determine the zone of interest. However, contractions were submaximal, and a rest period was allowed between each shock; thus, the first measurements should not alter the rest of the experiment.

V. Conclusion

The comparison between skin-mounted accelerometry and ultrafast ultrasonography revealed that the accelerometer exhibited limitations in accurately assessing muscle vibrations. More precisely, superficial tissues modify the acceleration signal when quantified by accelerometry compared to ultrasonography, by amplifying the vibration power under 20 Hz and attenuating it above 50 Hz. Moreover, when the subcutaneous fat was thicker, the underestimation of the damping properties and vibration frequency was greater. Consequently, accelerometry seems to be an appropriate method to depict the salient characteristics of muscle vibrations; however, the outcomes should be considered cautiously with respect to fat thickness. Further studies are needed to develop correction algorithms for muscle vibrations estimated with accelerometry, especially during sports activities.

VI. Conflict of interest statement

The authors declare no conflict of interest.

References

[1] J. M. Wakeling and B. M. Nigg, "Modification of soft tissue vibrations in the leg by muscular activity," *J. Appl. Physiol.*, vol. 90, no. 2, pp. 412–420, 2001.

[2] J. M. Wakeling, B. M. Nigg, and A. I. Rozitis, "Muscle activity damps the soft tissue resonance that occurs in response to pulsed and continuous vibrations," *J. Appl. Physiol.*, vol. 93, no. 3, pp. 1093–1103, Sep. 2002, doi: 10.1152/japplphysiol.00142.2002.

[3] K. A. Boyer and B. M. Nigg, "Soft tissue vibrations within one soft tissue compartment," *J. Biomech.*, vol. 39, no. 4, pp. 645–651, Jan. 2006, doi: 10.1016/j.jbiomech.2005.01.027.

[4] K. A. Boyer and B. M. Nigg, "Changes in Muscle Activity in Response to Different Impact Forces Affect Soft Tissue Compartment Mechanical Properties," *J. Biomech. Eng.*, vol. 129, no. 4, p. 594, 2007, doi: 10.1115/1.2746384.

[5] H. Enders, V. von Tscharner, and B. M. Nigg, "The effects of preferred and non-preferred running strike patterns on tissue vibration properties," *J. Sci. Med. Sport*, vol. 17, no. 2, pp. 218–222, Mar. 2014, doi: 10.1016/j.jsams.2013.03.015.

[6] A. Khassetarash, R. Hassannejad, H. Enders, and M. M. Ettefagh, "Damping and energy dissipation in soft tissue vibrations during running," *J. Biomech.*, vol. 48, no. 2, pp. 204–209, Jan. 2015, doi: 10.1016/j.jbiomech.2014.11.051.

[7] B. M. Nigg and J. M. Wakeling, "Impact forces and muscle tuning: a new paradigm," *Exerc. Sport Sci. Rev.*, vol. 29, no. 1, pp. 37–41, 2001.

[8] B. M. Nigg and W. Liu, "The effect of muscle stiffness and damping on simulated impact force peaks during running," *J. Biomech.*, vol. 32, no. 8, pp. 849–856, 1999.

[9] J. M. Wakeling, A.-M. Liphardt, and B. M. Nigg, "Muscle activity reduces soft-tissue resonance at heel-strike during walking," *J. Biomech.*, vol. 36, no. 12, pp. 1761–1769, Dec. 2003, doi: 10.1016/S0021-9290(03)00216-1.

[10] K. A. Boyer, "Muscle Tuning During Running: Implications of an Untuned Landing," *J. Biomech. Eng.*, vol. 128, no. 6, p. 815, Jun. 2006, doi: 10.1115/1.2354202.

[11] K. A. Boyer and B. M. Nigg, "Muscle activity in the leg is tuned in response to impact force characteristics," *J. Biomech.*, vol. 37, no. 10, pp. 1583–1588, Oct. 2004, doi: 10.1016/j.jbiomech.2004.01.002.

[12] A. Martínez, C. K.-Y. Lam, V. von Tscharner, and B. M. Nigg, "Soft tissue vibration dynamics after an unexpected impact," *Physiol. Rep.*, vol. 7, no. 2, p. e13990, Jan. 2019, doi: 10.14814/phy2.13990.

[13] B. Friesenbichler, L. M. Stirling, P. Federolf, and B. M. Nigg, "Tissue vibration in prolonged running," *J. Biomech.*, vol. 44, no. 1, pp. 116–120, Jan. 2011, doi: 10.1016/j.jbiomech.2010.08.034.

[14] A. Khassetarash, R. Hassannejad, M. M. Ettefagh, and V. Sari-Sarraf, "Fatigue and soft tissue vibration during prolonged running," *Hum. Mov. Sci.*, vol. 44, pp. 157–167, Dec. 2015, doi: 10.1016/j.humov.2015.08.024.

[15] S. Ehrström, M. Gruet, M. Giandolini, S. Chapuis, J.-B. Morin, and F. Vercruyssen, "Acute and Delayed Neuromuscular Alterations Induced by Downhill Running in Trained Trail Runners: Beneficial Effects of High-Pressure Compression Garments," *Front. Physiol.*, vol. 9, Nov. 2018, doi: 10.3389/fphys.2018.01627.

[16] W. Fu, Y. Liu, and S. Zhang, "Effects of Footwear on Impact Forces and Soft Tissue Vibrations during Drop Jumps and Unanticipated Drop Landings," *Int. J. Sports Med.*, vol. 34, no. 06, pp. 477–483, Nov. 2012, doi: 10.1055/s-0032-1327696.

[17] W. Fu, X. Wang, and Y. Liu, "Impact-induced soft-tissue vibrations associate with muscle activation in human landing movements: An accelerometry and EMG evaluation," *Technol. Health Care*, vol. 23, no. s2, pp. S179–S187, Jun. 2015, doi: 10.3233/THC-150952.

[18] W. Fu, Y. Fang, Y. Gu, L. Huang, L. Li, and Y. Liu, "Shoe cushioning reduces impact and muscle activation during landings from unexpected, but not self-initiated, drops," *J. Sci. Med. Sport*, vol. 20, no. 10, pp. 915–920, Oct. 2017, doi: 10.1016/j.jsams.2017.03.009.

[19] R. Trama, Y. Blache, and C. Hautier, "Effect of rocker shoes and running speed on lower limb mechanics and soft tissue vibrations," *J. Biomech.*, vol. 82, pp. 171–177, Jan. 2019, doi: 10.1016/j.jbiomech.2018.10.023.

[20] F. Hintzy, N. Gregoire, P. Samozino, X. Chiementin, W. Bertucci, and J. Rossi, "Effect of thigh-compression shorts on muscle activity and soft tissue vibration during cycling.:," *J. Strength Cond. Res.*, p. 1, Dec. 2017, doi: 10.1519/JSC.0000000000002402.

[21] M. Giandolini, M. Munera, X. Chiementin, S. Bartold, and N. Horvais, "Footwear influences soft-tissue vibrations in rearfoot strike runners," *Footwear Sci.*, vol. 9, no. sup1, pp. S25–S27, Jun. 2017, doi: 10.1080/19424280.2017.1313902.

[22] L. Necking, L. Dahlin, J. Friden, G. Lundborg, R. Lundstrom, and L. Thornell, "Vibration-induced muscle injury An experimental model and preliminary findings," *J. Hand Surg. J. Br. Soc. Surg. Hand*, vol. 17, no. 3, pp. 270–274, Jun. 1992, doi: 10.1016/0266-7681(92)90113-G.

[23] M. de Hoyo *et al.*, "Impact of an acute bout of vibration on muscle contractile properties, creatine kinase and lactate dehydrogenase response," *Eur. J. Sport Sci.*, vol. 13, no. 6, pp. 666–673, Nov. 2013, doi: 10.1080/17461391.2013.774052.

[24] J. Rittweger, M. Mutschelknauss, and D. Felsenberg, "Acute changes in neuromuscular excitability after exhaustive whole body vibration exercise as compared to exhaustion by squatting exercise," *Clin. Physiol. Funct. Imaging*, vol. 23, no. 2, pp. 81–86, 2003.

[25] J. E. Smeathers, "Transient vibrations caused by heel strike," *Proc. Inst. Mech. Eng. Part H*, vol. 203, no. 4, pp. 181–186, 1989, doi: 10.1243/PIME_PROC_1989_203_036_01.

[26] T. Kaddoura, A. Au, G. Kawchuk, R. Uwiera, R. Fox, and R. Zemp, "Non-invasive spinal vibration testing using ultrafast ultrasound imaging: A new way to measure spine function," *Sci. Rep.*, vol. 8, no. 1, p. 9611, Dec. 2018, doi: 10.1038/s41598-018-27816-0.

[27] D. Yamada, A. Degirmenci, and R. Howe, "Ultrasound Imaging for Identifying Dynamics of Soft Tissue," *IEEE 15th Int. Symp. Biomed. Imaging ISIB 2018*, pp. 1161–1165, Apr. 2018.

[28] H. J. Hermens, B. Freriks, C. Disselhorst-Klug, and G. Rau, "Development of recommendations for SEMG sensors and sensor placement procedures," *J. Electromyogr. Kinesiol.*, vol. 10, no. 5, pp. 361–374, Oct. 2000, doi: 10.1016/S1050-6411(00)00027-4.

[29] A. Fratini, M. Cesarelli, P. Bifulco, and M. Romano, "Relevance of motion artifact in electromyography recordings during vibration treatment," *J. Electromyogr. Kinesiol.*, vol. 19, no. 4, pp. 710–718, Aug. 2009, doi: 10.1016/j.jelekin.2008.04.005.

[30] S. Leutenegger, M. Chli, and R. Y. Siegwart, "BRISK: Binary Robust invariant scalable keypoints," in *2011 International Conference on Computer Vision*, Barcelona, Spain, Nov. 2011, pp. 2548–2555, doi: 10.1109/ICCV.2011.6126542.

[31] S. A. K. Tareen and Z. Saleem, "A comparative analysis of SIFT, SURF, KAZE, AKAZE, ORB, and BRISK," in *2018 International Conference on Computing, Mathematics and Engineering Technologies (iCoMET)*, Sukkur, Mar. 2018, pp. 1–10, doi: 10.1109/ICOMET.2018.8346440.

[32] J. M. Lilly and S. C. Olhede, "Higher-Order Properties of Analytic Wavelets," *IEEE Trans. Signal Process.*, vol. 57, no. 1, pp. 146–160, Jan. 2009, doi: 10.1109/TSP.2008.2007607.

[33] H. Enders, V. von Tscharner, and B. M. Nigg, "Analysis of damped tissue vibrations in time-frequency space: a wavelet-based approach," *J. Biomech.*, vol. 45, no. 16, pp. 2855–2859, Nov. 2012, doi: 10.1016/j.jbiomech.2012.08.027.

[34] T. C. Pataky, "Generalized n-dimensional biomechanical field analysis using statistical parametric mapping," *J. Biomech.*, vol. 43, no. 10, pp. 1976–1982, Jul. 2010, doi: 10.1016/j.jbiomech.2010.03.008.

[35] T. C. Pataky, "Spatial resolution in plantar pressure measurement revisited," *J. Biomech.*, vol. 45, no. 12, pp. 2116–2124, Aug. 2012, doi: 10.1016/j.jbiomech.2012.05.038.

[36] T. E. Nichols and A. P. Holmes, "Nonparametric permutation tests for functional neuroimaging: A primer with examples," *Hum. Brain Mapp.*, vol. 15, no. 1, pp. 1–25, Jan. 2002, doi: 10.1002/hbm.1058.

[37] D. Bates, M. Mächler, B. Bolker, and S. Walker, "Fitting Linear Mixed-Effects Models Using lme4," *J. Stat. Softw.*, vol. 67, no. 1, pp. 1–48, 2015, doi: 10.18637/jss.v067.i01.

[38] K. Kelley, "The Effects of Nonnormal Distributions on Confidence Intervals Around the Standardized Mean Difference: Bootstrap and Parametric Confidence Intervals," *Educ. Psychol. Meas.*, vol. 65, no. 1, pp. 51–69, Feb. 2005, doi: 10.1177/0013164404264850.

[39] R. Trama, C. Hautier, and Y. Blache, "Input and Soft-Tissue Vibration Characteristics during Sport-Specific Tasks:," *Med. Sci. Sports Exerc.*, p. 1, Jul. 2019, doi: 10.1249/MSS.0000000000002106.

4.2 INFLUENCE DES FACTEURS EXTERNES SUR LA VIBRATIONS

R. Trama, Y. Blache, C. Hautier. (2019a). Effect of rocker shoes and running speed on lower limb mechanics and soft tissue vibrations. Journal of Biomechanics, Vol. 82, pp. 171–177. 10.1016/j.jbiomech.2018.10.023

R. Trama, C. Hautier, Y. Blache. (2020). Input and Soft-Tissue Vibration Characteristics during Sport-Specific Tasks. Medicine & Science in Sports & Exercise, Vol. 52, No. 1, pp. 112–119. 10.1249/MSS.0000000000002106

R. Trama, T. Le Solliec, Y. Blache, C. Hautier. Heel Impact, Tibial Shock and Soft Tissue Vibrations in young basketball players: influence of movements and court construction. Numéro spécial congrès de la société de biomécanique, Computer Methods in Biomechanics and Biomedical Engineering (Accepté)

R. Trama, C. Hautier, Y. Blache. (2019b). Sport-related impact classification through a convolutional neural network. Computer Methods in Biomechanics and Biomedical Engineering, Vol. 22, No. sup1, pp. 267–269. 10.1080/10255842.2020.1714908

R. Trama, Y. Blache, F. Hintzy, J. Rossi, G. Y Millet, C. Hautier. Does neuromuscular fatigue generated by mountain ultra-marathon modify foot impact and soft-tissue vibrations during running? Medecine & Science in Sports & Exercise (Soumis)

4.2.1 Effet du type de pratique sportive

4.2.1.1 Influence de la vitesse de course et du type de mouvement

La plupart des études portant sur la vibration des tissus mous se sont focalisées sur la course à pied (Boyer & Nigg, 2004; Nigg et al., 1987) ou des réceptions de saut (Fu et al., 2015). Bien que lors de ces études différentes vitesses de course (Boyer & Nigg, 2004; Nigg et al., 1987) ou hauteurs de sauts (Fu et al., 2015) soient comparées, aucune étude n'a mesuré lors d'un même protocole ces deux mouvements en comparaison à des mouvements plus spécifiques aux sports collectifs. Les mouvements de sports collectifs, présentant des profils de force de réaction au sol différents de la course à pied (Kong et al., 2018), pourraient engendrer des vibrations différentes. Se focaliser sur ce type de mouvement a un double intérêt car cela permettra de 1) quantifier la charge vibratoire en fonction du type de pratique, et 2) de mieux comprendre comment le muscle vibre en fonction des caractéristiques de l'appui lors de l'impact au sol.

L'objectif des trois prochaines études était d'évaluer l'influence de la vitesse de course, des mouvements spécifiques aux sports collectifs, et des mouvements spécifiques au basketball, sur l'impact au sol et sur la vibration des tissus mous du membre inférieur.

Pour faire varier les conditions de pratique, la première étude se focalisait sur différentes vitesses de course, de 8 à 15.5 $km \cdot h^{-1}$, tandis que la deuxième et la troisième étude comparaient une condition de course à allure préférentielle à d'autres mouvements. Les participants de la seconde étude ont effectué différents mouvements de sports collectifs, comme des rebonds, des changements de directions, des pas latéraux et des fentes avant, et des réceptions de saut. Pour la troisième étude, des réceptions de sauts, du sprint, et un double pas (mouvement spécifique au basketball) ont été effectués. Lors de ces trois études, l'impact au sol a été mesuré grâce à une plateforme de force (étude 1) ou un accéléromètre positionné au niveau du talon de la chaussure (études 2 et 3), les vibrations des tissus mous du *gastrocnemius medialis* (étude 1, 2 et 3) et du *vastus lateralis* (étude 1 et 2) ont été mesurées avec des accéléromètres. L'amplitude, la fréquence, et l'amortissement de la vibration ont été quantifiés grâce à une transformée en ondelettes continue. Des modèles linéaires mixtes ont été utilisés pour comparer les différentes vitesses de course lors de la première étude, et pour comparer les différents mouvements lors

de la seconde étude. Une analyse SnPM a été réalisée sur les contenus fréquentiels des vibrations pour comparer les différents mouvements lors de la troisième étude.

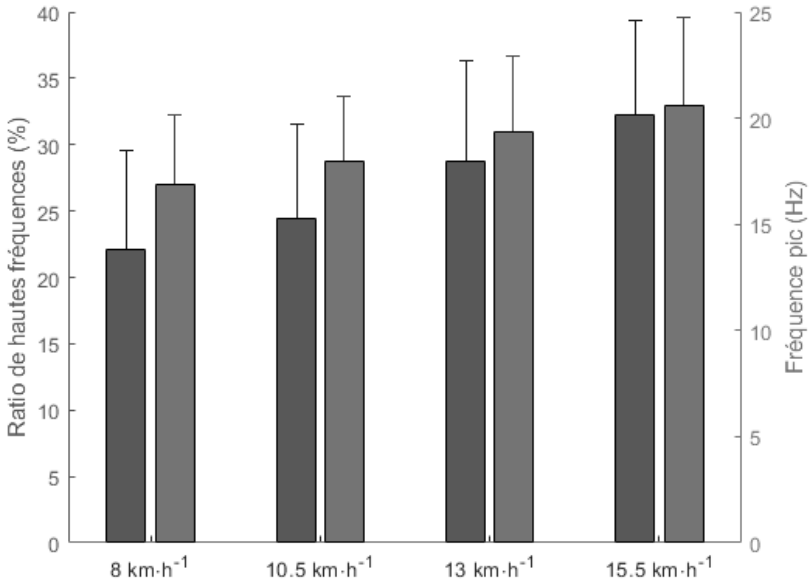

Figure 25 : Effet de la vitesse de course sur le ratio de hautes fréquences (foncé) et la fréquence principale de vibration (clair) du gastrocnemius medialis. Les barres ayant des lettres différentes sont significativement différentes. Adapté de Trama et al. (2019a).

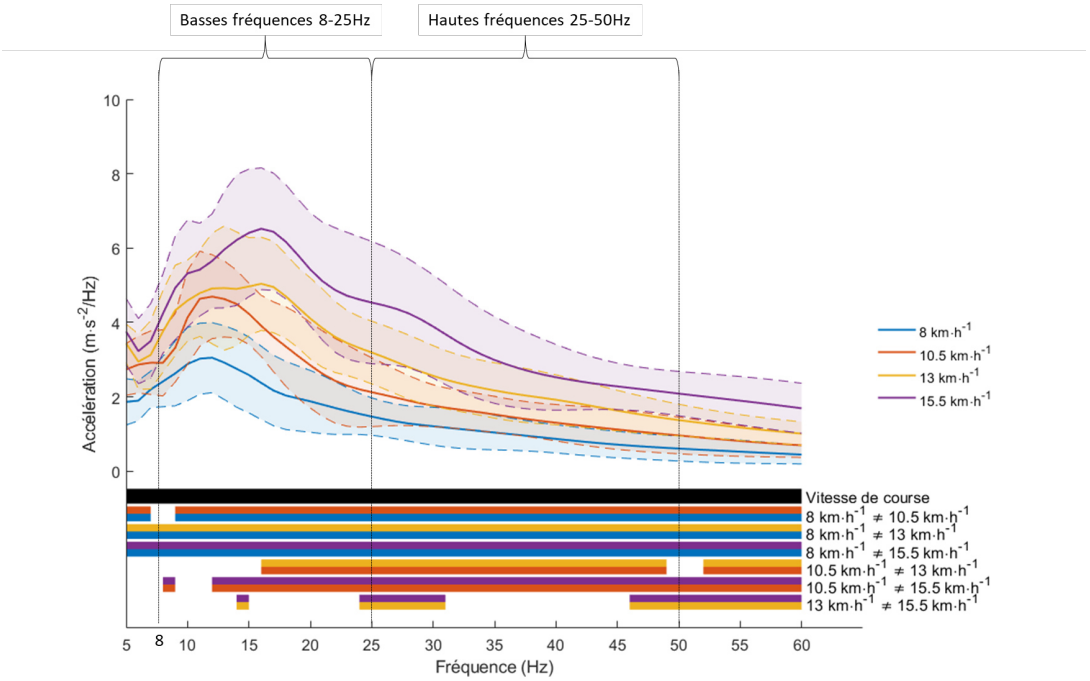

Figure 26 : Effet de la vitesse de course sur la représentation fréquentielle de la vibration du gastrocnemius medialis. En dessous des courbes, l'ANOVA (bande noire) et les tests post-hoc (bandes bicolores) sont représentés. Une couleur est au-dessus d'une autre, cette condition entraine plus d'énergie à ces fréquences que l'autre. Adapté de Trama et al. (2019a).

Les résultats principaux étaient que l'augmentation de la vitesse de course entrainait une augmentation de l'amplitude et de la fréquence de l'impact, ainsi qu'une augmentation plus marquée des hautes fréquences de vibration (25-50 Hz) comparé aux basses fréquences (8-25 Hz) (Figure 25 et Figure 26). De plus, les deux autres études ont montré que les mouvements spécifiques de sports collectifs et les réceptions de saut entrainaient un impact avec plus d'amplitude et une fréquence plus élevée que la course à allure préférentielle (Figure 27), tandis que la fréquence et l'amplitude des vibrations des tissus mous du membre inférieur étaient dépendantes du mouvement. D'une manière générale, plus l'amplitude de l'impact était importante, plus l'amplitude de la vibration était grande. Enfin, l'amortissement de la vibration était minimal pour la course à pied en comparaison aux autres mouvements dans la bande 10-50 Hz, alors qu'il existait peu de différences pour les plus hautes fréquences (Figure 28).

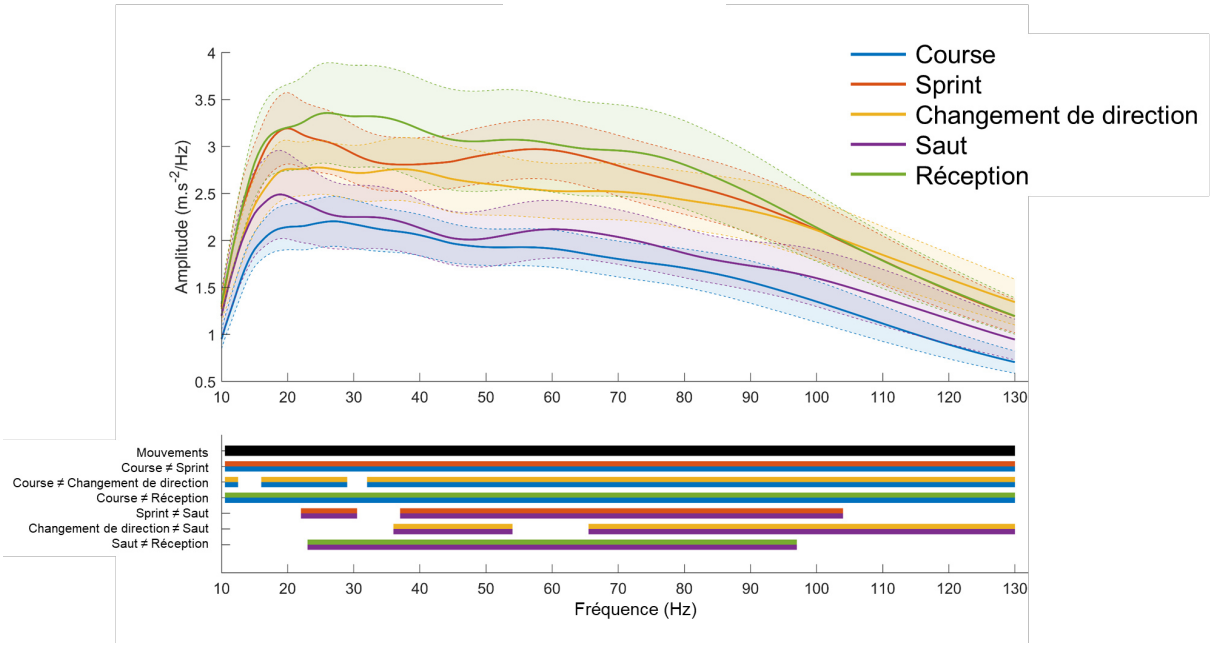

Figure 27 : Effet du type de mouvement sur la représentation fréquentielle de l'impact au sol après une analyse SnPM. En dessous des courbes, L'ANOVA (bande noire) montre un effet du mouvement de 10 à 130 Hz. Les différences significatives entre deux vitesses sont représentées par les bandes bicolores. Si une couleur est au-dessus d'une autre, cette condition entraine plus d'énergie à ces fréquences que l'autre. Adapté de Trama et al. (accepté).

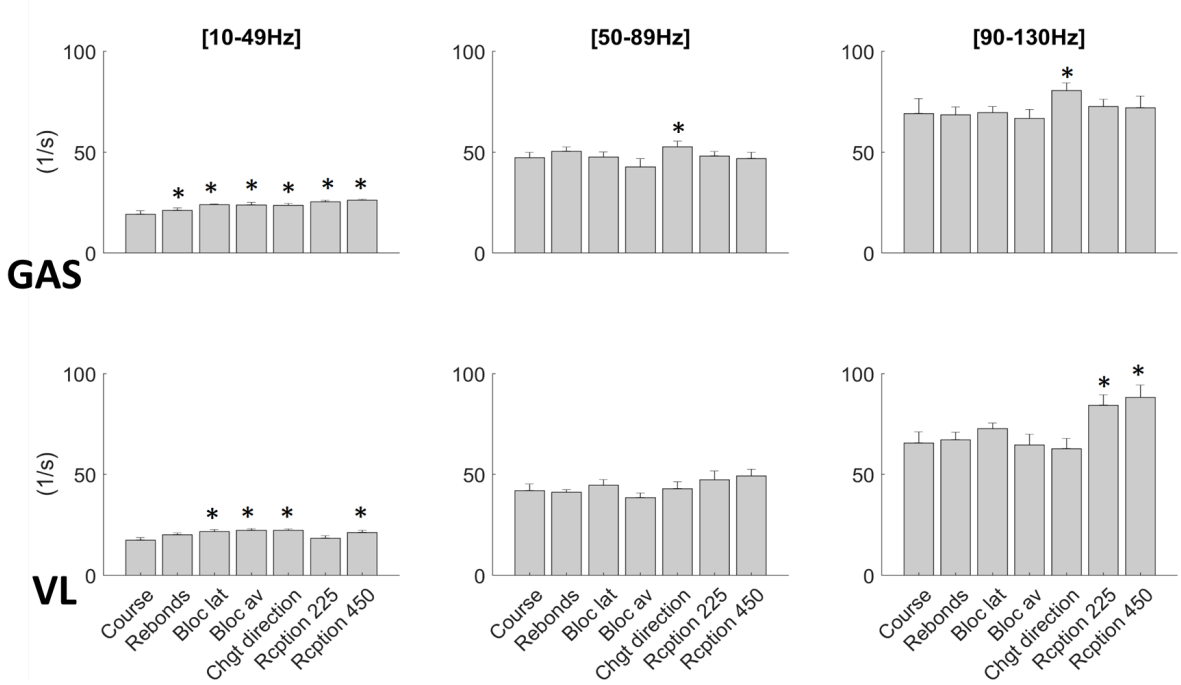

Figure 28 : Coefficient d'amortissement du gastrocnemius medialis (haut) et vastus lateralis (bas) en fonction de la bande de fréquence. Adapté de Trama et al. (2020).

L'augmentation des hautes fréquences de vibrations a été expliquée par l'augmentation conjointe de la fréquence d'impact et des activations musculaires avec la vitesse de course (Boyer & Nigg, 2004; Nilsson & Thorstensson, 1989; Tsuji et al., 2015). En ce qui concerne les différents mouvements, une combinaison spécifiques d'activations musculaires et d'angles articulaires pourrait expliquer la spécificité de chaque mouvement en terme de vibrations (Gindre et al., 2016; Gruber et al., 2014; Müller et al., 2012). Un amortissement plus important pour ce type de mouvement en comparaison à la course à pied pourrait s'expliquer par une adaptation du système neuromusculaire cherchant à limiter les vibrations induites par ces types de mouvements. En effet, il a été démontré qu'une énergie importante dans les fréquences de vibration supérieures à 50 Hz peut être à l'origine de fatigue neuromusculaire (Souron et al., 2017a). Ainsi, les mouvements spécifiques à certaines pratiques sportives ont été considérés comme plus contraignants pour le système musculo-squelettique et neuromusculaire (Figure 29). Plusieurs hypothèses peuvent être émises pour regrouper ces mouvements dans différentes familles. Les rebonds sont des mouvements dynamiques avec un contact se faisant sur l'avant du pied, avec une absence de pic passif. La mise en tension des muscles de la jambe et du pieds pour anticiper l'impact a pu entrainer une absorption de l'énergie au niveau des structures distales à la cheville, limitant donc l'amplitude du choc et de la vibration. Les mouvements de sauts, de fente et de pas latéraux entrainent

un freinage moins brusque que les changements de directions et les réceptions de sauts. Sur ces mouvements, le choc se produit aussi bien sur l'axe vertical que sur le plan horizontal. Plus le freinage est important, plus le choc et la vibration sont d'amplitudes importantes. Enfin, l'augmentation de la vitesse de course est possible grâce à une plus grande amplitude de foulée (Dorn et al., 2012; Schache et al., 2014), ceci entrainent un déplacement verticale du centre de masse plus important (Hamner et al., 2010; Hamner & Delp, 2013), et donc une vitesse d'impact entre le pied et le sol plus importante.

En conclusion, la diversité de mouvements et de contraintes mécaniques qu'entrainent les différents mouvements sportifs pose la question d'une quantification de la charge vibratoire et des différents impacts pour mieux estimer le stress mécanique subi par les athlètes de sports collectifs.

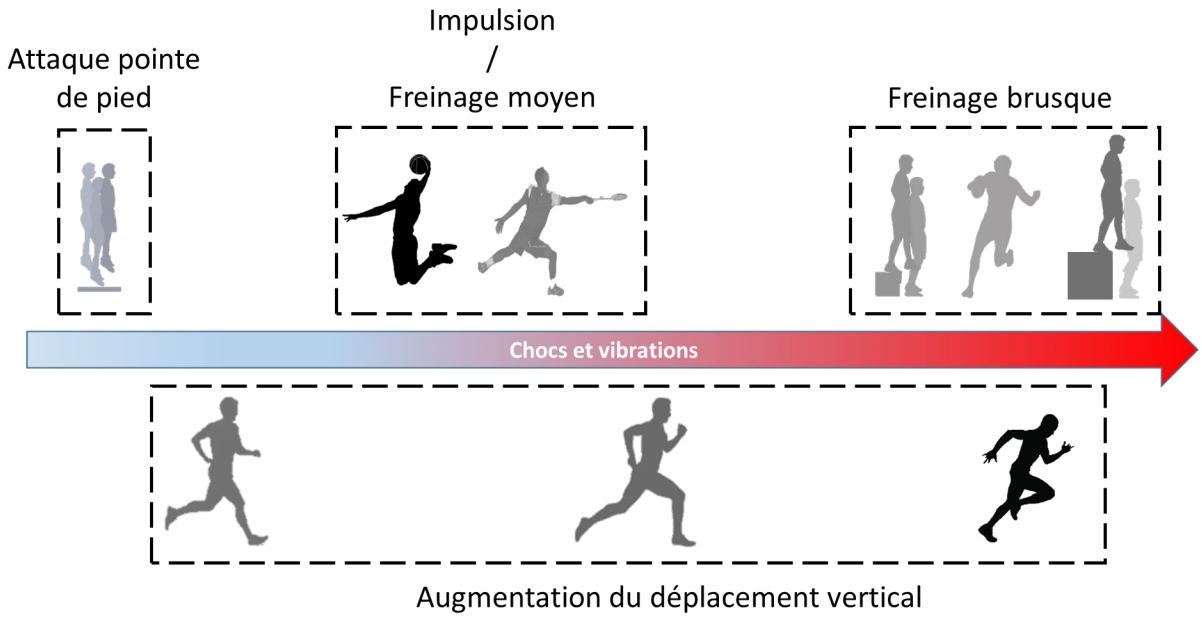

Figure 29 : Récapitulatif des études 3 à 5 montrant la diversité des chocs et des vibrations mesurées sur différents mouvements sportifs. Plus les mouvements se situent sur la droite, plus l'amplitude et la fréquence des chocs et vibrations sont importantes.

4.2.1.2 Classification des différents mouvements sportifs

Dans nos trois études précédentes, l'augmentation de la vitesse de course ainsi que les mouvements spécifiques à certains sports collectifs ont causé des vibrations de plus hautes fréquences à grande amplitude. Ce type de vibrations pouvant accroitre la fatigue neuromusculaire (Souron et al., 2017a), une quantification en pratique écologique permettrait de mieux caractériser la quantité de vibration subie par un athlète. Des méthodes émergentes comme la classification par intelligence artificielle, notamment

les méthodes se basant sur de l'apprentissage profond, ont été au centre de l'intérêt ces dernières années grâce à leur efficacité dans les domaines tels que la reconnaissance d'objet ou encore le diagnostic médical. Ces méthodes par apprentissage automatique sur un jeu de données labélisées par l'homme ont ensuite été popularisées dans le monde sportif (Perl, 2004, 2001) et de la biomécanique (Halilaj et al., 2018).

L'objectif de notre étude était de développer un réseau de neurones convolutifs pour classifier différents mouvements sportifs à partir du signal vibratoire de l'impact au sol

Les participants de cette étude ont effectué différents mouvements : des rebonds, des changements de directions, des pas latéraux, des fentes avant, et des réceptions de saut de deux hauteurs différentes (22.5 et 45 cm). L'impact au sol a été mesuré grâce à un accéléromètre positionné au niveau du talon de la chaussure Une transformée en ondelettes continue a été effectuée sur chacun des axes, et les cartes des coefficients d'ondelettes comprenaient les informations sur le signal entre 5 et 200 Hz, entre les 0.05 secondes avant et les 0.2 secondes après l'impact. Les trois cartes de coefficient ont été positionnées côte à côte et enregistrées sur une image de 88 par 270 pixels avec une résolution de 96 pixels par pouces. Le réseau de neurones convolutifs était composé de 16 couches (1 d'input, 13 d'apprentissage et 2 de classification), et était entrainé sur tous les impacts sauf celui à classifier. Différents entrainements, avec et sans considérer les impacts des autres participants, ou sans considérer les impacts effectués par le participant testé ont été effectués. Pour évaluer la précision du réseau, la sensibilité, qui est la capacité du réseau à correctement classifier le bon mouvement, et la spécificité, qui est la capacité du réseau à ne pas confondre le mouvement avec un autre, ont été calculées pour chaque mouvement.

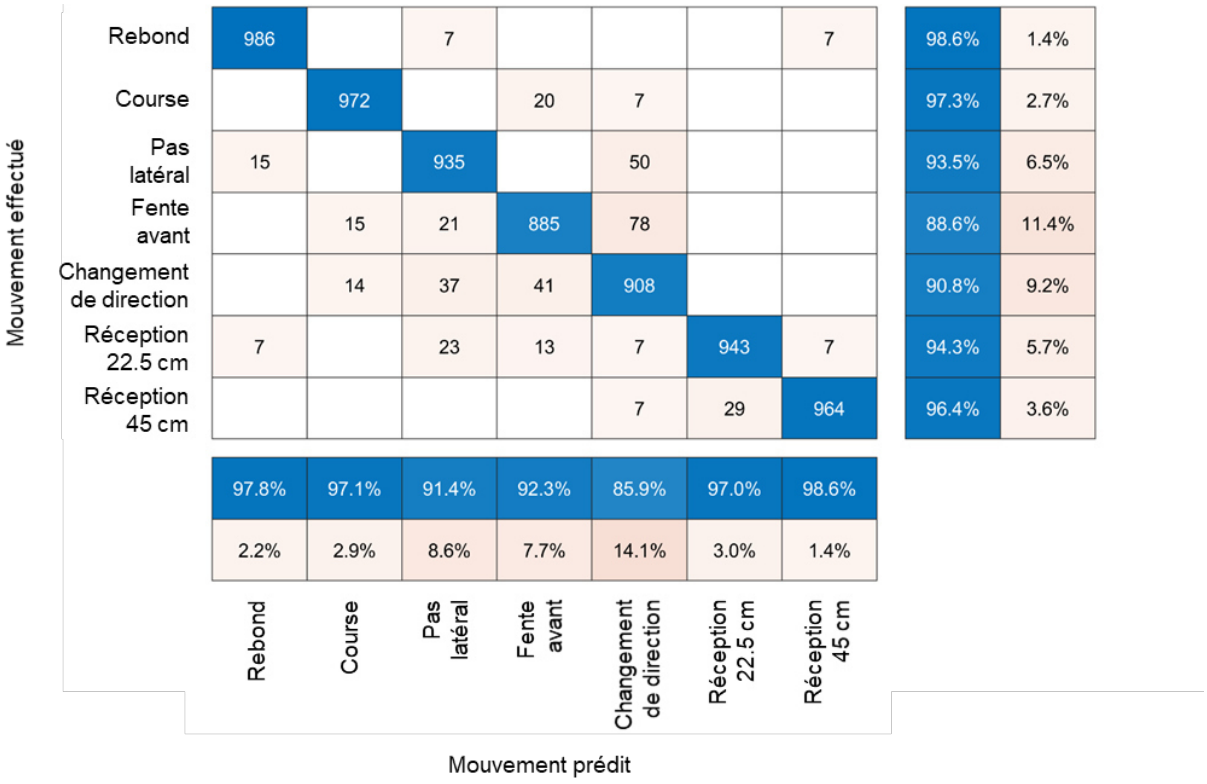

Figure 30 : Matrice de confusion normalisée à 1000 mouvements de chaque type indiquant les mouvements correctement classifié (vrais positifs, diagonale), les erreurs de classements (faux positifs, moitié inférieure gauche ; faux négatifs, moitié supérieure droite). La sensibilité est représentée dans la colonne de droite, tandis que la spécificité est représentée sur la ligne inférieure. Adapté de Trama et al. (2019b).

L'entrainement le plus performant a été celui où le réseau était entrainé spécifiquement sur les données du participant dont les impacts devaient être classifiés. Ce type d'entrainement a permis d'obtenir une précision moyenne de 93% (Figure 30), tandis qu'un entrainement sur les données des autres participants n'a permis de classifier correctement que 65% des impacts. Cependant, cet entrainement a permis au réseau de classifier la course et les rebonds à 94 et 97% de précision. Ce résultat a montré que les impacts induits par de la course à pied et des rebonds étaient communs aux différents participants, tandis que les autres mouvements entrainaient des impacts spécifiques au participant testé. Classifier ces impacts a donc demandé d'utiliser un réseau de neurones spécifique au sportif étudié.

En conclusion, il est possible d'utiliser un accéléromètre couplé à une transformée en ondelettes continue et un réseau de neurones spécifique au sportif afin de caractériser le type de mouvement effectué par ce dernier durant son activité.

4.2.2 Effet de la forme de la chaussure et de la raideur du sol

Au-delà des mécanismes de protections tels que le muscle tuning, le matériel sportif a été plébiscité pour réduire les forces d'impact au sol ainsi que les vibrations des tissus mous du membre inférieur. Parmi les différents matériels sportifs pour réduire les impacts et les vibrations, la chaussure (Boyer & Nigg, 2004; Fu et al., 2017; Gellaerts et al., 2017; Giandolini et al., 2020), le cuissard compressif (Borràs et al., 2011; Ehrström et al., 2018; Fu et al., 2015; Lussiana et al., 2015), et le revêtement du sol sportif (Bruce et al., 2019; Chen et al., 2019) ont été testés. Les travaux s'intéressant à l'effet de la chaussure sur les vibrations des tissus mous ont porté sur les matériaux composant la semelle (Giandolini et al., 2020), sa raideur (Boyer & Nigg, 2004) ou son épaisseur (Gellaerts et al., 2017), mais aucune étude ne s'est intéressée à la forme de la chaussure sur les vibrations des tissus mous. De plus en plus de chaussures à la forme arrondie, aussi appelée « rocker », ayant pour objectif de faciliter le passage vers l'avant du pied, sont utilisées en course à pied (Figure 31). Ces chaussures ont encore des effets peu connus sur les facteurs biomécaniques de la course à pied puisqu'elles ne modifient pas les activités musculaires du membre inférieur et ont un effet incertain sur l'impact au sol (Boyer & Andriacchi, 2009; Lin et al., 2017; Sobhani et al., 2016). En parallèle, le lien entre le revêtement du sol sportif et l'impact au sol ou les vibrations des tissus mous a été très peu été étudié (Bruce et al., 2019; Chen et al., 2019). Ces études ont montré qu'un sol moins raide sur l'axe antéropostérieur (i.e., dans le sens du déplacement) permettait de réduire la vitesse de la montée de la force de réaction du sol sur ce même axe (Chen et al., 2019), alors que des changement de raideur verticale n'avait pas d'effet (Bruce et al., 2019).

L'objectif de ces deux études était donc d'évaluer l'effet d'une chaussure à forme rocker sur les impacts, les activations musculaires et les vibrations des tissus mous du membre inférieur, ainsi que d'évaluer l'effet d'un sol formé de plaques coulissantes sur l'impact, et la vibration du mollet sur des mouvements spécifiques au basketball.

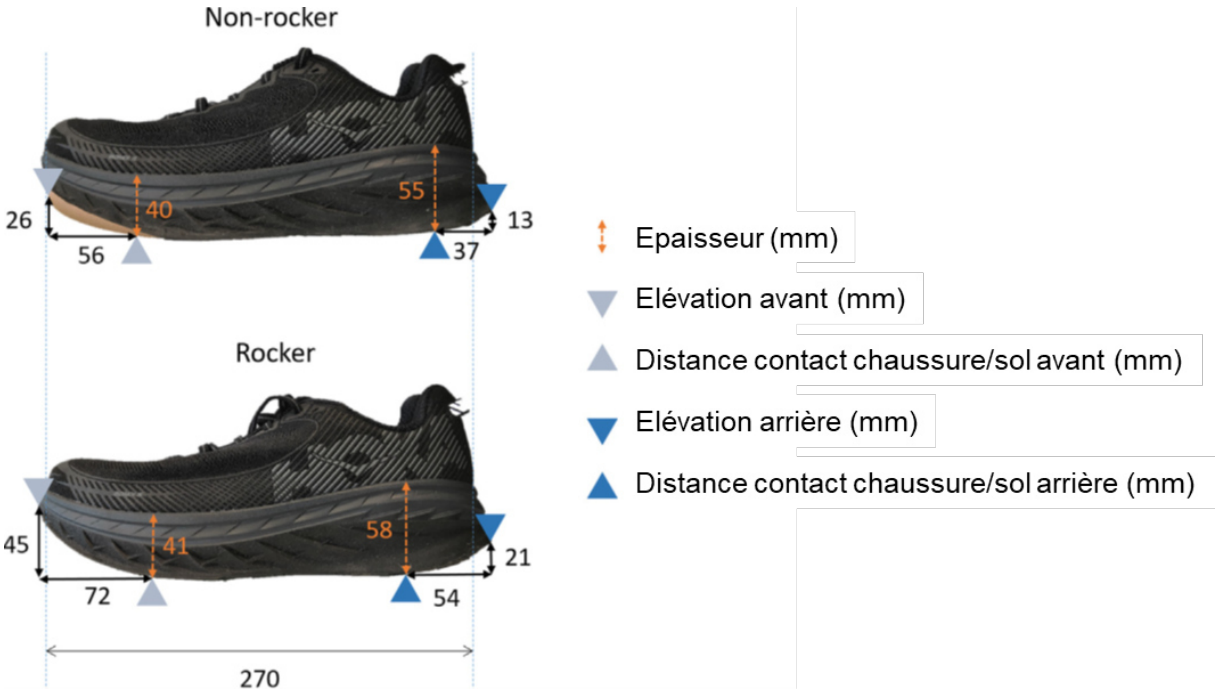

Figure 31 : Chaussure avec un faible rock comparé à une chaussure avec un rock prononcé. Les principales différences se situent sur la surface de contact au sol et les élévations avant et arrière. Adapté de Trama et al. (2019a).

Pour répondre à ces objectifs, les coureurs participants à la première étude ont couru avec deux types de chaussures différentes (Figure 31), tandis que les sportifs de la seconde étude ont effectué les mouvements sur deux sols différents : un sol référence en asphalte (REF), et un sol composé de dalles coulissantes (PowerGame +, Gerflor, France, PWG, Figure 32). Lors de la première étude, l'impact au sol a été mesuré grâce à une plateforme de force et les vibrations des tissus mous et activations musculaires du *gastrocnemius medialis* et du *vastus lateralis* ont été mesurées avec des accéléromètres et des électrodes d'électromyographie, respectivement. Lors de la deuxième étude, l'impact au sol a été

mesuré avec un accéléromètre positionné au niveau du talon de la chaussure et les vibrations des tissus mous du *gastrocnemius medialis* avec un accéléromètre.

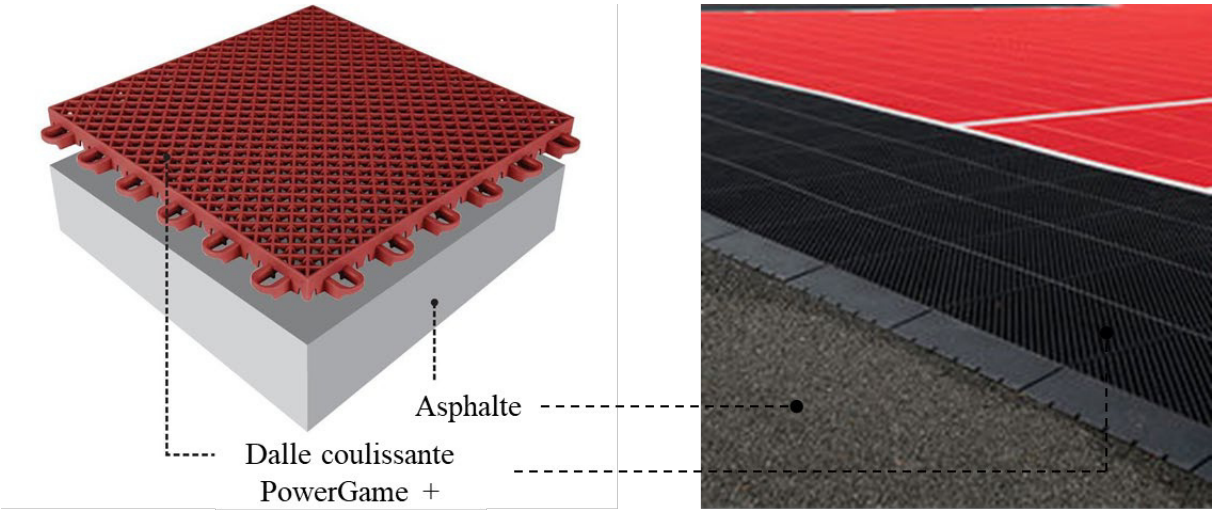

*Figure 32 : Dalles coulissantes PowerGame + (Gerflor, France) installées sur de l'asphalte (en noir). Les plaques (19*305*305 mm) coulissent entre elles sur une distance d'environ 1 cm lors d'un impact.*

La première étude n'a pas montré d'effet significatifs de la chaussure rocker par rapport à une chaussure sans rocker sur les paramètres de force de réaction au sol, de vibrations, et d'activations musculaires. Cependant, l'utilisation des chaussures rocker a engendré une augmentation de la variabilité de l'activité électrique du muscle, que ça soit durant la phase de préactivation avant le contact au sol ou pendant la phase d'appuis, notamment à haute vitesse de course (Figure 33). La seconde étude a montré que des plaques coulissantes permettaient de réduire l'impact au sol dans les trois axes (Figure 34), sans modifier les activations musculaires et les vibrations du *gastrocnemius medialis*.

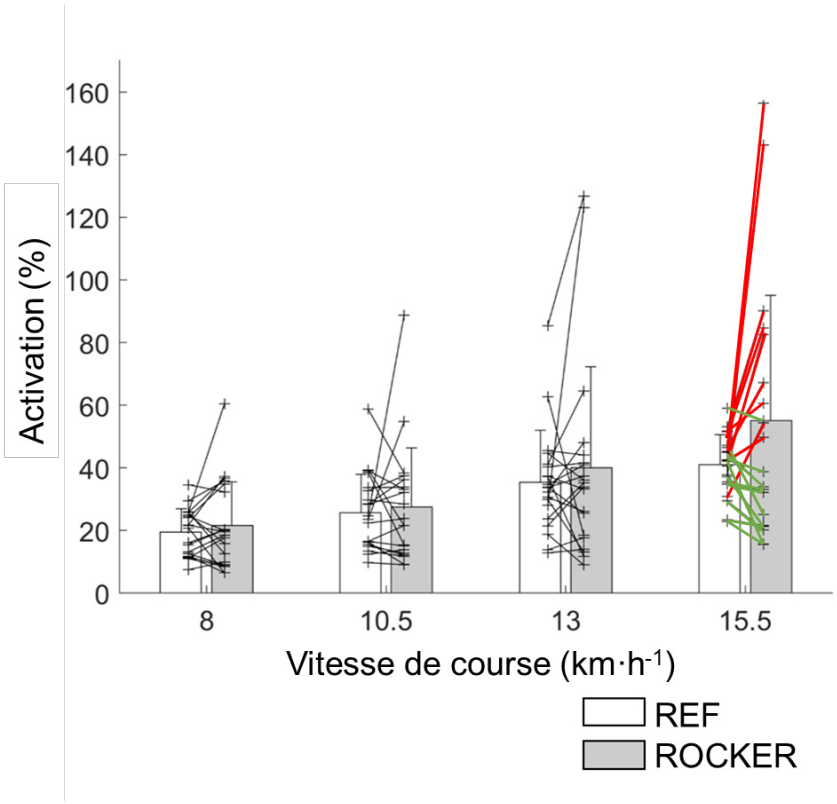

Figure 33 : Activité moyenne du muscle vastus lateralis lors de la phase d'appui. A 15.5 km·h^{-1}, les traits rouges indiquent une augmentation de l'activité du muscle avec la chaussure rocker tandis que les traits verts indiquent une baisse de l'activité.

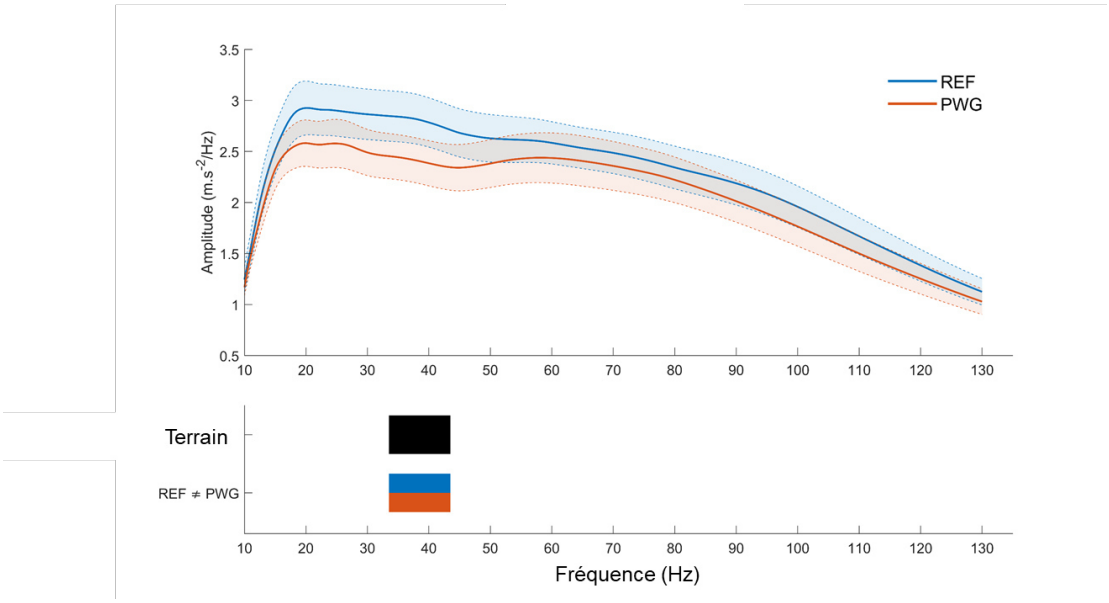

Figure 34 : Effet du type de terrain sur la représentation fréquentielle de l'impact au sol après une analyse SnPM sur les données présentées dans l'article. En dessous des courbes, L'ANOVA (bande noire) et la bande bicolore montrent un effet du terrain, avec moins d'amplitude pour le sol PWG comparé au sol REF, de 34 à 44 Hz. Adapté de Trama et al. (Accepté).

Les résultats de la première étude ont été expliqués par les faibles différences entre les deux chaussures testées (Figure 31) ainsi que par les capacités d'adaptation des coureurs comme l'a montré la forte variabilité des activations musculaires (Boyer, 2006). Cette variabilité peut aussi être expliquée par un

temps d'adaptation trop faible (Mohr et al., 2021) ne laissant pas le temps aux coureurs de retrouver une mécanique de course optimale (Nigg et al., 2017). Pour la seconde étude, la baisse de l'amplitude de l'impact était expliquée par la baisse de raideur du sol grâce aux plaques coulissante (Chen et al., 2019). Il est important de noter que les sportifs participants à cette étude avaient l'habitude d'utiliser le sol PWG durant leur pratique, ce qui peut expliquer qu'ils n'ont pas eu de phénomène d'adaptation sans modification de l'activité musculaire. Un temps d'adaptation est donc à considérer lorsque du matériel innovant est testé, afin que l'athlète puisse en tirer pleinement profit. Pour accroitre l'effet du matériel, la combinaison de différents équipements comme les chaussures et le sol pourraient permettre de limiter l'amplitude des vibrations pour avoir une pratique moins fatigante pour l'organisme et ainsi améliorer la performance.

4.2.3 Effet de la fatigue induite par différents trails et ultra-trails

Le phénomène du muscle tuning, c'est-à-dire de l'amélioration de l'amortissement et de l'éloignement de la fréquence de vibration du muscle par rapport à celle de l'impact, se produit pour des muscles non fatigués (Boyer & Nigg, 2007a; Wakeling et al., 2002). Ce phénomène étant initié par des modifications de recrutement musculaire, l'effet de la fatigue neuromusculaire sur ce mécanisme a été investigué au cours de la dernière décennie (Ehrström et al., 2018; Friesenbichler et al., 2011; Khassetarash et al., 2019, 2015a; Nikooyan & Zadpoor, 2012). Ces études ont montré une augmentation de l'amplitude de la vibration de 10 à 30% avec la fatigue (Ehrström et al., 2018; Friesenbichler et al., 2011; Khassetarash et al., 2019, 2015a), et une augmentation de 15 à 20% de l'amortissement (Khassetarash et al., 2019, 2015a). Cependant, l'augmentation de l'amortissement étant opposé aux prédictions du modèle proposé par Nikooyan et Zadpoor (2012), il est possible de faire l'hypothèse que les protocoles utilisés n'étaient pas assez longs pour induire une fatigue neuromusculaire importante et pour diminuer la capacité d'amortissement des muscles (Giandolini et al., 2016; Millet et al., 2011b; Saugy et al., 2013).

L'objectif de cette étude était de déterminer l'effet de courses plus longue de type ultra-trail sur les caractéristiques de la vibration.

Les participants de cette étude étaient 52 coureurs prenant le départ de 5 courses différentes de l'Ultra Trail du Mont Blanc 2019. Ces courses allaient de 40 à 171 km pour 2000 à 10000 m de dénivelé positif et négatif. Les mesures ont été effectuées avant la course, 48 à 24h avant le départ, et après la course, le plus rapidement possible après l'arrivée (81 ± 21 min). Durant ces deux temps de mesures, un premier test consistait à quantifié la force maximale isométrique des fléchisseurs plantaires et des extenseurs du genou sur un ergomètre isométrique (Millet et al., 2011a). Un indice de perte de force relative a été calculé pour caractériser la fatigue causée par les différentes courses. Pour le second test, les participants étaient équipés de 3 accéléromètres au niveau du talon, du *gastrocnemius medialis* et du *vastus lateralis* afin de quantifier d'une part l'impact au sol et d'autre part les vibrations de ces deux des tissus mous. Les participants devaient courir sur tapis roulant, à plat et à 10 $km \cdot h^{-1}$, pendant 1 minute durant laquelle les 30 dernières secondes ont été enregistrées pour quantifier les impacts et vibrations. Une transformée en ondelettes continue ainsi qu'une analyse SnPM ont été effectuées sur les différents signaux. Des

corrélations entre l'indice de perte de force et les modifications de vibrations ont été réalisées par le biais de régressions linéaires.

Nos résultats principaux étaient que l'amplitude, la fréquence, et l'amortissement des vibrations du *vastus lateralis* ont été réduites après une course de type ultra-trail, tandis qu'aucune modification n'a été observée pour le *gastrocnemius medialis* (Figure 35). De plus, la baisse de force n'expliquait pas les modifications de comportement vibratoires.

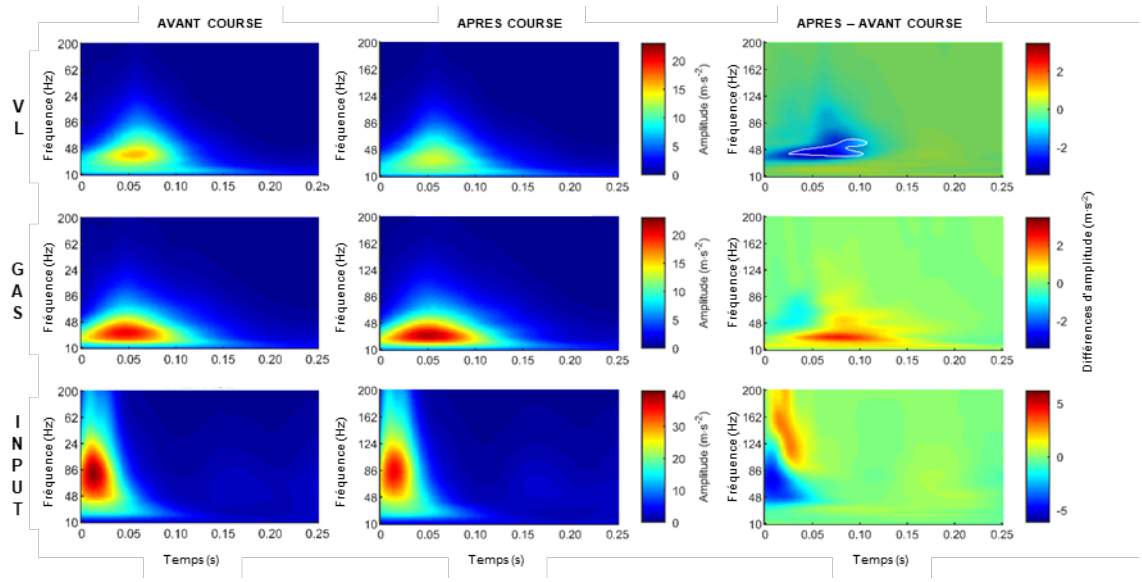

Figure 35 : Cartes d'ondelettes des vibrations des tissus mous (vastus lateralis, haut ; gastrocnemius medialis - milieu) et de l'impact au sol (bas) avant (gauche) et après (centre) les différentes courses de l'UTMB 2019. Les différences entre avant et après la course sont représentées à droite. La zone plus claire sur la carte en haut à droite montre qu'il y avait significativement moins d'amplitude de vibration pour le *vastus lateralis* après la course, durant les 0.12 secondes après l'impact, pour des fréquences de 40 à 60 Hz. Adapté de Trama et al. (soumis).

Une première explication serait que l'augmentation de la fréquence médiane de l'impact associée à la diminution de la fréquence de vibration du *vastus lateralis* entraine une diminution du phénomène de résonnance, un moindre transfert d'énergie aurait donc eu lieu et l'amplitude de vibration des tissus mous s'en serait trouvé réduite. Une seconde hyothèse, ne remettant pas en cause la première, était qu'une sollicitation plus grande du *vastus lateralis* lors d'effort sur terrain vallonné (Maeo et al., 2017; Park et al., 2019), pouvait potentiellement induire une plus grande altération de ce dernier et ainsi engendrer un comportement de protection à la suite de course d'ultra-trail. Ce comportement d'adaptation aurait modifié le comportement vibratoire en diminuant à la fois l'amplitude, la fréquence, et l'amortissement de la vibration. Lors d'une fatigue extrême, le muscle serait donc incapable d'amortir

de manière aussi efficace la vibration que lorsqu'il n'est pas fatigué, cependant, la diminution de fréquence et d'amplitude peuvent être la conséquence d'une diminution de raideur musculaire ou d'une augmentation locale de la masse dû à un œdème inflammatoire (Andonian et al., 2016). Bien que la baisse de force n'ait pas pu expliquer ces modifications, d'autres adaptations tels que celles de la cinématique de course ou des activations musculaires seraient des facteurs à explorer.

Author's own version
Published in Medicine & Science in Sports & Exercise (doi: 10.1249/MSS.0000000000002106)

INPUT AND SOFT-TISSUE VIBRATION CHARACTERISTICS DURING SPORT-SPECIFIC TASKS

Trama R.[1], Hautier C.[1], Blache Y.[1]

[1] Univ-lyon, Université Claude Bernard Lyon 1, LIBM EA 7424, Lyon, France

Corresponding author:

Trama Robin
UFR STAPS 1, 27/29 Boulevard du 11 Novembre 1918, 69622 Villeurbanne Cedex
+33649850040
robin.trama@univ-lyon1.fr

Published in Medicine & Science in Sport and Exercice (MSSE)

Medicine & Science in Sports & Exercise: January 2020 - Volume 52 - Issue 1 - p 112-119

doi: 10.1249/MSS.0000000000002106

https://journals.lww.com/acsm-msse/Abstract/2020/01000/Input_and_Soft_Tissue_Vibration_Characteristics.13.aspx

Author's own version
Published in Medicine & Science in Sports & Exercise (doi: 10.1249/MSS.0000000000002106)

Abstract

Purpose: To assess the influence of sport-specific tasks on the characteristics of input and soft-tissue vibrations. **Method:** Triaxial accelerometers were used to quantify the input (heel cup of the shoe) and soft-tissue vibrations of the *gastrocnemius medialis* and *vastus lateralis* muscles during seven sport-specific tasks performed by 10 healthy volunteers. A wavelet analysis was used to analyze the acceleration signals in the time-frequency domain. The energy and frequency of the input and soft-tissue vibrations, as well as the transmission of energy from the input to the muscles and the damping properties of soft tissues, were computed. **Results:** Different inputs, energy transmissions and damping properties were found between the various movements. Landings and side cuts induced the greatest input frequency and energy, as well as the greatest soft-tissue vibration energy. These tasks produced up to three times greater energy than in-line running. Positive energy transmission was found for frequencies under 50 Hz and for frequencies up to 90 Hz for some movements, indicating a possible change in the natural frequency of vibration within muscle. Only small differences in damping properties were found, which may indicate that the attenuation of the vibration was not the priority during these tasks. **Conclusion:** Athletes are subject to greater energy impacts and vibrations during some sport-specific tasks compared to running. It may be useful to decrease such input/vibration energy via the usage of footwear or compression tools in order to limit their potential deleterious effects on the musculoskeletal system. It is therefore recommended to quantify and control the number of impacts induced by the different sport-specific tasks. **Key words:** DAMPING, ENERGY TRANSMISSION, IMPACT, JUMPING, RUNNING, WAVELET

Introduction

Soft-tissue vibration (i.e., vibration of the muscle and the surrounding fat and skin) in sport has been studied since the late 1990s with a focus on running tasks (1–3). The soft-tissue vibration of the leg is initiated at the moment of the impact with the ground, which is considered an input into the musculoskeletal system (4). When the frequency of the input is close to the natural frequency of the soft tissues, a resonance effect is expected to occur. This may lead to an amplification of the soft-tissue vibrations at frequencies around the natural frequencies of soft tissues (5). The muscle-tuning paradigm suggests that the muscle adapts to reduce the vibration by adjusting its mechanical properties (3, 6–8), resulting in a modification of its natural frequency, and/or an increase in the damping properties (6). The natural frequency of the soft tissues ranges from 10 Hz for a relaxed muscle to 50 Hz for a contracted one (9). Consequently, during running, the energy transferred and amplified from the input to the muscles ranges from 10 Hz to 50 Hz, while energy at higher frequencies is attenuated (7). Once the vibration is initiated at the soft-tissue level, the latter is damped as an underdamped vibrating system. As higher frequencies of vibration are more damped (10) and transferred less to the soft tissues (7), less vibration energy is located in higher than in lower frequencies.

Several tools and methods have been used to characterize the input acceleration and its transfer to the musculoskeletal system. Firstly, the input is often assessed using a force platform or with an accelerometer placed on the medial face of the tibia (2, 11); nevertheless, an accelerometer placed on the heel cup of the shoe was shown as reliable to quantify the input during running (12, 13) and landing tasks (14). Secondly, the transfer between the input and the soft tissues is quantified at each frequency by the calculation of the ratio between the energy of soft-tissue acceleration signals and the energy of the input signal (15, 16). The frequency domain of acceleration signals can be investigated with wavelet transform, allowing a time-frequency

analysis and a quantification of both the energy and damping properties of several frequencies (17).

While input and soft-tissue vibration amplitude are up to 10 times greater during landing than in running (14, 18, 19), little is known on soft-tissue comportment in different sport tasks. For instance, the role of the *vastii* and the calf-muscle group in the force development differs between running and side cutting (20); additionally, the mechanical properties of the muscle may differ between the types of foot-strike pattern, as they induce diverse muscular preactivation and joint angles (21, 22). Thus, it could be hypothesized that input and soft-tissue vibration characteristics (i.e., main frequency and amplitude) may be different in other specific sport tasks (e.g., hopping, side cuts, landings) compared to in-line running, as these tasks may have different landing speeds, strike patterns and joint kinematics. However, previous studies focusing on whole-body or local-vibration exposure found that the increase in the frequency of the input led to an inefficient increase in muscular activity, namely, an increase in muscular activity without enhancement of the task performance (23–27). Furthermore, other studies found that the increase in vibration amplitude led to an increase in muscular activity (16, 19), or to a deficit in voluntary activation after a downhill run (28).

In consequence, the purpose of this study was to characterize the input and the soft-tissue vibrations of leg muscles during different sport-specific tasks. We hypothesized that some movements will produce greater input energy, and at higher frequency, compared to in-line running. Additionally, some movements will generate greater energy near the resonance frequency of the soft tissues, leading to greater soft-tissue vibration amplitude than in running.

Methods

Participants

A total of nine men and one woman—team-sports athletes or runners—volunteered to participate in this study (age: 32.2 ± 8.9 years, height: 171.4 ± 7.0 cm, mass: 70.9 ± 10.1 kg). They had been free from injury for six months prior to the experiment. Before the experiment, participants signed informed-consent documentation that was approved by the local university ethics committee, according to the Declaration of Helsinki.

Experimental procedure

Seven sport-specific tasks were performed. The first task was a hop test, consisting of three series of seven consecutive jumps (29). Participants were instructed to land on the forefoot and to bounce as quickly as possible while keeping the heel off the ground. The second task consisted of running in line at a preferred velocity for jogging. The third task was a side step, with instructions to stop before going back on the other side. The fourth task consisted of a front lunge, which is a typical movement of badminton, and participants were instructed to strike the floor with the heel first. The fifth task was a side cut, and participants were given instructions to turn at a 45 ± 15° angle on the left and to attack the ground with the heel first. Finally, the sixth and seventh tasks were two landing tasks: one from 22.5 cm and the other from 45 cm. Participants were instructed to keep their legs straight and to land with flat-foot contact.

Each subject underwent a 10-minute warm-up phase, during which he or she ran at a self-selected pace, and then participants executed each sport-specific task three times before beginning the tests. The test consisted of executing each task described above in a counterbalanced order. The footwear was standardized, and all participants wore the same indoor-sports shoes.

Instrumentation and data collection

Videos (200 Hz) of the impacts were made in order to identify the main strike patterns used by the participants (GoPro HERO7, GoPro, California, USA). Two triaxial accelerometers (Mega Electronics, Kuopio, Finland, ±100 g, 1,000 Hz) were taped to the muscle belly of the *gastrocnemius medialis* (GAS) and *vastus lateralis* (VL) in order to record the soft-tissue vibrations of the right leg with the y-axis oriented in order to be collinear to the longitudinal axis of the shank and the thigh, respectively. A third accelerometer was stuck on the heel cup of the shoe with the y-axis oriented vertically. All signals were recorded and synchronized with LabVIEW 3.0 (National Instrument, Massachusetts, USA).

Data treatment

A total of 15 impacts for each task were recorded. For the hop test, the five middle receptions were analyzed for each series, and for the side steps, the impact when the change of direction occurred was analyzed. The time-frequency domain of the acceleration signals was investigated with a continuous wavelet transform (30), using a filter bank of 39 Morse wavelets, with a symmetry parameter equal to 3, and a time bandwidth equal to 60 (31). The time resolution of the 39 scaled wavelets ranged from 0.3 (10 Hz) to 0.02 seconds (130 Hz; see supplementary files in appendix A for more details). A preliminary analysis showed that this mother wavelet was suitable to assess the vibrations of the sport-specific tasks, especially because the specific damping of the wavelets used were higher than the damping of the signal, allowing a nonbiased estimation of the signal damping (see supplementary files in appendix B for more details). The pseudo frequency of each scale was obtained using the center of frequency of each wavelet. As the scales were logarithmically spaced to allow a regular-frequency response, the map was linearly interpolated. The modulus of the coefficient given by the wavelet transform was computed for each axis of each accelerometer, and the norm of the three axes was calculated and considered as the power of the signal for each time and frequency ($p(t, f)$) (figure 1). The signal power ranging from 10 to 130 Hz was analyzed, as

frequencies under 10 Hz were related to movement artifacts, while frequencies above 130 Hz were related to electronic noise.

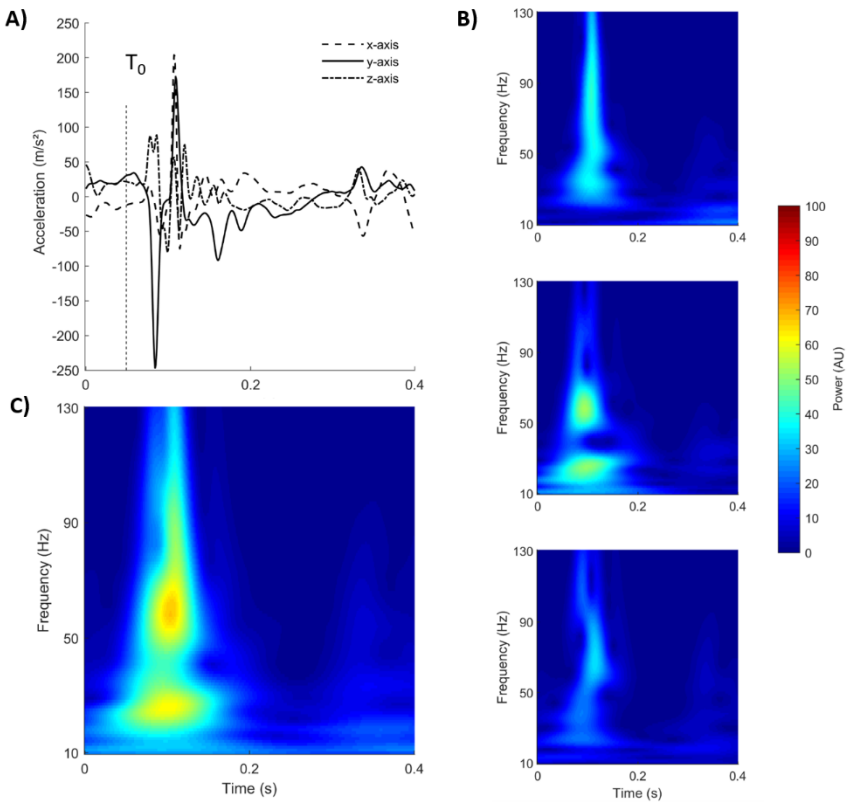

Figure 1 : A) Raw acceleration signals of the gastrocnemius medialis during running, with T0 corresponding to the impact; B) Wavelet transform for the three temporal signals (x, y and z axis from top to bottom); C) Norm of the three maps presented in B.

The damping properties for each muscle were calculated for each frequency, according to the method depicted by Enders et al. (17). Briefly, the damping coefficient ($D(f)$) was optimized to minimize the sum of squared errors between the measured signal power ($p(t,f)$) and the

theoretical power decay between the moment when the power decay was maximal ($T1$) and when the signal power was equal to 10% of the power at $T1$ ($T2$) (Eq. 1).

$$\min \mathrm{J} = \sum_{t=T1}^{T2} (p(T1,f) \cdot e^{-D(f)\cdot t} - p(t,f))^2, \text{ (Eq. 1)}$$

with t the time in seconds ranging from $T1$ to $T2$, $\boldsymbol{P(T1,f)} \cdot \boldsymbol{e^{-D(f)\cdot t}}$, the theoretical signal power decay at frequency f.

The signal energy ($S(f)$) was computed by integrating, for each frequency, the signal power over time during 0.2 s after the impact (Eq. 2).

$$S(f) = \int_{t=0}^{0.2} p(t,f)\,\mathrm{d}t, \text{ (Eq. 2)}$$

The main frequency was computed from the signal energy and corresponded to the frequency with the maximal energy. The energy transmission ($T(f)$) between the input and the two muscles was computed for each frequency (Eq. 3), in line with Hintzy et al. (16). A $T(f)$ value above zero meant an amplification of the energy of the input—a negative value corresponded to an attenuation—while a value of zero showed a simple transmission of the energy.

$$T(f) = \left(\frac{S_i(f)}{S_m(f)} - 1\right) \cdot 100, \text{ (Eq. 3)}$$

with $S_i(f)$ and $S_m(f)$ as the signal energy of the input and muscles, respectively.

For each parameter, 121 values corresponding to each frequency were obtained. These values were gathered in three frequency bands, ranging from 10 Hz to 49 Hz for the low frequencies, from 50 Hz to 89 Hz for the middle frequencies, and from 90 Hz to 130 Hz for the high frequencies. For the signal energy, the energy at each frequency within the band was added; for the damping properties and energy transmission, the mean of damping properties or energy transmission at each frequency within the band was calculated, respectively.

Statistics

The effects of sport-specific tasks (fixed effect) and frequency band (fixed effect) on energy, energy transmission and damping properties were tested using linear mixed models (32), while only the effects of the task were tested for the main frequency. Likewise, since participants may not share the same baseline, and since the effects of the task may differ among participants, the fixed effects were also set as random intercepts and slopes. The p-values were obtained from likelihood ratio tests, which were conducted by testing the full model against the model without the effect tested. In order to prevent false-positive results, the original alpha error (5%) was corrected with a sequential Bonferroni correction for each group test (i.e., interaction and main effects). When a significant interaction between the two fixed effects was observed, the two fixed effects were tested independently within each category of the other effect. Then, if there was a main effect, post-hoc pairwise comparisons were performed using Tukey's honestly significant difference, with an alpha error set at 5% and amended with a Bonferroni correction. The normality, homoscedasticity and linearity of the linear-mixed model residuals were graphically controlled. All models were performed using the package lme4 (33) of R software (R 3.5.0, RCore Team, Vienna, Austria).

Results

The analysis of videos revealed that the striking pattern differed between the tasks (table 1). The hop test was performed with a forefoot-strike pattern, and the heel was kept off the ground. The two landing tasks, despite our instructions, were also performed with a forefoot strike. However, they differed from the hop test, as the heel touched the ground within the following 0.02 seconds, no matter the height. The side-step and front-lunge strike techniques were subject specific, as they induced various strike techniques, predominantly midfoot and rearfoot, respectively. Lastly, running and side cuts were performed with a rearfoot-strike pattern.

Table 1: Strike pattern repartition between the different sport-specific tasks.

	Hop test	Running	Side-step	Front lunge	Side-cut	Landing 22.5	Landing 45
Rearfoot	0%	90%	20%	70%	90%	10%	0%
Midfoot	0%	10%	50%	30%	10%	20%	20%
Forefoot	100%	0%	30%	0%	0%	70%	80%

Main frequency

Considering the input signal, the two movements with the lowest input main frequency were the hop test and the running tasks, while input main frequencies were up to three to four times higher for the landings from 22.5 cm (table 2). For the GAS, the lowest main frequency was found for the front lunges and was maximal for the landings from 45 cm (table 2). Finally, for the VL, the main frequency was the lowest for the hop test and was maximal for the landings from 45 cm (table 2).

Table 2: Means ± standard deviations of the main frequency of vibrations (Hz) for each sport-specific task.

	Hop test	Running	Side-step	Front lunge	Side-cut	Landing 22.5 cm	Landing 45 cm
VL	18.6±5.1 $_{ab}$	20.9±3.8 $_{bc}$	16.6±2.7 $_{a}$	16.2±2.2 $_{a}$	17.2±2.4 $_{ab}$	18.8±4.3 $_{a}$	26.8±9.4 $_{c}$
GAS	26.5±6.0 $_{bc}$	22.5±6.3 $_{ab}$	23.2±5.2 $_{b}$	18.2±2.7 $_{a}$	22.7±4.4 $_{b}$	24.2±4.7 $_{b}$	29.1±3.4 $_{c}$
INPUT	21.8±6.2 $_{a}$	23.4 ± 6.8 $_{a}$	46.4±21.6 $_{bc}$	68.8±15.9 $_{d}$	67.3±29.7 $_{cd}$	78.2±18.4 $_{d}$	55.2±11.7 $_{c}$

For each row, means ± standard deviations that do not share the same letter are significantly different at $p<0.05$.

Energy

Considering the input signal, the hop test was the only movement with significant differences between the three frequency bands, as the 10–49 Hz band contained 1.5 and 2 times more energy than 50–89 Hz and 90–130 Hz bands, respectively ($p<0.001$). Additionally, the energy of the input was the highest for the two landing conditions and the side cuts, while energy measured during the hop test and the running task was the lowest (figure 2). Considering the two muscles, energy at 10–49 Hz was 1.5 times higher than energy at 50–89 Hz ($p<0.001$),

which was itself twice significantly greater than energy at 90–130 Hz ($p<0.001$). Moreover, for the two muscles and for the three frequency bands, movements with the most energy were the side cuts and landings from 45 cm. These movements generated between two and three times more energy than running (figure 2).

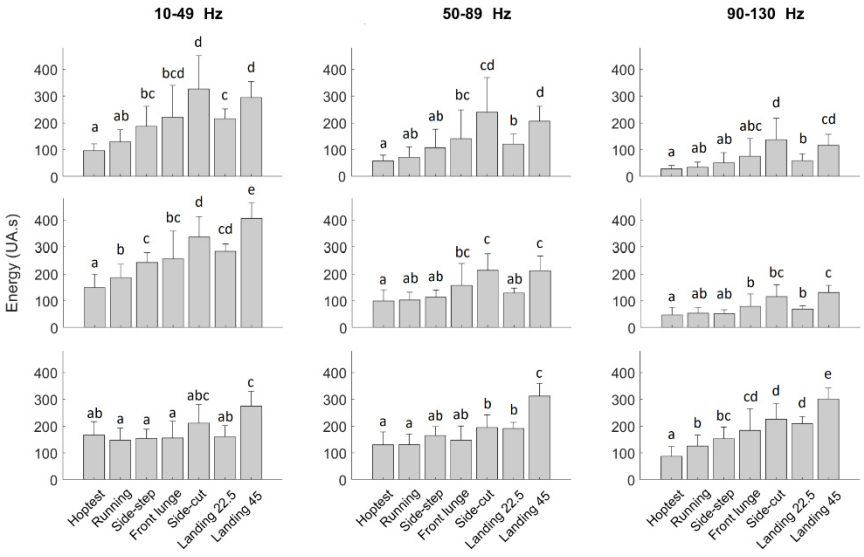

Figure 2 : Means ± standard deviations of the energy for the input (bottom), the gastrocnemius medialis (middle) and vastus lateralis (top) for the seven sport-specific tasks. For each graphic, bars that do not share the same letter are significantly different at $p<0.05$.

Energy transmission

For the two muscles, the transferred energy at 10–49 Hz was significantly greater than transferred energy measured at 50–89 Hz ($p<0.001$), which was also greater than transferred energy recorded at 90–130 Hz ($p<0.001$). Concerning the GAS, energy transmission in the 10–49 Hz band was positive for six of the seven tasks. The maximum was depicted for the side cuts, where twice the energy of the input was found at the muscle level, while the minimal transmission was found for the hop test, where no amplification was observed. For the 50–

89 Hz band, a small positive transfer was observed only for the side steps and side cuts, while the input energy of other tasks was attenuated. For the 90–130 Hz band, almost all energy was attenuated for all the tasks (figure 3). Concerning the VL, energy transmission in the 10–49 Hz band was positive for five of the seven tasks. The maximums were depicted for the side cuts and landings from 22.5 cm, while energy was attenuated for the hop test and running tasks. At last, energy was attenuated for the two higher-frequency bands (50–89 Hz and 90–130 Hz), with no significant differences between the tasks (figure 3).

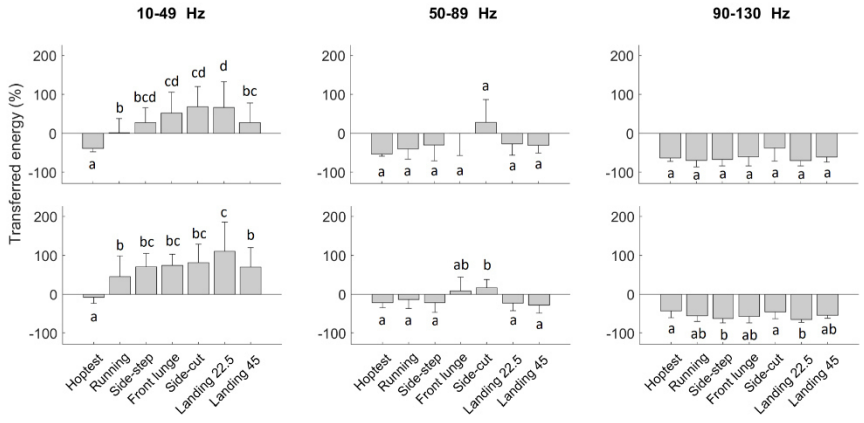

Figure 3 : Means ± standard deviations of the transferred energy from the input to the gastrocnemius medialis (bottom) and vastus lateralis (top) for the seven sport-specific tasks. For each graphic, bars that do not share the same letter are significantly different for $p<0.05$.

Damping properties

For the two muscles, damping properties at 10–49 Hz were two times lower than the ones measured at 50–89 Hz, which were 1.5 times lower than the ones recorded at 90–130 Hz ($p<0.001$). Concerning the GAS, damping properties in the 10–49 Hz band were maximal for the two landings, front lunge and side cut, and they were up to 30% higher in comparison to the running and hop tests. For the 50–89 Hz band, the damping properties were minimal for

the running and front lunges, and they were up to 15% higher for all the other movements. No significant differences between the tasks were observed for the 90–130 Hz band (figure 4). Concerning the VL, the damping properties in the 10–49 Hz band were minimal during running, hop test and landing from 22.5 cm, and they were up to 25% smaller compared to the other movements. For the 50–89 Hz band, the damping properties were minimal for the hop test, as other tasks led to damping properties up to 15% higher. Finally, for the 90–130 Hz band, the damping properties were maximal for the two landing tasks and front lunges, and they were up to 40% greater in comparison to the other movements (figure 4).

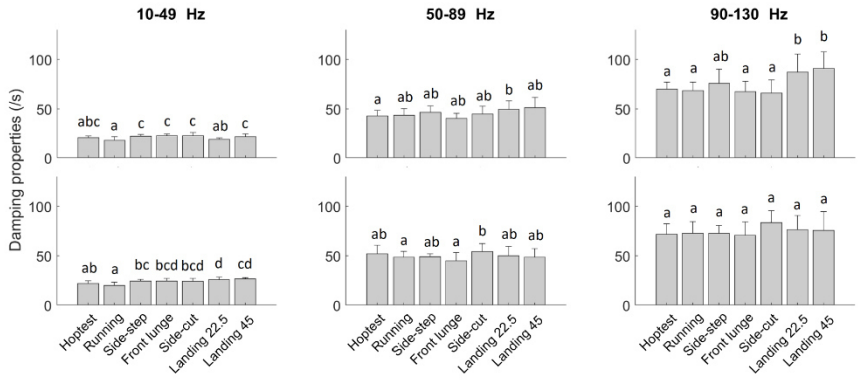

Figure 4 : Means ± standard deviations of the damping property for the gastrocnemius medialis (bottom) and vastus lateralis (top) for the seven sport-specific tasks. For each graphic, bars that do not share the same letter are significantly different at p <0.05.

Discussion

The purpose of this study was to characterize the input and the soft-tissue vibrations of leg muscles during different sport-specific tasks. The main results were that greater input and soft-tissue frequency and energy were found for most movements compared to running. In addition, positive energy transmission was found for the low frequency band but also for the middle

frequencies, with some discrepancies between movements. However, only minor modifications of damping properties were depicted between the tasks.

Soft-tissue compartment vibrations are initiated at the instant of the impact between the foot and the ground; thus, the energy and frequency of the impact characterized the input into the musculoskeletal system (4). When the input frequency is close to the natural frequency of the soft tissues, a resonance effect is expected to occur (6). Previous studies have found that input frequency in running is around 20 Hz (12) and is likely to be transferred to the soft tissues (6). In our study, only the running and the hop tests produced an input main frequency close to this frequency of 20 Hz, while the other tasks generated input main frequencies above 50 Hz, as well as greater energy in higher-frequency bands. Based on studies that focused on whole-body vibration exposure, the increase in the input frequency may lead to an ineffective increase in muscular activity during these tasks (23–27). The differences of input frequency between the movements may be the consequence of combinations of different landing speed, joint kinematics, muscle preactivation and strike patterns (11, 21, 22). Moreover, the distribution of the signal energy on the frequency spectrum depicted that the energy was not only localized around the main frequency, but also that peaks of energy were localized at several frequencies. Therefore, movements with main frequencies above 50 Hz also generated more energy under 50 Hz than the running and hop tests.

Once the impact occurs, the input energy is transferred to the lower limbs and causes soft-tissue vibrations. The transfer function depicted that all movements except for the hop test led to an amplification of the input signal under 50 Hz. While the main frequencies of the input for the hop test and running were similar, the transfer of energy in the lower band was different. Previous studies found that greater knee flexion led to greater attenuation of the vibration (34, 35), potentially thanks to the eccentric work of the quadriceps muscles (36). During the hop test, the strike was made with the forefoot in order to keep the heel off the ground, potentially

increasing the eccentric work of the calf muscles compared to heel-toe running. It may be assumed that the energy was transmitted less, thanks to the eccentric work of the calf muscles (36). Within the middle-frequency band, front lunges and side cuts produced an amplification of the input, while it was attenuated for other tasks. Based on the resonance principle, only the energy at frequencies close to the natural frequency of the muscle must have been transferred (5). It may be hypothesized that the motor organization required to perform these two tasks (i.e., lunges and side cuts) led to an increase in the natural frequencies of the soft tissues.

Consequently, regardless of the task, the soft-tissue vibration energy was mainly located under 90 Hz, with main frequencies between 15 and 30 Hz. The energy of the vibration in each frequency band was higher for the movements with the greater input energy, and therefore, some movements produced up to three times more vibration energy than in running. There is little evidence that transient soft-tissue vibrations have negative effects on the musculoskeletal system. However, three studies reported that the reduction of the amplitude of the soft-tissue vibrations achieved with compression garments was concomitant with a reduction of muscular activity during cycling (16) and landing tasks (19). Additionally, the reduction of the vibration amplitude during downhill run decreased the muscle soreness and limit the decrease in the voluntary activation after the run (28). Consequently, it may be hypothesized that the movements that produced more vibration energy may require more muscular activation to damp the vibrations, and that repetition of vibrations may have deleterious effects on the neuromuscular system and may negatively impact performance. In our study, the landings and side cuttings were the two tasks in which greater soft-tissue vibration energy was found.

Once the vibration is initiated at the muscle level, muscles tend to damp the vibrations as quickly as possible (10, 37). Our results depicted some movement-related changes in damping properties. In line with the implications of the muscle-tuning paradigm (37), movement with more energy in the low-frequency bands close to the main frequency had greater damping

properties. However, even if the damping properties differed between tasks, they remained too small to keep vibration energy at a level as low as in running. One hypothesis could be that the increase in damping properties aimed to reduce the vibration amplitude was not the main goal sought by the musculoskeletal system during these sport-specific tasks. It may be possible that the main goal of the neuromuscular system was to correctly execute the movements and to deal with a performance/protection tradeoff that limited the reduction of the vibration amplitude.

Practical applications

When athletes perform sport-specific tasks, they may be subject to input and soft-tissue vibrations with more energy and at a greater frequency than in running. As these characteristics were shown to led to an increase in the neuromuscular demand, the reduction of the latter may become a possible solution to limit their deleterious effects. Footwear design has been shown to influence input characteristics (14, 38, 39), but the specificity of the movements and the variations between participants may lead to subject-specific changes (2). Therefore, the use of compression garments was shown to be efficient to decrease soft-tissue vibrations (16, 19, 28). While compression is frequently used in mountain running, it may also be used by athletes who experiment with numerous tasks such as landings or side cuttings. However, before drawing any conclusions, further experiments are needed to better understand how input and transient soft-tissue vibrations are linked to neuromuscular adaptations.

Limitations

Our study suffered from some limitations. Firstly, electromyograms of lower-limb muscles and three-dimensional kinematics were not recorded, whereas they could help in understanding the influence of muscle activity and joint kinematics on the input transmission and damping of soft-tissue vibrations of the muscles concerned. Secondly, the slippage of the foot relative to the shoe during the side steps may lead to a biased estimation of the input characteristics.

Further studies are needed to estimate how the slippage of the foot may alter impact-vibration measurements.

Conclusion

In our study, input and muscle-vibration characteristics were modified by the various sport-specific tasks. We posit that some sport-specific tasks lead to greater energy and frequency of vibration than in-line running. Sports with repetitive landings and side cuttings are the most exposed to greater energy impact and vibrations. Authors suggest that an accurate quantification of these tasks should be completed, as it may help to better understand the constraints experienced by the musculoskeletal system during sporting practice.

Acknowledgments

The authors thank Babolat and Gerflor for the provision of technical assistance (i.e., gymnasium, track field, standardized shoes). This study was financed by the European Regional Development Fund, FUI VIBRINNOV. The results of the study are presented clearly, honestly and without fabrication, falsification or inappropriate data manipulation. The results of the present study do not constitute endorsement by ACSM.

Conflict of interest statement

None of the authors are in conflict of interest with regards to this research.

References

1. Boyer KA. Muscle Tuning During Running: Implications of an Un-tuned Landing. *J Biomech Eng.* 2006;128(6):815.
2. Boyer KA, Nigg BM. Muscle activity in the leg is tuned in response to impact force characteristics. *J Biomech.* 2004;37(10):1583–8.
3. Nigg BM, Liu W. The effect of muscle stiffness and damping on simulated impact force peaks during running. *J Biomech.* 1999;32(8):849–856.

4. Nigg BM, Wakeling JM. Impact forces and muscle tuning: a new paradigm. *Exerc Sport Sci Rev*. 2001;29(1):37–41.

5. Wakeling JM, Liphardt A-M, Nigg BM. Muscle activity reduces soft-tissue resonance at heel-strike during walking. *J Biomech*. 2003;36(12):1761–9.

6. Wakeling JM, Nigg BM, Rozitis AI. Muscle activity damps the soft tissue resonance that occurs in response to pulsed and continuous vibrations. *J Appl Physiol*. 2002;93(3):1093–103.

7. Boyer KA, Nigg BM. Changes in Muscle Activity in Response to Different Impact Forces Affect Soft Tissue Compartment Mechanical Properties. *J Biomech Eng*. 2007;129(4):594.

8. Zadpoor AA, Nikooyan AA. Modeling muscle activity to study the effects of footwear on the impact forces and vibrations of the human body during running. *J Biomech*. 2010;43(2):186–93.

9. Wakeling JM, Nigg BM. Modification of soft tissue vibrations in the leg by muscular activity. *J Appl Physiol*. 2001;90(2):412–420.

10. Khassetarash A, Hassannejad R, Enders H, Ettefagh MM. Damping and energy dissipation in soft tissue vibrations during running. *J Biomech*. 2015;48(2):204–9.

11. Gruber AH, Boyer KA, Derrick TR, Hamill J. Impact shock frequency components and attenuation in rearfoot and forefoot running. *J Sport Health Sci*. 2014;3(2):113–21.

12. Boyer KA, Nigg BM. Quantification of the input signal for soft tissue vibration during running. *J Biomech*. 2007;40(8):1877–80.

13. Giandolini M, Pavailler S, Samozino P, Morin J-B, Horvais N. Foot strike pattern and impact continuous measurements during a trail running race: proof of concept in a world-class athlete. *Footwear Sci*. 2015;7(2):127–37.

14. Fu W, Fang Y, Gu Y, Huang L, Li L, Liu Y. Shoe cushioning reduces impact and muscle activation during landings from unexpected, but not self-initiated, drops. *J Sci Med Sport*. 2017;20(10):915–20.

15. Boyer KA, Nigg BM. Soft tissue vibrations within one soft tissue compartment. *J Biomech*. 2006;39(4):645–51.

16. Hintzy F, Gregoire N, Samozino P, Chiementin X, Bertucci W, Rossi J. Effect of thigh-compression shorts on muscle activity and soft tissue vibration during cycling.: *J Strength Cond Res*. 2017;1.

17. Enders H, von Tscharner V, Nigg BM. Analysis of damped tissue vibrations in time-frequency space: a wavelet-based approach. *J Biomech*. 2012;45(16):2855–9.

18. Fu W, Liu Y, Zhang S. Effects of Footwear on Impact Forces and Soft Tissue Vibrations during Drop Jumps and Unanticipated Drop Landings. *Int J Sports Med*. 2012;34(06):477–83.

19. Fu W, Wang X, Liu Y. Impact-induced soft-tissue vibrations associate with muscle activation in human landing movements: An accelerometry and EMG evaluation. *Technol Health Care*. 2015;23(s2):S179–87.

20. Maniar N, Schache AG, Cole MH, Opar DA. Lower-limb muscle function during sidestep cutting [Internet]. *J Biomech*. 2018 [cited 2018 Oct 29]; available from: https://linkinghub.elsevier.com/retrieve/pii/S002192901830798X. doi:10.1016/j.jbiomech.2018.10.021.

21. Gindre C, Lussiana T, Hebert-Losier K, Mourot L. Aerial and Terrestrial Patterns: A Novel Approach to Analyzing Human Running. *Int J Sports Med*. 2016;37(1):25–9.

22. Müller R, Siebert T, Blickhan R. Muscle preactivation control: simulation of ankle joint adjustments at touchdown during running on uneven ground. *J Appl Biomech*. 2012;28(6):718–725.

23. Rittweger J, Mutschelknauss M, Felsenberg D. Acute changes in neuromuscular excitability after exhaustive whole body vibration exercise as compared to exhaustion by squatting exercise. *Clin Physiol Funct Imaging*. 2003;23(2):81–86.

24. Padulo J, Filingeri D, Chamari K, et al. Acute effects of whole-body vibration on running gait in marathon runners. *J Sports Sci*. 2014;32(12):1120–6.

25. Rittweger J, Ehrig J, Just K, Mutschelknauss M, Kirsch KA, Felsenberg D. Oxygen uptake in whole-body vibration exercise: influence of vibration frequency, amplitude, and external load. *Int J Sports Med*. 2002;23(06):428–432.

26. Bongiovanni LG, Hagbarth KE, Stjernberg L. Prolonged muscle vibration reducing motor output in maximal voluntary contractions in man. *J Physiol*. 1990;423(1):15–26.

27. Munera M, Bertucci W, Duc S, Chiementin X. Analysis of muscular activity and dynamic response of the lower limb adding vibration to cycling. *J Sports Sci*. 2017;1–11.

28. Ehrström S, Gruet M, Giandolini M, Chapuis S, Morin J-B, Vercruyssen F. Acute and Delayed Neuromuscular Alterations Induced by Downhill Running in Trained Trail Runners: Beneficial Effects of High-Pressure Compression Garments [Internet]. *Front Physiol*. 2018 [cited 2019 Jan 7];9 available from: https://www.frontiersin.org/article/10.3389/fphys.2018.01627/full. doi:10.3389/fphys.2018.01627.

29. Dalleau G, Belli A, Viale F, Lacour JR, Bourdin M. A simple method for field measurements of leg stiffness in hopping. *Int J Sports Med*. 2004;25(3):170–6.

30. Trama R, Blache Y, Hautier C. Effect of rocker shoes and running speed on lower limb mechanics and soft tissue vibrations. *J Biomech*. 2019;82:171–7.

31. Lilly JM, Olhede SC. Higher-Order Properties of Analytic Wavelets. *IEEE Trans Signal Process*. 2009;57(1):146–60.

32. Bates D, Mächler M, Bolker B, Walker S. Fitting Linear Mixed-Effects Models Using **lme4** [Internet]. *J Stat Softw*. 2015 [cited 2017 Mar 15];67(1) available from: http://www.jstatsoft.org/v67/i01/. doi:10.18637/jss.v067.i01.

33. Bates D, Maechler M, Bolker B, et al. Package 'lme4' [Internet]. *R Found Stat Comput Vienna*. 2014 [cited 2017 Mar 29]; available from: ftp://alvarestech.com/pub/plan/R/web/packages/lme4/lme4.pdf.

34. Lafortune MA, Lake MJ, Hennig EM. Differential shock transmission response of the human body to impact severity and lower limb posture. *J Biomech*. 1996;29(12):1531–7.

35. Edwards WB, Derrick TR, Hamill J. Musculoskeletal Attenuation of Impact Shock in Response to Knee Angle Manipulation. *J Appl Biomech*. 2012;28(5):502–10.

36. Garrett WE, Safran MR, Seaber AV, Glisson RR, Ribbeck BM. Biomechanical comparison of stimulated and nonstimulated skeletal muscle pulled to failure. *Am J Sports Med*. 1987;15(5):448–54.

37. Wakeling JM, Nigg BM, Rozitis AI. Muscle activity damps the soft tissue resonance that occurs in response to pulsed and continuous vibrations. *J Appl Physiol*. 2002;93(3):1093–103.

38. Hamill J, Russell EM, Gruber AH, Miller R. Impact characteristics in shod and barefoot running. *Footwear Sci*. 2011;3(1):33–40.

39. Herbaut A, Chavet P, Roux M, et al. The influence of shoe drop on the kinematics and kinetics of children tennis players. *Eur J Sport Sci*. 2016;16(8):1121–9.

Supplementary files

Appendix A: Center of frequency and time resolution for the 39 wavelet used.

#	Centre Frequency (Hz)	Time resolution (s)	#	Centre Frequency (Hz)	Time resolution (s)	#	Centre Frequency (Hz)	Time resolution (s)
1	9.59	0.300	14	23.62	0.122	27	58.16	0.050
2	10.28	0.280	15	25.32	0.114	28	62.33	0.046
3	11.02	0.262	16	27.13	0.106	29	66.81	0.044
4	11.81	0.244	17	29.08	0.100	30	71.60	0.040
5	12.66	0.228	18	31.17	0.092	31	76.74	0.038
6	13.57	0.212	19	33.40	0.086	32	82.25	0.036
7	14.54	0.198	20	35.80	0.080	33	88.15	0.032
8	15.58	0.184	21	38.37	0.076	34	94.48	0.030
9	16.70	0.172	22	41.13	0.070	35	101.26	0.028
10	17.90	0.160	23	44.08	0.066	36	108.53	0.026
11	19.19	0.150	24	47.24	0.060	37	116.32	0.024
12	20.56	0.140	25	50.63	0.056	38	124.67	0.024
13	22.04	0.130	26	54.27	0.054	39	133.62	0.022

Effect of rocker shoes and running speed on lower limb mechanics and soft tissue vibrations

Trama R.[1], Blache Y.[1], Hautier C.[1]
[1] Univ-lyon, Université Claude Bernard Lyon 1, LIBM EA 7424, Lyon, France

Corresponding author
Trama Robin
Univ Lyon, University Claude Bernard Lyon 1, EA 7424 - Inter-university Laboratory of Human Movement Science, Lyon, France
Email: robin.trama@univ-lyon1.fr

Please cite this article as : R. Trama, Y. Blache, C. Hautier, Effect of rocker shoes and running speed on lower limb mechanics and soft tissue vibrations, Journal of Biomechanics (2018).
doi : https://doi.org/10.1016/j.jbiomech.2018.10.023

Abstract

Previous studies have shown a possible effect of running speed and the sole material of footwear on lower-limb mechanics and soft tissue vibrations, while little information has been offered concerning the influence of the shape of the footwear's sole. The purpose of this study is to assess the effect of running speed and rocker shoes on muscular activity, ground reaction force, and soft tissue vibrations. Twenty participants performed heel-toe running with two shoes, differentiated only by their sole shape (i.e. rocker and non-rocker), at four running speeds. Ground reaction force and electromyograms of the *gastrocnemius medialis* and *vastus lateralis* were measured, and soft tissue accelerations of the same muscles were recorded with tri-axial accelerometers. A continuous wavelet transform was applied to the accelerometer's signals to analyse them in the time-frequency domain. The rocker of the shoes did not change the muscular activations, ground reaction force, nor power of soft tissue vibrations. In opposite, increased running speed led to an augmentation of all of the measured parameters. Interestingly, running speed augmentation led to a greater increase in high frequencies component of soft tissue vibrations (25 to 50 Hz, 242 %) than lower ones (8 to 25 Hz, 111 %). Consequently, we indicated a 10 % increase in the relative part of the high frequencies of the total power. In

conclusion, although rocker shoes have shown an effect on lower-limb kinetics in some studies, no influence on soft tissue vibration is denoted. By contrast, soft tissue vibrations may be modulated by changing running speed.

1. Introduction

Running is one of the most commonly practiced sports, with hundreds of millions of runners worldwide. Despite running's positive effects on health (Lee et al., 2017), inappropriate management of the training load may lead to increased risk of injury. Indeed, the incidence of lower-limb injuries varied from 19 % and 79 % of runners (van Gent et al., 2007). One of the causes of such injuries is excessive mechanical stress (Zadpoor and Nikooyan, 2011), which is characterized by a succession of muscular contractions, impact with the ground, and vibration of soft tissues (i.e. muscles, fat, and skin) caused by the impact. Moreover, some authors showed that continuous vibrations above 30 Hz cause muscular damages (de Hoyo et al., 2013) and fatigue (Cardinale and Lim, 2003; Rittweger et al., 2003).

Running speed is one of the factors that influences lower-limb mechanics. Indeed, studies have shown that lower-limb muscular activity during the stance phase (Dorn et al., 2012; Hamner et al., 2010; KyrÖlÄinen et al., 1999), as well as leg muscle pre-activation (Boyer and Nigg, 2004), increased with higher running speeds. Concerning ground reaction force, it has been observed that increasing running velocity led to an increase in passive and active peaks, vertical loading rate (VLR), and impact frequency (Boyer and Nigg, 2004; Nilsson and Thorstensson, 1989). Finally, only one study has quantified the effect of running speed on soft tissue vibrations (Boyer and Nigg, 2004), and the results showed that soft tissue acceleration amplitude and frequency were higher when running velocity increased.

Footwear type may also modify lower-limb mechanics. Studies in which the hardness or stiffness of shoes were changed did not detect altered muscular activity (Azevedo et al., 2012; Kahle et al., 2016; Roy and Stefanyshyn, 2006) or consequent subject-specific changes (Nigg

et al., 2003; Wakeling et al., 2002), but other authors reported decreased muscular activity at low running speeds with increased shoe stiffness (Chen et al., 2014). Concerning ground reaction force, it has been demonstrated that running with harder or less cushioned shoes increased the impact peak and VLR (Logan et al., 2010; Ly et al., 2010; Zadpoor and Nikooyan, 2010), while some studies indicated that wearing softer shoes raised the impact peak (Baltich et al., 2015). By contrast, increasing the thickness of the sole did not alter the ground reaction force during running (Chambon et al., 2014; Hamill et al., 2011). Soft tissue vibrations have also been shown to be sensitive to changes in the sole material. Indeed, elastic soles increased the magnitude of vertical accelerations of the *tibialis anterior* during running in some works (Giandolini et al., 2017), while some authors did not find any differences (Boyer and Nigg, 2004).

Although the previous studies have yielded relevant insights about the influence of footwear type and running velocity on lower-limb mechanics, some concerns remain. Firstly, only the sole material, thickness or hardness, has been tested, and very few studies have investigated the effect of the sole shape, especially rocker shoes (i.e. with a curved sole), on muscular activity, ground reaction force, and soft tissue vibrations. Despite that rocker shoes did not modify muscular activity (Sobhani et al., 2013), their possible effect on ground reaction force is still debated. Indeed, some authors found that wearing rocker shoes decreased impact and passive peaks during running (Lin et al., 2017), though others did not find any effect (Boyer and Andriacchi, 2009). In addition, no study has yet investigated the influence of rocker shoes on soft tissue vibrations, although a reduction of soft tissue vibrations could be one mechanism to explain the popularity of such running shoes. Secondly, soft tissue acceleration signals are often not stationary, and they therefore require a more appropriate treatment than fast Fourier transform (Gao and Yan, 2011). In this context, a wavelet-based approach was developed to obtain a relevant time-frequency analysis (Enders et al., 2012). In addition, such an analysis

makes it possible to calculate the power and a damping coefficient for several bandwidth frequencies (Khassetarash et al., 2015b).

The purpose of this study is to assess the effect of running speed and rocker shoes on muscular activity, ground reaction force, and soft tissue vibrations. On one hand, we hypothesized that increasing running speed leads to an augmentation of muscular activity, ground reaction force, and soft tissue acceleration parameters. On the other hand, running with rocker shoes should not affect muscular activity, decrease impact peak and therefore, decrease the shock and its propagation.

2. Methods

2.1. Participants

In total, 20 healthy male recreational runners (age: 23.9 ± 2.1 years, height: 1.77 ± 0.05 m, mass: 73.6 ± 7.4 kg) volunteered to partake in this study. None of the participants presented any history of lower-limb injury for six months prior to the experiment. All participants were rear-foot strikers, which was monitored with video during the warm-up period (Enders et al., 2014; Rice et al., 2016). The participants signed an informed consent document, which was approved by the local university ethics committee according to the Declaration of Helsinki.

2.2. Experimental procedure

Before beginning the tests, each subject underwent a 20-minute warm-up phase during which time they ran at different velocities on the indoor running track used for the tests with two types of shoes: rocker and non-rocker running shoes (Fig. 1). The rocker shoes were specially designed and characterized by greater rear and front elevation of the sole and a smaller ground contact surface, compared to the non-rocker shoes (Table 1). The apexes were defined as the point where the sole was not in contact with the ground anymore. The mean thickness of the

sole, corresponding to the mean sole height calculated at the rear and front apexes, were only 2 mm different (corresponding to less than 5 %) between the two shoes (Table 1).

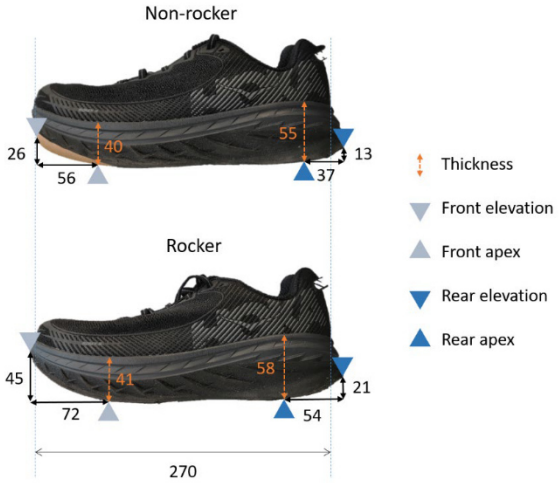

Fig. 1. Shoe without rock (top) and with a rock (bottom). All distances are in millimeters.

Table 1 : Shoe characteristics for a man US size 9 (270 mm).

	Non-rocker shoe	Rocker shoe
Mass (g)	237	241
Sole material	EVA 40 - 45 C	EVA 40 - 45 C
Mean thickness (mm)	48	50
Front apex (%)	21	27
Rear apex (%)	14	20
Ground contact (%)	65	53

The tests consisted of running at 8, 10.5, 13, and 15.5 km/h on a running track with the rocker and non-rocker shoes in a counter-balanced order. Participants were instructed to land on the force plate with their right foot without modifying their natural gait. Running speed was controlled with photocells placed 1.5 m from each side of the centre of the force plate. Trials were excluded from the analysis if the running pattern was changed to ensure the runner landed

on the force plate (visually controlled) or if the running speed was 5 % above or below the required running speed. A condition was completed when five valid trials were documented.

2.3. Instrumentation and data collection

In line with previous studies (Boyer and Nigg, 2004; Enders et al., 2014; Khassetarash et al., 2015a; Wakeling et al., 2003; Wakeling and Nigg, 2001), electromyograms of each participant's *gastrocnemius medialis* (GAS) and *vastus lateralis* (VL) of the right leg were recorded with pairs of surface electrodes (Trigno Wireless EMG, Delsys, MA, USA, 1,000 Hz). After having shaved and cleaned the skin with alcohol, electrodes were placed on GAS and VL according to SENIAM recommendations. Ground reaction force was recorded with a force plate (AMTI, OR6-7-2000, Watertown, MA, USA, 1,000 Hz). Soft tissue accelerations of the right leg were recorded with two tri-axial accelerometers (Mega Electronics, Kuopio, Finland, ±100 g, 1,000 Hz). In line with the work of Boyer (2006), the accelerometers were firmly tapped on the muscle belly of the GAS and VL. The y-axis was oriented in order to be collinear to the longitudinal axis of the thigh and shank respectively. All signals were synchronized with LabChart 8.0 (ADinstrument, Sydney, Australia).

2.4. Data treatment

The stance phase corresponded to the time when the vertical ground reaction force was superior to 3 N. Raw electromyograms were firstly filtered with a band-pass Butterworth filter at 10-499 Hz (De Luca, 1997). Then, signals were rectified, and a low-pass Butterworth filter with a cut-off frequency at 8 Hz was applied to obtain signal envelops. The signals were normalized for each participant with the maximum values obtained at 15.5 km/h with the non-rocker shoes during the stance phase (Albertus-Kajee et al., 2011). According to Boyer's (2006) methodology, the mean activity of GAS and VL was calculated for the pre-activation phase, during the 50 ms before impact (EMG_{pre}), and during the stance phase (EMG_{stance}). Ground reaction force was normalized relative to the participants' body weight. In accordance with

Boyer and Nigg's (2007a) work, only the vertical ground reaction force was analysed. The impact peak, which corresponds to the first peak after the impact, and the active peak, which corresponds to the second peak, were automatically detected. The VLR, as corresponds to the average slope between 20 % and 80 % of the impact peak, and the impact frequency (Eq. 1), were then computed with the following equation (Boyer and Nigg, 2004).

$$\text{Impact frequency} = \frac{1}{2\ (\text{Impact peak} / \text{VLR})} \quad \text{(Eq. 1)}$$

In line with the recommendations from Khassetarash et al. (2015a), only the longitudinal axis of soft tissue accelerations was analysed. In the temporal domain, peak accelerations (Acc_{peak}) were calculated as the maximal absolute value of the acceleration signal during the stance phase (Fig. 2). For the frequency analysis, a continuous wavelet transform was applied to the raw accelerometer's signals in order to analyse the time-frequency characteristics of these signals (Fig. 2). The method described by Phinyomark et al. (2009) was used to select the mother wavelet, which was the Complex Gaussian 56. Then, the modulus of the coefficients obtained from the continuous wavelet transform were split into two frequency components: low frequencies (LF, between 8 Hz and 25 Hz) and high frequencies (HF, between 25 Hz and 50 Hz) (Fig. 2) (Boyer and Nigg, 2006). The very low frequencies under 8 Hz, which represent movement (Winter, 2009), and the very-high frequencies above 50 Hz, which represent the noise of the attachment system (Shorten and Winslow, 1992), were not analysed. The main frequency, which corresponds to the mean of the median frequencies measured at each sample time, was computed for each muscle (i.e. GAS and VL). The mean power (P_{mean}) and the maximal power (P_{max}) were calculated for each frequency band (Fig. 2). The relative part of HF was determined by calculating the ratio between P_{mean} of HF and the total mean power (HF_{ratio}). A 500 ms window after impact was considered to compute the damping coefficient (DAMP) of GAS and VL for the two frequency bands (LF and HF). To avoid side effects, DAMP

corresponded to the slope of the curve between 80 % and 20 % of the power range computed between the maximal and minimal power (Fig. 2).

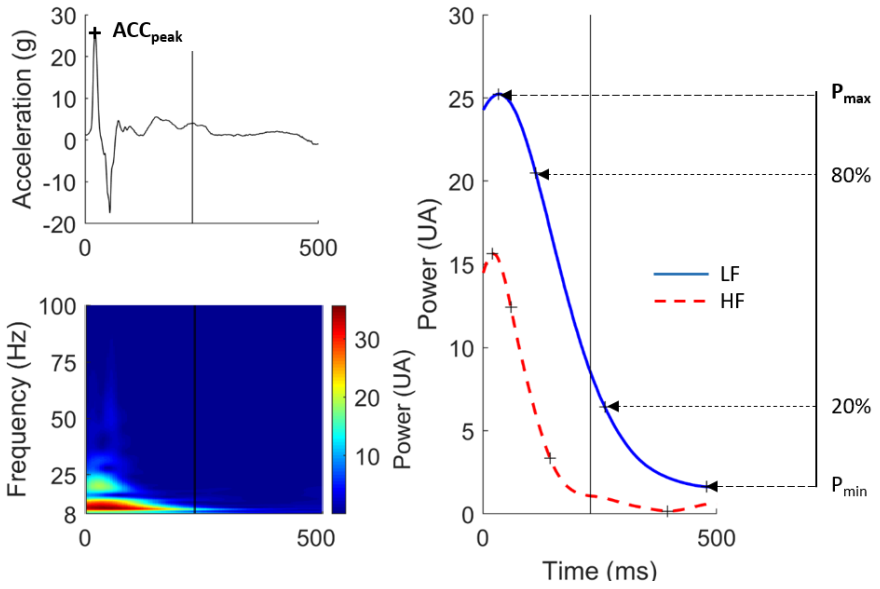

Fig. 2. top left: acceleration signal of the *gastrocnemius medialis* at 15.5 km/h; bottom left: The map represents the power at each time and frequency obtained by the wavelet analysis; right: Low (LF, blue solid line) and high (HF, red dashed line) frequency components of the signal. The damping coefficient corresponds to the mean slope between 80% and 20%. The black vertical line represents the end of the stance phase.

2.5. Statistics

The interaction effect between the shoes (rocker vs non-rocker shoes; fixed effect) and running speed (8 vs 10.5 vs 13 vs 15.5 km/h; fixed effect) on the parameters cited in the previous section were tested using linear mixed models (Bates et al., 2015) with the participants entered as a random intercept. Likewise, since the effect of the shoes or running speed may differ among participants, the fixed effects were also set as random slopes. We obtained the p-values from likelihood ratio tests, which were conducted by testing the full model against the model without the effect tested. The level of significance was set at $p < 0.0017$ (Bonferroni correction:

0.05/30). If an interaction effect was found, main effects were calculated for each specific running speed and shoes. When main effect was found, post-hoc pairwise comparisons were performed using Tukey's honestly significant difference. The normality, homoscedasticity, and linearity of the linear-mixed model residuals were graphically controlled. All models were performed using the package lme4 (Bates et al., 2014, p. 4) of R software (R 3.3.3, RCore Team 2014, Vienna, Austria).

3. Results

3.1. Muscular activity

The linear mixed models revealed an interaction effect of the shoes and running speed on EMG_{pre} of GAS ($p < 0.0017$) and EMG_{stance} for GAS and VL, while only a running speed effect was observed for EMG_{pre} of VL ($p < 0.0017$). However, for both muscles, there was no effect of the shoe condition on EMG_{pre} and EMG_{stance} at a given running velocity.

Concerning pre-activations, the EMG_{pre} of GAS was not influenced by running speed when the non-rocker shoes were used ($p = 0.003$; 12.7 ± 2.3 %). However, when running with rocker shoes, EMG_{pre} was superior (up to 143 %) at 15.5 km/h compared to two other speeds (8 and 10.5 km/h), and it was superior at 13 km/h compared to 8 km/h (Fig. 3). For the EMG_{pre} of VL, a significant increase (up to 74 %) was observed between 8 and 15.5 km/h (Fig. 3). Concerning activations during the stance phase, EMG_{stance} of GAS when running with the non-rocker shoes was significantly smaller (up to -59 %) at 8 km/h compared to the other running velocities. When running with the rocker shoes, $EMG_{stance\ at}$ 8 km/h was inferior (up to -54 %) to those measured at 13 and 15.5 km/h (Fig. 4). EMG_{stance} of VL was superior (up to 106 and 172, for the non-rocker and rocker shoes respectively) at 15.5 km/h compared to two other speeds (8 and 10.5 km/h), and it was superior at 13 km/h compared to 8 km/h (Fig. 4).

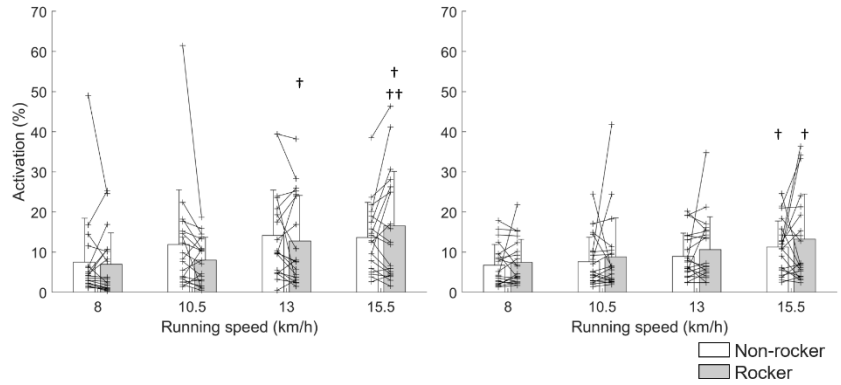

Fig. 3. Mean ± standard deviation (bars) and individual responses (thin cross) of EMG_{pre} for the *gastrocnemius medialis* (left) and *vastus lateralis* (right) at different running speeds with non-rocker (white) and rocker shoes (grey).
† different from 8 km/h for the similar shoe condition (p<0.0017).
†† different from 10.5 km/h for the similar shoe condition (p<0.0017).

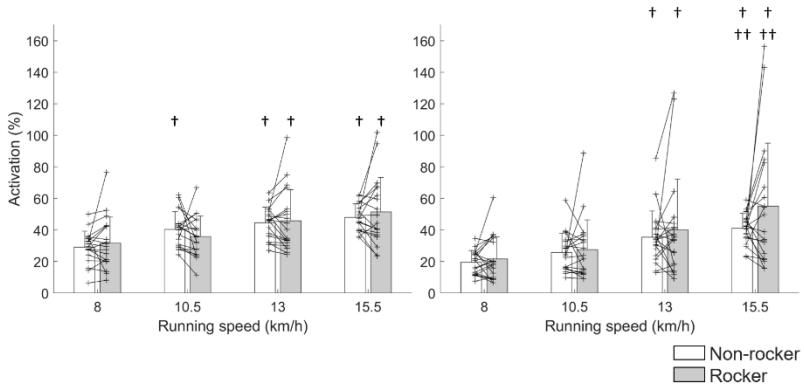

Fig. 4. Mean ± standard deviation (bars) and individual responses (thin cross) of EMG_{stance} for the *gastrocnemius medialis* (left) and *vastus lateralis* (right) at different running speeds with non-rocker (white) and rocker shoes (grey).
† different from 8 km/h for the similar shoe condition (p<0.0017).
†† different from 10.5 km/h for the similar shoe condition (p<0.0017).

3.2. Ground reaction force

The linear mixed models did not reveal any interaction effect of the shoes and running speed on the impact peak, active peak, VLR, nor impact frequency. However, there was a running speed effect on these four variables ($p < 0.0017$).

Significant increases of the impact peak, active peak, and VLR (up to 29 %, 53 %, and 115 % respectively) were observed with the augmentation of running velocity (Table 2). A significant increase (up to 42 %) of the impact frequency was revealed with running speed augmentation, except between 10.5 km/h and 8 km/h or 13 km/h, and between 13 and 15.5 km/h (Table 2).

Table 2 : Mean ± SD values of ground reaction force parameters with respect to running speed.

	8 km/h	10.5 km/h	13 km/h	15.5 km/h
Impact peak (bw)	1.56 ± 0.36 $_{a}$	1.81 ± 0.35 $_{b}$	2.07 ± 0.54 $_{c}$	2.40 ± 0.57 $_{d}$
Active peak (bw)	2.16 ± 0.17 $_{a}$	2.43 ± 0.18 $_{b}$	2.63 ± 0.23 $_{c}$	2.79 ± 0.23 $_{d}$
VLR (bw.s^{-1})	49.47 ± 19.13 $_{a}$	64.73 ± 18.65 $_{b}$	83.69 ± 26.87 $_{c}$	106.34 ± 29.37 $_{d}$
Impact frequency (Hz)	16.16 ± 5.14 $_{a}$	18.26 ± 4.88 $_{a,b}$	21.63 ± 9.71 $_{b,c}$	23.02 ± 7.22 $_{c}$

For a given parameter, means that does not share the same letter are significantly different ($p < 0.0017$). bw: body weight, VLR: Vertical Loading Rate.

3.3. Soft tissue vibrations

The linear mixed models did not reveal any interaction effect of the shoes and running speed, but there was a main effect of the running speed ($p < 0.0017$) on the soft tissue acceleration parameters (Table 3).

The Acc_{peak} increased significantly with running speed augmentation, regardless of the muscle (up to 134 % and 144 % for GAS and VL, respectively). The main frequency increased with running velocity augmentation (up to 22 % and 27 % for GAS and VL, respectively), with the following exceptions: between 10.5 km/h and 8 km/h or 13 km/h, and between 13 and 15.5 km/h for GAS, and between 8 and 10.5 km/h, and between 13 and 15.5 km/h for VL.

Regardless of the muscle, P_{mean} raised significantly with increased running speed in LF (up to 119 % and 104 % for GAS and VL, respectively) and HF bands (up to 257 % and 228 % for GAS and VL, respectively). In addition, HF_{ratio} increased with running velocity augmentation (up to 46 % and 45 % for GAS and VL. respectively) except between 8 and 10.5 km/f for GAS. Furthermore, for both GAS and VL, P_{max} raised significantly with increased running speed in LF (up to 91 % and 80 % for GAS and VL, respectively) and HF (up to 167 % and 153 % for GAS and VL, respectively). Finally, DAMP significantly increased with running speed augmentation in LF (up to 100 % and 80 % for GAS and VL, respectively) and HF bands (up to 159 % and 150 % for GAS and VL, respectively).

Table 3 : Mean ± SD values of soft tissue acceleration parameters with respect to running speed.

		8 km/h	10.5 km/h	13 km/h	15.5 km/h
GAS	Acc_{peak} (g)	9.36 ± 3.77 $_a$	12.23 ± 4.39 $_b$	16.53 ± 5.26 $_c$	21.86 ± 7.09 $_d$
	Main frequency (Hz)	16.87 ± 3.31 $_a$	17.95 ± 3.05 $_a$	19.34 ± 3.57 $_{a,b}$	20.58 ± 4.13 $_b$
	HF_{ratio} (%)	22.07 ± 7.44 $_a$	24.48 ± 7.02 $_b$	28.79 ± 7.51 $_c$	32.25 ± 7.07 $_d$
	P_{mean} LF(UA)	7.79 ± 2.02 $_a$	10.68 ± 2.30 $_b$	13.83 ± 3.07 $_c$	17.06 ± 3.56 $_d$
	P_{max} LF (UA)	10.93 ± 3.28 $_a$	14.01 ± 3.43 $_b$	17.22 ± 4.12 $_c$	20.86 ± 4.90 $_d$
	DAMP LF (UA/s)	37.57 ± 12.59 $_a$	48.75 ± 13.70 $_b$	60.55 ± 17.25 $_c$	75.01 ± 21.33 $_d$
	P_{mean} HF (UA)	2.36 ± 1.35 $_a$	3.63 ± 1.75 $_b$	5.79 ± 2.54 $_c$	8.45 ± 3.47 $_d$
	P_{max} HF (UA)	5.16 ± 3.04 $_a$	7.10 ± 3.60 $_b$	10.11 ± 4.57 $_c$	13.80 ± 6.15 $_d$
	DAMP HF (UA/s)	35.59 ± 23.96 $_a$	48.44 ± 29.56 $_b$	68.11 ± 38.77 $_c$	92.33 ± 51.71 $_d$
VL	Acc_{peak} (g)	10.77 ± 7.65 $_a$	13.66 ± 8.01 $_b$	20.12 ± 11.36 $_c$	26.40 ± 13.01 $_d$
	Main frequency (Hz)	15.90 ± 3.23 $_a$	17.18 ± 2.87 $_a$	19.04 ± 4.13 $_b$	20.26 ± 5.00 $_b$
	HF_{ratio} (%)	25.12 ± 6.62 $_a$	29.59 ± 6.60 $_b$	34.38 ± 6.71 $_c$	36.51 ± 5.91 $_d$
	P_{mean} LF (UA)	8.51 ± 4.01 $_a$	10.72 ± 4.13 $_b$	14.02 ± 5.07 $_c$	17.35 ± 6.01 $_d$
	P_{max} LF (UA)	11.06 ± 5.48 $_a$	13.03 ± 5.17 $_b$	16.30 ± 6.18 $_c$	19.91 ± 7.18 $_d$
	DAMP LF (UA/s)	39.28 ± 18.30 $_a$	48.21 ± 18.52 $_b$	60.17 ± 22.65 $_c$	70.70 ± 25.33 $_d$
	P_{mean} HF (UA)	3.22 ± 2.25 $_a$	4.93 ± 3.10 $_b$	7.94 ± 4.21 $_c$	10.56 ± 4.99 $_d$
	P_{max} HF (UA)	6.08 ± 4.85 $_a$	8.07 ± 5.19 $_b$	11.93 ± 6.67 $_c$	15.39 ± 7.76 $_d$
	DAMP HF (UA/s)	39.00 ± 30.34 $_a$	52.08 ± 33.38 $_b$	76.94 ± 43.88 $_c$	97.55 ± 48.82 $_d$

For a given parameter, means that does not share the same letter are significantly different ($p < 0.0017$). Acc_{peak}: peak acceleration, P_{mean}: mean power, P_{max}: maximum power, DAMP: damping coefficient, HF_{ratio}: relative part of HF, $g = 9.81\ m.s^{-1}$.

4. Discussion

The purpose of this study was to assess the effect of running speed and rocker shoes on muscular activity, ground reaction force, and soft tissue accelerations. As expected, increasing running speed led to an augmentation of muscular activity, ground reaction force, and soft tissue vibrations. By contrast, running with rocker shoes did not alter these parameters.

Running mechanics can be described as a chain of consequences involving muscular activity, ground reaction force, and soft tissue vibrations. A running cycle may be seen as the activation of the prime mover muscles (for example, GAS and VL), which leads to a flying phase that ends with ground impact at landing, thus creating a shockwave that propagates along the lower-limbs and causes soft tissue vibrations (Nigg and Wakeling, 2001). These soft tissue vibrations may also be damped by appropriate activation of the leg muscles (Wakeling and Nigg, 2001). Before the impact, muscle pre-activation is necessary in order to increase joint stiffness and adapt the landing angle of the joint (Kyröläinen et al., 1999). With the exception of GAS with the non-rocker shoes, we observed that increasing running speed requires higher muscle pre-activation, which confirms the results of Boyer and Nigg (2004). Changes in muscular pre-activations with changed footwear could have been expected as rocker shoes may modify running kinematics (Boyer and Andriacchi, 2009; Sobhani et al., 2016). However, rocker shoes did not alter pre-activations of GAS and VL in our study. It can be assumed that kinematic changes between the two shoes were too small for rear-foot strikers to experience modifications in muscular pre-activations. However, running kinematics were not controlled in the current study, and therefore the link between muscular pre-activation and kinematics should be investigated. Once the foot strikes the ground, muscular activations are necessary to brake and then propel the body in a forward direction. As expected, we observed that increasing GAS and

VL activities during the stance phase is necessary to run faster (Nilsson and Thorstensson, 1989; Tsuji et al., 2015). As running speeds were identical between our two shoe conditions, footwear did not alter muscular activations during the stance phase, which confirms the ideas in the study of Sobhani et al. (2013).

Human strategies for increasing running speed consist of increasing step frequency and amplitude (Dorn et al., 2012), which involves an increase in the vertical displacement of the centre of gravity (Hamner et al., 2010). Consequently, as observed in a previous study (Boyer and Nigg, 2004), we indicated that greater running velocities are associated with greater ground impact magnitude and frequency. Rocker shoes were designed with a curved sole in order to smooth the roll of the foot, especially during the braking phase. However, contrary to our hypotheses, we did not observe a decrease in ground impact peak and VLR in comparison to the non-rocker shoes. Our results differ from those of Lin et al. (2017); however, an explanation for these discrepancies may be that Lin et al. (2017) did not test exactly same sole material and thickness in their study, and these parameters are known to influence ground reaction force (Nikooyan and Zadpoor, 2011).

As previously depicted, ground impact leads to the propagation of a shockwave, which creates soft tissue vibrations (Boyer and Nigg, 2007b). Therefore, in line with Boyer and Nigg (2004), we observed that increasing running speed induced an augmentation of all of the parameters linked to soft tissue accelerations. By contrast, as the rocker shoes did not modify muscular activations nor ground reaction force, soft tissue accelerations parameters were not modified by the rocker shoes. Running faster required higher muscular activity and induced greater impact frequency, which led to an increased main frequency of soft tissue vibrations (Boyer and Nigg, 2004). In addition, an increase in peak acceleration with running speed explained the greater mean and maximal powers regardless of the frequency bandwidth and muscle. More precisely, the proportion of the high frequencies increased with running velocity, which indicates that the increase in the total power is mainly due to an increase in the high frequencies

power. This result may confirm that the frequency component of soft tissue vibration signals is influenced by impact frequency and muscular activity (Wakeling and Nigg, 2001). Furthermore, vibrations may be damped by controlling the muscular activity (Boyer and Nigg, 2007b), which may influence the apparition of muscular fatigue caused by high vibration frequencies (Cardinale and Lim, 2003; Rittweger et al., 2003). In our study, increasing running speed led to an increased damping coefficient, mainly for high frequencies, which may be partly explained by the notion that the neuromuscular system tends to adopt a protective mechanism to avoid excessive vibrations (Nigg and Wakeling, 2001).

Our study suffers from some limitations, including a short adaptation time for running with rocker shoes. We have only assessed the short-term adaptations to rocker shoes, and thus a longer period of adaptation may lead to different results. The second limitation is that all runners were rear-foot strikers, and therefore our results cannot be applied to fore-foot strikers.

5. Conclusion

Although rocker shoes could have an effect on joint kinematics and kinetics during running, they did not modify GAS or VL activities, ground reaction force, nor soft tissue vibrations. This finding can be explained by the fact that, contrary to other studies, the sole material and thickness of the two shoes were identical. In common use, rocker shoes are "maximalists", with thicker and softer soles than non-rocker ones. This combination of characteristics, compared to the only change in the shape of the sole, could modify lower-limb mechanics and soft tissue vibrations. By contrast, running speed augmentation increased muscular activity, ground reaction force, and soft tissue vibrations. Interestingly, running speed augmentation led to a greater increase in soft tissue acceleration parameters in high frequencies, which are known to induce muscular fatigue or damages. Nevertheless, further studies are needed to better understanding the link between soft tissue vibrations in running and fatigue or damages.

Acknowledgments

The authors thank the company HOKA ONE ONE ® for creating and providing the prototype shoes.

Conflict of interest statement

None of the authors are in conflict of interest with regards to this research

Reference

Albertus-Kajee Y., Tucker R., Derman W., Lamberts R.P. and Lambert M.I., Alternative methods of normalising EMG during running, *J. Electromyogr. Kinesiol.* **21**, 2011, 579–586.

Azevedo A.P.D.S., Brandina K., Bianco R., Oliveira V.H.D., Souza J.R.D., Mezencio B., Amadio A.C. and Serrão J.C., Effects of replica running shoes upon external forces and muscle activity during running, *J. Sports Sci.* **30**, 2012, 929–935.

Baltich J., Maurer C. and Nigg B.M., Increased vertical impact forces and altered running mechanics with softer midsole shoes, *PloS One* **10**, 2015, e0125196.

Bates D., Mächler M., Bolker B. and Walker S., Fitting linear mixed-effects models using lme4, *J. Stat. Software* **67**, 2015.

Bates D., Maechler M., Bolker B., Walker S., Christensen R.H.B., Singmann H., Dai B., Grothendieck G., Eigen C. and Rcpp L., Package 'lme4', 2014, R Foundation for Statistical Computing; Vienna.

Boyer K.A., Muscle tuning during running: implications of an un-tuned landing, *J. Biomech. Eng.* **128**, 2006, 815.

Boyer K.A. and Andriacchi T.P., Changes in running kinematics and kinetics in response to a rockered shoe intervention, *Clin. Biomech.* **24**, 2009, 872–876.

Boyer K.A. and Nigg B.M., Changes in muscle activity in response to different impact forces affect soft tissue compartment mechanical properties, *J. Biomech. Eng.* **129**, 2007a, 594.

Boyer K.A. and Nigg B.M., Quantification of the input signal for soft tissue vibration during running, *J. Biomech.* **40**, 2007b, 1877–1880.

Boyer K.A. and Nigg B.M., Soft tissue vibrations within one soft tissue compartment, *J. Biomech.* **39**, 2006, 645–651.

Boyer K.A. and Nigg B.M., Muscle activity in the leg is tuned in response to impact force characteristics, *J. Biomech.* **37**, 2004, 1583–1588.

Cardinale M. and Lim J., The acute effects of two different whole body vibration frequencies on vertical jump performance, *Medicina Dello Sport* **56**, 2003, 287–292.

Chambon N., Delattre N., Guéguen N., Berton E. and Rao G., Is midsole thickness a key parameter for the running pattern?, *Gait Posture* **40**, 2014, 58–63.

Chen C.-H., Tu K.-H., Liu C. and Shiang T.-Y., Effects of forefoot bending elasticity of running shoes on gait and running performance, *Hum. Mov. Sci.* **38**, 2014, 163–172.

de Hoyo M., Carrasco L., Da Silva-Grigoletto M.E., Sañudo B., Caballero-Villarraso J., Arriaza E. and Escobar M.D.C., Impact of an acute bout of vibration on muscle contractile properties, creatine kinase and lactate dehydrogenase response, *Eur. J. Sport Sci.* **13**, 2013, 666–673.

De Luca, C.J., 1997. The use of surface electromyography in biomechanics. J. Appl. Biomech. **13**, 135–163.

Dorn T.W., Schache A.G. and Pandy M.G., Muscular strategy shift in human running: dependence of running speed on hip and ankle muscle performance, *J. Exp. Biol.* **215**, 2012, 2347.

Enders H., von Tscharner V. and Nigg B.M., The effects of preferred and non-preferred running strike patterns on tissue vibration properties, *J. Sci. Med. Sport* **17**, 2014, 218–222.

Enders H., von Tscharner V. and Nigg B.M., Analysis of damped tissue vibrations in time-frequency space: a wavelet-based approach, *J. Biomech.* **45**, 2012, 2855–2859.

Gao R.X. and Yan R., From Fourier transform to wavelet transform: a historical perspective, In: *Wavelets,* 2011, Springer US; Boston, MA, 17–32.

Giandolini M., Munera M., Chiementin X., Bartold S. and Horvais N., Footwear influences soft-tissue vibrations in rearfoot strike runners, *Footwear Sci.* **9**, 2017, S25–S27.

Hamill J., Russell E.M., Gruber A.H. and Miller R., Impact characteristics in shod and barefoot running, *Footwear Sci.* **3**, 2011, 33–40.

Hamner S.R., Seth A. and Delp S.L., Muscle contributions to propulsion and support during running, *J. Biomech.* **43**, 2010, 2709–2716.

Kahle A., Brown G.A., Shaw I. and Shaw B.S., Mechanical and physiological analysis of minimalist versus traditionally-shod running, *J. Sports Med. Phys. Fitness* **56**, 2016, 974–979.

Khassetarash A., Hassannejad R., Enders H. and Ettefagh M.M., Damping and energy dissipation in soft tissue vibrations during running, *J. Biomech.* **48**, 2015a, 204–209.

Khassetarash A., Hassannejad R., Ettefagh M.M. and Sari-Sarraf V., Fatigue and soft tissue vibration during prolonged running, *Hum. Mov. Sci.* **44**, 2015b, 157–167.

Kyröläinen H., Komi P.V. and Belli A., Changes in muscle activity patterns and kinetics with increasing running speed, *J. Strength Condition. Res.* **13**, 1999, 400–406.

Lee D., Brellenthin A.G., Thompson P.D., Sui X., Lee I.-M. and Lavie C.J., Running as a key lifestyle medicine for longevity, *Prog. Cardiovasc. Dis.* **60**, 2017, 45–55.

Lin S.-Y., Su P.-F., Chung C.-H., Hsia C.-C. and Chang C.-H., Stiffness effects in rocker-soled shoes: biomechanical implications, *PLoS One* **12**, 2017, e0169151.

Logan S., Hunter I.J., Ty Hopkins J.T., Feland J.B. and Parcell A.C., Ground reaction force differences between running shoes, racing flats, and distance spikes in runners, *J. Sports Sci. Med.* **9**, 2010, 147–153.

Ly Q.H., Alaoui A., Erlicher S. and Baly L., Towards a footwear design tool: influence of shoe midsole properties and ground stiffness on the impact force during running, *J. Biomech.* **43**, 2010, 310–317.

Nigg B.M., Stefanyshyn D., Cole G., Stergiou P. and Miller J., The effect of material characteristics of shoe soles on muscle activation and energy aspects during running, *J. Biomech.* **36**, 2003, 569–575.

Nigg B.M. and Wakeling J.M., Impact forces and muscle tuning: a new paradigm, *Exerc. Sport Sci. Rev.* **29**, 2001, 37–41.

Nikooyan A.A. and Zadpoor A.A., An improved cost function for modeling of muscle activity during running, *J. Biomech.* **44**, 2011, 984–987.

Nilsson J. and Thorstensson A., Ground reaction forces at different speeds of human walking and running, *Acta Physiol. Scand.* **136**, 1989, 217–227.

Phinyomark A., Limsakul C. and Phukpattaranont P., A Comparative Study of Wavelet Denoising for Multifunction Myoelectric Control, 2009, IEEE, 21–25.

Rice H.M., Jamison S.T. and Davis I.S., Footwear matters: influence of footwear and foot strike on load rates during running, *Med. Sci. Sports Exerc.* **48**, 2016, 2462–2468.

Rittweger J., Mutschelknauss M. and Felsenberg D., Acute changes in neuromuscular excitability after exhaustive whole body vibration exercise as compared to exhaustion by squatting exercise, *Clin. Physiol. Funct. Imaging* **23**, 2003, 81–86.

Roy J.-P.R. and Stefanyshyn D.J., Shoe midsole longitudinal bending stiffness and running economy, joint energy, and EMG, *Med. Sci. Sports Exerc.* **38**, 2006, 562–569.

Shorten M.R. and Winslow D.S., Spectral analysis of impact shock during running, *Int. J. Sport Biomech.* **8**, 1992, 288–304.

Sobhani S., Hijmans J., van den Heuvel E., Zwerver J., Dekker R. and Postema K., Biomechanics of slow running and walking with a rocker shoe, *Gait Posture* **38**, 2013, 998–1004.

Sobhani S., van den Heuvel E.R., Dekker R., Postema K., Kluitenberg B., Bredeweg S.W. and Hijmans J.M., Biomechanics of running with rocker shoes, *J. Sci. Med. Sport* **20**, 2016, 38–44.

Tsuji K., Ishida H., Oba K., Ueki T. and Fujihashi Y., Activity of lower limb muscles during treadmill running at different velocities, *J. Phys. Therapy Sci.* **27**, 2015, 353–356.

van Gent, R.N., Siem, D., van Middelkoop, M., van Os, A.G., Bierma-Zeinstra, S.M.A., Koes, B.W., 2007. Incidence and determinants of lower extremity running injuries in long distance runners: a systematic review. Br. J. Sports Med. **41**, 469–480.

Wakeling J.M., Liphardt A.-M. and Nigg B.M., Muscle activity reduces soft-tissue resonance at heel-strike during walking, *J. Biomech.* **36**, 2003, 1761–1769.

Wakeling J.M. and Nigg B.M., Modification of soft tissue vibrations in the leg by muscular activity, *J. Appl. Physiol.* **90**, 2001, 412–420.

Wakeling J.M., Pascual S.A. and Nigg B.M., Altering muscle activity in the lower extremities by running with different shoes, *Med. Sci. Sports Exerc.* **34**, 2002, 1529–1532.

Winter D.A., Biomechanics and Motor Control of Human Movement, fourth ed., 2009, Wiley; Hoboken, NJ.

Zadpoor A.A. and Nikooyan A.A., The relationship between lower-extremity stress fractures and the ground reaction force: a systematic review, *Clin. Biomech.* **26**, 2011, 23–28.

Zadpoor A.A. and Nikooyan A.A., Modeling muscle activity to study the effects of footwear on the impact forces and vibrations of the human body during running, *J. Biomech.* **43**, 2010, 186–193.

Heel Impacts, Tibial Shocks and Soft Tissue Vibrations in young basketball players: influence of movements and court construction

R. Trama[a]*, T. Le Solliec[a], Y. Blache[a], and C. Hautier[a]

[a] *Univ-lyon, Université Claude Bernard Lyon 1, LIBM EA 7424, Lyon, France*

Keywords: Acceleration; Continuous Wavelet Transform; Statistical Parametric Mapping

1. Introduction

Basketball is practiced by 450M people according to the International Basketball Federation. This sport is characterized by intermittent efforts, with high-intensity phases composed of sprints, side-cuts, and jumps. Compared to in-line running, some of these sport-specific movements induce greater heel impacts (HI) amplitude and frequency, involving higher soft-tissue vibrations (STV) amplitude and frequency (Trama et al. 2020). Such characteristics of STV are related to quicker and higher muscle fatigue during continuous exposure (Lienhard et al. 2015). To reduce HI and tibial shocks (TS), the stiffness of a basketball court was modified, however, these courts have no effects on HI or TS (Bruce et al. 2019). Still, only the vertical stiffness of the ground was modified, while anteroposterior (AP) and mediolateral (ML) forces are major components of the resultant force in basketball practice. To reduce the horizontal components of the force, a reduced shear stress stiffness might be required (Chen et al. 2019). Although reduced AP stiffness reduced HI amplitude in the AP axis (Chen et al. 2019), the reduction of HI amplitude induced by sport-specific tasks was not evaluated with such a court modification.

This study aimed to evaluate the influence of a basketball court with a decreased AP and ML stiffness on HI, TS, and STV. We hypothesized that this specific court construction would decrease HI, TS, and STV amplitude and frequency for the AP and ML axes, and not for the vertical axis.

2. Methods

2.1 Participants

Nine young men basketball players (french division II level), volunteered to participate in this study (age: 16 ± 3 years, height: 172 ± 11 cm, mass: 70 ± 25 kg). They were free from injury and signed an informed consent document approved by the local university ethics committee.

2.2 Basketball courts

A control ground (asphalt, REF) was compared to a specific court (PowerGame +, PWG, Gerflor, France). PWG is composed of several square plates 19*305*305 mm). When an impact occurs, plates slide horizontally to each other (≈1 cm).

2.3 Experimental procedure and data collection

Four different movements were performed: in-line running (3.6 ± 0.6 $m \cdot s^{-1}$), in-line sprinting (all out, 20 m), side-cuts (45° toward in opposite direction of supporting leg), and layups (jumps and landing impacts). For each court, five trials per movement were randomly performed.

HI (heel cup of the shoe), TS, and STV of the *gastrocnemius medialis* of the supporting leg were recorded with three triaxial accelerometers (Dytran Instrument Inc., USA, ± 1000 $m \cdot s^{-2}$, 2000 Hz). The electromyography (EMG) of the GAS was recorded with pairs of surface electrodes (Trigno Wireless EMG, Delsys, USA, 2000 Hz).

HI was detected with the heel accelerometer. A filter bank of Morse (3,60) mother wavelets was used to perform the continuous wavelet transform on raw signals. The modulus of the map of coefficients given by the wavelet transform was computed for each axis of the accelerometer. Amplitude for each frequency was computed by integrating the maps in the time domain during the 0.25 seconds after the impact (Trama et al. 2020). The same analysis was performed for EMG signal, during the 0.1 seconds before (preactivation) and after the impact (early impact phase).

2.4 Statistics

Statistical Parametric Mapping (SPM) with three three-way ANOVA with repeated measures was performed to evaluate the effect of the movement, court, and axes on the amplitude in the frequency domain of HI, TS, and STV. The alpha risk was set at 0.05/3 and 20000 permutations were performed to achieve numerical stability. The same analysis with a two-way ANOVA (movement and court) and an alpha risk of 0.05 was employed for the EMG analysis.

3. Results and discussion

Three-way ANOVA revealed a main effect of the court without interaction with the axes or movement for HI, while no effect of the court was observed for TS and STV. A main effect of the axes was denoted for HI and

TS, but not for STV. Differences between movements were depicted for HI, TS, and STV, with strong and little interactions within each axis for HI and STV, respectively. As a rule, PWG reduced the amplitude of HI by 30% (0.95% CI: 10-50%) between 34 and 44 Hz compared to REF, while the frequency repartition of the energy was not modified (Figure 1). Besides for HI and TS only, more amplitude was found for the vertical axis, then for the ML, and then for the AP axis. Considering all axes together, landing and sprinting led the greatest HI, TS, and STV, followed by side-cuts, then by jumping and running (Figure 2).

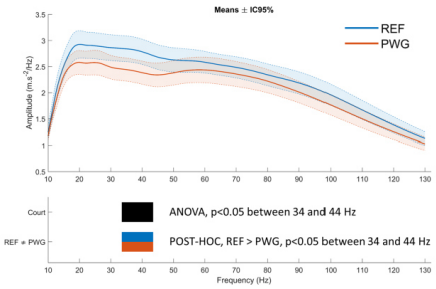

Figure 1: Heel impact amplitude in the frequency domain (means ± 95% CI) for each court.

No effect of the court, nor interactions between movement and court, were observed on the EMG. Movements elicited differences in EMG, with greater preactivations during landings compared to the majority of the other movements. Concerning the early contact phase, maximum EMG was found for sprinting, side-cutting, and jumping, while landing elicited lesser EMG.

The sliding court acted similarly to a decreased stiffness platform by reducing HI amplitude (Chen et al. 2019). This reduction was similar among the three axes and was only found for HI. Most movements differed mainly from the vertical and AP axes, but less from the ML axis. Although differences between the importance of each axis were denoted for certain movements, court construction did not act specifically on the movements with more ML and AP accelerations contributions. Besides, the reduction of HI did not lead to a reduction of TS or STV, nor of the EMG. Consequently, the transfer of energy between the heel and the other structures (bones and soft-tissues) increased. This increase could have been reflected by modifications in the EMG, but no differences were denoted. A greater time of adaptation to this surface might have led to different changes, for instance, several minutes of running are necessary to decrease EMG when changing shoes.

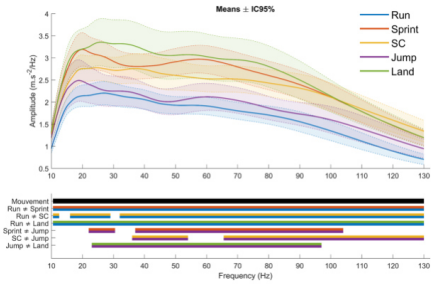

Figure 2: Heel impact amplitude in the frequency domain (means ± 95% CI) for each movement. Black line represents the ANOVA significant effect for the movements and colored lines are the significant differences between the different movements (post- hoc tests). SC: side-cuts

4. Conclusions

ML and AP sliding court was efficient to decrease HI with the ground, independently of the axis. As this court did not elicit changes in TS, STV, and EMG, they should be used as a safe alternative to asphalt courts. Further studies, with more participants and with more experience are needed to conclude the benefits of playing on such a court.

References

Bruce OL, Firminger CR, Wannop JW, Stefanyshyn DJ, Edwards WB. 2019. Effects of basketball court construction and shoe stiffness on countermovement jump landings. Footwear Science. 11(3):171–179.

Chen W-H, Hsieh C-F, Chan M-S, Shih Y, Chen C-H, Shiang T-Y. 2019. Optimal shear cushion stiffness at different gait speeds. Journal of Biomechanics. 93:226–230.

Lienhard K, Vienneau J, Nigg S, Meste O, Colson SS, Nigg BM. 2015. Relationship Between Lower Limb Muscle Activity and Platform Acceleration During Whole-Body Vibration Exercise: Journal of Strength and Conditioning Research. 29(10):2844–2853.

Trama R, Hautier C, Blache Y. 2020. Input and Soft-Tissue Vibration Characteristics during Sport-Specific Tasks: Medicine & Science in Sports & Exercise. 52(1):112–119.

***Corresponding author. trama.robin@gmail.com**

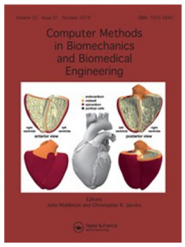

Taylor & Francis
Taylor & Francis Group

Computer Methods in Biomechanics and Biomedical Engineering

ISSN: 1025-5842 (Print) 1476-8259 (Online) Journal homepage: https://www.tandfonline.com/loi/gcmb20

Sport-related impact classification through a convolutional neural network

R. Trama, C. Hautier & Y. Blache

To cite this article: R. Trama, C. Hautier & Y. Blache (2019) Sport-related impact classification through a convolutional neural network, Computer Methods in Biomechanics and Biomedical Engineering, 22:sup1, S267-S269, DOI: 10.1080/10255842.2020.1714908

To link to this article: https://doi.org/10.1080/10255842.2020.1714908

Published online: 22 May 2020.

COMPUTER METHODS IN BIOMECHANICS AND BIOMEDICAL ENGINEERING
2019, VOL. 22, NO. S1, S267–S269
https://doi.org/10.1080/10255842.2020.1714908

Sport-related impact classification through a convolutional neural network

R. Trama, C. Hautier and Y. Blache

Univ-lyon, Université Claude Bernard Lyon 1, Lyon, France

1. Introduction

Athletes, and particularly team-sport athletes, are experiencing numerous high energy impacts caused by running, sprinting, side-cutting, landing, and others movements. Previous studies depicted that the different sport-related impacts lead to different shock characteristics, both in terms of acceleration amplitude and frequency (Fu et al. 2015; Trama et al. 2019), causing different mechanical stress to the musculoskeletal system. An excess of mechanical stress could lead to injuries (Hreljac 2004), and therefore, the quantification of such impacts may help to prevent these injuries. Wearable sensors, such as accelerometers, combined with a wavelet transform, allows the analyse of acceleration caused by the impact in the time-frequency domain. The recent development in artificial intelligence (i.e., neural networks) make it possible to classify various images with great precision.

Input characteristics are well characterized in running (Boyer and Nigg 2007), however, no study aimed to quantify and classify the impact for other sport movements. The purpose of this study was to determine if the wavelet transform of the accelerations measured at the heel, combined with a convolutional neural network, were powerful enough to classify accurately several sport-related movements.

2. Methods

2.1. Participants

A total of nine men and one woman, team sport athletes or runners, volunteered to participate in this study (age: 32.2 ± 8.9 years, height: 171.4 ± 7.0 cm, mass: 70.9 ± 10.1 kg). They were free from injury for six months prior to the experiment, and signed an informed consent document approved by the local university ethics committee.

2.2. Experimental procedure and data collection

Seven sport-related tasks were executed. The first task was a hop test; the second consisted in running in line at preferred velocity; the third task was a side-step; the fourth task was a front lunge; the fifth task was a sidecut at 45 ± 15°; the sixth and seventh tasks consisted in two landing tasks (22.5 and 45 cm). A tri-axial accelerometer (Mega Electronics, Kuopio, Finland, ±100 g, 1,000 Hz) was stuck and secured on the heel cup of the right shoe in order to record 3 D accelerations caused by the ground impacts. A total of 15 impacts for each movement was recorded with the accelerometer.

2.3. Wavelet transform

A filter bank of Morse (3,60) mother wavelets was used to performed the continuous wavelet transform (Lilly and Olhede 2012). The modulus of the map of coefficients given by the wavelet transform was computed for the three axis. Thereafter, an image of the three maps located side by side was saved in .jpeg format, with a dimension of 270*88 pixels, and a resolution of 96 dpi.

2.4. Convolution neural network

In this study, a convolution neural network, composed of 16 layers, was created to classify the different images representing the impacts. The network was composed by an input layer, followed by three times the succession of a convolution layer, normalisation layer, rectifier layer, and a pooling layer. The last layers were a fully connected layer, a softmax layer, and, a classification output layer. Adaptive Moment Estimation (Adam) optimisation algorithm was used with this network.

2.5. Training protocols

A total of 13 training protocols were tested, differing by three parameters: The first parameter was the presence or not of a pre-training (PRE) on the nontested participants (n = 10-1 = 9). The second was the type of specific training performed on the participant's data: No training (NONE); a training with the data of

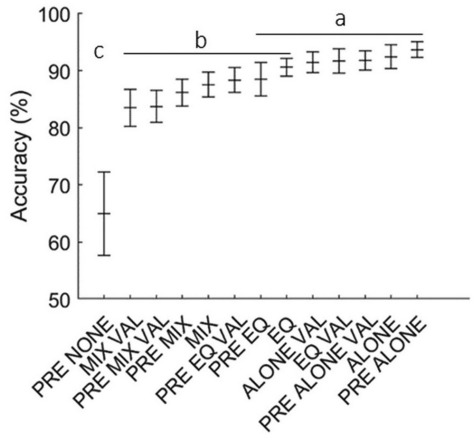

Figure 1. Accuracy (95% CI) for each training protocol. Trainings that do not share the same letter are different.

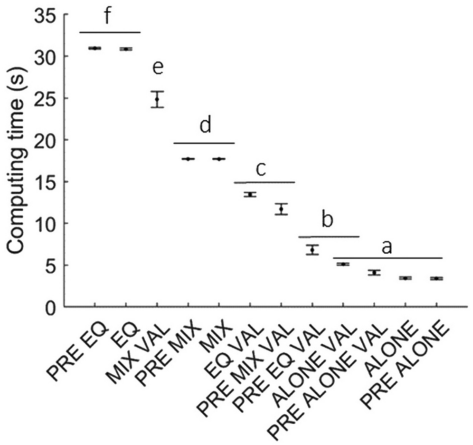

Figure 2. Computing time (95% CI) for each training protocol. Trainings that do not share the same letter are different.

the evaluated participant alone (ALONE); a training for which the data of the evaluated participant were mixed with the data of other participants (MIX); a training for which the data of the participant were oversampled by nine, then mixed with the data of other participants (EQ). The last parameter was the presence or not of validation process during the participant specific training (VAL). When PRE or VAL was performed, the training was performed on 70% of the data, while 30% were kept for the validation process. Trainings were performed with Matlab software, through a GPU with a compute capability of 6.1.

2.6. Test and outcomes

As the data were not numerous enough to have a sample for training, validation, and test, leave one out cross validation method was used. The average accuracy of the training, as well as the computing time needed to performed the training were computed. The confusion matrixes, depicting the sensitivity and the specificity of the network, were also computed.

2.7. Statistics

Linear mixed models and post-hoc tests were performed to compared the effect of the different trainings protocol on the accuracy and the computing time. This analysis was performed with R software.

3. Results and discussion

Our results depicted that the combination of PRE and VAL shortened the computing time only for MIX and EQ, with no effect on the accuracy. Confusion matrixes showed that the hoptest and running tasks were the only movements that any network can recognise with at least 90% of accuracy. Thus, it is possible that these impacts were similar between subjects, while impacts characteristics from other tasks were subject specific. ALONE were always part of the most accurate trainings (hoptest, running, and landings at 45 cm (97% of accuracy); landing 22.5 cm (94% of accuracy), side-step and side-cut (92% of accuracy), front lunge (88% of accuracy)) and of the fastest group of training (less than 6 seconds) (Figure 1).

Therefore, we recommend to perform one measurement session with the aim to train a neural network on the different movements executed by the athlete in its practice. This is a first step to quantify with accuracy the athlete's activity (i.e., number of movements executed, intensity of each impact) and estimate the associated mechanical stress underwent by the athlete, even without prior database.

However, some limitations remain. The movements tested were standardised, and the accuracy might decrease with other movements. Additionally, the athlete's fatigue caused by the session might modify the impact characteristics, and possibly, decrease the accuracy of the network (Figure 2).

4. Conclusions

The main outcome of this study was that the analysis of the impact through a wavelet analysis, combined with convolutional network, enabled a classification

with accuracy of different types of impacts. Our results depicted that the ALONE trainings were the fastest and most accurate.

References

Boyer KA, Nigg BM. 2007. Quantification of the input signal for soft tissue vibration during running. J Biomech. 40(8):1877–1880.

Fu W, Wang X, Liu Y. 2015. Impact-induced softtissue vibrations associate with muscle activation in human landing movements: an accelerometry and EMG evaluation. Technol Health Care. 23(s2):S179–S187.

Hreljac A. 2004. Impact and overuse injuries in runners. Med Sci Sports Exerc. 36(5):845–849.

Lilly JM, Olhede SC. 2012. Generalized morse wavelets as a superfamily of analytic wavelets. Ieee Trans Signal Process. 60(11):6036–6041.

Trama R, Blache Y, Hautier C. 2019. Effect of rocker shoes and running speed on lower limb mechanics and soft tissue vibrations. J Biomech. 82:171–177.

KEYWORDS Accelerometer; wavelet; artificial intelligence

robin.trama@univ-lyon1.fr

Medicine & Science in Sports & Exercise

Does neuromuscular fatigue generated by mountain ultra-marathons alter foot impact and soft-tissue vibrations during running?

--Manuscript Draft--

Manuscript Number:	
Full Title:	Does neuromuscular fatigue generated by mountain ultra-marathons alter foot impact and soft-tissue vibrations during running?
Short Title:	Muscle fatigue and soft-tissue vibrations
Article Type:	Original Investigation
Keywords:	ACCELERATION; DAMPING; INPUT; SHOCK; STATISTICAL PARAMETRIC MAPPING; WAVELET
Corresponding Author:	Robin Trama Universite Claude Bernard Lyon 1 Villeurbanne, FRANCE
Corresponding Author Secondary Information:	
Corresponding Author's Institution:	Universite Claude Bernard Lyon 1
Corresponding Author's Secondary Institution:	
First Author:	Robin Trama
First Author Secondary Information:	
Order of Authors:	Robin Trama
	Yoann Blache
	Frédérique Hintzy
	Jérémy Rossi
	Guillaume Millet
	Christophe Hautier
Order of Authors Secondary Information:	
Abstract:	Purpose: To assess the influence of a preceding mountain ultra-marathon on soft-tissue vibrations (STV) resulting from the impact between the foot and the ground. Methods: Two sessions of measurements were performed on 52 trail runners, before and just after mountain trail running races of various distances (from 40 to 171 km). Triaxial accelerometers were used to quantify the acceleration at the heel (INPUT) and STV of both gastrocnemius medialis (GAS) and vastus lateralis (VL) muscles during flat treadmill running at 10 km•h -1 . A continuous wavelet transform was used to analyze the acceleration signals in the time–frequency domain, and the maps of coefficients as well as the frequency and damping properties of soft tissues were computed. Isometric maximal voluntary contraction forces of knee extensors (KE) and plantar flexors (PF) were also assessed before and after each race. Statistical Parametric Mapping and linear mixed models were used to analyze the data. Results: INPUT amplitude and GAS STV were not modified after the race, while VL STV amplitude, frequency, and damping were significantly decreased similarly for all running distances. However, the 26% (for PF) and 27% (for KE) significant loss of force were not correlated to the changes observed in STV. Conclusions: Mountain ultra-marathons induced a decrease in VL STV amplitude, damping, and frequency, that has never been observed on shorter distances investigated before the present study. These diminutions were not correlated to neuromuscular fatigue indexes and may be interpreted as a protection mechanism of the muscle indicating that biomechanical and/or physiological adaptations may occur in mountain ultra-marathons to limit STV and muscle damage of knee extensors.

DOES NEUROMUSCULAR FATIGUE GENERATED BY MOUNTAIN ULTRA-MARATHONS MODIFY FOOT IMPACT AND SOFT-TISSUE VIBRATIONS DURING RUNNING?

Robin Trama[1], Yoann Blache[1], Frédérique Hintzy[2], Jérémy Rossi[3], Guillaume Y Millet[3,4], Christophe Hautier[1]

[1] Univ. Lyon, UCBL-Lyon 1, Laboratoire Interuniversitaire de Biologie de la Motricité, EA 7424, F-69622, Villeurbanne, France

[2] Univ. Lyon, USMB, Laboratoire Interuniversitaire de Biologie de la Motricité, EA 7424, F-69622 Villeurbanne, France, EA 7424, F-73376, Le-Bourget-du-Lac, France

[3] Univ. Lyon, UJM-Saint-Etienne, Univ. Lyon, UCBL-Lyon 1, Laboratoire Interuniversitaire de Biologie de la Motricité, EA 7424, F-42023, Saint-Etienne, France

[4] Institut Universitaire de France (IUF)

Corresponding author:
Trama Robin
UFR STAPS, 27/29 Boulevard du 11 Novembre 1918, 69622 Villeurbanne Cedex
+33649850040
trama.robin@gmail.com

Abstract

Purpose: To assess the influence of a preceding mountain ultra-marathon on soft-tissue vibrations (STV) resulting from the impact between the foot and the ground. **Methods:** Two sessions of measurements were performed on 52 trail runners, before and just after mountain trail running races of various distances (from 40 to 171 km). Triaxial accelerometers were used to quantify the acceleration at the heel (INPUT) and STV of both *gastrocnemius medialis* (GAS) and *vastus lateralis* (VL) muscles during flat treadmill running at 10 $km \cdot h^{-1}$. A continuous wavelet transform was used to analyze the acceleration signals in the time–frequency domain, and the maps of coefficients as well as the frequency and damping properties of soft tissues were computed. Isometric maximal voluntary contraction forces of knee extensors (KE) and plantar flexors (PF) were also assessed before and after each race. Statistical Parametric Mapping and linear mixed models were used to analyze the data. **Results:** INPUT amplitude and GAS STV were not modified after the race, while VL STV amplitude, frequency, and damping were significantly decreased similarly for all running distances. However, the 26% (for PF) and 27% (for KE) significant loss of force were not correlated to the changes observed in STV. **Conclusions:** Mountain ultra-marathons induced a decrease in VL STV amplitude, damping, and frequency, that has never been observed on shorter distances investigated before the present study. These diminutions were not correlated to neuromuscular fatigue indexes and may be interpreted as a protection mechanism of the muscle indicating that biomechanical and/or physiological adaptations may occur in mountain ultra-marathons to limit STV and muscle damage of knee extensors.

Key Words: ACCELERATION, DAMPING, INPUT, SHOCK, STATISTICAL PARAMETRIC MAPPING, WAVELET.

45 ## Introduction

46 Soft-tissue vibrations (STV) in running are the direct consequences of the impacts between the
47 foot and the ground. The muscle tuning paradigm suggests that the musculoskeletal system
48 adapts to reduce STV by adjusting muscle activations in regard to the characteristics of the early
49 moment of the impact phase, that is to say, to the passive peak and the vertical loading rate
50 which are considered as an input signal (1, 2). However, it has been proposed that muscle
51 fatigue can limit the muscle tuning efficiency in running by altering the muscle force production
52 capacity. To that extent, a computer model depicted an increase of 20% of the vibration
53 amplitude of the lower limb soft tissues without any increase in the input amplitude in muscle
54 fatigue condition (3). In addition, it has been shown that running to exhaustion on even ground
55 for 4 or 10 km increased the vibration amplitude of the *triceps surae* (4–6), without altering its
56 frequency (4), whereas running downhill during 40 minutes led to an increased *vastus lateralis*
57 STV amplitude, without altering the amplitude of the *gastrocnemius medialis* STV (7).
58 Inversely to the computer model (3), the damping of the vibration increased with fatigue (5, 6),
59 without altering the vibration duration (6). Consequently, the five above mentioned studies put
60 forward different effects of fatigue on STV, indicating that the causes of the increase in
61 vibration amplitude and damping alterations are still not clearly understood.

62 Mountain ultra-marathons are extreme endurance races combining long running distances and
63 duration as well as large ascending and descending elevations. Running this type of race has
64 been associated with a 25% to 40% loss of maximal voluntary force, the origin being both
65 central (i.e. within the nervous system) and peripheral (i.e. within the muscle) (8, 9). In addition,
66 the hilly characteristic of trail running induces muscle damage and inflammation (10) and alter
67 the muscle mechanical properties (11). However, no study investigated the modification of STV
68 after prolonged to extreme exercises. It can be hypothesized that these races can modify
69 differently the vibration behavior compared to shorter running bouts, and thus, bring new

insights on how the musculoskeletal system deals with vibrations under extreme fatigue. Thus, it could be very interesting to study these modifications to better adapt physical training and sport gears to this extreme exercises and limit muscle fatigue.

The purpose of this study was to investigate the fatigue-induced changes in STV after the 40 to 171 km races of the "Ultra-Trail du Mont-Blanc". We hypothesized that 1) the amplitude and damping of STV will increase while the frequency of STV will not be modified after the races, and 2) there will be a correlation between neuromuscular fatigue and changes in STV.

Methods

Participants

Fifty-two experienced ultra-marathon runners, out of 70 initially recruited, were able to complete the race and underwent the post-race protocol. Consequently, 32 men and 20 women were included in this study. Their characteristics are reported in Table 1 while Table 2 depicts the repartition of finishers between the races.

Table 1. Runner's characteristics.

	Total	Men	Women
Number	52	32	20
Age (years)	36.3 ± 8.1	36.0 ± 8.1	36.9 ± 8.4
Height (cm)	173.4 ± 10.0	178.3 ± 6.5	165.7 ± 6.7
Weight PRE RACE (kg)	66.7 ± 10.9	72.2 ± 9.3	57.8 ± 6.4
Weight POST RACE (kg)	65.0 ± 10.5	70.3 ± 9.1	56.5 ± 6.1
Body Fat (%)	18.0 ± 7.5	14.5 ± 5.4	24.0 ± 7.7
$\dot{V}O_2max$ ($ml \cdot min^{-1} \cdot kg^{-1}$)	60.2 ± 18.0	63.51 ± 13.7	54.1 ± 20.3

PRE- and POST RACE corresponded to the values obtained before and after the race, respectively.

Table 2. Races distances and number of finishers for each race.

Race	Type of races	Distance (km)	Ascending / descending elevation (km)	# men	# women	# total
MCC	Prolonged	40	2.3 / 2.1	6	6	12
OCC	Prolonged	56	3.5 / 3.3	7	5	12
CCC	Extreme	101	6.1 / 6.3	11	4	15
TDS	Extreme	145	9.1 / 9.3	1	1	2
UTMB	Extreme	171	10.3 / 10.3	7	4	11

Before the experiment, participants signed informed-consent documentation that was approved by the French Ethical Research committee (Comité de Protection des Personnes Ouest VI), according to the Declaration of Helsinki. The study was registered at ClinicalTrials.gov (NCT04025138).

Instrumentation and data collection

Accelerometry. Two triaxial accelerometers (Dytran Instrument Inc., Chatsworth, California, ± 1000 $m \cdot s^{-2}$, sample rate: 2000 Hz) were taped and secured with cohesive tape to the right muscle belly of the *gastrocnemius medialis* (GAS) and *vastus lateralis* (VL) in order to record the STV of the right lower limb (12, 13). The y-axis was oriented in order to be collinear to the longitudinal axis of the shank and the thigh, respectively. A third accelerometer was fixed on the heel cup of the shoe (INPUT) with the y-axis oriented vertically (12). The locations of the accelerometers were marked on the skin with an indelible marker. Furthermore, runners wore the same shoes (Kiprun TRAIL TR, Kalenji, France) during the measurement session which were different from the pair used during the race. This allowed to standardize the sole shape and stiffness between the subjects and avoid any influence of the race distance on shoes mechanical properties.

Isometric force measurements. Plantar flexors (PF) and knee extensors (KE) maximal voluntary contractions forces (MVC) were recorded on right leg. For both muscle groups, participants were asked to fold their arms over their chest, subjects were strongly encouraged and were provided with real-time visual feedback of the generated torque displayed on a monitor. The force signal was recorded at a sampling frequency of 2000 Hz using a PowerLab System (16/30; ADInstruments, Bella Vista, Australia) and LabChart 8 software (ADInstruments). For PF, a custom-built isometric ergometer equipped with a pedal coupled to a strain gauge was used (CS1060 300 Nm; FGP Sensors, Les Clayes-sous-Bois, France). Subjects were seated upright on the ergometer with the foot securely strapped to the pedal with a custom-made hook and loop fastener, to limit heel lift. Hip, knee, and ankle angles were set at 90°. Subjects were asked to concentrate on contracting exclusively the calf muscles. For KE, force was measured thanks to an isometric knee dynamometer (ARS dynamometry, SP2, Ltd., Ljubljana, Slovenia). The leg was attached to the chair by a noncompliant strap just proximal to the malleoli. Subjects were seated in an upright position with both right knee and hips at 90° of flexion with chest and hips securely strapped.

Experimental design

Participants underwent the pre-race tests (PRE RACE) 1 to 3 days before the start of their race, and the post-race evaluation (POST RACE) as soon as possible after the end of the race. The vibration evaluation started 81 ± 21 min after the end of the race. This delay is explained by the traveling time to the laboratory and the other measures carried out, this experiment being part of a larger protocol.

The warm-up consisted in 8 min of running on a motorized treadmill (h/p/cosmos, Munich, Germany), corresponding to another test not mentioned in the current study. Warm-up consisted in 4 min of level running at 90% of the speed sustained during the last minute of a maximal test performed the 6-8 weeks before the race (slope 12%), followed by 1 minute of rest, and 4 min

on a 15% incline at 70% of their maximal speed sustained during the maximal test. INPUT and STV were assessed when running at 10 $km \cdot h^{-1}$ during 30 s on a motorized treadmill (CMTD 20 LAROQ). After the race, 41 runners were not able to run during 30 s due to the extreme fatigue and the data were retained if we could record at least 10 impacts. The subjects then performed the neuromuscular function evaluation. The testing protocol was the same for KE and PF and consisted on a standardized warm-up (for PRE sessions only) of 10 submaximal contractions (5 s of contraction, 5 s of rest) followed by 3 MVCs lasting between 3 and 5 s (the contraction stops when a plateau was found) with a 1-min resting period between each maximal contraction to avoid fatigue. For PRE RACE, subjects underwent the vibrations assessment first, while during POST RACE, subjects performed the MVC measurement first.

Data treatment

The impacts were detected thanks to the heel-cup accelerometer, when the time derivate of the norm of the acceleration signal (i.e., the jerk) reached 2500 $m \cdot s^{-3}$. To analyze the same number of impacts PRE and POST RACE, the number of impacts kept for analysis was selected in function of the number of impacts obtained in POST RACE. The maximum of the norm of the three axes was considered as the peak acceleration (in $m \cdot s^{-2}$). The time-frequency domain of the acceleration signals was investigated with a continuous wavelet transform (12), using a filter bank of Morse wavelets with $\gamma = 3$ and $P^2 = 60$ (14). Primary analysis of the INPUT signal depicted that the signal energy ranged from 10 to 200 Hz, and this range was set as limits of the wavelet transform for both INPUT and STV analysis. A second-order Butterworth band-pass filter was also applied between 10 and 200 Hz to avoid movement artifacts on the peak acceleration and standardized the different analyses. The pseudo frequency of each scale was obtained using the center of frequency of each wavelet and presented in supplementary files (Appendix A). As the scales were logarithmically spaced with 48 voices per octave to allow a regular-frequency response, the maps were linearly interpolated by 2 Hz in the frequency

domain. The 0.25 s after the impact were investigated, and this duration was interpolated to 100 samples. Thus, the number of nodes of the maps corresponded to 100 [time] × 96 [frequency] = 9600 nodes. The modulus of the coefficient given by the wavelet transform was computed for each axis of each accelerometer, and the norm of the three axes was calculated for each node. Then, the amplitude spectrum, expressing the amplitude of the vibration at each frequency, was computed from the maps by integrating the coefficients over the time. The frequency with the most amplitude was considered as the peak frequency (in Hz), and the frequency that split the spectrum in half was the median frequency (in Hz). Moreover, the overall amplitude in the time domain was computed by integrating the coefficients over the frequencies. For both muscles, the damping properties (in s^{-1}) were calculated according to the method depicted by Enders et al. (15) and previously employed by our team (12), and the settling time (in ms) corresponded to the time between the peak overall amplitude and the moment when the amplitude reached 10% of its maximum (6).

The best MVC (in Nm) of the three trials was retained for PRE and POST conditions and the index of neuromuscular fatigue (in %) corresponded to the relative loss of force and was calculated as $(MVC_{PRE} - MVC_{POST}) / MVC_{PRE}$.

Statistics

A primarily analysis on the maps of INPUT, GAS and VL with a two-way ANOVA with one repeated measure (independent effect: Distance (prolonged vs. extreme); repeated measure effect: Time of measurement (PRE vs. POST)) depicted no effect of the distance, nor interaction effect between the distance and the time of measurement. By contrast, a main effect of the time of the measurement was found. Consequently, all data from different races were pooled together to standardize the further analysis.

177 A student paired t-test was used to compare the level of force between PRE and POST RACE
178 both for KE and PF. Statistical Parametric Mapping (SPM) analysis was conducted in two
179 dimensions on the maps obtained from the wavelet transform, using the spm1d package for
180 Matlab (16). The mean maps of all the impacts for each subject were considered for the analysis.
181 The maps corresponded to a 2D-1D continuum (i.e., the amplitude is expressed as a function of
182 time and frequency), but a 1D-1D continuum was required to perform the SPM analysis. Thus,
183 the maps were flattened into a 1D-1D continuum for the analysis and then reshaped to their
184 original dimensions for interpretation. Maps were analyzed with paired t-tests (PRE RACE
185 versus POST RACE) with an alpha error at 0.05/3 as three tests were performed (i.e., one for
186 each accelerometer). To define the threshold of the statistical tests performed, permutation tests
187 were used with 10000 permutations. Additionally, using R software (v3.5.0, R Core Team,
188 Vienna, Austria), linear mixed models (17) were used to investigate the effect the time of
189 measurement (fixed effect: PRE RACE versus POST RACE) on extracted variables (i.e., peak
190 acceleration, peak and median frequencies, damping and settling time). All the impacts were
191 included in these models, and the fixed effect was set as random intercepts and slopes to adapt
192 the model to each participant's specificity. The p-values were obtained from likelihood ratio
193 tests, which were conducted by testing the full model against the model without the effect
194 tested. The normality, homoscedasticity, and linearity of the linear mixed model residuals were
195 graphically controlled.

196 Therewith, effect sizes (ES) were calculated for each node of the maps, for extracted variables,
197 and for muscle force. The Hedges' g value was used, and for the maps only, these values were
198 corrected for non-normal data (18). The ESs were considered as *small* when $0.2 \leq g < 0.5$, and
199 *medium* when $0.5 \leq g < 0.8$.

200 Two non-parametric regressions were performed between the changes in maps (between PRE
201 and POST RACE) and the relative change of force of the same muscle, using the spm1d package

for Matlab (16). The alpha error was set at 2.5%, and to define the threshold of significance, permutation tests were used with 10000 permutations in order to achieve computational stability (19). The Pearson's r-values for each node was also computed. Furthermore, linear regressions were performed between the index of neuromuscular fatigue and the extracted variables such as the maximal acceleration, main and median frequencies, damping properties and settling time. The alpha error for significance was set at 0.5%.

Results

Comparisons between pre and post-race. From PRE to POST RACE, runners experienced a 26 ± 14% decreased in PF MVC (143 ± 38 to 104 ± 32 Nm, p<0.001, ES=1.10), and a 27 ± 16% decreased in KE MVC (244 ± 70 to 177 ± 62 Nm, p<0.001, ES=1.01).

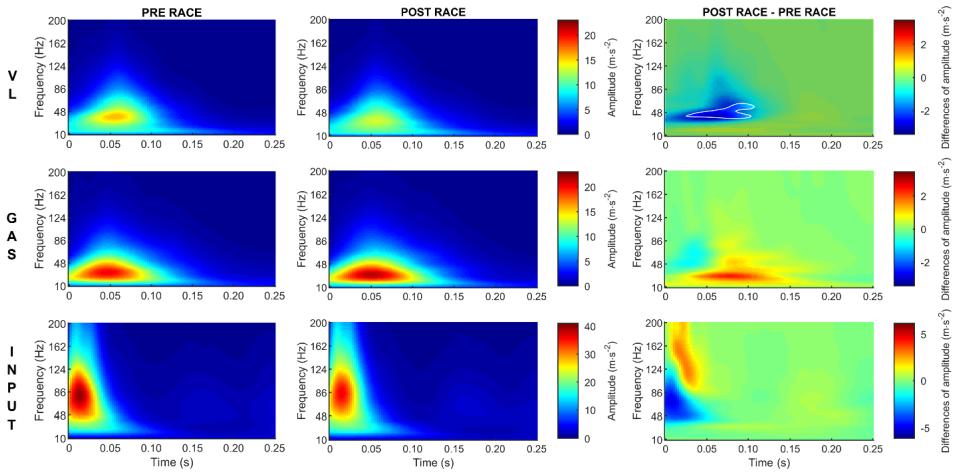

Figure 1. Mean maps (PRE RACE: left column; POST RACE: middle column) and differences of amplitude between POST RACE and PRE RACE (right column) for INPUT (bottom row), the *gastrocnemius medialis* (GAS, middle row), and *vastus lateralis* (VL, top row). The cluster highlighted for the VL depicted significant differences between PRE and POST RACE with PRE>POST.

A total of 2,012 impacts were analyzed (19.3 ± 10.5 impacts per runner for each test session). SPM analysis (Figure 1) depicted no significant differences in the maps between PRE and

POST RACE for the INPUT, however, the linear mixed models (Table 3) depicted that the median frequency of the INPUT increased POST RACE (+4.3 ± 7.3%, *small*). For the GAS, neither the SPM analysis nor the linear mixed model depicted any differences between PRE and POST RACE. Considering the VL, SPM analysis (Figure 1) revealed a 10 to 15% (*medium*) decrease in amplitude POST RACE from 40 to 60 Hz, and between 0.03 and 0.1 s after the impact. These differences were greater than the mean intra-subject variability (see Appendix B in Supplementary files). Linear mixed models (Table 3) depicted a decrease after the race of the peak acceleration (-5.3 ± 27.3%, *small*), the peak and median frequencies (-8.9 ± 28.8%, *small*, and -6.1 ± 12.6%, *medium*, respectively), and the damping (-5.3 ± 28.2%, *small*) of VL.

Table 3. Input and soft-tissue vibrations parameters

	INPUT				GAS				VL			
	PRE	POST	Effect size	p	PRE	POST	Effect size	p	PRE	POST	Effect size	p
Peak acceleration ($m \cdot s^{-2}$)	161.6 ± 41.8	156.6 ± 43.9	0.12	NS	71.4 ± 33.6	74.4 ± 42.1	0.08	NS	57.7 ± 18.9	52.6 ± 16.8	0.29	<0.05
Peak frequency (Hz)	53.6 ± 15.0	51.8 ± 17.4	0.11	NS	24.4 ± 6.4	23.6 ± 6.3	0.13	NS	25.3 ± 9.4	21.6 ± 7.9	0.42	<0.01
Median frequency (Hz)	78.7 ± 7.3	82.0 ± 8.3	0.42	<0.01	41.1 ± 3.5	40.6 ± 3.4	0.14	NS	43.6 ± 5.8	40.6 ± 5.4	0.54	<0.001
Damping (s^{-1})					18.8 ± 6.5	19.8 ± 5.7	0.15	NS	24.5 ± 6.2	22.3 ± 5.8	0.37	<0.05
Settling time (ms)					136.8 ± 34.0	134.5 ± 28.0	0.08	NS	116.3 ± 26.4	121.1 ± 23.7	0.19	NS

Correlation with neuromuscular fatigue. The SPM analysis did not depict any significant correlation between the index neuromuscular fatigue and the changes in vibration amplitude (Figure 2). Moreover, no linear correlation was found between the index of neuromuscular fatigue and the other extracted variables.

234 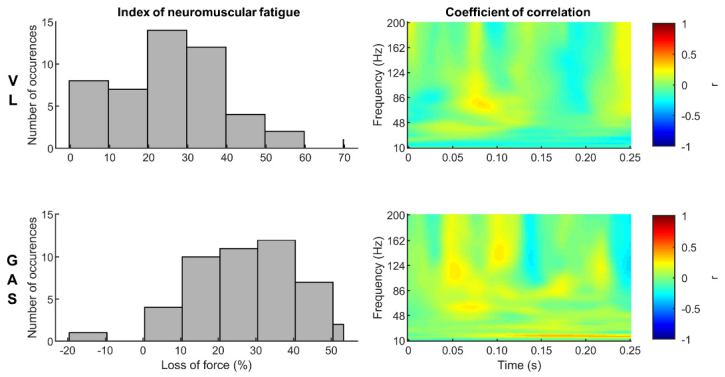

235 **Figure 2.** Distribution of the index of neuromuscular fatigue used for the regressions (left) and the coefficient of
236 correlation (right) with the changes in vibration amplitude for the *vastus lateralis* (VL, top row) and the
237 *gastrocnemius medialis* (GAS, bottom row).

238 ## Discussion

239 The purpose of this study was to investigate the fatigue-induced changes in STV after the 40 to
240 171 km races of the "Ultra-Trail du Mont-Blanc". The main results are that despite an
241 unchanged input amplitude and a similar index of neuromuscular fatigue for the PF and KE
242 muscles, GAS STV were not modified after the race, while the VL amplitude, frequency, and
243 damping were decreased. Another important finding of the present study is that the index of
244 neuromuscular fatigue of KE muscles failed to explain the changes observed in characteristics
245 of the VL STV.

246 *Impact modifications.* Several studies showed that trail running did not modify input
247 characteristics (20–22), while our results depicted a *small* increase in INPUT median frequency.
248 The differences with previous results may be explained by the method used to acquire and/or
249 analyze the input signal. In contrast with previous studies investigating the input from ground
250 reaction force (i.e., the vertical loading rate) (21, 22) or shank accelerations (20), we considered
251 the input from the heel-cup of the shoe (12, 23). The differences may originate from the surface

252 in contact with the accelerometer (i.e., skin or textile), or from the proximity with the impact
253 location (24). Furthermore, these studies only investigated the time (21) or the frequency
254 domain (20) separately, while wavelet transforms may allow for more discriminant outputs for
255 non-stationary signals like accelerations during human locomotion (15). Consequently, the
256 *small* frequency changes observed in our study might have no significant outcomes in practice,
257 as no modification was observed in other studies (20–22).

258 *Vibrations after short vs. long term running.* The model proposed by Nikooyan and Zadpoor
259 (3) suggests that muscle fatigue lead to an increase of vibration amplitude, which is supported
260 by experimental studies (4–7), to a decrease in damping properties, which is opposed to
261 experimental studies (5, 6). Both model and experimental studies are in contradiction with our
262 results, as we observed a decrease in the VL vibration amplitude, frequency, and damping, and
263 no modification of the GAS vibrations in POST RACE condition. In contrast, the settling time
264 (i.e., the time before the vibration was completely dampened) of both muscles was not modified
265 after the races, as after an exhaustive run in rear foot strike runners (6). However, too few
266 studies have been conducted to determine if the settling time depends on fatigue. The
267 differences between these experimental studies (4–7) and ours lied in the fatiguing protocols.
268 To induce fatigue, three studies used a flat and relatively intense running sessions, either of
269 4 km (6) or 10 km (4, 5), with running speeds and durations ranging between 3.1 and 4.3 $m \cdot s^{-1}$
270 and between 15 and 55 minutes, respectively. The fourth protocol of the literature used a
271 downhill running session of 40 minutes (10 km) with a slope of -15% (-1500 m) at 55% of
272 $\dot{V}_{O_2}max$ (4.2 $m \cdot s^{-1}$). In contrast, the shortest race in our study (i.e., MCC) was about 40 km with
273 2100 m of positive and negative elevation and was run in 4.4 hours by the fastest participant
274 (average speed: 2.5 $m \cdot s^{-1}$). Consequently, the protocols used in the aforementioned studies
275 cannot be compared with the present one. As the alterations of the present INPUT where *small*
276 and concerned only the median frequency, and in the absence of correlation between fatigue

277 and modifications of vibrations, it was assumed that the changes in all the parameters of VL
278 STV, and the lack of changes for GAS STV, were induced by the specificity of trail running,
279 and especially by its duration and hilly characteristic.

280 *Specificity of long term running.* The running time in our study ranged from 4.4 to 44.4 hours,
281 which was at least 5 times longer than the other studies (4–7). A first hypothesis that can explain
282 the differences of modification of STV between short and long term running is the strategies
283 that can be developed to limit muscle fatigue and damage. Several authors suggested that in a
284 non-fatigued state, the muscle damping is optimal and the STV and impact amplitudes are
285 minimal (3, 25). When fatigue increases during a short and intense running exercise, muscle
286 adaptations seem to be made to maintain running performance, despite increased impact (6),
287 vibration amplitude (4–7), and damping (5, 6). However, the reason why damping capacity is
288 increased in these studies remains unclear. It was hypothesized that it could originate from an
289 increase in the viscous damping coefficient (5) or from non-contractile structures in the muscle
290 (6). Khassetarash et al. (6) also suggested that constant vibration settling time might either be
291 an objective for muscle tuning, which in turn may increase damping if vibration amplitude is
292 increased. In our study, the vibration measurement took place after the race while other studies
293 quantified vibration during the fatiguing protocol, and it can be hypothesized that the runners'
294 primary goal was not the performance, but to protect the musculoskeletal system from damage
295 and/or minimize pain. Our results, obtained after prolonged and extreme endurance running,
296 depicted that the damping capacity of the VL was diminished, and adaptations may be aimed
297 to protect the musculoskeletal system by a reduction of vibration amplitude and a re-lowered
298 impact. These adaptations were observed even for the shortest races in our study (i.e., 4.4
299 hours), however, our experimental protocol does not allow to explain how the reduction of the
300 STV amplitude, considered as a protection mechanism, was achieved. As reported in a previous
301 study (20), runners may have change their running patterns after fatigue to modify muscle

activations and STV. A second hypothesis that could partly explain the reduction of STV amplitude and frequency is the alterations of muscle properties that have been reported after a 330 km trail running race (11). A decrease in muscle stiffness (11) could explain the decrease of the vibration frequency, as the frequency is proportional to the stiffness and inversely proportional to the mass of the soft tissue (26). Only one study reported vibration frequency after fatigue, it is very likely that their protocol was not strenuous enough to alter muscle stiffness or mass (4). Less likely, an increase in muscle mass is probably not the cause of the present decrease in frequency, as a 1.7 ± 1.2 kg reduction of body weight was found at POST RACE. Still, a local edema at the superficial part of the muscle after a 330 km trail running, that was observed in a previous study (11), may increase the mass locally. A local increase in muscle mass could also explain the present diminished amplitude of vibration, as the acceleration is the ratio of the force by the mass. In addition, the differences between the two muscles investigated in the present study could be explained by the large amount of downhill running during our races, which was comprised between 2,100 and 10,000 m of negative elevation. Downhill running increases the muscle eccentric work compared to flat running, especially for knee extensors compared to plantar flexor muscles (27), which induces more damages to thigh muscles compared to calf ones (10). Although we denoted an opposite effect of fatigue on STV amplitude in comparison to Ehrström et al. (7), these authors also observed modifications for VL but not for GAS after downhill running. It is conceivable that the most affected muscles are the ones that are tuned in order to modify the vibration characteristics, and/or are the ones with the most altered properties.

Neuromuscular fatigue and vibrations - Neuromuscular fatigue measured in the present study is in line with the literature for similar running duration (28, 29). Yet the lake of correlations in our results depicted that neuromuscular fatigue index did not appear to be a good indicator of the muscle inability to damp the vibrations. One may suggest that the rate of force development

(30) is a better indicator of the ability of the muscle to produce quickly the right amount of force to damp the vibration. Further studies should focus on the continuous measurement of vibration characteristics (amplitude, frequency, and damping) during prolonged running bout, in association with biomechanical (e.g. joint angles) and physiological parameters (e.g. neuromuscular fatigue, rate of force development, energy cost of running).

Limitations. Although the locations of the accelerometers were marked on the skin to be placed at the same location before and after the races, the pressure of the tape to secured them was not measured. Yet, the same investigator equipped the runners, which limits the variability between PRE and POST RACE. Approximations can occur when estimating the threshold for post hoc tests with a Bonferonni correction, as the method assumes that the post hoc tests are independent which is usually not the case. However, the errors are expected to be small, the results reported agreed with the ANOVA performed during the preliminary analysis, and the significant t-values were truly above the threshold (4.2 vs 3.4).

Conclusion

This study aimed to quantify the changes in STV induced by fatigue after mountain ultra-marathon races. Heel impact and *gastrocnemius medialis* vibrations were not modified, whereas *vastus lateralis* vibration amplitude, frequency and damping were reduced after the different races. The results also depicted that changes in STV were not correlated to the index of neuromuscular fatigue, indicating that other parameters like muscle tissue characteristics and/or running patterns adaptation may modify the STV. Further studies are needed to better understand how the different muscles deal with the inclination, intensity and duration of the effort, as well as the possible trade-off between performance and protection of the musculoskeletal system that may occur during prolonged to extreme endurance running.

Acknowledgments

The results of the study are presented clearly, honestly, and without fabrication, falsification, or inappropriate data manipulation, and statement that results of the present study do not constitute endorsement by ACSM. None of the authors are in conflict of interest with regards to this research.

References

1. Nigg BM, Wakeling JM. Impact forces and muscle tuning: a new paradigm. *EXERC SPORT SCI REV*. 2001;29(1):37–41.

2. Wakeling JM, Nigg BM. Modification of soft tissue vibrations in the leg by muscular activity. *Journal of applied physiology*. 2001;90(2):412–420.

3. Nikooyan AA, Zadpoor AA. Effects of Muscle Fatigue on the Ground Reaction Force and Soft-Tissue Vibrations During Running: A Model Study. *IEEE Transactions on Biomedical Engineering*. 2012;59(3):797–804.

4. Friesenbichler B, Stirling LM, Federolf P, Nigg BM. Tissue vibration in prolonged running. *Journal of Biomechanics*. 2011;44(1):116–20.

5. Khassetarash A, Hassannejad R, Ettefagh MM, Sari-Sarraf V. Fatigue and soft tissue vibration during prolonged running. *Hum Mov Sci*. 2015;44:157–67.

6. Khassetarash A, Hassannejad R, Ettefagh MM, Oskouei AE. Vibration settling time of the gastrocnemius remains constant during an exhaustive run in rear foot strike runners. *Journal of Biomechanics*. 2019;93:140–6.

7. Ehrström S, Gruet M, Giandolini M, Chapuis S, Morin J-B, Vercruyssen F. Acute and Delayed Neuromuscular Alterations Induced by Downhill Running in Trained Trail Runners: Beneficial Effects of High-Pressure Compression Garments. *Frontiers in Physiology* [Internet]. 2018 [cited 2019 Jan 7];9 Available from: https://www.frontiersin.org/article/10.3389/fphys.2018.01627/full. doi:10.3389/fphys.2018.01627.

8. Millet GY, Tomazin K, Verges S, et al. Neuromuscular Consequences of an Extreme Mountain Ultra-Marathon. *PLoS One* [Internet]. 2011 [cited 2016 Feb 3];6(2) Available from: http://www.ncbi.nlm.nih.gov/pmc/articles/PMC3043077/. doi:10.1371/journal.pone.0017059.

9. Saugy J, Place N, Millet GY, Degache F, Schena F, Millet GP. Alterations of Neuromuscular Function after the World's Most Challenging Mountain Ultra-Marathon. *PLoS One* [Internet]. 2013 [cited 2016 Jan 27];8(6) Available from: http://www.ncbi.nlm.nih.gov/pmc/articles/PMC3694082/. doi:10.1371/journal.pone.0065596.

10. Maeo S, Ando Y, Kanehisa H, Kawakami Y. Localization of damage in the human leg muscles induced by downhill running. *Sci Rep* [Internet]. 2017 [cited 2020 Feb 17];7 Available from: https://www.ncbi.nlm.nih.gov/pmc/articles/PMC5515850/. doi:10.1038/s41598-017-06129-8.

11. Andonian P, Viallon M, Le Goff C, et al. Shear-Wave Elastography Assessments of Quadriceps Stiffness Changes prior to, during and after Prolonged Exercise: A Longitudinal Study during an Extreme Mountain Ultra-Marathon. *PLOS ONE*. 2016;11(8):e0161855.

12. Trama R, Hautier C, Blache Y. Input and Soft-Tissue Vibration Characteristics during Sport-Specific Tasks: *Medicine & Science in Sports & Exercise*. 2020;52(1):112–9.

13. Trama R, Blache Y, Hautier C. Effect of rocker shoes and running speed on lower limb mechanics and soft tissue vibrations. *J Biomech*. 2019;82:171–7.

14. Lilly JM, Olhede SC. Higher-Order Properties of Analytic Wavelets. *EEE Trans Signal Process*. 2009;57(1):146–60.

15. Enders H, von Tscharner V, Nigg BM. Analysis of damped tissue vibrations in time-frequency space: a wavelet-based approach. *J Biomech*. 2012;45(16):2855–9.

16. Pataky TC. Generalized n-dimensional biomechanical field analysis using statistical parametric mapping. *Journal of Biomechanics*. 2010;43(10):1976–82.

17. Bates D, Mächler M, Bolker B, Walker S. Fitting Linear Mixed-Effects Models Using lme4. *Journal of Statistical Software* [Internet]. 2015 [cited 2017 Mar 15];67(1) Available from: http://www.jstatsoft.org/v67/i01/. doi:10.18637/jss.v067.i01.

18. Kelley K. The Effects of Nonnormal Distributions on Confidence Intervals Around the Standardized Mean Difference: Bootstrap and Parametric Confidence Intervals. *Educational and Psychological Measurement*. 2005;65(1):51–69.

19. Nichols TE, Holmes AP. Nonparametric permutation tests for functional neuroimaging: A primer with examples. *Human Brain Mapping*. 2002;15(1):1–25.

20. Giandolini M, Gimenez P, Temesi J, et al. Effect of the Fatigue Induced by a 110-km Ultramarathon on Tibial Impact Acceleration and Lower Leg Kinematics. *PLOS ONE*. 2016;11(3):e0151687.

21. Vernillo G, Aguiar M, Savoldelli A, et al. Regular changes in foot strike pattern during prolonged downhill running do not influence neuromuscular, energetics, or biomechanical parameters. *European Journal of Sport Science*. 2019;1–10.

22. Degache F, Guex K, Fourchet F, et al. Changes in running mechanics and spring-mass behaviour induced by a 5-hour hilly running bout. *Journal of Sports Sciences*. 2013;31(3):299–304.

23. Boyer KA, Nigg BM. Quantification of the input signal for soft tissue vibration during running. *J Biomech*. 2007;40(8):1877–80.

24. Lucas-Cuevas AG, Encarnación-Martínez A, Camacho-García A, Llana-Belloch S, Pérez-Soriano P. The location of the tibial accelerometer does influence impact acceleration parameters during running. *Journal of Sports Sciences*. 2017;35(17):1734–8.

25. Jalali P, Noorani M-RS, Hassannejad R, Ettefagh MM. Modeling the central nervous system functionality in controlling the calf muscle activity during running with sport shoes. *Proceedings of the Institution of Mechanical Engineers, Part H: Journal of Engineering in Medicine*. 2019;095441191882139.

26. Smeathers JE. Transient vibrations caused by heel strike. *Proc Inst Mech Eng H*. 1989;203(4):181–6.

27. Park S-K, Jeon H-M, Lam W-K, Stefanyshyn D, Ryu J. The effects of downhill slope on kinematics and kinetics of the lower extremity joints during running. *Gait & Posture*. 2019;68:181–6.

28. Millet GY. Can Neuromuscular Fatigue Explain Running Strategies and Performance in Ultra-Marathons?: The Flush Model. *Sports Medicine*. 2011;41(6):489–506.

29. Giandolini M, Vernillo G, Samozino P, et al. Fatigue associated with prolonged graded running. *European Journal of Applied Physiology*. 2016;116(10):1859–73.

30. Maffiuletti NA, Aagaard P, Blazevich AJ, Folland J, Tillin N, Duchateau J. Rate of force development: physiological and methodological considerations. *Eur J Appl Physiol*. 2016;116:1091–116.

Supplementary files

Appendix A: Center of frequency and time resolution for the wavelets used.

#	Center Frequency (Hz)	Time resolution (ms)	#	Hz	ms	#	Hz	ms	#	Hz	ms	#	Hz	ms
1	9.9	101.3	43	18.1	55.2	85	33.2	30.1	127	60.9	16.4	169	111.7	9.0
2	10.0	99.8	44	18.4	54.4	86	33.7	29.7	128	61.8	16.2	170	113.3	8.8
3	10.2	98.4	45	18.6	53.6	87	34.2	29.3	129	62.7	16.0	171	115.0	8.7
4	10.3	97.0	46	18.9	52.9	88	34.7	28.8	130	63.6	15.7	172	116.7	8.6
5	10.5	95.6	47	19.2	52.1	89	35.2	28.4	131	64.5	15.5	173	118.4	8.4
6	10.6	94.2	48	19.5	51.4	90	35.7	28.0	132	65.5	15.3	174	120.1	8.3
7	10.8	92.9	49	19.7	50.6	91	36.2	27.6	133	66.4	15.1	175	121.8	8.2
8	10.9	91.5	50	20.0	49.9	92	36.7	27.2	134	67.4	14.8	176	123.6	8.1
9	11.1	90.2	51	20.3	49.2	93	37.3	26.8	135	68.4	14.6	177	125.4	8.0
10	11.2	88.9	52	20.6	48.5	94	37.8	26.4	136	69.4	14.4	178	127.2	7.9
11	11.4	87.7	53	20.9	47.8	95	38.4	26.1	137	70.4	14.2	179	129.1	7.7
12	11.6	86.4	54	21.2	47.1	96	38.9	25.7	138	71.4	14.0	180	130.9	7.6
13	11.7	85.2	55	21.5	46.4	97	39.5	25.3	139	72.4	13.8	181	132.8	7.5
14	11.9	83.9	56	21.8	45.8	98	40.1	25.0	140	73.5	13.6	182	134.8	7.4

15	12.1	82.7	57	22.2	45.1	99	40.7	24.6	141	74.6	13.4	183	136.7	7.3
16	12.3	81.6	58	22.5	44.5	100	41.2	24.2	142	75.6	13.2	184	138.7	7.2
17	12.4	80.4	59	22.8	43.8	101	41.8	23.9	143	76.7	13.0	185	140.7	7.1
18	12.6	79.2	60	23.1	43.2	102	42.5	23.6	144	77.9	12.8	186	142.8	7.0
19	12.8	78.1	61	23.5	42.6	103	43.1	23.2	145	79.0	12.7	187	144.9	6.9
20	13.0	77.0	62	23.8	42.0	104	43.7	22.9	146	80.1	12.5	188	147.0	6.8
21	13.2	75.9	63	24.2	41.4	105	44.3	22.6	147	81.3	12.3	189	149.1	6.7
22	13.4	74.8	64	24.5	40.8	106	45.0	22.2	148	82.5	12.1	190	151.3	6.6
23	13.6	73.7	65	24.9	40.2	107	45.6	21.9	149	83.7	11.9	191	153.5	6.5
24	13.8	72.7	66	25.2	39.6	108	46.3	21.6	150	84.9	11.8	192	155.7	6.4
25	14.0	71.6	67	25.6	39.0	109	47.0	21.3	151	86.1	11.6	193	158.0	6.3
26	14.2	70.6	68	26.0	38.5	110	47.7	21.0	152	87.4	11.4	194	160.3	6.2
27	14.4	69.6	69	26.4	37.9	111	48.3	20.7	153	88.7	11.3	195	162.6	6.1
28	14.6	68.6	70	26.7	37.4	112	49.0	20.4	154	90.0	11.1	196	165.0	6.1
29	14.8	67.6	71	27.1	36.9	113	49.8	20.1	155	91.3	11.0	197	167.4	6.0
30	15.0	66.6	72	27.5	36.3	114	50.5	19.8	156	92.6	10.8	198	169.8	5.9
31	15.2	65.7	73	27.9	35.8	115	51.2	19.5	157	93.9	10.6	199	172.3	5.8
32	15.4	64.7	74	28.3	35.3	116	52.0	19.2	158	95.3	10.5	200	174.8	5.7
33	15.7	63.8	75	28.7	34.8	117	52.7	19.0	159	96.7	10.3	201	177.3	5.6
34	15.9	62.9	76	29.2	34.3	118	53.5	18.7	160	98.1	10.2	202	179.9	5.6
35	16.1	62.0	77	29.6	33.8	119	54.3	18.4	161	99.5	10.0	203	182.5	5.5
36	16.4	61.1	78	30.0	33.3	120	55.1	18.2	162	101.0	9.9	204	185.2	5.4
37	16.6	60.2	79	30.5	32.8	121	55.9	17.9	163	102.4	9.8	205	187.9	5.3
38	16.8	59.4	80	30.9	32.4	122	56.7	17.6	164	103.9	9.6	206	190.6	5.2
39	17.1	58.5	81	31.3	31.9	123	57.5	17.4	165	105.4	9.5	207	193.4	5.2
40	17.3	57.7	82	31.8	31.4	124	58.3	17.1	166	107.0	9.3	208	196.2	5.1
41	17.6	56.8	83	32.3	31.0	125	59.2	16.9	167	108.5	9.2	209	199.0	5.0
42	17.8	56.0	84	32.7	30.5	126	60.0	16.7	168	110.1	9.1	210	201.9	5.0

Note that the number of wavelets is important as 48 voices per octave were chosen (i.e., 48 wavelets are used for each doubling frequency interval). This increases the frequency resolution, especially for higher frequencies, and allows a smoother interpolation as more points are used for the interpolation.

Appendix B: Mean intra-subject standard deviation

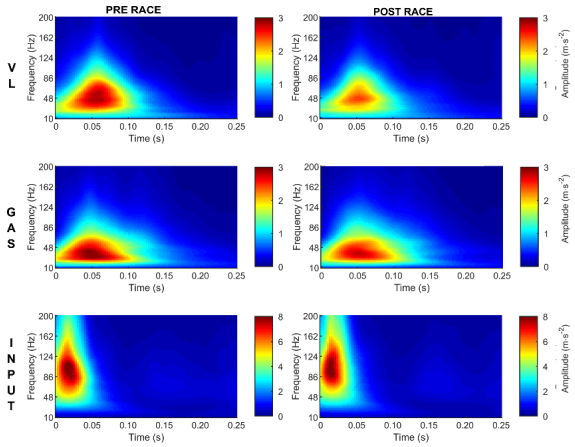

The mean intra-subject standard deviation of the VL was inferior to the differences depicted for both PRE and POST RACE.

5 CONCLUSIONS ET PERSPECTIVES

Cette thèse s'est focalisée sur l'étude des vibrations transitoires lors de la pratique sportive, initiées par un impact entre le pied et le sol. L'impact avec le sol (input), et les vibrations de deux muscles, le *gastrocnemius medialis* et le *vastus lateralis*, ont majoritairement été étudiées afin de répondre à deux objectifs. Premièrement, cette thèse a permis de développer des méthodes innovantes en termes de mesure, traitement du signal et d'analyse statistique afin de mieux caractériser la vibration transitoire, notamment au niveau musculaire. Deuxièmement, différents facteurs externes, tels que les pratiques sportives, le matériel et la fatigue, ont été étudiés pour comprendre leurs effets sur le comportement vibratoire des tissus mous en pratique écologique.

La vibration est analysée classiquement avec un traitement temporel ou fréquentiel, avec des paramètres scalaires limitant ainsi une interprétation approfondie du signal vibratoire. Méthode de traitement émergente, l'analyse temps-fréquence, c'est-à-dire une transformée en ondelettes ou une décomposition en modes intrinsèques, a permis d'améliorer la pertinence des indicateurs extraits. Cependant, l'utilisation de paramètres scalaires après ce genre d'analyse reste prépondérante. Notre premier objectif était donc, après une analyse temps-fréquence, d'adopter une méthode statistique permettant d'analyser les nouveaux indicateurs obtenus : les cartes de coefficients d'ondelettes. La méthode SnPM a été choisie et développée afin de réaliser des inférences statistiques sur les cartes temps-fréquence. De ce fait, deux algorithmes ont été créés et mise en ligne en libre accès, ceci permettant à d'autres chercheurs de bénéficier du travail effectué durant ces années de thèse. Le premier répertoire de fonctions permet, en plus des analyses classiquement utilisées (analyste temporelle, transformée de Fourier rapide…), de faire des analyses temps-fréquences de types analyse en ondelettes et décompositions en mode intrinsèques. Celui-ci est disponible à l'adresse suivante : https://github.com/tramarobin/vibAnalyzer. Le second répertoire de fonctions proposé répond à deux objectifs. 1) permettre de faire des inférences statistiques sur des courbes et des cartes avec une mise en forme uniformisée et 2) simplifier les analyses par comparaison de moyennes tout en considérant les intersections avec les tests effectués en amont. Celui-ci est disponible à l'adresse suivante : https://github.com/tramarobin/fctSnPM. Les paramètres de

la vibrations obtenus grâce à des indicateurs scalaires et en une ou deux dimensions ont été comparés. Quel que soit le type d'analyse, les conclusions sont similaires, à la différence près que les analyses en une ou deux dimensions apportent des informations plus complètes et précises. Ces nouvelles méthodes d'analyse ne remettent donc pas en cause les résultats des précédentes études, toutefois, celles-ci devraient être utilisées à l'avenir pour obtenir une analyse complète du signal vibratoire.

En comparant la vibration des tissus mous mesurée par accéléromètres avec la vibration musculaire mesurée par échographie ultra-rapide, nous avons démontré que l'accéléromètre sous-estimait la fréquence et l'amortissement de la vibration comparée à l'échographie. De plus, les différences entre ces deux méthodes de mesure étaient plus grandes lorsque le muscle était contracté, et quand l'épaisseur du pli sous-cutané était importante. Il a été conseillé de filtrer les fréquences du signal inférieures à 20 Hz afin de limiter les effets de la masse graisseuse sur le signal vibratoire, ainsi que de sélectionner des participants avec un faible pourcentage de masse grasse. Ces deux recommandations peuvent permettre d'améliorer la caractérisation de la vibration musculaire grâce aux accéléromètres, mais de par les différences entre un choc induit avec un marteau et un impact entre le pied et le sol, il est difficile de généraliser cette étude à la pratique sportive. De plus, nous avions étudié uniquement le muscle *vastus lateralis*, laissant une part d'inconnu importante en ce qui concerne les autres muscles. Cette étude donne une piste de développement pour une future correction du signal des accéléromètres afin qu'ils puissent refléter plus précisément la vibration musculaire. En effet, il a été montré que l'imagerie par échographie peut suivre efficacement le déplacement des muscles sous les tissus mous superficiels, même en pratique écologique grâce à un changement de plan des images recueillie par la sonde (Rasske & Franz, 2018). L'utilisation de l'échographie pour quantifier le déplacement musculaire pendant la course permettra de surmonter l'imprécision des accéléromètres pour mesurer directement la fréquence des vibrations musculaires causées par un impact en course à pied. Grâce à une mesure conjointe de la vibration des tissus mous et du muscle, des caractéristiques musculaires, de l'impact au sol, des activations musculaires et de la cinématique de course à pied, il est envisageable de corriger les caractéristiques de vibration des tissus mous obtenues avec les accéléromètres pour mieux refléter les vibrations musculaires lors de la pratique écologique. Cette caractérisation plus précise permettra de mieux

comprendre le lien entre la vibration et la fatigue neuromusculaire, et notamment de mettre en avant l'effet des hautes fréquences de vibrations difficilement observables par accélérométrie.

L'augmentation de la vitesse de course et les mouvements spécifiques aux sports collectifs génèrent des impacts et des vibrations potentiellement plus délétères pour le système musculo-squelettique. Bien que certains matériels sportifs semblent efficaces pour réduire l'amplitude de l'impact au sol, mais pas nécessairement la vibration, une quantification de ces deux paramètres semble nécessaire. En se basant sur le signal mesuré au niveau du talon de la chaussure, d'une transformée en ondelettes continue des vibrations dans les trois plans de l'espace, ainsi que d'un réseau de neurones convolutifs, il serait possible d'identifier les différents mouvements pratiqués. Cette méthodologie peut être appliquée à différents sports collectifs afin de mieux quantifier la charge d'entrainement, d'identifier les mouvements effectués et calculer une dose d'exposition aux chocs et aux vibrations en situation écologique de pratique sportive. Bien que nous n'ayons pas encore de données qui établissent un lien indiscutable entre la vibration et le risque de blessure, la quantification de la dose d'exposition aux vibrations est une première étape importante.

Afin de réduire l'exposition aux vibrations, le matériel sportif a montré des effets contrastés. Bien que le revêtement sportif testé ait permis de légèrement réduire l'amplitude de l'impact sans modification du comportement vibratoire, la modification de la forme de la chaussure n'a pas eu d'effet sur l'impact et la vibration. En plus des paramètres de vibrations, il est essentiel de considérer l'activité musculaire lorsque du matériel sportif est testé, cette dernière étant intrinsèquement liée à la vibration des tissus mous via le muscle tuning. De plus, il est important d'établir une période d'adaptation afin que le sportif puisse retrouver un pattern et une amplitude d'activation stable lorsque du matériel inhabituel est testé. Enfin, considérer des groupes fonctionnels, que ça soit à priori avec des caractéristiques anthropométriques ou à postériori avec des bons ou mauvais répondants, devrait être au centre des prochaines recherches afin d'optimiser le lien entre l'humain et le matériel.

Concernant l'effet de la fatigue sur le comportement vibratoire, nous avons montré que les courses de trails et ultra-trails modifiaient l'impact et les vibrations de manière différente par rapport à des efforts courts. L'augmentation de la fréquence d'impact ainsi que la diminution de la fréquence de vibrations

du *vastus lateralis* ont minimisé le phénomène de résonance et en conséquence, ce muscle vibrait moins amplement, à plus basse fréquence, et de manière moins amortie après la course. La diminution de la fréquence de vibration du muscle pouvait être dû à une augmentation locale de la masse, causée par la formation d'un œdème superficiel. De plus, il est possible que des stratégies de protection aient été mise en place afin de limiter une trop grande amplitude de vibration et la génération de douleur. Cette hypothèse est renforcée par le fait que seul le *vastus lateralis*, muscle le plus sollicité dans les épreuves de trails (Maeo et al., 2017), ait été affecté. Des études complémentaires, notamment avec une analyse de la cinématique de course, de l'activation musculaire, et de la localisation des dommages musculaires, seront nécessaires pour compléter les hypothèses faites par cette étude.

Les vibrations transitoires du membre inférieur, et notamment des muscles *gastrocnemius medialis* et *vastus lateralis* ont été étudiées lors de cette thèse. Le choix de ces deux muscles a été effectué car ce sont deux des muscles très sollicités au niveau des membres inférieurs lors de la course à pied (Hamner et al., 2010; Hamner & Delp, 2013) et que leur amplitude de vibrations est importante (Boyer & Nigg, 2004; Wakeling et al., 2003). Dans la pratique sportive, les chocs peuvent aussi survenir à d'autres localisations qu'entre le pied et le sol, c'est le cas notamment des sports de raquettes où l'impact est initié au moment du contact entre la balle/volant et la raquette. Des études sur le tennis ont montré que la raquette vibrait à des fréquences proches de celles des tissus mous et que la vibration se transmettait au niveau de l'avant-bras (Blache et al., 2017; Chadefaux et al., 2016). Le matériel, la force de préhension, ainsi que le niveau d'activations des muscles de l'avant-bras jouent un rôle dans le transfert de la vibration de la raquette à l'organisme (Chadefaux et al., 2017, 2016). Les premières pistes montrent donc que le muscle tuning pourrait s'effectuer au niveau du membre supérieur, et l'étude de la vibration du membre supérieur après induction de fatigue permettrait de compléter l'analyse déjà initiée par les travaux de Chadefaux et collaborateurs.

Enfin, certaines hypothèses et axes de développement de cette thèse se sont appuyés sur des données venant de la vibration continue, notamment sur le lien entre les vibrations et la fatigue et/ou dommages musculaires. En effet, ajouter des vibrations continues durant la pratique sportive crée des dommages musculaires, de la fatigue, de l'inconfort, provoque une augmentation de l'activité musculaire et de la

dépense énergétique (Cardinale & Lim, 2003; Hintzy et al., 2019; de Hoyo et al., 2013; Munera et al., 2017; Necking et al., 1996a, 1992; Rittweger et al., 2002). Cependant, l'effet de l'exposition à des vibrations transitoires, c'est-à-dire initiées par un impact et amorties entre deux impacts consécutifs, n'a pas été mis en relation avec les dommages ou la fatigue musculaire. Il serait possible d'étudier le lien entre les vibrations et la fatigue et/ou dommages musculaires grâce à une réduction localisée de l'amplitude de la vibration. Pour cela, l'utilisation d'un cuissard de compression sur une des deux jambes permettrait d'observer des différences de vibrations entre la jambe compressée et non compressée, et de corréler ces différences à de potentielles différences de fatigue neuromusculaire après l'effort. En parallèle, une mesure de l'impact, de la cinématique de course et de l'activité musculaire sera nécessaire pour isoler d'autres facteurs explicatifs si une différence de fatigue et/ou dommages musculaires est observée.

BIBLIOGRAPHIE

Andonian P, Viallon M, Le Goff C, de Bourguignon C, Tourel C, Morel J, et al. Shear-Wave Elastography Assessments of Quadriceps Stiffness Changes prior to, during and after Prolonged Exercise: A Longitudinal Study during an Extreme Mountain Ultra-Marathon. PLOS ONE 2016;11:e0161855. https://doi.org/10.1371/journal.pone.0161855.

Bercoff J. Ultrafast Ultrasound Imaging. Ultrasound Imaging - Medical Applications 2011. https://doi.org/10.5772/19729.

Bigland-Ritchie B, Jones DA, Hosking GP, Edwards RH. Central and peripheral fatigue in sustained maximum voluntary contractions of human quadriceps muscle. Clin Sci Mol Med 1978;54:609–14.

Blache Y, Hautier C, Lefebvre F, Djordjevic A, Creveaux T, Rogowski I. Analysis of the tennis racket vibrations during forehand drives: Selection of the mother wavelet. Journal of Biomechanics 2017;61:94–101. https://doi.org/10.1016/j.jbiomech.2017.07.006.

Borràs X, Balius X, Drobnic F, Til L, Turmo A, Valle J. Effects of lower body compression garment in muscle oscillation and tissular injury during intense exercise 2011:4.

Boyer KA. Muscle Tuning During Running: Implications of an Un-tuned Landing. Journal of Biomechanical Engineering 2006;128:815. https://doi.org/10.1115/1.2354202.

Boyer KA, Andriacchi TP. Changes in running kinematics and kinetics in response to a rockered shoe intervention. Clinical Biomechanics 2009;24:872–6. https://doi.org/10.1016/j.clinbiomech.2009.08.003.

Boyer KA, Nigg BM. Changes in Muscle Activity in Response to Different Impact Forces Affect Soft Tissue Compartment Mechanical Properties. Journal of Biomechanical Engineering 2007a;129:594. https://doi.org/10.1115/1.2746384.

Boyer KA, Nigg BM. Quantification of the input signal for soft tissue vibration during running. J Biomech 2007b;40:1877–80. https://doi.org/10.1016/j.jbiomech.2006.08.008.

Boyer KA, Nigg BM. Soft tissue vibrations within one soft tissue compartment. Journal of Biomechanics 2006;39:645–51. https://doi.org/10.1016/j.jbiomech.2005.01.027.

Boyer KA, Nigg BM. Muscle activity in the leg is tuned in response to impact force characteristics. J Biomech 2004;37:1583–8. https://doi.org/10.1016/j.jbiomech.2004.01.002.

Broatch JR, Brophy-Williams N, Phillips EJ, O'Bryan SJ, Halson SL, Barnes S, et al. Compression Garments Reduce Muscle Movement and Activation during Submaximal Running: Medicine & Science in Sports & Exercise 2019:1. https://doi.org/10.1249/MSS.0000000000002182.

Bruce OL, Firminger CR, Wannop JW, Stefanyshyn DJ, Edwards WB. Effects of basketball court construction and shoe stiffness on countermovement jump landings. Footwear Science 2019;11:171–9. https://doi.org/10.1080/19424280.2019.1668867.

Cardinale M, Lim J. The acute effects of two different whole body vibration frequencies on vertical jump performance. Medicina Dello Sport 2003;56:287–92.

Chadefaux D, Rao G, Androuet P, Berton E, Vigouroux L. Active tuning of stroke-induced vibrations by tennis players. Journal of Sports Sciences 2016:1–9. https://doi.org/10.1080/02640414.2016.1227868.

Chadefaux D, Rao G, Le Carrou J-L, Berton E, Vigouroux L. The effects of player grip on the dynamic behaviour of a tennis racket. Journal of Sports Sciences 2017;35:1155–64. https://doi.org/10.1080/02640414.2016.1213411.

Chen C-H, Yang W-W, Chen Y-P, Chen VC-F, Liu C, Shiang T-Y. High vibration frequency of soft tissue occurs during gait in power-trained athletes. Journal of Sports Sciences 2020:1–7. https://doi.org/10.1080/02640414.2020.1824366.

Chen W-H, Hsieh C-F, Chan M-S, Shih Y, Chen C-H, Shiang T-Y. Optimal shear cushion stiffness at different gait speeds. Journal of Biomechanics 2019;93:226–30. https://doi.org/10.1016/j.jbiomech.2019.07.018.

Chen X, Li L, Guo J, Zhang L, Yuan Y, Chen B, et al. Treadmill running exercise prevents senile osteoporosis and upregulates the Wnt signaling pathway in SAMP6 mice. Oncotarget 2016;7:71072–86. https://doi.org/10.18632/oncotarget.12125.

Coza A, Nigg BM. Compression apparel effects on soft tissue vibrations 2008:2.

Coza A, Nigg BM, Fliri L. Quantification of Soft-Tissue Vibrations in Running: Accelerometry versus High-Speed Motion Capture. Journal of Applied Biomechanics 2010;26:367–72. https://doi.org/10.1123/jab.26.3.367.

Dorn TW, Schache AG, Pandy MG. Muscular strategy shift in human running: dependence of running speed on hip and ankle muscle performance. Journal of Experimental Biology 2012;215:2347–2347. https://doi.org/10.1242/jeb.075051.

Ehrström S, Gruet M, Giandolini M, Chapuis S, Morin J-B, Vercruyssen F. Acute and Delayed Neuromuscular Alterations Induced by Downhill Running in Trained Trail Runners: Beneficial Effects of High-Pressure Compression Garments. Frontiers in Physiology 2018;9:1627. https://doi.org/10.3389/fphys.2018.01627.

Enders H, von Tscharner V, Nigg BM. Analysis of damped tissue vibrations in time-frequency space: a wavelet-based approach. J Biomech 2012;45:2855–9. https://doi.org/10.1016/j.jbiomech.2012.08.027.

Friesenbichler B, Stirling LM, Federolf P, Nigg BM. Tissue vibration in prolonged running. Journal of Biomechanics 2011;44:116–20. https://doi.org/10.1016/j.jbiomech.2010.08.034.

Fu W, Fang Y, Gu Y, Huang L, Li L, Liu Y. Shoe cushioning reduces impact and muscle activation during landings from unexpected, but not self-initiated, drops. Journal of Science and Medicine in Sport 2017;20:915–20. https://doi.org/10.1016/j.jsams.2017.03.009.

Fu W, Wang X, Liu Y. Impact-induced soft-tissue vibrations associate with muscle activation in human landing movements: An accelerometry and EMG evaluation. Technol Health Care 2015;23:S179–87. https://doi.org/10.3233/THC-150952.

Gandevia SC. Spinal and Supraspinal Factors in Human Muscle Fatigue. Physiological Reviews 2001;81:1725–89. https://doi.org/10.1152/physrev.2001.81.4.1725.

Gellaerts J, Pirard M, Muzic J, Peseux M, Ménétrier A. Maximalist vs. minimalist shoes: dose-effect response of elastic compression on muscular oscillations. The Journal of Sports Medicine and Physical Fitness 2017. https://doi.org/10.23736/S0022-4707.16.06721-9.

Giandolini M, Bartold S, Horvais N. Interaction between body composition and impact-related parameters in male and female heel-toe runners. Gait & Posture 2019;70:355–60. https://doi.org/10.1016/j.gaitpost.2019.03.026.

Giandolini M, Pavailler S, Samozino P, Morin J-B, Horvais N. Foot strike pattern and impact continuous measurements during a trail running race: proof of concept in a world-class athlete. Footwear Science 2015;7:127–37. https://doi.org/10.1080/19424280.2015.1026944.

Giandolini M, Romain J-P, Horvais N, Nigg BM. Midsole Properties Affect the Amplitude of Soft Tissue Vibrations in Heel–Toe Runners. Medicine & Science in Sports & Exercise 2020;52:884–91. https://doi.org/10.1249/MSS.0000000000002194.

Giandolini M, Vernillo G, Samozino P, Horvais N, Edwards WB, Morin J-B, et al. Fatigue associated with prolonged graded running. European Journal of Applied Physiology 2016;116:1859–73. https://doi.org/10.1007/s00421-016-3437-4.

Gindre C, Lussiana T, Hebert-Losier K, Mourot L. Aerial and Terrestrial Patterns: A Novel Approach to Analyzing Human Running. Int J Sports Med 2016;37:25–9. https://doi.org/10.1055/s-0035-1555931.

Gruber AH, Boyer KA, Derrick TR, Hamill J. Impact shock frequency components and attenuation in rearfoot and forefoot running. Journal of Sport and Health Science 2014;3:113–21. https://doi.org/10.1016/j.jshs.2014.03.004.

Halilaj E, Rajagopal A, Fiterau M, Hicks JL, Hastie TJ, Delp SL. Machine learning in human movement biomechanics: Best practices, common pitfalls, and new opportunities. Journal of Biomechanics 2018;81:1–11. https://doi.org/10.1016/j.jbiomech.2018.09.009.

Hamner SR, Delp SL. Muscle contributions to fore-aft and vertical body mass center accelerations over a range of running speeds. Journal of Biomechanics 2013;46:780–7. https://doi.org/10.1016/j.jbiomech.2012.11.024.

Hamner SR, Seth A, Delp SL. Muscle contributions to propulsion and support during running. Journal of Biomechanics 2010;43:2709–16. https://doi.org/10.1016/j.jbiomech.2010.06.025.

Hintzy F, Gregoire N, Samozino P, Chiementin X, Bertucci W, Rossi J. Effect of Thigh-Compression Shorts on Muscle Activity and Soft-Tissue Vibration During Cycling: Journal of Strength and Conditioning Research 2019;33:2145–52. https://doi.org/10.1519/JSC.0000000000002402.

Hoerzer S, von Tscharner V, Jacob C, Nigg BM. Defining functional groups based on running kinematics using Self-Organizing Maps and Support Vector Machines. J Biomech 2015;48:2072–9. https://doi.org/10.1016/j.jbiomech.2015.03.017.

Horvais N, Samozino P, Chiementin X, Morin J-B, Giandolini M. Cushioning perception is associated with both tibia acceleration peak and vibration magnitude in heel-toe running. Footwear Science 2019;11:35–44. https://doi.org/10.1080/19424280.2018.1555863.

de Hoyo M, Carrasco L, Da Silva-Grigoletto ME, Sañudo B, Caballero-Villarraso J, Arriaza E, et al. Impact of an acute bout of vibration on muscle contractile properties, creatine kinase and lactate dehydrogenase response. European Journal of Sport Science 2013;13:666–73. https://doi.org/10.1080/17461391.2013.774052.

Hreljac A. Impact and overuse injuries in runners. Med Sci Sports Exerc 2004;36:845–9.

Hulteen RM, Smith JJ, Morgan PJ, Barnett LM, Hallal PC, Colyvas K, et al. Global participation in sport and leisure-time physical activities: A systematic review and meta-analysis. Preventive Medicine 2017;95:14–25. https://doi.org/10.1016/j.ypmed.2016.11.027.

Jalali P, Noorani MRS, Hassannejad R, Ettefagh MM. Modeling the central nervous system functionality in controlling the calf muscle activity during running with sport shoes. Proceedings of the Institution of Mechanical Engineers, Part H: Journal of Engineering in Medicine 2019;233:254–66. https://doi.org/10.1177/0954411918821390.

Kerdok AE, Biewener AA, McMahon TA, Weyand PG, Herr HM. Energetics and mechanics of human running on surfaces of different stiffnesses. Journal of Applied Physiology 2002;92:469–78. https://doi.org/10.1152/japplphysiol.01164.2000.

Khassetarash A, Hassannejad R, Enders H, Ettefagh MM. Damping and energy dissipation in soft tissue vibrations during running. Journal of Biomechanics 2015a;48:204–9. https://doi.org/10.1016/j.jbiomech.2014.11.051.

Khassetarash A, Hassannejad R, Ettefagh MM, Oskouei AE. Vibration settling time of the gastrocnemius remains constant during an exhaustive run in rear foot strike runners. Journal of Biomechanics 2019;93:140–6. https://doi.org/10.1016/j.jbiomech.2019.06.026.

Khassetarash A, Hassannejad R, Ettefagh MM, Sari-Sarraf V. Fatigue and soft tissue vibration during prolonged running. Hum Mov Sci 2015b;44:157–67. https://doi.org/10.1016/j.humov.2015.08.024.

Kiernan D, Hawkins DA, Manoukian MAC, McKallip M, Oelsner L, Caskey CF, et al. Accelerometer-based prediction of running injury in National Collegiate Athletic Association track athletes. Journal of Biomechanics 2018;73:201–9. https://doi.org/10.1016/j.jbiomech.2018.04.001.

Kong PW, Lam WK, Ng WX, Aziz L, Leong HF. In-Shoe Plantar Pressure Profiles in Amateur Basketball Players. Journal of the American Podiatric Medical Association 2018;108:215–24. https://doi.org/10.7547/16-123.

Lai AKM, Hodson-Tole EF. In vivo oscillations of the soleus muscle can be quantified using b-mode ultrasound imaging during walking and running in humans. Scientific Reports 2020;10:20230. https://doi.org/10.1038/s41598-020-77266-w.

Lee D, Brellenthin AG, Thompson PD, Sui X, Lee I-M, Lavie CJ. Running as a Key Lifestyle Medicine for Longevity. Progress in Cardiovascular Diseases 2017. https://doi.org/10.1016/j.pcad.2017.03.005.

Lilly JM, Olhede SC. Generalized Morse Wavelets as a Superfamily of Analytic Wavelets. EEE Trans Signal Process 2012;60:6036–41. https://doi.org/10.1109/TSP.2012.2210890.

Lilly JM, Olhede SC. Higher-Order Properties of Analytic Wavelets. EEE Trans Signal Process 2009;57:146–60. https://doi.org/10.1109/TSP.2008.2007607.

Lin S-Y, Su P-F, Chung C-H, Hsia C-C, Chang C-H. Stiffness Effects in Rocker-Soled Shoes: Biomechanical Implications. PLOS ONE 2017;12:e0169151. https://doi.org/10.1371/journal.pone.0169151.

Lucas-Cuevas AG, Encarnación-Martínez A, Camacho-García A, Llana-Belloch S, Pérez-Soriano P. The location of the tibial accelerometer does influence impact acceleration parameters during running. Journal of Sports Sciences 2017;35:1734–8. https://doi.org/10.1080/02640414.2016.1235792.

Lussiana T, Terrillon A, Raynaud J-L, Tordi N, Mourot L, Ménétrier A. Effet dose-réponse de la compression élastique sur les vibrations musculaires. Science & Sports 2015;30:101–4. https://doi.org/10.1016/j.scispo.2014.09.004.

Maeo S, Ando Y, Kanehisa H, Kawakami Y. Localization of damage in the human leg muscles induced by downhill running. Sci Rep 2017;7. https://doi.org/10.1038/s41598-017-06129-8.

Mair SD, Seaber AV, Glisson RR, Garrett WE. The Role of Fatigue in Susceptibility to Acute Muscle Strain Injury. Am J Sports Med 1996;24:137–43. https://doi.org/10.1177/036354659602400203.

Major WF. The Benefits and Costs of Serious Running. World Leisure Journal 2001;43:12–25. https://doi.org/10.1080/04419057.2001.9674226.

Manin L, Poggi M, Havard N. Vibrations of table tennis racket composite wood blades: modeling and experiments. Procedia Engineering 2012;34:694–9. https://doi.org/10.1016/j.proeng.2012.04.118.

Martínez A, Lam CKY, von Tscharner V, Nigg BM. Soft tissue vibration dynamics after an unexpected impact. Physiological Reports 2019;7:1–11. https://doi.org/10.14814/phy2.13990.

Millet GY, Martin V, Martin A, Vergès S. Electrical stimulation for testing neuromuscular function: from sport to pathology. Eur J Appl Physiol 2011a;111:2489–500. https://doi.org/10.1007/s00421-011-1996-y.

Millet GY, Tomazin K, Verges S, Vincent C, Bonnefoy R, Boisson R-C, et al. Neuromuscular Consequences of an Extreme Mountain Ultra-Marathon. PLoS One 2011b;6. https://doi.org/10.1371/journal.pone.0017059.

Mohr M, von Tscharner V, Nigg S, Nigg BM. Systematic reduction of leg muscle activity throughout a standard assessment of running footwear. Journal of Sport and Health Science 2021:S209525462100003X. https://doi.org/10.1016/j.jshs.2021.01.003.

Müller R, Siebert T, Blickhan R. Muscle preactivation control: simulation of ankle joint adjustments at touchdown during running on uneven ground. Journal of Applied Biomechanics 2012;28:718–25.

Munera M, Bertucci W, Duc S, Chiementin X. Analysis of muscular activity and dynamic response of the lower limb adding vibration to cycling. Journal of Sports Sciences 2017:1–11. https://doi.org/10.1080/02640414.2017.1398407.

Necking L, Dahlin L, Friden J, Lundborg G, Lundstrom R, Thornell L. Vibration-induced muscle injury An experimental model and preliminary findings. The Journal of Hand Surgery: Journal of the British Society for Surgery of the Hand 1992;17:270–4. https://doi.org/10.1016/0266-7681(92)90113-G.

Necking L, Lundborg G, Fridén J. Hand Muscle Weakness in Long-Term Vibration Exposure. Journal of Hand Surgery 2002;27:520–5. https://doi.org/10.1054/jhsb.2002.0810.

Necking L, Lundström R, Dahlin LB, Lundborg G, Thornell L-E, Fridén J. Tissue displacement is a causative factor in vibration-induced muscle injury. The Journal of Hand Surgery: British & European Volume 1996a;21:753–7. https://doi.org/10.1016/S0266-7681(96)80180-X.

Necking L, Lundström R, Lundborg Gör, Thornell L-E, Fridén J. Skeletal Muscle Changes After Short Term Vibration. Scandinavian Journal of Plastic and Reconstructive Surgery and Hand Surgery 1996b;30:99–103. https://doi.org/10.3109/02844319609056390.

Nichols TE, Holmes AP. Nonparametric permutation tests for functional neuroimaging: A primer with examples. Human Brain Mapping 2002;15:1–25. https://doi.org/10.1002/hbm.1058.

Nigg BM. The Role of Impact Forces and Foot Pronation: A New Paradigm: Clinical Journal of Sport Medicine 2001;11:2–9. https://doi.org/10.1097/00042752-200101000-00002.

Nigg BM. Impact forces in running: Current Opinion in Orthopaedics 1997;8:43–7. https://doi.org/10.1097/00001433-199712000-00007.

Nigg BM, Bahlsen HA, Luethi SM, Stokes S. The influence of running velocity and midsole hardness on external impact forces in heel-toe running. Journal of Biomechanics 1987;20:951–9.

Nigg BM, Liu W. The effect of muscle stiffness and damping on simulated impact force peaks during running. Journal of Biomechanics 1999;32:849–56.

Nigg BM, Mohr MM, Nigg SR. Muscle tuning and preferred movement path – a paradigm shift. Current Issues in Sport Science (CISS) 2017;2:1–12. https://doi.org/10.15203/CISS_2017.007.

Nigg BM, Wakeling JM. Impact forces and muscle tuning: a new paradigm. Exerc Sport Sci Rev 2001;29:37–41.

Nikooyan AA, Zadpoor AA. Effects of Muscle Fatigue on the Ground Reaction Force and Soft-Tissue Vibrations During Running: A Model Study. IEEE Transactions on Biomedical Engineering 2012;59:797–804. https://doi.org/10.1109/TBME.2011.2179803.

Nilsson J, Thorstensson A. Ground reaction forces at different speeds of human walking and running. Acta Physiol Scand 1989;136:217–27. https://doi.org/10.1111/j.1748-1716.1989.tb08655.x.

Park S-K, Jeon H-M, Lam W-K, Stefanyshyn D, Ryu J. The effects of downhill slope on kinematics and kinetics of the lower extremity joints during running. Gait & Posture 2019;68:181–6. https://doi.org/10.1016/j.gaitpost.2018.11.007.

Pataky TC. Generalized n-dimensional biomechanical field analysis using statistical parametric mapping. Journal of Biomechanics 2010;43:1976–82. https://doi.org/10.1016/j.jbiomech.2010.03.008.

Perl J. A neural network approach to movement pattern analysis. Human Movement Science 2004;23:605–20. https://doi.org/10.1016/j.humov.2004.10.010.

Perl J. Artificial Neural Networks in Sports: New Concepts and Approaches. International Journal of Performance Analysis in Sport 2001;1:106–21. https://doi.org/10.1080/24748668.2001.11868253.

Phinyomark A, Limsakul C, Phukpattaranont P. A Comparative Study of Wavelet Denoising for Multifunction Myoelectric Control, IEEE; 2009, p. 21–5. https://doi.org/10.1109/ICCAE.2009.57.

Piéron H. V. Recherches expérimentales sur la sensation vibratoire cutanée. psy 1935;36:82–102. https://doi.org/10.3406/psy.1935.30647.

Rasske K, Franz JR. Aging effects on the Achilles tendon moment arm during walking. Journal of Biomechanics 2018;77:34–9. https://doi.org/10.1016/j.jbiomech.2018.06.001.

Rittweger J. Vibration as an exercise modality: how it may work, and what its potential might be. European Journal of Applied Physiology 2010;108:877–904. https://doi.org/10.1007/s00421-009-1303-3.

Rittweger J, Ehrig J, Just K, Mutschelknauss M, Kirsch KA, Felsenberg D. Oxygen uptake in whole-body vibration exercise: influence of vibration frequency, amplitude, and external load. International Journal of Sports Medicine 2002;23:428–32.

Rittweger J, Mutschelknauss M, Felsenberg D. Acute changes in neuromuscular excitability after exhaustive whole body vibration exercise as compared to exhaustion by squatting exercise. Clinical Physiology and Functional Imaging 2003;23:81–6.

Saugy J, Place N, Millet GY, Degache F, Schena F, Millet GP. Alterations of Neuromuscular Function after the World's Most Challenging Mountain Ultra-Marathon. PLoS One 2013;8. https://doi.org/10.1371/journal.pone.0065596.

Schache AG, Dorn TW, Williams GP, Brown NAT, Pandy MG. Lower-limb muscular strategies for increasing running speed. J Orthop Sports Phys Ther 2014;44:813–24. https://doi.org/10.2519/jospt.2014.5433.

Shorten MR, Winslow DS. Spectral analysis of impact shock during running. International Journal of Sport Biomechanics 1992;8:288–304.

Smeathers JE. Transient vibrations caused by heel strike. Proc Inst Mech Eng H 1989;203:181–6. https://doi.org/10.1243/PIME_PROC_1989_203_036_01.

Sobhani S, van den Heuvel ER, Dekker R, Postema K, Kluitenberg B, Bredeweg SW, et al. Biomechanics of running with rocker shoes. J Sci Med Sport 2016. https://doi.org/10.1016/j.jsams.2016.04.008.

Souron R, Besson T, McNeil CJ, Lapole T, Millet GY. An Acute Exposure to Muscle Vibration Decreases Knee Extensors Force Production and Modulates Associated Central Nervous System Excitability. Front Hum Neurosci 2017a;11. https://doi.org/10.3389/fnhum.2017.00519.

Souron R, Besson T, Millet GY, Lapole T. Acute and chronic neuromuscular adaptations to local vibration training. European Journal of Applied Physiology 2017b;117:1939–64. https://doi.org/10.1007/s00421-017-3688-8.

Stegeman DF, Hermens HJ. Standards for surface electromyography: the European project "Surface EMG for non-invasive assessment of muscles (SENIAM)". Enschede Roessingh Res Dev 2007;1:108–12.

Trama R, Blache Y, Hautier C. Effect of rocker shoes and running speed on lower limb mechanics and soft tissue vibrations. J Biomech 2019a;82:171–7. https://doi.org/10.1016/j.jbiomech.2018.10.023.

Trama Robin, Hautier C, Blache Y. fctSnPM: Factorial ANOVA and post-hoc tests for Statistical nonParametric Mapping in MATLAB. JOSS 2021;6:3159. https://doi.org/10.21105/joss.03159.

Trama R, Hautier C, Blache Y. Input and Soft-Tissue Vibration Characteristics during Sport-Specific Tasks: Medicine & Science in Sports & Exercise 2020;52:112–9. https://doi.org/10.1249/MSS.0000000000002106.

Trama R, Hautier C, Blache Y. Sport-related impact classification through a convolutional neural network. Computer Methods in Biomechanics and Biomedical Engineering 2019b;22:S267–9. https://doi.org/10.1080/10255842.2020.1714908.

Trama R., Hautier CA, Souron R, Lapole T, Fouré A, Blache Y. Is Accelerometry an Effective Method to Assess Muscle Vibrations in Comparison to Ultrafast Ultrasonography? IEEE Transactions on Biomedical Engineering 2021;68:1409–16. https://doi.org/10.1109/TBME.2020.3035838.

Tsuji K, Ishida H, Oba K, Ueki T, Fujihashi Y. Activity of lower limb muscles during treadmill running at different velocities. Journal of Physical Therapy Science 2015;27:353–6.

Valle X, Til L, Drobnic F, Turmo A, Montoro JB, Valero O, et al. Compression garments to prevent delayed onset muscle soreness in soccer players. Muscle Ligaments and Tendons Journal 2013;03:295. https://doi.org/10.32098/mltj.04.2013.10.

Wakeling JM, Liphardt A-M, Nigg BM. Muscle activity reduces soft-tissue resonance at heel-strike during walking. Journal of Biomechanics 2003;36:1761–9. https://doi.org/10.1016/S0021-9290(03)00216-1.

Wakeling JM, Nigg BM. Soft-tissue vibrations in the quadriceps measured with skin mounted transducers. Journal of Biomechanics 2001a;34:539–43. https://doi.org/10.1016/S0021-9290(00)00203-7.

Wakeling JM, Nigg BM. Modification of soft tissue vibrations in the leg by muscular activity. Journal of Applied Physiology 2001b;90:412–20.

Wakeling JM, Nigg BM, Rozitis AI. Muscle activity damps the soft tissue resonance that occurs in response to pulsed and continuous vibrations. Journal of Applied Physiology 2002;93:1093–103. https://doi.org/10.1152/japplphysiol.00142.2002.

Wang T-G, Hsiao T-Y, Wang C-L, Shau Y-W. Resonance frequency in patellar tendon: Resonance frequency in tendon. Scandinavian Journal of Medicine & Science in Sports 2007;17:535–8. https://doi.org/10.1111/j.1600-0838.2006.00618.x.

Wu G, van der Helm FCT, (DirkJan) Veeger HEJ, Makhsous M, Van Roy P, Anglin C, et al. ISB recommendation on definitions of joint coordinate systems of various joints for the reporting of human joint motion—Part II: shoulder, elbow, wrist and hand. Journal of Biomechanics 2005;38:981–92. https://doi.org/10.1016/j.jbiomech.2004.05.042.

Wu G, Siegler S, Allard P, Kirtley C, Leardini A, Rosenbaum D, et al. ISB recommendation on definitions of joint coordinate system of various joints for the reporting of human joint motion—part I: ankle, hip, and spine. Journal of Biomechanics 2002;35:543–8.

Yamada D, Degirmenci A, Howe R. Ultrasound Imaging for Identifying Dynamics of Soft Tissue. IEEE 2018:1161–5.

Zadpoor AA, Nikooyan AA. The relationship between lower-extremity stress fractures and the ground reaction force: A systematic review. Clinical Biomechanics 2011;26:23–8. https://doi.org/10.1016/j.clinbiomech.2010.08.005.